NTNU
Norwegian University of
Science and Technology

Trailer Suspension Rig for Virtual and Physical Testing

Ask Arildsønn Falch

Master of Science in Mechanical Engineering
Submission date: September 2016
Supervisor: Terje Rølvåg, IPM

Norwegian University of Science and Technology
Department of Engineering Design and Materials

NTNU - NORWEGIAN UNIVERSITY
OF SCIENCE AND TECHNOLOGY
DEPARTMENT OF ENGINEERING DESIGN
AND MATERIALS

MASTER THESIS FALL 2016
FOR
STUD.TECHN. ASK FALCH

TRAILER SUSPENSION RIG FOR VIRTUAL AND PHYSICAL TESTING

Tilhenger hjuloppheng rig for virtuell og fysisk dynamisk testing

IPM professors are teaching various courses in static and dynamic analysis of mechanical systems. Different methods and cases are used and it's hard for the students to know when and where the different methods and tools are applicable. Analytical calculations are sometimes applicable while simulation tools are required for more complex analysis.

The intention with the physical test rig is to establish a common benchmark model and link between the different methods and tools used in various courses. Then the students can compare calculations with physical test results and evaluate the difference in accuracy and speed.

This master thesis is based on the candidates project and will prepare the test rig for use in several IPM courses. The learning objective is to give the students a better understanding of structural dynamics and motivate them for further studies in this challenging area.

Tasks to be completed:

1. Identify structural and mechanism key performance indicators (KPIs) to be tested and benchmarked
2. Build and instrument the virtual and physical test rig with sensors to capture the KPIs
3. Perform physical tests and document the performance (KPIs)
4. Perform analytical calculations, virtual tests and compare with physical test KPIs
5. Prepare suspension test rig exercises for TMM4112 (Maskindeler), TMM4135 (Elementmetoden grunnkurs) and TMM4155 (FEAinME).

Formal requirements:

Three weeks after start of the thesis work, an A3 sheet illustrating the work is to be handed in. A template for this presentation is available on the IPM's web site (see https://www.ntnu.edu/web/ipm/master-thesis). This sheet should be updated one week before the master's thesis is submitted.

Risk assessment of experimental activities shall always be performed. Experimental work defined in the problem description shall be planed and risk assessed up-front and within 3 weeks after receiving the problem text. Any specific experimental activities which are not properly covered by the general risk assessment shall be particularly assessed before performing the experimental work. Risk assessments should be signed by the supervisor and copies shall be included in the appendix of the thesis.

The thesis should include the signed problem text, and be written as a research report with summary both in English and Norwegian, conclusion, literature references, table of contents, etc. During preparation of the text, the candidate should make efforts to create a well arranged and well written report. To ease the evaluation of the thesis, it is important to cross-reference text, tables and figures. For evaluation of the work a thorough discussion of results is appreciated.

The thesis shall be submitted electronically via DAIM, NTNU's system for Digital Archiving and Submission of Master's theses.

The contact persons at IPM are Bjørn Haugen and Torgeir Welo.

Torgeir Welo
Head of Division

Terje Rølvåg
Professor/Supervisor

NTNU
Norges teknisk-
naturvitenskapelige universitet
Institutt for produktutvikling
og materialer

Abstract

The objective of this Master's thesis was to finalize the construction of a physical torsion bar suspension test rig, and perform analytical calculations and virtual simulations related to the rig. This thesis is a continuation of the candidates Project Thesis. The basis for this work are two exams from TMM4112 Machine Elements of 2009. The rig is to be used by lecturers and students in several courses at the Department of Engineering Design and Materials, NTNU.

The physical rig has been instrumented with numerous sensors and equipment, and a PC with Catman Data Acquisition software to analyze the physical static and dynamic suspension response. Physical testing of the rig was conducted and evaluated. These results laid the foundation for comparing physical test data with analytical calculations, and computer simulations. Multiple Finite Element Analysis (FEA) solvers has been utilized to simulate the quasi-static- and dynamic response of the suspension system. The analytical calculation model presented in the exams has also been revised to improve the correlation with the physical rig.

All the design and constitution work of the rig has been performed by the author of this thesis. The final result is a turnkey-product rig, ready to be used in lectures. Student exercises related to the rig was also created for the courses; TMM4112 - Machine Elements, TMM4135 -Analysis and Assessment Based on the Finite Element Method, and TMM4155 - FEA in ME.

Sammendrag

Formålet med denne masteroppgaven var å ferdigstille en fysisk testrigg for et torsjonsstav-hjuloppheng, samt utføre analytiske kalkulasjoner og data simuleringer relatert til riggen. Denne masteroppgaven er en videreføring av undertegnedes prosjektoppgave. Bakgrunnen for dette arbeidet er to eksamener i faget TMM4112 maskindeler i fra 2009. Riggen vil bli brukt av forelesere og studenter i flere fag på Institutt for produktutvikling og materialer, NTNU.

Riggen ble utrustet med diverse sensorer og utstyr, samt en pc med Catman datainnsamlings-programvare for å analysere den fysiske statiske og dynamiske oppførselen til riggen. Fysisk testing ble gjennomført og evaluert. Disse resultatene la deretter grunnlaget for å sammenligne den fysiske ytelsen av riggen med analytiske beregninger og data-simuleringer. Flere typer elementmetode (FEA) simuleringer ble brukt for å simulere den statiske- og dynamiske responsen til hjulopphenget. Den analytiske beregningsmodellen presentert i eksamenene har også blitt revidert for å forbedre korrelasjon med den fysiske riggen.

Hele designet og byggingen av riggen ble utført av undertegnede. Det ferdige resultatet er en nøkkelferdig rigg som er klar til å bli benyttet i undervisning. Øvingsoppgaver for studenter tilknyttet riggen har også blitt laget for fagene; TMM4112 - Maskindeler, TMM4135 -Dimensjonering basert på elementmetoden, og TMM4155 - Anvendelse av elementmetoden i maskinkonstruksjon.

Preface

This rig-project marks the end of five years of mechanical engineering education. The idea for this projects was provided by supervisor Professor Terje Rølvåg, on the basis of two exams created by Professor Torgeir Welo. The project has been a absolute pleasure to work with. The versatility of this project has required skills acquired from almost every discipline learned the past five years. It involves, mechanics, design, calculus, CAD, FEA, electronics, construction, fatigue design, material science, statistics, and dynamics. The result is a rig which enables students to acquire more practical experience with physical testing, and testing of theory. And hopefully this project will inspire new candidates to perform similar project themselves.

During this project I have been fortunate to get to demonstrate the rig by lecturing in Terje Rølvågs class, and demonstrate the rig for representatives from Lockhead Martin and Jotne.

I would like to thank the following people for their great help during my master thesis. Supervisor, Professor Terje Rølvåg has been a great help and support, throughout this project.By providing an exciting project I find interesting, and expecting great results, he has pushed me to preform my best. A big thanks goes to Halvard Støwer for being a great asset concerning the sensors and software. I would also like to give credit to fellow M.sc. student Pål Duus for constructive dialogues and feedback concerning the thesis. Gabriela Dahle has also been a great help, by dealing with orders and vendors during this project.

Oslo, 18-09-2016

Ask A. Falch

Contents

Abstract . . . iii
Preface . . . v

1 Introduction **1**
1.1 Background . . . 1
1.2 Approach . . . 3
1.3 Structure of the Report . . . 4

2 Basis for this Master Thesis **5**

3 KPIs from Exams **11**
3.1 Quasi Static Key Performance Indicators . . . 11
3.2 Dynamical Key Performance Indicator . . . 12

4 Instrumentation **13**
4.1 Sensors and Equipment . . . 14
4.2 Installing Sensors . . . 16
4.3 Electronics Bay . . . 20
4.4 Wiring . . . 22
4.5 Finished Rig . . . 24

5 Physical Quasi Static Testing **27**
5.1 Calibration . . . 27
5.2 Test Procedure . . . 30
5.3 Physical test results . . . 31

6 Analytical Static Response **35**
6.1 Complex Geometry Calculation . . . 37
6.1.1 Torsion bar stiffness . . . 37
6.1.2 Effective beam deflection . . . 41
6.1.3 Rotation of the Torsion Arm . . . 47

6.1.4 Evaluation of assumptions . . . 49
6.2 Calculation Models . . . 50
6.3 Results and Evaluation . . . 55

7 Virtual Static Simulation **59**
7.1 3D Solid Elements Simulation Setup . . . 60
7.2 1D Beam Elements Simulation Setup . . . 65
7.3 Results and Comparison with Analytical and Physical Test . . . 68
7.4 Fatigue . . . 72

8 Dynamic Response **75**
8.1 Analytical Approach . . . 76
8.2 Frequency Simulation . . . 78
8.3 Physical Testing . . . 78
8.4 Evaluation of the Results . . . 79

9 Exercises **81**
9.1 TMM4112 - Machine Elements - Exercises Suggestion . . . 82
9.2 TMM4135 - Analysis and Assessment Based on FEM - Exercises Suggestion . . . 87
9.3 TMM4155 - FEA in ME - Exercises Suggestion . . . 90

10 Summary **95**
10.1 Summary and Conclusions . . . 95
10.2 Further Work . . . 97

A As Built, Technical Drawings

B Rig Computer Background Image

C Physical Test Manual

D Exercises Solutions
D.1 TMM4112 - Machine Elements - Exercises Solution . . .
D.2 TMM4135 - Analysis and Assessment Based on FEM - Exercises Solutions . . .
D.3 TMM4155 - FEA in ME - Exercises Solutions . . .

E Material Certificate & Strain Gauge Data

F Risk Assessment

G Project Thesis

H Exams of 2009 in Machine Elements

Bibliography

List of Figures

2.1 Technical Drawing from 2009 Exam . . . 5
2.2 Technical Drawing of the Built Rig . . . 7
2.3 Technical Drawing of the Suspension System, Built Rig . . . 8
2.4 Visual Illustration of Angles and Height Constants, Exam Model . . . 10

4.1 HBM QuantumX DAQ . . . 14
4.2 Computer & Catman Software . . . 14
4.3 HBM U2a Load Cell . . . 15
4.4 HBM WA100 Displacement . . . 15
4.5 Kelag KAS903 Accelerometer . . . 15
4.6 Stain Gauges . . . 15
4.7 Load Cell Assembled on the Rig . . . 16
4.8 Displacement Sensor and Accelerometer Placement . . . 17
4.9 Stain Gauge Direction and Placement . . . 18
4.10 Visual Torsion Angle and Displacement Indicators, CAD illustration . . . 19
4.11 Electronics Bay . . . 20
4.12 Bottom/Back Section of the Electronics Bay . . . 20
4.13 Assembly Order of the Electronics Bay . . . 22
4.14 DAQ Channels with Corresponding Sensors and Color Code . . . 23
4.15 Wiring and Connectors inside the Electronics Bay Door . . . 23
4.16 CAD of Finished Rig . . . 24
4.17 Photo of Finished Rig, Front/Right . . . 25
4.18 Photo of Finished Rig, Front/Left . . . 26

5.1 Strain Gauge Setup in Catman . . . 28
5.2 Calibration of Displacement Sensor . . . 29
5.3 Load versus Height from Physical Tests . . . 31
5.4 Average Stresses from Physical Tests . . . 33

6.1 Angles and Height Parameters, Visual Illustration . . . 36
6.2 Suspension System, Built Rig . . . 37
6.3 Technical Drawing from the Exams . . . 41
6.4 Dimensions Related to the Bearing Calculation . . . 47
6.5 Free Body Diagram for Torsion Arm/Bearings . . . 48
6.6 Description of Angles and Height constants . . . 51
6.7 Height/Load: Analytical- vs Physical Test Results . . . 56
6.8 Height/Load: Analytical- vs Physical Test Results, 2200 - 3200N . . . 57
6.9 Stress/Load: Analytical- vs Physical Test Results . . . 57
6.10 Height/Load: Analytical- vs Physical Test, included Friction Factor . . . 58

7.1 Simulation Constrains . . . 61
7.2 20 Nodes to Sample Torsion Bar Stress . . . 62
7.3 1D Model Sketch . . . 65
7.4 1D Model Constraints, Node numbering . . . 65
7.5 1D SOL 112 Post-Processor; Displacement, and Nodal Stress at 80mm . . . 66
7.6 Height/Load: Simulation Results vs Analytical, and Physical Test . . . 68
7.7 Height/Load: Simulation Results vs Analytical, and Physical Test. 2200 - 3200N . . . 69
7.8 Nominal Von Mises Stress: Simulation Results vs Analytical, and Physical Test . . . 70
7.9 Zero-to-Tension, Cycles between 0 and σ_{max} . . . 73
7.10 Fatigue Analysis Parameters . . . 73
7.11 Load Pattern, Full Cycles with 50% Offset . . . 73
7.12 Cycles to Failure. Zero-to-Tension (F = 3200N) . . . 73
7.13 S-N diagram for S165M [Pic: Industeel [1]] . . . 74

8.1 Technical Drawing of the Wheel Hub Weight . . . 76
8.2 Frequency Simulation Models . . . 78
8.3 Natural Frequency: Only Wheel Hub . . . 79
8.4 Natural Frequency: Wheel Hub And Extra Weight . . . 79

9.1 Technical Drawing of the Suspension System . . . 82
9.2 Stress Concentration Factor [Fig. 2-11, Peterson] . . . 85
9.3 Idealized Suspension System . . . 88
9.4 1D Sketch of the Suspension System . . . 89
9.5 FEM Models Accompanying these Exercises . . . 90
9.6 Zero-to-Tension, Cycles between 0 and σ_{max} . . . 93
9.7 Fatigue Analysis Parameters . . . 93

9.8 Load Pattern, Full Cycles with 50% Offset 93
9.9 S-N diagram for S165M (Torsion Bar) [Fig: Industeel] 94

10.1 Further work suggestion, Eccentric Flywheel 97

D.1 S-N diagram for S165M [Pic: Industeel [1]] . . . . . .

List of Tables

2.1 Constant Declaration 9

3.1 Exam KPIs and Related Values 11
3.2 Selected Static KPIs 12
3.3 Selected Dynamic KPIs 12

5.1 Test Procedure Data 30
5.2 Confidence Interval Test Results 31
5.3 Physical Test Results, Average 32

6.1 Assumption Declaration 35
6.2 Constant Declaration 36
6.3 Values included in the Complex Stiffness Factor Computation 38
6.4 Radii Torsional Constant Computation 39
6.5 Comparison of Torsion Bar Stiffness 40
6.6 Material Properties 42
6.7 Assumptions to Include in the Calculation Models 50
6.8 Dimensions and Constants 51
6.9 Results Calculated at 2940 Newtons 56

7.1 Material Properties in the FEM-model 60
7.2 3D Mesh Details and Constraints 60
7.3 SOL101 Results of 3D Elements Simulation 62
7.4 SOL109 Direct Transient Response of 3D Elements Simulation 64
7.5 SOL112 Modal Transient Response of 3D Elements Simulation 64
7.6 1D Mesh Details and Constraints 66
7.7 SOL 101 Simulation Results 1D Beam Elements 67
7.8 SOL 109 & 112 Simulation Results 1D Beam Elements 67
7.9 Fatigue Parameters and Simulated Maximum Stress 72

7.10 Cycles to Failure Results 73

8.1 Frequency Results with Different Mass 77
8.2 Frequencies with Different Simulated Mass 78
8.3 Frequencies Obtained from Physical Testing 79
8.4 Natural Frequency Results from all Approaches 79

9.1 Material and Fatigue Parameters 93

Abbreviations

CAD Computer-Aided Design

CAE Computer-Aided Engineering

DAQ Data Acquisition Amplifier

FEA Finite Element Analysis

FEM Finite Element Method

GF Gauge Factor

IPM Institutt for Produktutvikling og Materialer, Department of Engineering Design and Materials

NTNU Norwegian University of Science and Technology

KPI Key Performance Indicator

PDS Product Demand Specifications

RMS Root Mean Square

SG Strain Gauge

SIM Simulation

SINTEF Selskapet for industriell og teknisk forskning ved Norges tekniske høgskole, The company for industrial and technical research at the Norwegian technical collage

Chapter 1

Introduction

Throughout five years of a Mechanical Engineering education, students primary learn the necessary theory to construct mechanical components. This leaves some students to have limited hands on experience with transferring their theoretical knowledge into manufactured components. - And to experience deviations and unforeseen obstacles that may occur. This thesis' objective is to provide students with an opportunity to compare theory and practice in a convenient setting. This by construing a physical version of a theoretical exercise most IPM students have tried to solve. Hopefully, this thesis will inspire other students to conduct similar projects themselves.

1.1 Background

IPM professors are teaching various courses in static and dynamic analysis of mechanical systems. Different methods and cases are used and it is hard for students to know when and where the different methods and tools are applicable. Analytical calculations are sometimes applicable while simulation tools are required for more complex analysis. The intention with the physical test rig is to establish a common benchmark model and link between the different methods and tools used in various courses. Then, students can compare calculations with physical test results and evaluate the difference in accuracy and speed. This master thesis will prepare the test rig for use in several IPM courses. The learning objective is to give the students a better understanding of structural dynamics and motivate them for further studies in this challenging area.

Problem Formulation

The objective of this thesis is to construct a physical test rig, on the basis of two exams in Machine Elements of 2009. The test rig is to be utilized by professors and students at IPM, to compare physical testing with analytical calculations and FEA.

Tasks to be completed:

1. Identify structural and mechanism key performance indicators (KPIs) to be tested and benchmarked.
2. Build and instrument the virtual and physical test rig with sensors to capture the KPIs.
3. Perform physical tests and document the performance (KPIs).
4. Perform analytical calculations, virtual tests and compare with physical test KPIs.
5. Prepare suspension test rig exercises for TMM4112 (Maskindeler), TMM4135 (Elementmetoden grunnkurs) and TMM4155 (FEAinME).

1.2 Approach

The foundation of this rig project was machine elements exams concerning a trailer suspensions static and dynamic response. These became the basis for developing the suspension test rig. The exams with solutions were analyzed to retrieve important KPIs. These became the basis for a set of engineering criteria, essential to designing the physical version of the suspension system. In the project thesis, Product Demand Specifications, (PDS), were created on the basis of the intended use of the rig. Different component/material solutions where analyzed and chosen in regards to cost/benefit. To ensure that the design was adequate, Finite Element Analysis (FEA) simulations were performed of the design throughout the design process. The construction of the mechanical structure og the rig was performed by the candidate at the Institutes' realization workshop. The finished mechanical structure defines the transition between the project and master thesis.

This first step of the master thesis was to revise and specify the KPIs. These became the basis for selecting the instrumentation of the rig. The rig was then equipped with sensors and monitoring system. This also involved constructing an electronics bay to house the electronic equipment. The finished rig was then subjected to thorough calibration before performing the testing. The physical test results would then act as a baseline benchmark for further use in the thesis. This baseline showed that the analytical approach presented in the exams did not fully represent the actual static response of the rig. This was the basis for performing extensive analytical calculation to derive an extended calculation model, which better captures the rigs response. In addition to the analytical calculation, virtual simulations has been performed. Both a 3D model and a 1D representation was evaluated with different solvers. The simulation results was then compared with the physical testing and analytical results. The student exercises related to the suspension rig was then mainly created on the basis of the results acquired during the thesis work.

1.3 Structure of the Report

The report is structured in order of the problem formulation. It begins by presenting the work performed to complete the physical rig. Physical tests was then carried out. These results subsequently served as a benchmarks for the following analytical calculations and virtual simulations. Due to the variety of topics, results and evaluations are presented in each associated section.

Chapter 2 Presents the basis for this master thesis, including a summary of the project thesis, and the essence of calculation model from the exams.

Chapter 3 In this chapter, Key Performance Indicators are defined.

Chapter 4 Describes the selected sensors and installation of the rig instrumentation. The finished rig is presented at the end of the chapter.

Chapter 5 Presents the physical testing of the rig. This includes the calibration, test procedure, and physical test results.

Chapter 6 Concerns extensive analytical calculations of the quasi-static response of the suspension system. The calculation model from the exams is revised, leading to an extended calculation model, which better suits the physical test rig. Analytical results are presented and compared with the physical test results.

Chapter 7 Describes the virtual simulations of the suspension system. This includes 3D solid elements, and 1D beam elements simulations. The results are compared with the physical and analytical results. This chapter also includes a fatigue analysis to evaluate the expected service lifetime of the rig.

Chapter 8 Concerns the dynamic response in terms of the natural frequency of the suspension system. Analytical calculations are compared with virtual simulations and physical testing.

Chapter 9 Presents student exercises related to the rig. The exercises are divided into three different sections, one for each respective course; TMM4112 - Machine Elements, TMM4135 - Analysis and Assessment Based on the Finite Element Method, and TMM4155 - FEA in ME.

Chapter 10 Summary and further work.

Chapter 2

Basis for this Master Thesis

The objective of this project is to construct a physical suspension rig based on the TMM4112 - Machine Elements exams of 2009. The exams revolves around different calculations based on the technical drawing of a trailer suspension in fig. 2.1. The trailer suspension consists of a torsion bar, torsion arm, wheel hub, and bushings. The common thread though-out the exams is the relationship between the applied load, rotation of the torsion bar, and critical stresses, based on the geometry. Due to the extensive amount of work connected to this project, this rig-project extends to both a Project- and this Master Thesis, performed by the author of this paper. This Chapter gives a recap of the work performed prior to this master thesis, and is the foundation for this master thesis.

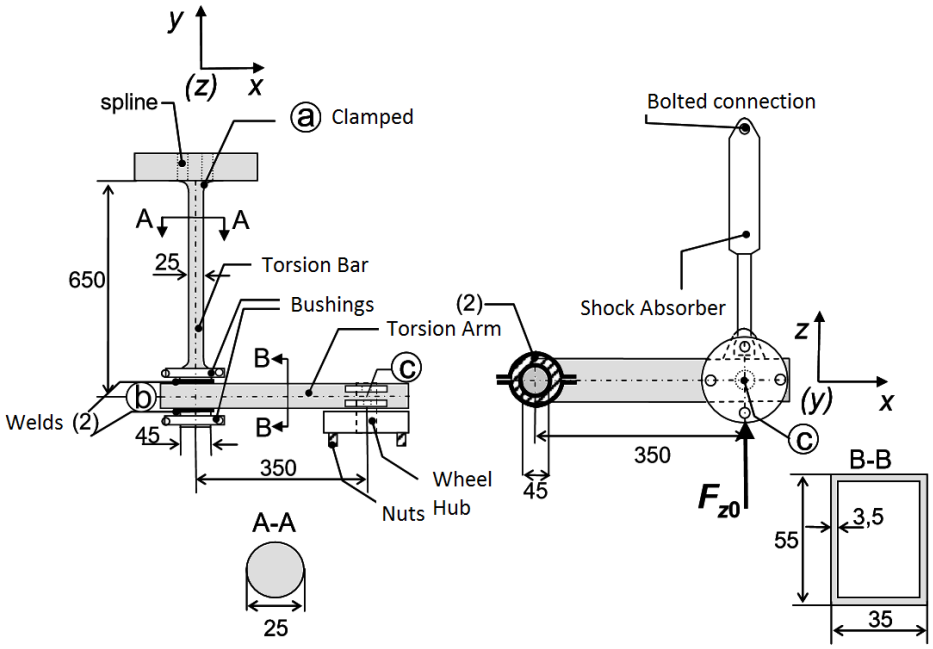

Figure 2.1: Technical Drawing from 2009 Exam

Project thesis summary

The objective of the Project Thesis was to construct the physical foundation for the rig. This in terms of designing and building the suspension system, and a rigid trolley to support it. Technical drawings of the built rig is seen in fig. 2.2 and figure 2.3. These drawings displays the rig prior to the initiation of the master thesis.

The rig consists of a rig frame with the suspension system mounted on top. The suspension system consists of two main parts; a torsion arm, and a torsion bar which acts as the spring. The torsion bar stretches across the rig, and is welded to frame on the right-side, and to the torsion arm on the left-side. Ball bearings on each side of the torsion bar/arm-joint, allows for force-transfer without significant bending the torsion bar. To elevate the torsion arm, a hydraulic jack is utilized as force-applier. The rig is designed withstand workloads up to 3200N. This corresponds to elevating the torsion arm to about 13°, or 80mm. Which generates a maximum torsion bar stress of about 600 Mpa.

The design is a result of multiple design revisions to ensure that the design criteria were met. These criteria concerned the stiffness of the rig frame, user friendliness, and the practicality of constructing the rig in the IPM workshop. FEA was performed in Siemens NX to ensure the stiffness of the rig frame . The simulation revealed that the rig frame can be considered to be totally rigid [2]. - Which is essential to be able to assume when performing physical tests and analytical calculations. Detailed simulation of the suspension system was not performed in the project thesis, as this is a part of this Master thesis.

The rig was built in the IPM workshop, in the course of six weeks, by the candidate. The only outsourced construction work, was the machining of the torsion bar. Unfortunately, the finished diameter of the slender section proved to be 1% larger than designed. This results in a 4% stiffer torsion bar than intended.

Detailed information of computations, materials, and component geometry will be presented in relevant sections throughout this thesis.

Remark:The project thesis is found in Appendix G.

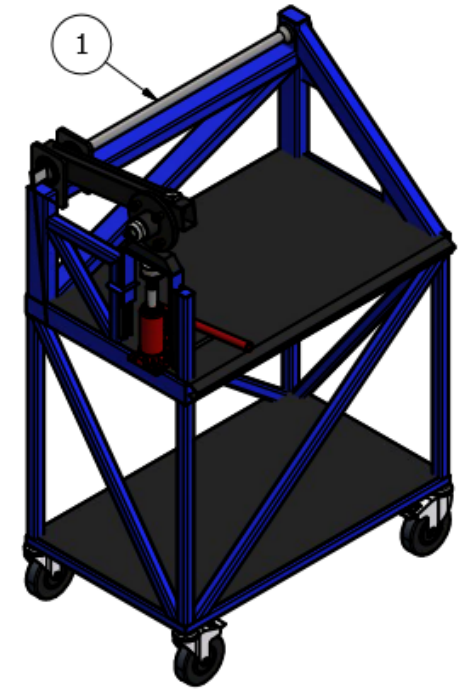

PARTS LIST		
ITEM	PART	DESCRIPTION
1	Torsion Bar	Stainless S165M
2	Torsion Arm	Steel S355
3	Hydraulic Jack	2 Ton
4	Lift Plate	
5	Wheel Hub	
6	Wheel Spacer	
7	Frame	Steel S355
8	Bearings	10 kN/pcs
9	Slider	

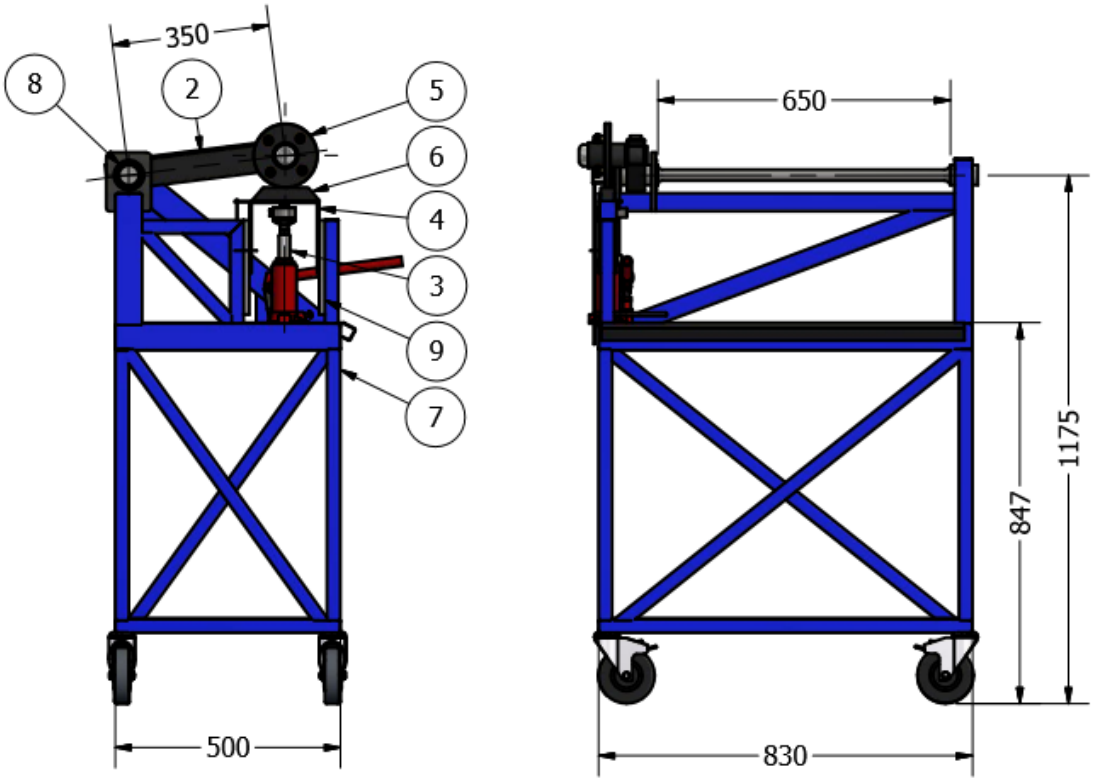

Figure 2.2: Technical Drawing of the Built Rig

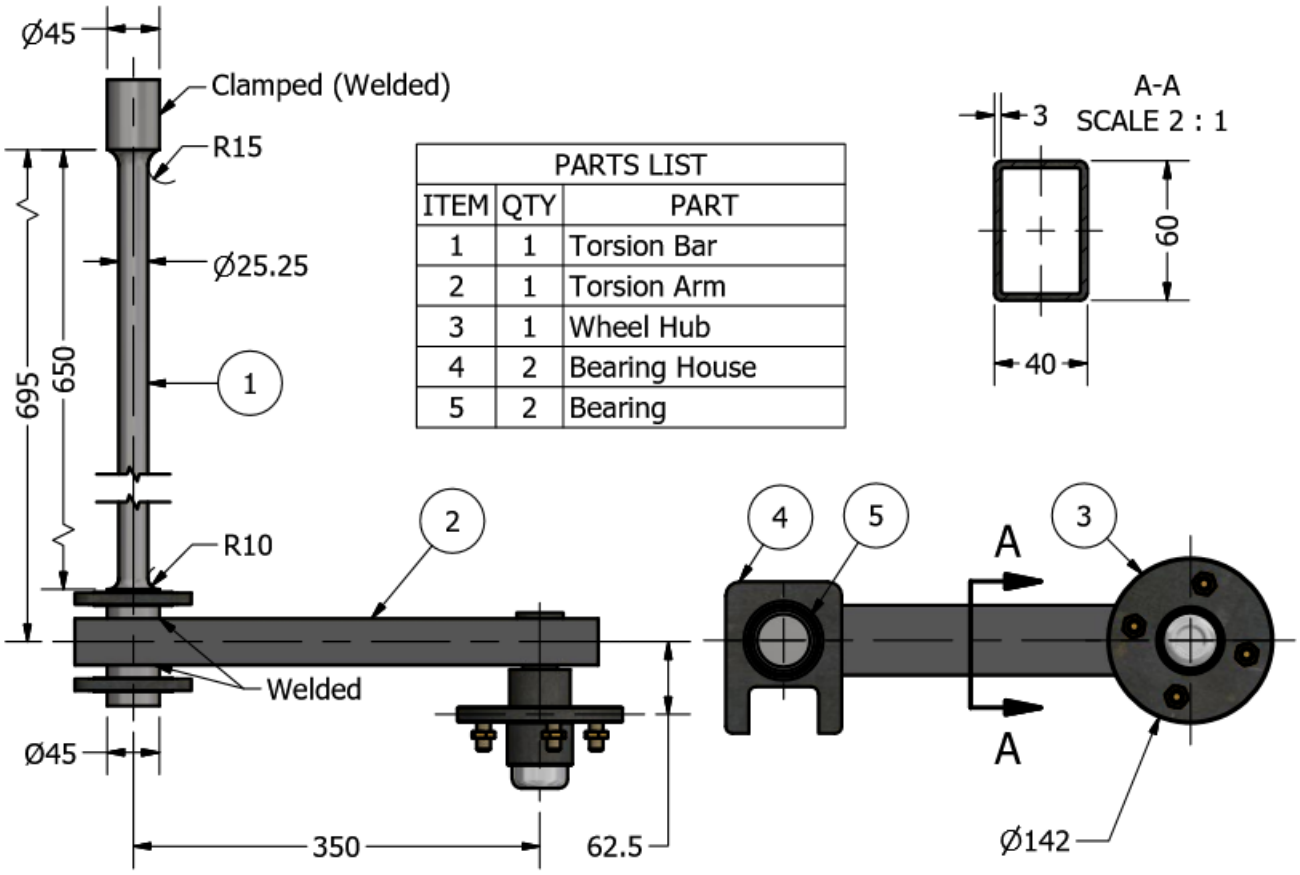

Figure 2.3: Technical Drawing of the Suspension System, Built Rig

Static Calculation Model from the Exam

The Machine Elements Exams include a variety of different exercises to analyze the quasi-static and dynamic response and limitations of the system. The primary focus in the exams and this thesis is the quasi-static response of the suspension system. To provide an introduction, the essence of the static calculation model from the exams is presented below. This calculation model a starting basis of this master thesis. The purpose of the calculations is to relate the elevation height of the wheel hub, Eq. 2.6, and the stresses in the torsion bar, Eq. 2.8, to the applied force. The dimensioning criteria is mainly the maximum allowed stress, which is a result of pure torsion. To ease the calculations, a number of assumptions are given. These include the assumptions of; Infinite stiff support bearings, Simplified geometry, and small angular displacement. It is also calculated with both infinite- and non-infinite stiff torsion arm. The small angular displacement assumption results in a system response equal to constant applied torque, which becomes imprecise at large torsion angles [3]. This is due to that the vertical applied load, generates less torque at large angles. The calculations are based on basic theory which is found in the student formula tables [4]. Algebraic calculation are displayed on the next page. Numeric values will be presented in Chapter 6, Analytical Static Response.

Table 2.1: Constant Declaration

ϕ	torsion angle
α	torsion arm angle
T	applied torque
F	applied force
L	length of torsion bar
D	diameter of torsion bar
R	radius of torsion bar
l	length of torsion arm
b	width of torsion arm
h	height of torsion arm
t	wall thickness of torsion arm
I_p	polar moment, torsion bar = J_T
E	elastic modulus
G	shear modulus
h_ϕ	vertical height, no beam deflection
$h_{\phi+}$	vertical beam deflection, basic theory
H_ϕ	total vertical height, with beam deflection
τ_{xy}	shear stress, torsion bar
σ_{max}	maximum stress, Von Mises

Torsion constant, Torsion bar:

$$J_T = \frac{\pi D^4}{32} \tag{2.1}$$

Second moment of area, arm:

$$I_x = \frac{bh^3}{12} - \frac{(b-2t)(h-2t)^3}{12} \tag{2.2}$$

Torsion Angle:

$$\underline{\underline{\phi = \frac{T \cdot L}{J_T G} \Rightarrow \frac{Fl \cdot L}{J_T G}}} \tag{2.3}$$

Height, no beam deflection:

$$h_\phi = l \cdot sin\phi \tag{2.4}$$

Height from beam deflection:

$$h_{\phi+} = u_{max} = \frac{F \cdot l^3}{3EI_x} \tag{2.5}$$

Total height:

$$\underline{\underline{H_\phi = h_\phi + h_{\phi+}}} \tag{2.6}$$

Principal stress:

$$\tau_{xy} = \frac{T \cdot R}{I_{p,bar}} \Rightarrow \frac{Fl}{J_T} \cdot \frac{D}{2} \tag{2.7}$$

Von Mises stress, Torsion Bar:

$$\underline{\underline{\sigma_{max} = \sqrt{3} \cdot \tau_{xy}}} \tag{2.8}$$

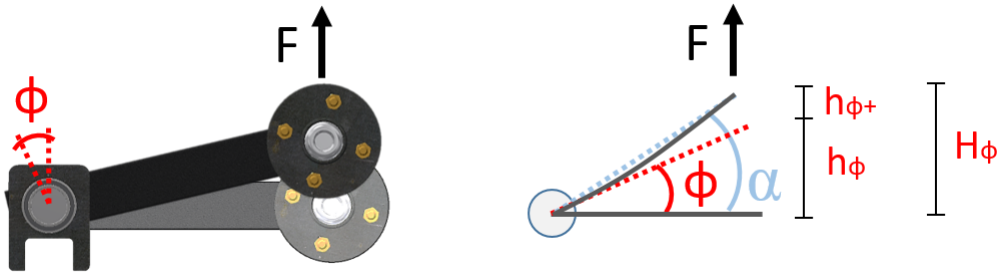

Figure 2.4: Visual Illustration of Angles and Height Constants, Exam Model

Chapter 3

Key Performance Indicators

The suspension rigs objective is to reveal any differences between analytical calculation models, virtual simulation, and the physical reality. To quantify the differences, Key Performance Indicators (KPIs) are needed. In this chapter, both static and dynamical KPIs are to be defined.

3.1 Quasi Static Key Performance Indicators

To define the static KPIs, the exams was used as a reference. The exercises revolves around the corresponding response values to a given applied load. Most importantly; the vertical elevation of the hub, and the Von Mises stress. Those response values may be regarded as the KIPs in the exams. Table 3.1 displays the system response from the exam, given two different force values; 1000 and 2940 Newtons (Original exam dimensions). 1000N is just a random even value, whilst 2940N relates to the dimensioning maximum allowed stress in the exams.

Table 3.1: Exam KPIs and Related Values

Applied Force	Elevation of the Hub	Von Mises, Torsion Bar
1000N	26.2 mm	198 Mpa
2940N	76.4 mm	581 Mpa (max. allowed)

As these exam KPIs describes the main characteristics of the system response, they are also assessed as the main KPIs considering the rig. And they will form the basis of the parameters to evaluate in the physical testing, calculation and simulations. The assumptions given in the exams allows for using basic formulas without transient expressions. This results is that the exam model KPIs are linear dependant. The only factor which is not directly linear is the height $[h = l \cdot sin(\theta)]$, but the angular change is so small, that it can be considered to be linear.

Considering the physical rig, it was suspected that some of the theoretical assumptions was incomplete. And that the system will not behave directly linear. To evaluate this, the rig needs to be equipped with sensors that independently monitor each KPI. Decoupling the KPIs also allows for detecting deviations and possible errors in the monitor system. In addition to the the mentioned KPIs in Table 3.1, other KPIs should be incorporated. This includes the torsion angle, θ, torsion arm angle, α, and the principal stress in the torsion bar. And considering the large stresses the torsion bar, failure due to fatigue, may occur. To evaluate this, the life expectancy of the physical rig is also incorporated as a KPI. All the quasi-static KPIs to include are listed in Table 3.3. These acts as the benchmarks for the physical tests, virtual simulation, and analytical computation. But it the main KPIs are those which will be focused on. No specific numeric values was selected at this point. Instead, a comparison of the different tests and calculation results are assessed in the full capacity range of the rig, 0 - 3200N. As the physical rig is designed to surpass the maximum capacity in the exam's-theory by 9%, also allows for extrapolating the theory.

Table 3.2: Selected Static KPIs

#	**Main Static Key Performance Indicators**
1.	Force, (vertically applied)
2.	Vertical elevation of the wheel hub
3.	Von Mises stress, Torsion bar
#	**Additional Static Key Performance Indicators**
4.	Principal stress, Torsion bar
5.	Torsion angle, (θ)
6.	Torsion arm angle, (α)
7.	Fatigue (Life expectancy)

3.2 Dynamical Key Performance Indicator

The rig is primarily constructed to test the quasi-static response. Nevertheless, it desirable to be able to perform simple dynamic analyzes. One of the exam exercises concerns calculating the natural frequency and the required damping factor of the suspension system. Due to the focus on static response, the rig is not designed to include a damper. Hence, it is to identify the natural frequency which is the only desired dynamic KPI.

Table 3.3: Selected Dynamic KPIs

#	**Dynamic Key Performance Indicator**
8.	Undamped Natural Frequency

Chapter 4

Instrumentation of the rig

This chapter describes the work performed to instrument the rig. This includes the selection of equipment, and the installation of the sensors. The process of constructing an electronics bay to house the wiring and equipment, is also described. This work finalized the building process of the rig, and made it ready for testing.

Prior to this project, the author of this thesis had limited knowledge concerning electronic sensoring and data collection. As the incorporation of sensors and equipment is an essential part of the rig, it was important to facilitate the sensor incorporation from the beginning of the project. Therefore, a brief introduction of available equipment and possibilities was given by IPM Staff Engineer Halvard Støwer. Støwer gave great guidelines, but did not select the types of components to include, leaving an opportunity to make mistakes.

The initial concept from the project thesis was to be able to easily remove all the electronic equipment from the rig, when not in use. Which leaves the possibility for other students to use the equipment. But due to great feedback on the finished built rig, it was decided to make all the equipment permanent. This made it possible to incorporate the sensors and equipment in a more esthetic manner. And it saves a preparation time before using the rig due to re-installation of the equipment, and the calibration of sensors.

4.1 Sensors and Equipment

Based on the KPIs, equipment and sensors were selected to capture the dynamic and static response. An overview of the selected equipment is presented in this section.

Figure 4.1: HBM QuantumX DAQ

Figure 4.2: Computer & Catman Software

Data Collector

To collect the sensor data, a 8-channel HBM QuantumX DAQ was chosen. This is a universal Data Acquisition amplifier (DAQ) which allows for using a variety of different passive and active sensors, and connect it to a computer. The only limitation of this DAQ is the number of sensors. Otherwise it is was a perfect basis for a monitoring system. The DAQ is seen in figure 4.1

Computer and Software

A computer with Catman AP software is to be permanent on the rig. The Catman AP is a Data Acquisition & Analysis Software, which is used to process the measurement data from the DAQ. The software is intuitive to use, and makes it easy to analyze and visualise the measurements. Catman also allows for exporting data to other software as Excel or Matlab if desired. Figure 4.2

Load Cell

To capture the force (KPI #1), a load cell was chosen. The selected component is named HBM U2a load cell. It is a good quality load cell with a maximum capacity of 500kg, giving a 50% capacity headroom. It is captures the vertical applied force from the hydraulic jack. The load cell is displayed in figure 4.3

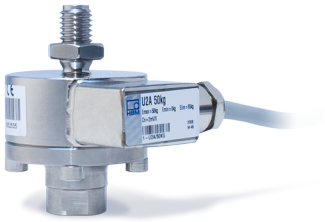

Figure 4.3: HBM U2a Load Cell

Figure 4.4: HBM WA100 Displacement

Figure 4.5: Kelag KAS903 Accelerometer

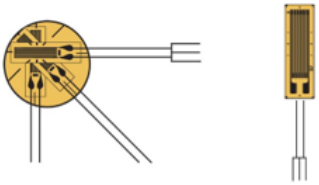

Figure 4.6: Stain Gauges

Displacement sensor

The vertical elevation of the wheel hub (KPI #2) is monitored by a displacement sensor . The HBM WA100 Displacement Sensor is an passive inductive sensor, with a 100mm stroke-length. This produces a continuous step-less reading, and should produce high accuracy results. The displacement sensor is also used to capture the torsion arm angle (KPI #6), based on trigonometry. Figure 4.4

Accelerometer / Torsion Angle

To capture the dynamic response of the rig, it was chosen to use an accelerometer. The Kelag KAS903 Accelerometer, is able to capture two axis, but only the vertical axis is to to be connected. In addition to capture the frequency, the accelerometer is used to collect the torsional angle (KPI #5). It is an active sensor which requires an additional power source. Figure 4.5

Stain gauges

Strain gauges are utilized to compute stresses in the torsion bar (KPI #3/4). Five strain gauges are connected to the DAQ. These are attached to the torsion bar at different angles and locations. This is to determine effect of the installation-direction of the stain gauges. Figure 4.6

4.2 Installing Sensors

This section describes the installation of the different sensors on the rig.

Load cell

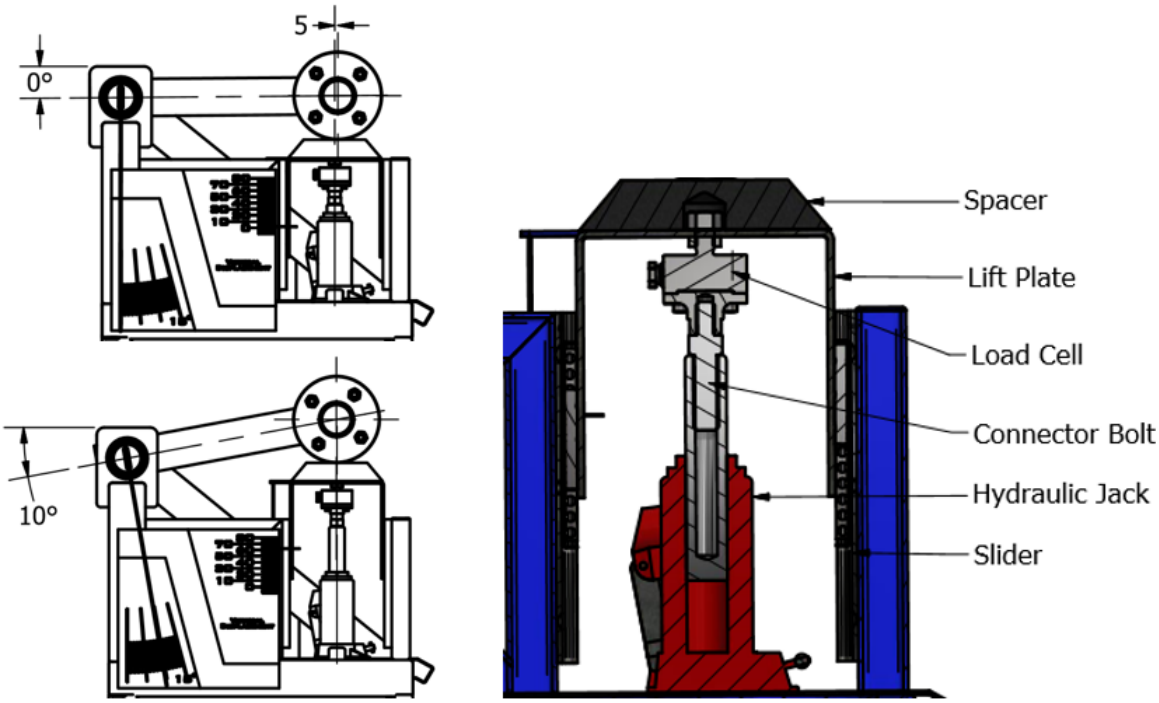

Figure 4.7: Load Cell Assembled on the Rig

The load cell is mounted directly above, and in-line with the hydraulic jack, by a custom M16 - M12 connector bolt. This causes the load cell to be subjected to the full vertical force from the jack. See figure 4.7. A supporting structure, in terms of a Lift plate mounted to four linear sliders, has multiple functions. The primary function of the support structure, is to reduces any play in the top of the hydraulic jack/load cell system. The jack base is bolted to the frame, but there is some play in the piston cylinder which the supporting structure eliminates. As the wheel hub elevates, it has horizontal travel distance of approx. 8 mm from 0 to 12 degrees of elevation. A spacer is placed on top of the lift plate to act as a smooth surface to allow the wheel hub roll across. The spacer is easily removed, leaving a 40mm gap between the hub and lift plate. This is done when performing dynamical testing, leaving the hub to move freely. To ensure that the load cell is subjected to minimal moment forces, the lift system is mounted in a manner so the wheel hub and jack becomes vertical in-line as the force increase. The lift plate also acts as attachment-point for the displacement sensor.

Displacement sensor

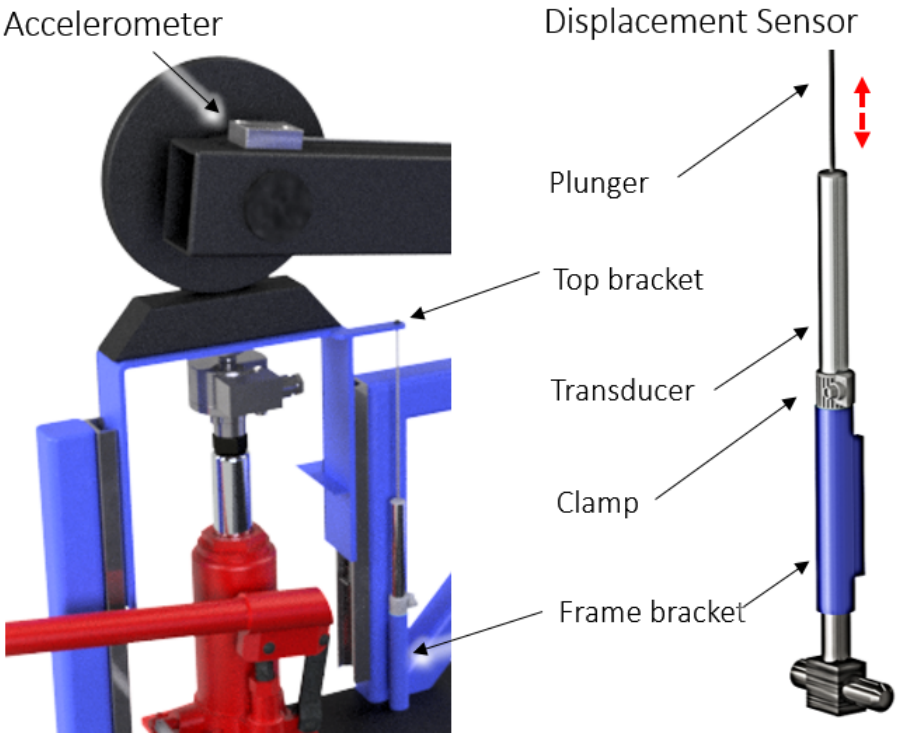

Figure 4.8: Displacement Sensor and Accelerometer Placement

The linear displacement sensor it mounted to capture the vertical elevation of the wheel hub. The sensor consists of two parts, see figure 4.8. A transducer, and a slender plunger which travels freely trough the transducer. A tube-bracket is welded to the rig frame to house the transducer. A clamp makes it easy to adjust the height, or to remove the transducer. The plunger is connected to a top bracket attached to the lift plate. This enables the sensor to read the vertical displacement of the wheel hub as lift-plate elevates.

Accelerometer

The accelerometer is mounted on top of the torsion arm, and attached by two bolts. See figure 4.8. The sensor is situated directly above the wheel hub axle 350mm from the torsion bar centre. This enables it to capture the oscillation frequency. At this location, the accelerometer is able to capture the torsion angle or torsion arm angle dependant on the calibration.

Stain gauges

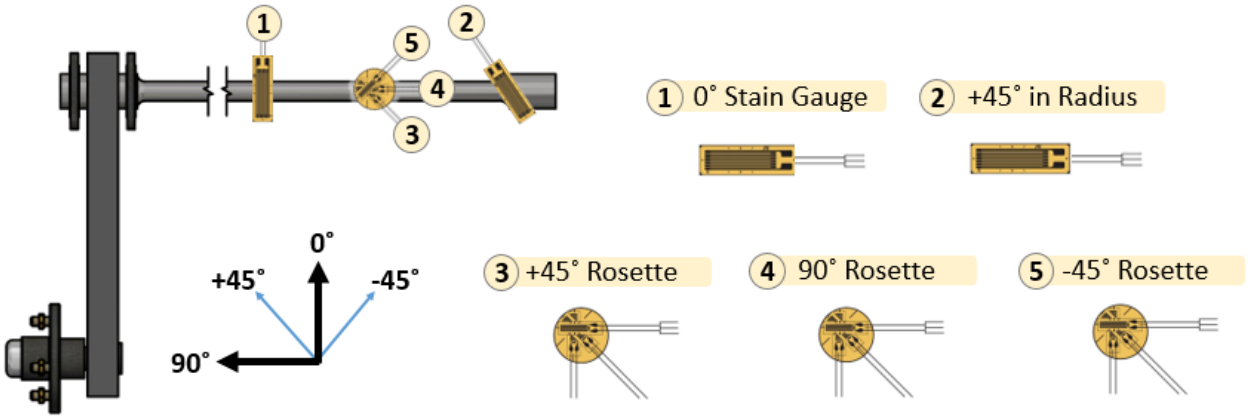

Figure 4.9: Stain Gauge Direction and Placement

Five channels of strain gauges (SG) has been attached to the torsion bar. These are mounted in four different directions to capture strains. Figure 4.9 displays the strain gauge placements and angles. Theoretically, if the rig is considered as an ideal system with pure torsion without any bending moments, principal strains are found ±45 degrees along the torsion bar. At 0° and 90°, positive and negative strains cancels, generating zero readable strains, despite large internal stresses.

As the rig is created for educational purposes, SG number (1) has been installed transverse to the torsion bar at 0°. This it to be able to show that there is no readable strain transverse to the axle. SG number (2), is a placed in the R15 radius at +45°, at a larger diameter of ≈ Ø30mm. This is to be able to capture the effect of enhanced diameter on the stain.

SG number (3), (4) and (5) are channels on a tri-axial "rosette" stain gauge. The rosette is positioned in the correct procedure to evaluate torsion [5]. The rosette captures the maximum tension- and compressive- principle stains at ±45°, and strains long the torsion bar at 90°. The rosette is placed 40 mm away from the radius to avoid the stress concentration. The advantage of a tri-axial SG is that it allows for computing corrected maximum principle strains, if the assumption of pure torsion is incorrect. This is used to calculate principal and Von Mises stresses, (KPI #3/4).

To attach the strain gauges, the surface was first prepared with a fin grained sandpaper, before cleaning with isopropanol. Superglue was then used to instantly secure the stain gauge.

Visual Indicators

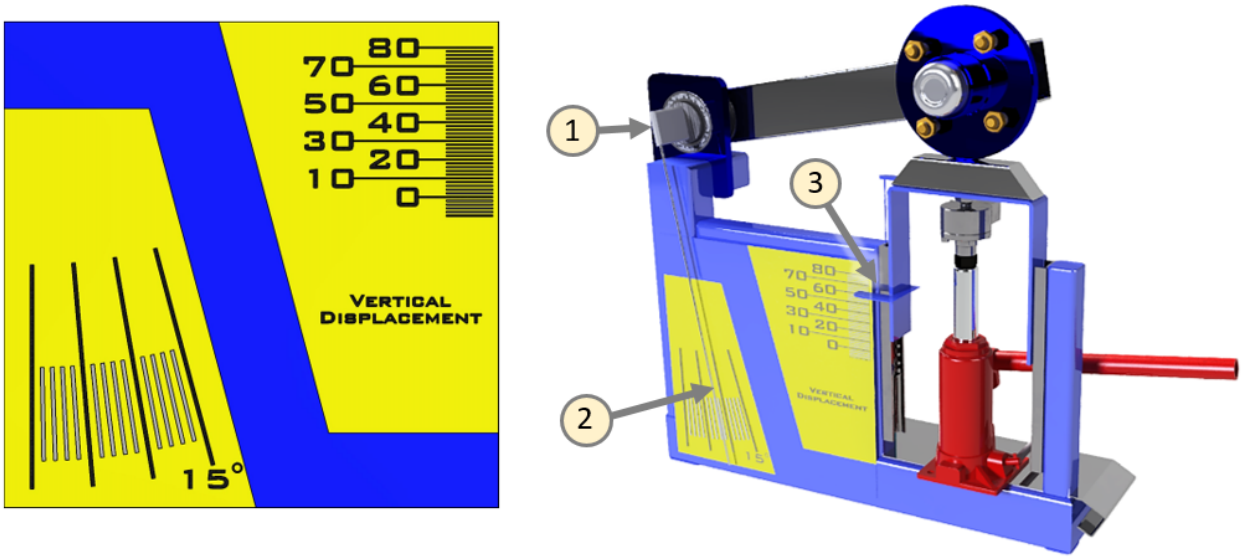

Figure 4.10: Visual Torsion Angle and Displacement Indicators, CAD illustration

In addition to the electronic instruments, visual indicators for vertical displacement and torsion angle was created. See figure 4.10. The purpose of this is to make it easy for an audience to observe the physical changes when utilizing the rig in lectures. Large text font and the layout makes is possible to observe the changes from about 10 meters. (1) The torsion angle is indicated by a 380mm arm attached to the torsion bar. (2) Clear lines makes it easy to observe the angular change. Range: 0 to 15 degrees. (3) A bracket attached to the lift plate indicates the vertical elevation. Range: -10 to +80 mm.

The indicator panel was generated in CAD, and printed as a picture. The picture was then laminated to ensure good durability and finish. The indicator panel is attached to the rig with double-sided tape.

4.3 Electronics Bay

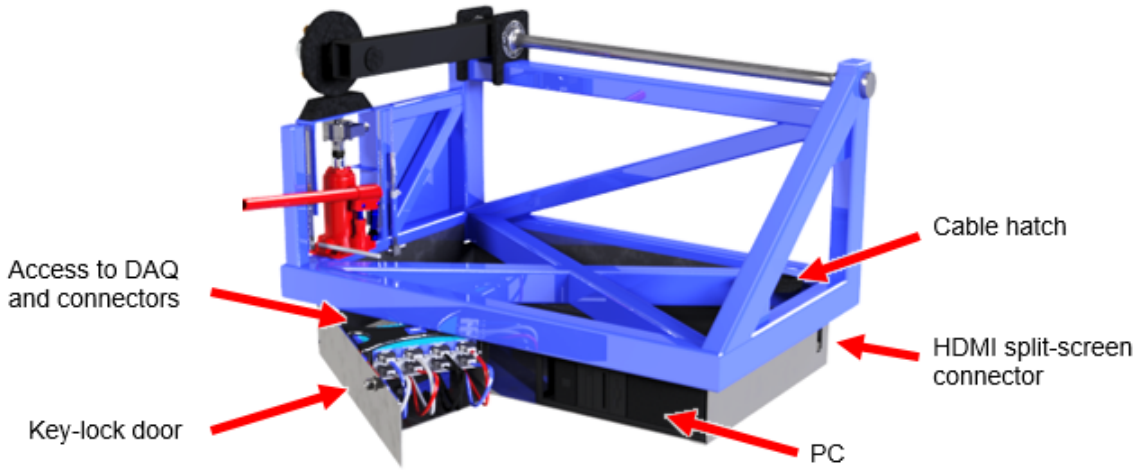

Figure 4.11: Electronics Bay

As the electronic components are to remain permanent on the rig, it was decided to create an enclosed electronics bay on the rig. This is a locker underneath the table top that houses all the electronic components, including the PC and HBM DAQ. In addition to hide most of the wiring, the electronics bay has a key-lock, which prevents unwanted "borrowing" of equipment. See Fig. 4.11

Construction

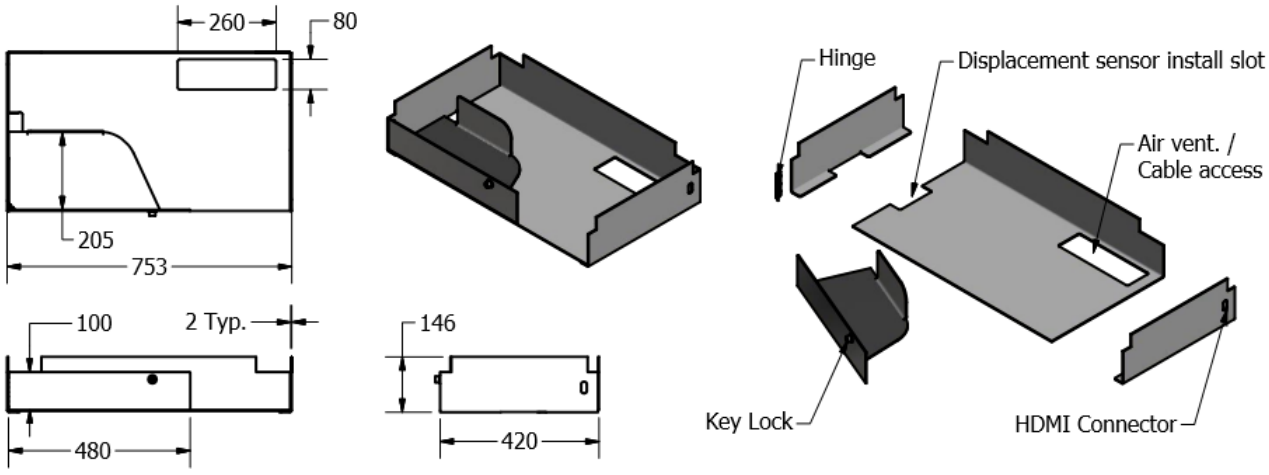

Figure 4.12: Bottom/Back Section of the Electronics Bay

The electronics bay consists of four main components; A bottom/back panel, two side panels, and front door. See figure 4.12. The components are made of 2mm stainless steel sheet-metal. The sheet metal was first trimmed to size, and features cut out, before using a plate bending machine, to create the angels on the panels. Ideally the side- and bottom- panels could be one single panel, but due to the crossbeams in the rig frame, it would have been impossible to install. In which led to that the panel had to be designed in three parts, plus the front door. The door is designed to house the HBM DAQ and stain gauge connectors. The door acts as a carousel shelf bringing the DAQ and connectors out of the electronics bay. This gives easy access to switch cables and connectors if desired. When built, the angle between flat- and front- section of the door was bent to about 85°, not 90°. This is to compensate for the weight of the components it holds, deflecting the flat section. This makes the door easy to open without the door substantially rubbing against the bottom panel. Hinges connects the door to the left panel. On the right side panel there is a cutout to install a HDMI split-screen connector. This makes it easy to connect a projector to the rig when lecturing. The bottom panel has a 260x80mm cutout behind where the computer is to be situated. This acts as an air vent, and enables cable access to the computer. A Ø70mm cable hatch for keyboard and monitor cables is situated in the table top directly above the cutout. This also acts as an inspection hatch from above if (dis)connecting of computer cables are desired. The left- and bottom- panel have cutouts to be able to install the displacement sensor. When the door is locked, this cutout is blocked by the door.

The panels were attached to the rig frame by pre-drilling holes though the panel and frame, before using self-tapping bolts. The side- and bottom- panels are bolted together with bolts and nuts. Figure 4.13 displays the assembly procedure of the electronics bay. (1) The bottom panel was clamped in place. (2) The side panels were clamped, and the panels bolted to the frame. (3) The hinges and door was installed.(4) Electronic components and sensors inserted. Wiring of the system performed. (5) Inserting the tabletop. (6) Installing hydraulic jack, and connect computer monitor, keyboard and mouse.

The initial plan was to paint the bay black. But during construction it was chosen to keep the stainless steel finish, as it gives the rig an extra mechanical expression.

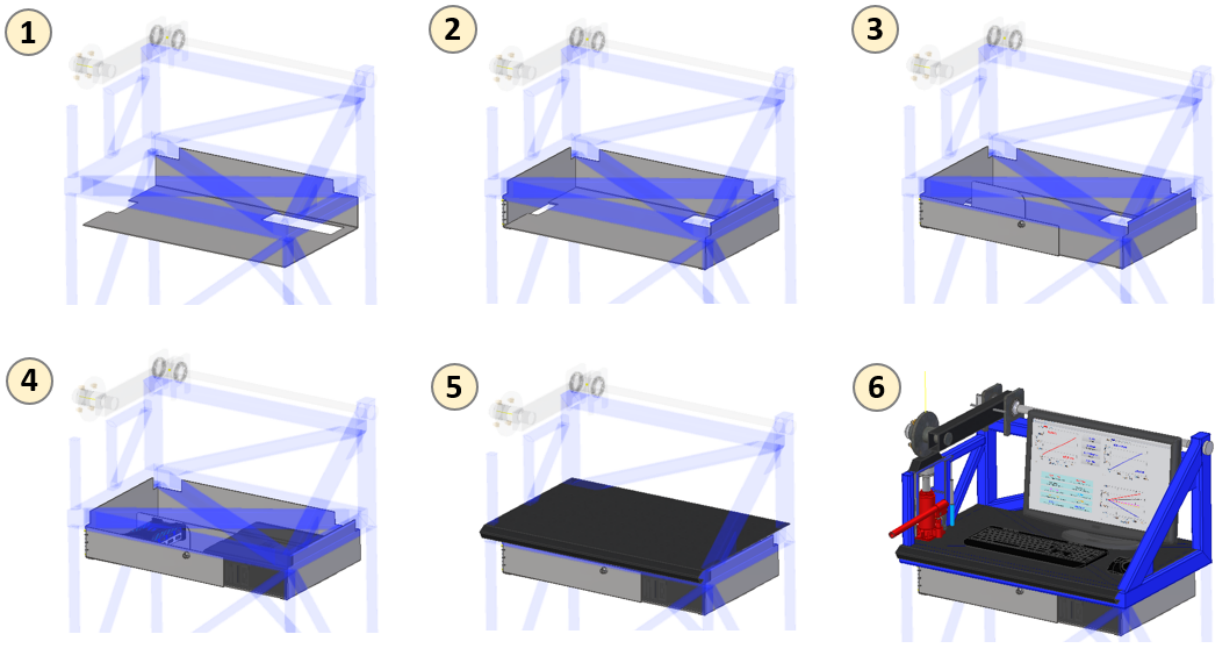

Figure 4.13: Assembly Order of the Electronics Bay

4.4 Wiring

The electronic system consists of dozens of cables. Every single strain gauge is linked by four stages of wires before the signal reaches the HBM DAQ. Keeping track of the wiring harness is therefore crucial. To make it easier to distinguish the different sensor channels, each channel has a designated color code on all its wires, from the source to the DAQ. Figure 4.14 displays the different channels with corresponding color code and DAQ input channel. Channel 1 - 3 are connected to the Load Cell, Displacement sensor, and the vertical direction of the accelerometer. Channel 4 - 8 are stain gauge inputs. The color codes are the vertical colored lines to the left of each sensor. A modified version of Figure 4.14 is set at the background image on the rig computer. Is is also found in Appendix B. This is to give students and future rig operators an easy overview of the system wiring. The left picture in figure 4.15 displays five connector boxes attached to the inside of the electronics bay door. This is where the strain gauges are connected. If it is desired to switch or connect other stain gauges, these are to be reconnected here. The right picture displays the finished wired door including the DAQ. Inside the electronics bay, cables have been orderly put in place by using cable warps and trunks. All the power cables are internally connected to a power cord extender, which makes it necessary to only connect a single power cord to run the rig.

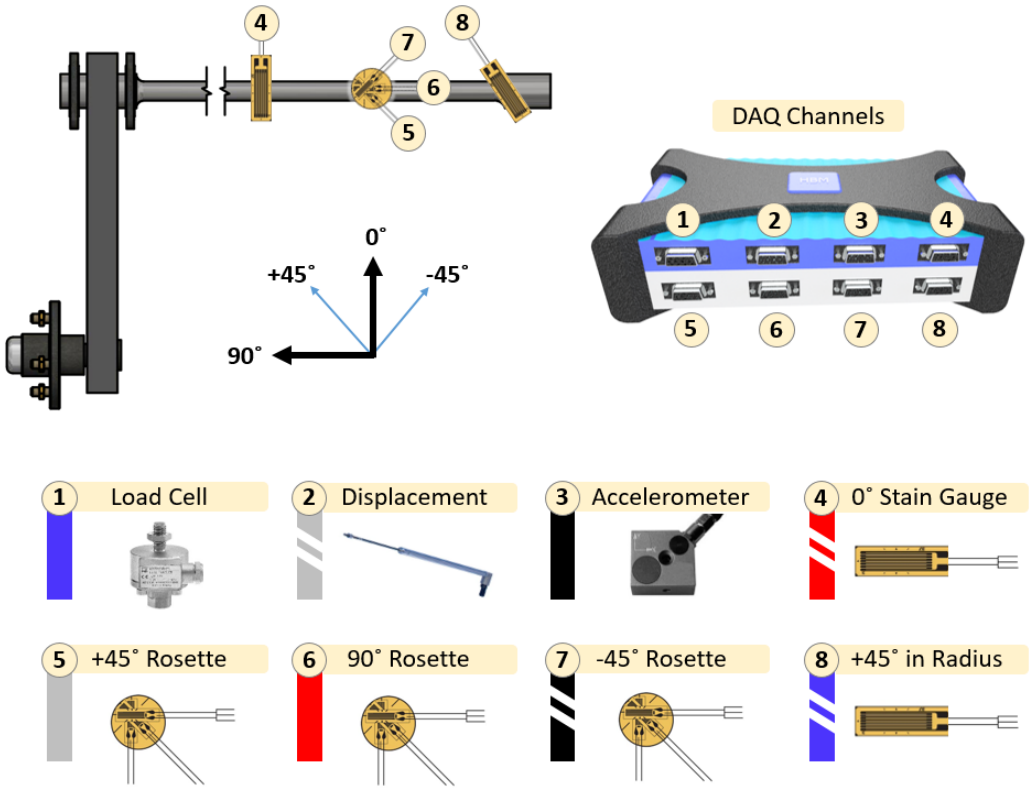

Figure 4.14: DAQ Channels with Corresponding Sensors and Color Code

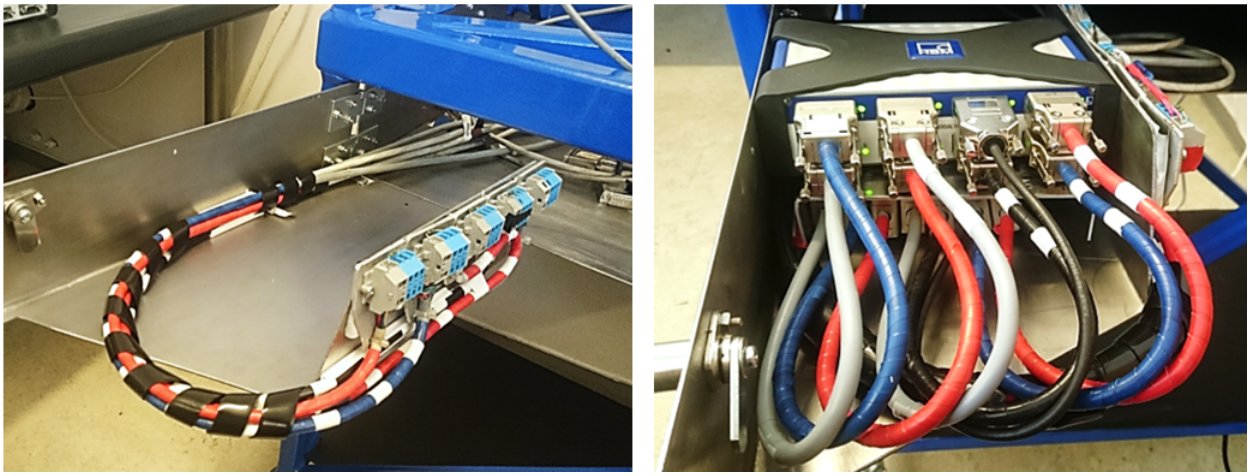

Figure 4.15: Wiring and Connectors inside the Electronics Bay Door

4.5 Finished Rig

Figure 4.16: CAD of Finished Rig

The finished rig is a result of seven months of work, including the project thesis. The ambition to design, build and equip the rig, has pleasingly been realized during the project and this master thesis. Both the mechanical and electrical features behaves as intended. The only slightly displeasing feature is the torsion bar. The diameter is machined 1% larger than intended, which yields a 4% stiffer structure than intended. Subjectively speaking, the rig looks as great at planned. Photographs of the finished rig are seen in Fig. 4.17-4.18. With a user-friendly layout, it is easy and comfortable to operate both while standing or sitting. To highlight some features based on feedback, the analog angle- and height- indicator makes the intention of the rig more visual intuitive. The electronics bay which gives access to all the electronic connections, works great. The most pleasing feature is the fact that it is a stand alone instrument. A single power cord is connected, and it works and runs. This eliminates the a lot of potential technical issues. And if the rig is used in lectures, it is simple to run split-screen to a projector with the HDMI connector.

Figure 4.17: Photo of Finished Rig, Front/Right

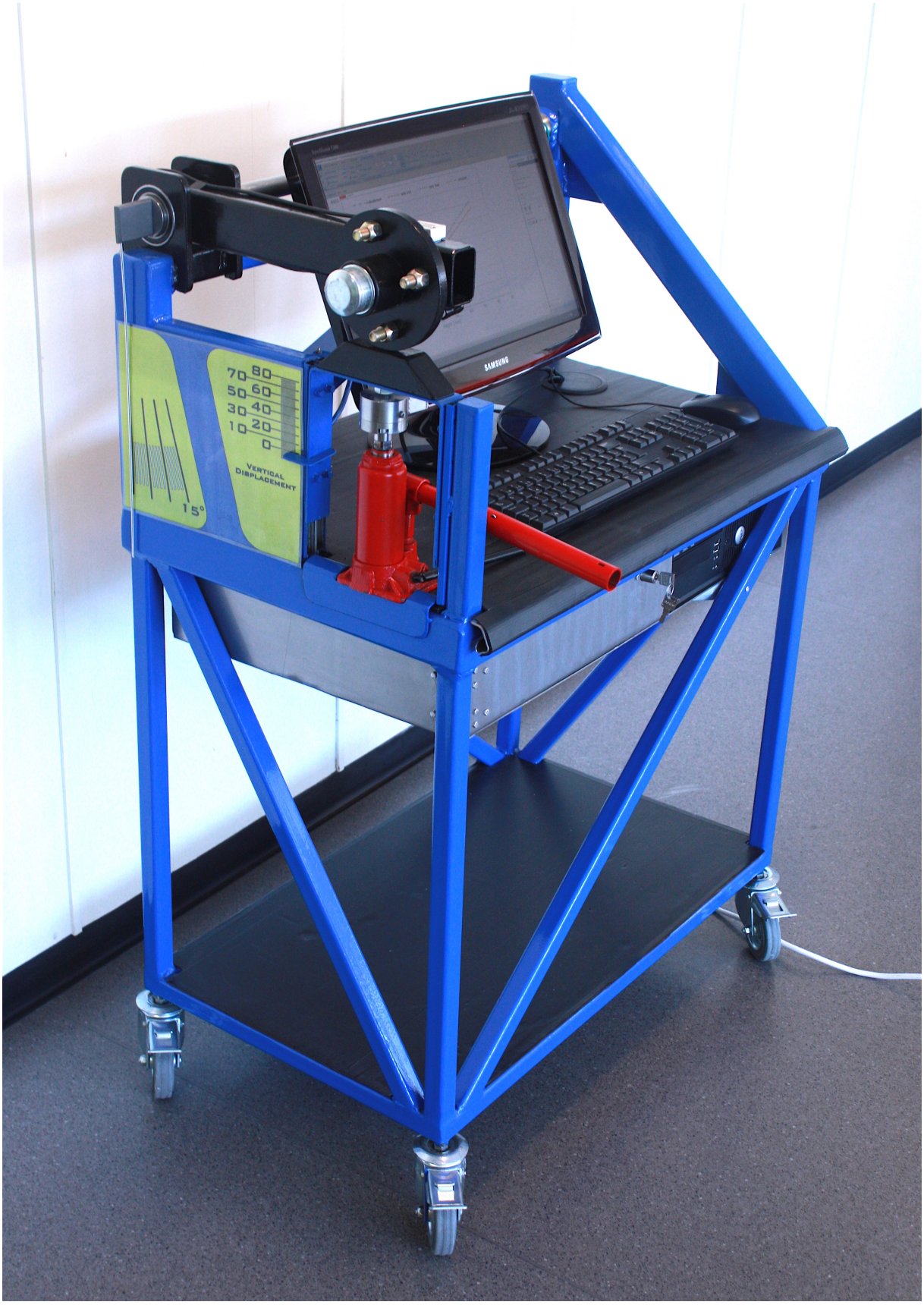

Figure 4.18: Photo of Finished Rig, Front/Left

Chapter 5

Physical Quasistatic Testing

This chapter describes the physical testing process of the rig. This includes the calibration of the sensors, test procedure, and presentation of the results. This Chapter only concerns the quasi static testing of the rig. The dynamic testing is included in Chapter 8, Dynamic response.

5.1 Calibration

Load Cell

The load cell itself does not need calibration, as it is an enclosed sensor. And Catman automatically adjusts the software calibration based on an embedded database. When testing the load cell the first time, there was obviously something wrong. Elevating the wheel hub produced a load-reading that was only a third of what to expect. A different load cell was then tested with the same result, eliminating component error. After troubleshooting, the error proved to be slightly incorrect installation of the load cell. The issue occurred because the lift plate was situated directly on-top of the flat section of the load cell. This was solved by adding a nut underneath the lift plate, which directs the force through the threaded top stem of the load cell.

Stain gauges

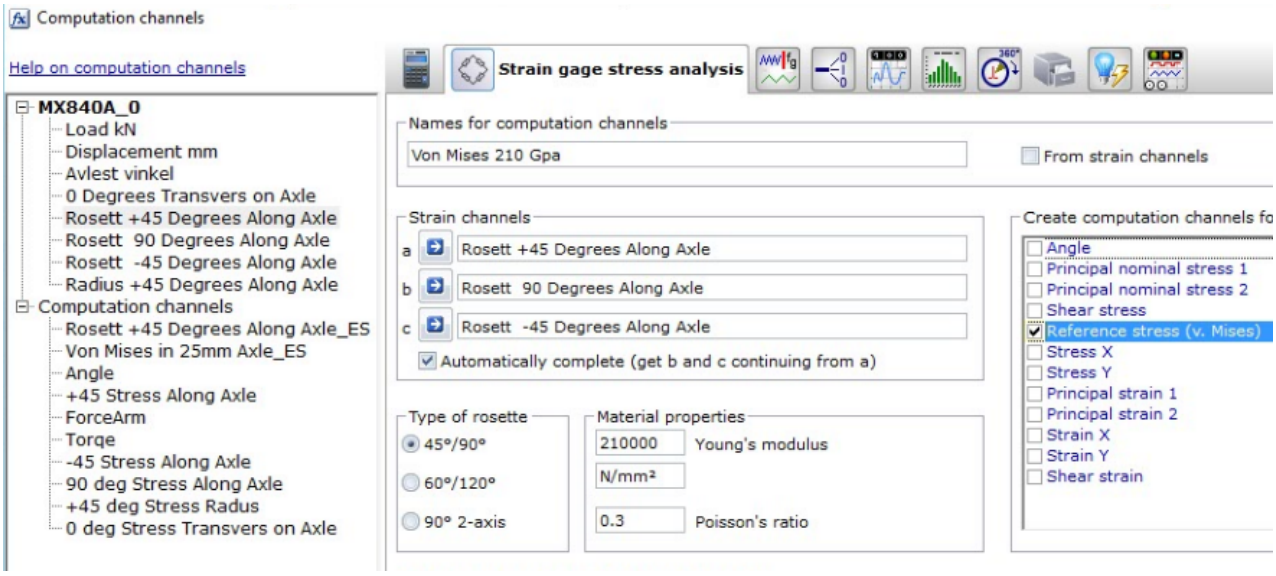

Figure 5.1: Strain Gauge Setup in Catman

A stain gauge (SG) comes in many variations with different properties and configurations. The configuration used on the rig is called a quarter-bridge with 120Ω SGs. This is when only one active stain gauge is used on each channel. Other configurations as a half-bridge and full-bridge, with respectively 2 and 4 active stain gauges, may be used to increase the strain-sensitivity. The strain gauge configuration needs to be accounted for in the Catman software. This is done by selecting a bridge factor. As the rigs strain gauges are a in a quarter-brige configuration, the bridge factor is 1. An other important factor is what is called a Gauge factor (GF). The Gauge Factor of a strain gauge is the ratio of relative change in electrical resistance R, to the mechanical strain ϵ. This factor is varies with the type of strain gauges used. This Gauge Factor is found on the data sheet for each strain gauge. For the rosette strain gauge, this factor is 2.11, whilst it is 2.12 for the two other SGs. When these two factors are added in the Catman software, the program is able to measure the correct strains. To convert the strain to stress, material properties was selected. The advantage of using the rosette stain gauge is that Catman can automatically compute results such as the Principal- and Von Mises stress. To enable this feature, a strain gauge stress analysis was configured in Catman. See Fig. 5.1. Here the included SGs are added, and desired stress computation outputs are selected. Principal and Von Mises output was selected at this point.

Displacement sensor

Figure 5.2: Calibration of Displacement Sensor

Calibrating the displacement sensor was the most comprehensive. Initially it was calibrated with a two-point linear calibration. This is done by selecting the two point end-points (0 and 80mm) , and correlate the electric values to physical values in Catman. This first calibration resulted in a poor and inaccurate readout. Compared to the analog displacement indicator, the readout displayed a variable drift up to 2mm. In addition, there was an unphysical inclining gradient in the readout the first 10mm of the elevation. This gradient proved to be incorrect installation. The issue occurred because plunger passed though the bottom of the transducer, creating an unlinear magnetic field. This was solved by lowering the transducer 15mm. Due to this, the readout still drifted. The cause of this is probably the physical sensor itself. It is old and heavily used, and the plunger is not 100% straight. To compensate for this, it was necessary to perform a multi point interpolation calibration. The calibration was performed by attaching a digital caliper to the rig, and correlate the electrical values, and physical reading from the caliper in Catman. This was done for every 10mm, from 0 to 80 mm elevation. This procedure was performed multiple times to ensure the quality of the calibration. The final calibration is displayed in Figure 5.2. The calibration has a 3% linear deviation at 60mm elevation.

5.2 Test Procedure

Table 5.1: Test Procedure Data

Height calibration		**Test data**	
Calibration date	16. May 2016	Date	16. May 2016
Calibration mode	Multi point interpolation	Sample rate	50 Hz
Max. Calibration deviation	3 %	Test duration	75 - 130 sec.
		Number of tests	4
		Preloading	46 N
		Force Range	0 - 3200 N

The quasi-statical testing was preformed May 16. 2016, the same day as the displacement sensor was calibrated. Due to the weight of the torsion arm and wheel hub, the torsion bar gets negatively prestressed by a magnitude of 46 Newtons. Which equals the weight of the wheel hub and half the torsion arm. This prestressing needs to be compensated for prior to testing. This is done by preloading the wheel hub with 46N before zeroing all sensor channels, prior to every test. The force range of the test was 0-3200N. This allows for extrapolating the exam theory with 9To compare the different tests later on, the applied force was chosen to be used as benchmark, with sample points every 200 N. The purpose of this, was to focus on collecting accurate data from these sample points, by running the test slower at these sections. The data sample rate was set to 50Hz. Test duration time varied between 75 and 130 seconds. The Catman software was set to save test data to Microsoft Excel format.

5.3 Physical test results

Four tests were preformed to sample the physical quasi-static response of the rig. Figure 5.3 displays vertical elevation of the wheel hub versus the applied load, sampled every 200 N. The black dotted line is the average of these results. A confidence interval test, between each test and the test average, revealed great consistency in the results. The larges statistical margin of error (CI 95%) between the test average and a single test is 0.0337 mm. See Table 5.2. This implies that the average result from the four tests is good basis for further use, without running more tests.

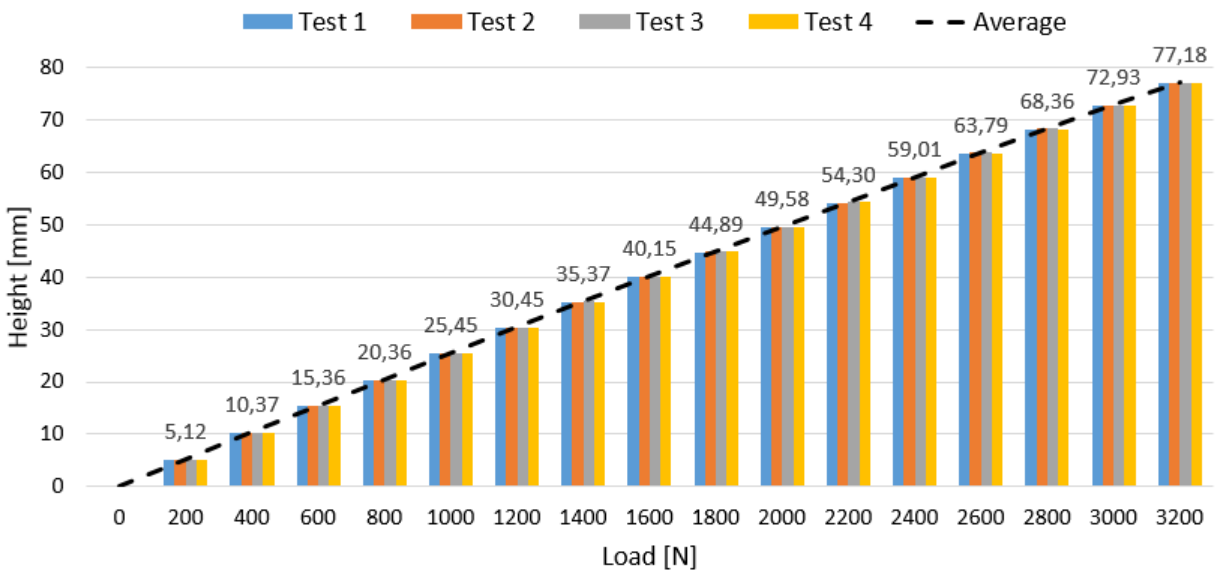

Figure 5.3: Load versus Height from Physical Tests

Table 5.2: Confidence Interval Test Results

Deviation from test average		**Test 1**	**Test 2**	**Test 3**	**Test 4**
Average	[mm]	0.0380	-0.0047	-0.0174	-0.0150
Standard Deviation	[mm]	0.0376	0.0277	0.0218	0.0438
Sample Size, N		17	17	17	17
Confidence Coff. 95%	N <20	3.17	3.17	3.17	3.17
Margin of Error	[mm]	0.0289	0.0213	0.0168	**0.0337**
Upper Bound 95%	[mm]	0.0669	0.0166	-0.0006	0.0187
Lower Bound 95%	[mm]	0.0091	-0.0260	-0.0341	-0.0487

Table 5.3 displays the average numerical values from the tests. This includes the applied load, height of the wheel hub, and the corresponding measured stresses. At 3200N the wheel hub is elevated to 77.18mm, and there is a Von Mises stress of 578.5 Mpa in the torsion bar. A graphical representation of the stresses related to the applied load, is seen in Figure 5.4 . Theoretically, the $+45°$ and $-45°$ stain gauge values should produce equal absolute values. And the $90°$ should read equal to zero stain (and stress). As seen in Table 5.3, this is not the fact in this case. There is $\approx 1.4\%$ deviation between the $\pm 45°$ strain gauges. This is probably caused by a slightly imperfect installation of the rosette, $< 1°$. This small deviation is considered to be acceptable for further use. This phenomenon can be clearly observed on the transverse $0°$ strain gauge. This SG should not produce any readable strain. Nevertheless, it reads strain equivalent to 45.4 Mpa. Some troubleshooting was performed, at it resulted in discovering that strain gauge is visually out of the intended angle of $0°$. But as this stain gauge is exclusively installed for learning purposes only, and does not influence the KPIs. Nothing was therefore done with this issue, and it will instead serve as a perfect troubleshooting assignment in e.g. lectures. The $+45°$ stain gauge in the radius computes a stress which seems to be as expected, generating less stress than the in the slender section.

Table 5.3: Physical Test Results, Average

Load	Height	Von Mises	Stress				
		Rosette	$+45°$	$-45°$	$90°$	$0°$	Radius
[N]	[mm]	[Mpa]	[Mpa]	[Mpa]	[Mpa]	[Mpa]	[Mpa]
0	0	0	0	0	0	0	0
200	5,12	36,7	21,3	-21,6	0,2	2,9	11,8
400	10,37	74,0	42,9	-43,6	0,4	5,8	23,7
600	15,36	111,4	64,5	-65,6	0,7	8,7	35,7
800	20,36	148,5	86,1	-87,4	1,1	11,7	47,7
1000	25,45	185,7	107,6	-109,4	1,1	14,5	59,5
1200	30,45	222,5	128,9	-131,1	1,4	17,4	71,3
1400	35,37	259,3	150,3	-152,8	1,6	20,2	83,0
1600	40,15	295,6	171,4	-174,1	2,0	23,1	94,7
1800	44,89	331,6	192,3	-195,3	2,3	25,9	106,2
2000	49,58	367,7	213,2	-216,6	2,6	28,7	117,8
2200	54,30	403,5	234,0	-237,6	3,0	31,6	129,3
2400	59,01	439,3	254,8	-258,6	3,4	34,4	140,7
2600	63,79	474,8	275,5	-279,5	4,1	37,3	152,2
2800	68,36	510,0	295,9	-300,2	4,2	39,9	163,4
3000	72,93	544,9	316,2	-320,7	4,8	42,7	174,7
3200	77,18	578,5	335,8	-340,4	5,4	45,4	185,5

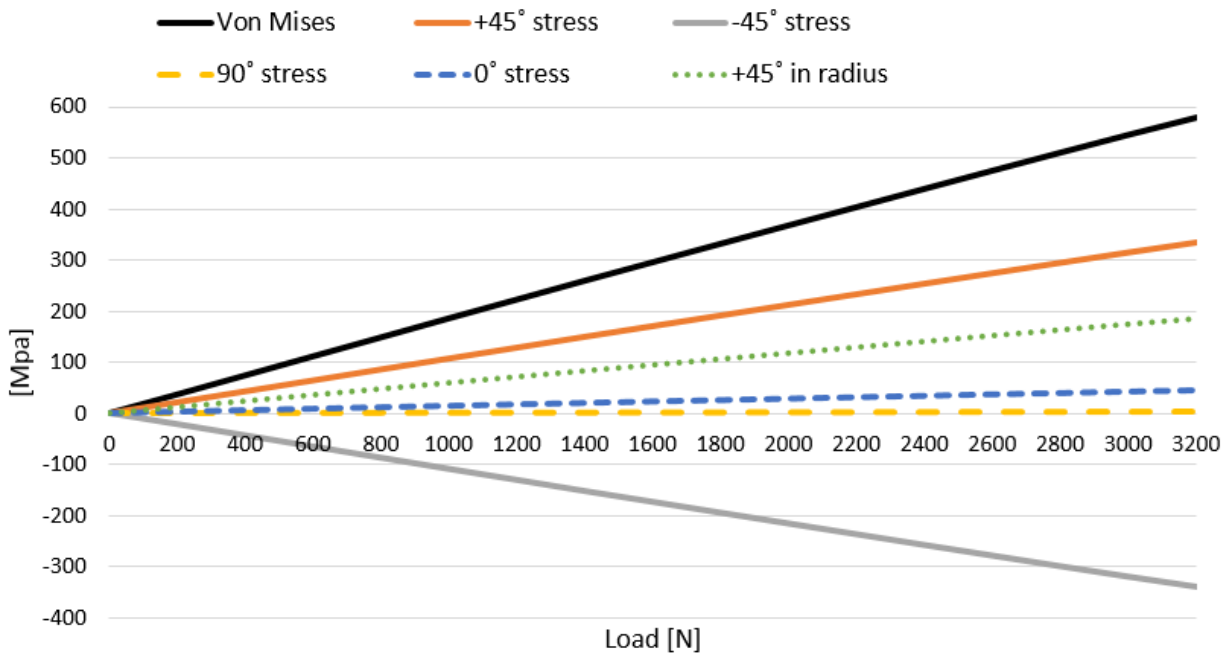

Figure 5.4: Average Stresses from Physical Tests

Chapter 6

Analytical Quasi Static Calculation

This chapter concerns the quasi static analytical calculation of the suspension system. In the exams, the exercises includes different assumptions on different tasks to ease the calculation. In this chapter those assumption will be evaluated on whether they are applicable to the rig. In addition, a new extended calculation model will be presented. The objective with this model is numerically capture the realistic response of the rig. This involves partiality comprehensive calculations, which results in effective geometric values that can be used to calculate the rig response. Table 6.1 presents the assumptions included in the exams. This table also includes three new extended assumptions which are evaluated if whether they are more physical correct. All assumption are numbered , and will be noted above the calculation models. e.g. [Ass: 1a, 2b, 3a, 4a, 5a] , where *a* and *b* indicates opposing assumptions. Assumption 6. applies for all models, and will not be listed.

Table 6.1: Assumption Declaration

	Assumptions from the exams	Effect
1a.	Infinite stiff torsion arm	Beam deflection ignored
1b.	Not Infinite stiff torsion arm	Physical correct
2a.	Infinite stiff support bearings	Simplifies calculation
2b.	Soft support bearings	Induces bending stresses in torsion bar
3a.	Idealized geometry	Simplifies calculation
4a.	Small angular displacement	Incorrect at large angular displacement
5a.	Force applied to the torsion arm	Torsion arm rotation neglected
6.	Fixed clamping of torsion bar end section	Acts as calculation reference point

	Extended assumption declaration	Effect
3b	Complex geometry calculation	To determine whether there is a difference
4b.	Large angular displacement	Angular changing force vector
5b.	Force applied on the wheel hub	Torsion arm rotation included

Table 6.2: Constant Declaration

CONSTANT DECLARATION

ϕ	torsion angle in radians	
θ	torsion angle in radians, corrected for changing force direction	
α	angle of torsion arm, corrected for force direction and geometry	
T	applied torque	
F	applied force	
F_θ	force vector perpendicular to the torsion arm	
F_α	force vector perpendicular to the torsion arm	
l	effective torsion arm length	
L	length of torsion bar	
D	diameter of torsion bar	
J	torsional constant, torsion bar	
I	second moment of area, torsion arm	
κ_f	stiffness factor	
G	shear modulus	
E	elastic modulus	
h_ϕ	vertical height with basic theory, no beam deflection	[Ass: 1a, 2a, 3a/b, 4a]
$h_{\phi+}$	vertical beam deflection, basic theory	[Ass: 1b, 2a, 3a/b, 4a]
H_ϕ	total vertical height with basic theory, with beam deflection	[Ass: 1b, 2a, 3a/b, 4a]
h_θ	vertical height, force direction corrected, no beam deflection	[Ass: 1a, 2a, 3a/b, 4b]
$h_{\alpha+}$	vertical beam deflection. force direction and geometry corrected	[Ass: 1b, 2a, 3a/b, 4b]
H_α	total vertical height. Real height	[Ass: 1b, 2a, 3a/b, 4b]

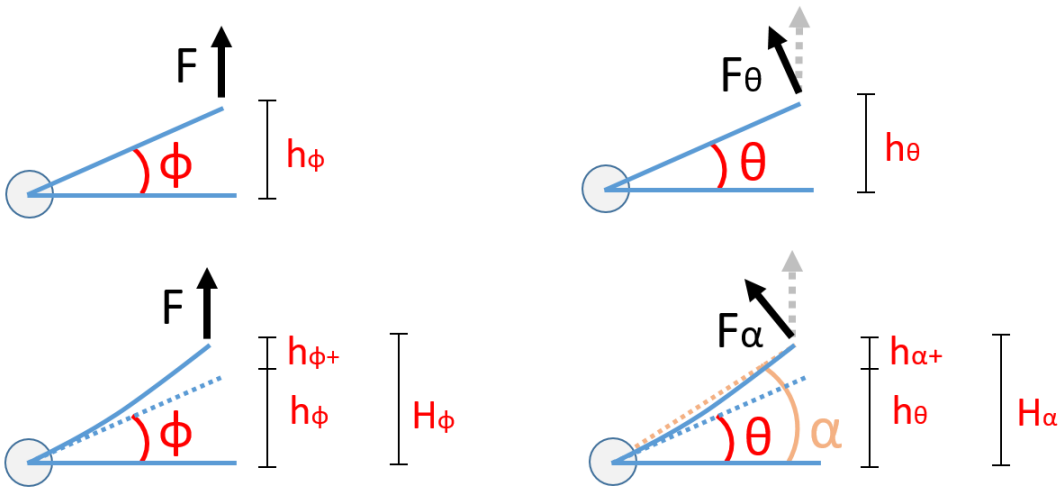

Figure 6.1: Angles and Height Parameters, Visual Illustration

6.1 Complex Geometry Calculation

In this section complex geometry calculation will be assessed. The purpose is to be able to conclude what effect the geometrical idealization constitutes. The calculation assess four sub-sections; The torsion bar stiffness [Ass.3], torsion arm deflection [Ass. 1], torsion arm rotation [Ass. 1], and the bearing stiffness [Ass. 2].

The result of these calculations are corrected geometry values, in term of an effective torsion bar stiffness and effective beam deflection length. These values are further utilized in the process to try to create a physical realistic calculation model for the rig response. Later in this chapter, this extended calculation model is compared with the original exam model and the physical test.

6.1.1 Torsion bar stiffness

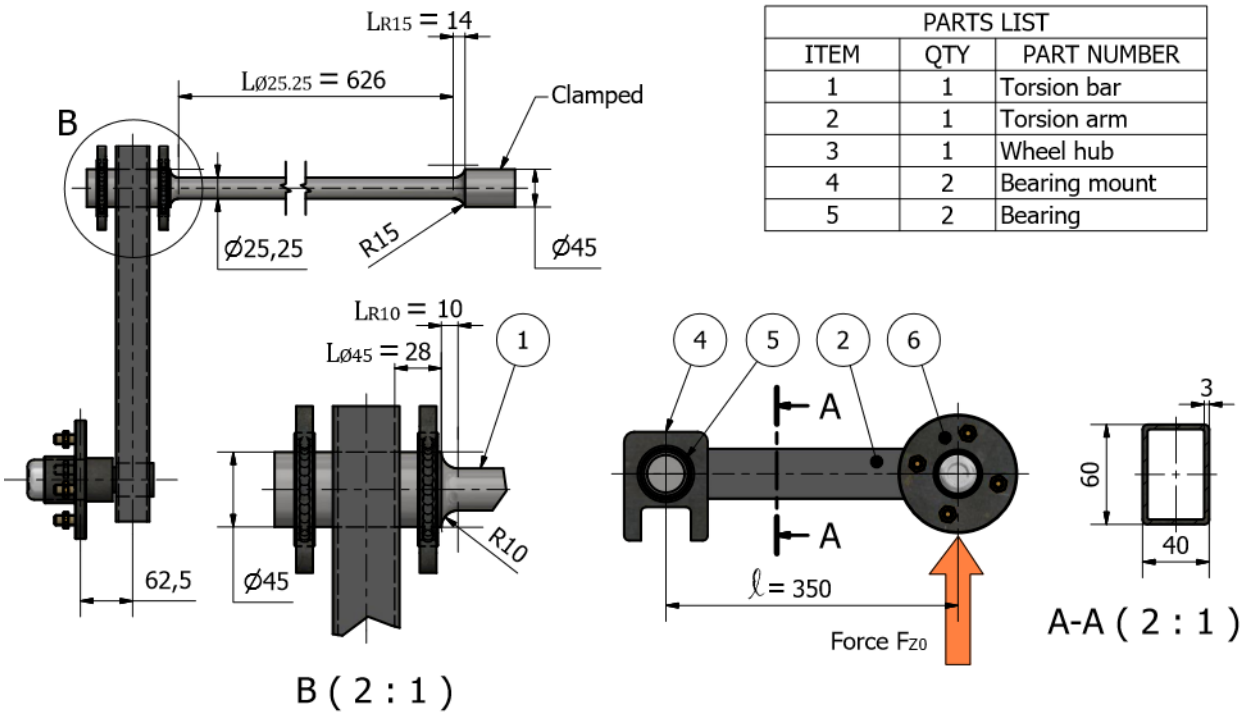

PARTS LIST		
ITEM	QTY	PART NUMBER
1	1	Torsion bar
2	1	Torsion arm
3	1	Wheel hub
4	2	Bearing mount
5	2	Bearing

Figure 6.2: Suspension System, Built Rig

In the idealized geometry of the exam, the calculation is based on the torsion bar having a uniform diameter, and an effective torsional length of 650 mm. -Where the length is calculated from the centre of the torsion arm, to the clamped section. Due to practical reasons the built rig is not physical equal to the exam model. On the rig, the hole slender section is shifted further out to make it possible to install the inner bearing. The slender section is still 650mm, including

the radii on each side. In this section computation is performed to examine the stiffness of the rig torsion bar, compared to the idealized model. This computation includes the radii of R10 and R15 on the torsion bar. See figure 6.2.

To easily compare the stiffness, a stiffness factor, κ_f, is introduced. This factor is the effective torsional length divided by the torsional constant. The idealized model has the following stiffness factor, based on the build dimension, D=25.25mm torsion bar diameter.

Idealized geometry stiffness factor:

$$\kappa_{f,Ideazlied} = \frac{L}{J_T} = \frac{650}{\frac{\pi}{32}D^4} = 0.01629mm^{-3} \tag{6.1}$$

To compute a stiffness factor which is true to the actual build rig, it is necessary to include the radii and the Ø45 section between the torsion arm and the slender Ø25.25 section. This is done numerically by summing the individual sections' stiffness factors. This results in a stiffness factor, $\kappa_{f,complex}$.

Complex geometry stiffness factor:

$$\kappa_{f,complex} = \sum \frac{L_i}{J_i} = \frac{L_{Ø25.25}}{J_{Ø25.25}} + \frac{L_{Ø45}}{J_{Ø45}} + \frac{L_{Radii}}{J_{Radii}} \tag{6.2}$$

All the values, besides the J_{Radii} can be found and computed from the technical drawing of the torsion bar in figure 6.2. The values are listed in table 6.3. The $L_{Ø45}$ is set to not extend to the centre of the torsion arm. Instead it extends to the inner wall of the torsion arm, as this is assumed to be more realistic. The J_{Radii} is unknown as the radii diameter is variable.

Table 6.3: Values included in the Complex Stiffness Factor Computation

Diameter		Length		Torsion constant, J	
$D_{Ø25.25}$	$22.25mm$	$L_{Ø25.25}$	$326mm$	$J_{Ø25.25}$	$39907mm4$
$D_{Ø45}$	$45mm$	$L_{Ø45}$	$28mm$	$J_{Ø45}$	$402578mm4$
D_{Radii}	Variable	L_{Radii}	$10+14mm$	J_{Radii}	Unknown

To establish the value of the J_{Radii}, the CAD model of the torsion bar was utilized to numerically compute the radii torsional constant. By extracting the cross section diameters with an increment of 1mm, a summation of the corresponding torsional constants yields a good approximation. To increase the accuracy, trapezoidal values of the diameters were computed.

Trapezoidal section diameter:

$$D_{trap,i} = \frac{[D_i + D_{i-1}]}{2} \tag{6.3}$$

Section torsional constant:

$$J_i = \frac{\pi \cdot [D_{trap,i}]^4}{32} \Rightarrow \frac{\pi}{512}[D_i + D_{i-1}]^4 \tag{6.4}$$

Table 6.4: Radii Torsional Constant Computation

R15 radius			**R10 radius**		
$Increment$	$D_{trap,i}[mm]$	$J_i[mm^4]$	$Increment$	$D_{trap,i}[mm]$	$J_i[mm^4]$
n=1	25.28	40116	n=1	25.30	40224
n=2	25.24	39862	n=2	25.50	41524
n=3	25.51	41592	n=3	25.91	44263
n=4	26.10	45523	n=4	26.55	48745
n=5	26.65	49517	n=5	27.42	55529
n=6	27.36	54997	n=6	28.59	65584
n=7	28.23	62378	n=7	30.11	80668
n=8	29.29	72271	n=8	32.11	104328
n=9	30.56	85599	n=9	34.89	145455
n=10	32.07	103789	n=10	40.76	271099
n=11	33.87	129146			
n=12	36.05	165731			
n=13	38.76	221548			
n=14	42.64	324449			
	$\sum_{i=1}^{14} J_{R15,i}$	**1436519**		$\sum_{i=1}^{10} J_{R10,i}$	**897418**

The values and results of the increment torsional constants are listed in Table 6.4. As the increments are small and identical, the total torsional constant for both the radii, J_{Radii}, is equal to the average of the increment torsional constants.

Total torsional constant for the R15 and R10 radii:

$$J_{Radii} = \frac{\sum_{i=1}^{N_1} J_{R15,i} + \sum_{i=1}^{N_2} J_{R10,i}}{N_1 + N_2} \tag{6.5}$$

$$\underline{\underline{J_{Radii} = \frac{1436519 + 897418}{14 + 10} = 97247 mm^4}} \tag{6.6}$$

Corresponding effective diameter of the radii:

$$D_{radii} = \sqrt[4]{\frac{32 \cdot J_{Radii}}{\pi}} = 31.55mm \tag{6.7}$$

All the values for computing the stiffness factor for the rig torsion bar are now accessible. Inserted in the complex stiffness factor equation, Eq.6.2, provides a comparative basis for the stiffness relationship between the idealized and complex computed geometry.

Complex geometry stiffness factor:

$$\kappa_{f,complex} = \sum \frac{L_i}{J_i} = \frac{326}{39907} + \frac{28}{402578} + \frac{14+10}{97247} = 0.01600mm^{-3} \tag{6.8}$$

Stiffness ratio between idealized and complex computed geometry:

$$R_{stiffness} = \frac{\kappa_{f,complex}}{\kappa_{f,Ideazlied}} = \frac{0.0160}{0.01629} = 98.2\% \tag{6.9}$$

The stiffness ratio reveals that the idealized model is slightly softer than the complex computed. (larger κ_f equals softer stiffness). The the main contributor to this deviation is the implementation of the radii. Whether the stiffness deviation of 1.8% can be called significant, can be discussed, but in this thesis it is a significant contributor to create an accurate calculation model. The geometric and computed values for the idealized- and complex computed geometry is summarized in Table 6.5.

Table 6.5: Comparison of Torsion Bar Stiffness

	IDEALIZED GEOMETRY		COMPLEX GEOMETRY	
Diameters:	$D_{Ø25.25}$	25.25 mm	$D_{Ø25.25}$	25.25 mm
			$D_{Ø45}$	45 mm
			D_{Radii}	31.55 mm
Torsional lengths:	$L_{Ø25.25}$	650 mm	$L_{Ø25.25}$	626 mm
			$L_{Ø45}$	28 mm
			L_{Radii}	24 mm
Torsional constants:	$J_{Ø25.25}$	39907 mm^4	$J_{Ø25.25}$	39907 mm^4
			$J_{Ø45}$	402578 mm^4
			J_{Radii}	97247 mm^4
Stiffness factors:	$\kappa_{f,idealized}$	0.01629 mm^{-3}	$\kappa_{f,complex}$	0.0160 mm^{-3}

6.1.2 Effective beam deflection

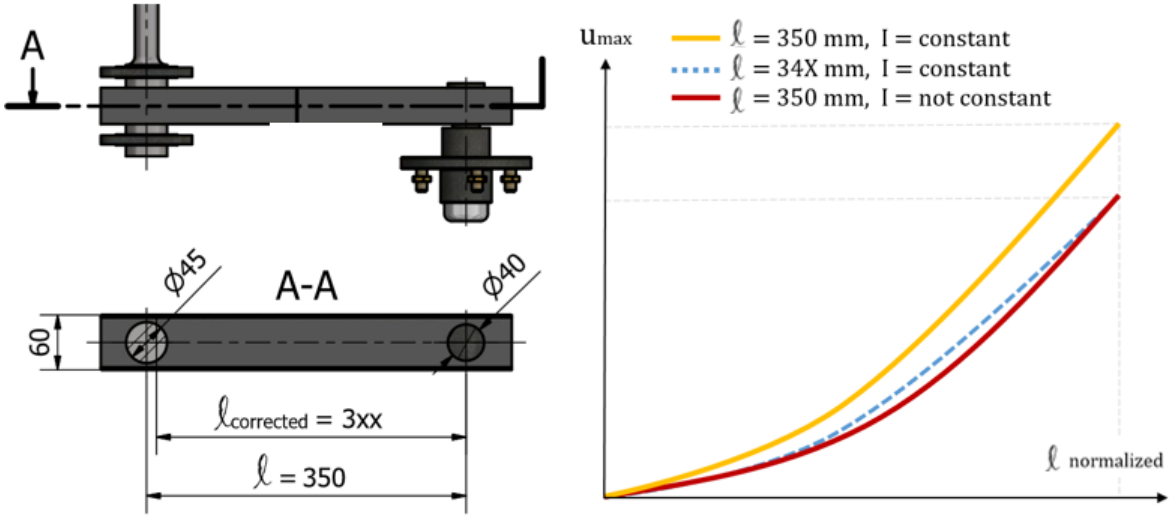

Figure 6.3: Technical Drawing from the Exams

The physical length of the torsion arm between the centre of the torsion bar and the wheel hub axle is 350mm. This length is declared as $l = 350$. Idealized, the torsion arm is considered to have a uniform cross section across this length. This allows for utilizing a standard deflection formula when calculating the beam deflection. Physically, the torsion arm cross section is not constant due to the torsion bar and wheel hub axle. As the beam deflection is a cubic function of the length, it is important to get this factor correct. In this section the effective beam deflection length is calculated, named l_{corr}, corrected deflection length. The result of the calculation shows that the effective beam deflection length is 342.7 mm, giving a 6.5% lower deflection. This value is valid for any given applied load and E-modulus. The logic behind this calculation is visualized in figure 6.3. The yellow graph represents a beam deflection of a 350 mm beam with constant second moment of area, I. The red graph represents the physical rig where the physical length is 350, but the I is a variable. The mission is to find the dashed blue line. A unknown deflection length with constant I which generates a end-point value equal to the red graph. This is to be able (and allow other people) to easily compute the real end-point deflection, with the standard deflection formula.

The calculation has been performed both analytically, and numerically to confirm the result. The analytical calculations is to be presented first. The numerical is afterwards briefly presented.

Analytical calculation of effective beam deflection length

Constant Declaration	
θ_B	tangent angle at end point, basic theory
θ_{corr}	corrected tangent angle at end point
u_{max}	maximum beam deflection
E	elastic modulus
G	shear modulus
F	applied force
$V(x)$	acting internal shear force along torsion arm
$M(x)$	acting moment along torsion arm
l	beam deflection length
l_{corr}	corrected effective beam deflection length
L	physical length of torsion arm
R	radius of torsion bar axle
B	section width of torsion bar axle
$H(x)$	section height of torsion bar axle
I_{beam}	second moment of area, torsion arm
$I_{bar}(x)$	second moment of area, torsion bar cylinder
$I(x)$	combined second moment of area, torsion arm and cylinder

Table 6.6: Material Properties

S165M, Stainless steel (Torsion bar)				Ref.
Young's Modulus	E	210	Gpa	Matweb
Poisson's Ratio	ν	0.346	-	Matweb
Shear Modulus	G	78	Gpa	Matweb
Yield Strength	σ_{ys}	885	Mpa	Mat. Certificate
Ultimate Tensile	σ_u	1010	Mpa	Mat. Certificate

S355 J2H, Construction Steel (Torsion Arm)				Ref.
Young's Modulus	E	210	Gpa	ThyssenKrupp
Yield Strength	σ_{ys}	355	Mpa	ThyssenKrupp
Ultimate Tensile	σ_u	510	Mpa	ThyssenKrupp

Below, Eg.6.10-6.11, the standard formulas for beam deflection and tangent angle at end-point, are presented. These formulas relies on constant second moment of area, I.
Max beam deflection and angle from moment [4]:

$$u_{max} = \frac{M_e \cdot L^2}{2EI}, \quad \theta_B = \frac{M_e \cdot L}{EI} \tag{6.10}$$

Max beam deflection and angle from force [4]:

$$u_{max} = \frac{F \cdot L^3}{3EI}, \quad \theta_B = \frac{F \cdot L^2}{2EI} \quad \rightarrow \quad u_{max} = \frac{2L}{3} \cdot \theta_B \tag{6.11}$$

To analytical calculate the beam deflection with non constant I, one must do a double integration of the shear load, including the variable $I(x)$. Moment is found by integrating the shear load:

$$M(x) = \int V(x) = F(l-x) \tag{6.12}$$

The variable $I(x)$ consists of a constant, I_{beam}, which is the torsion arm beam, and a variable $I_{bar}(x)$. The $I_{bar}(x)$ refers to the half cylinder of the torsion bar which extends from the centre into to torsion arm, and contributes to stiffen the structure. The wheel hub axle is not included, as it does not contribute to the beam deflection. This is due to the flattening of the deflection tangent angle.
Variable second moment of area:

$$I(x) = I_{beam} + I_{bar}(x) \tag{6.13}$$

The $I_{bar}(x)$ is found by introducing a variable section height of the cylinder, $H(x)$:

$$H(x) = 2\sqrt{R^2 - x^2}, \quad Domain: \ [x < \pm R] \tag{6.14}$$

$$I_{bar}(x) = \frac{B \cdot H(x)^3}{12} \Rightarrow \frac{B \cdot [2\sqrt{R^2 - x^2}]^3}{12} \Rightarrow \frac{2B}{3}[\sqrt{R^2 - x^2}]^3 \tag{6.15}$$

The new corrected deflection angle tangent is found by integrating the moment, divided by E and I(x), over the physical length:

$$\theta_{corr} = \int_0^L \frac{M(x)dx}{EI(x)} \Rightarrow \int_0^L \frac{F(l-x)dx}{EI(x)} = \frac{[N][mm^2]}{[N/mm^2][mm^4]} = [rad] \tag{6.16}$$

Due to the Domain of the I_{bar}, the integral is split:

$$\theta_{corr} = \int_0^L \frac{F(l-x)dx}{EI(x)} \Rightarrow \frac{F}{E}\int_0^{L_1=R} \frac{(l-x)dx}{I_{beam} + I_{bar}(x)} + \frac{F}{E}\int_{L_1=R}^L \frac{(l-x)dx}{I_{beam}} \tag{6.17}$$

I_{bar} inserted:

$$\theta_{corr} = \frac{F}{E}\int_0^R \frac{(l-x)dx}{I_{beam} + \frac{2B}{3}[\sqrt{R^2-x^2}]^3} + \frac{F}{E}\int_R^L \frac{(l-x)dx}{I_{beam}} \tag{6.18}$$

Due to the complexity, it is unattainable to perform algebraic integration. Values inserted:

$$\theta_{corr} = \frac{F}{E}\int_0^{22.5} \frac{(350-x)dx}{273852 + \frac{2\cdot 34}{3}[\sqrt{22.5^2-x^2}]^3} + \frac{F}{E}\int_{22.5}^{350} \frac{(350-x)dx}{273852} \tag{6.19}$$

Computation performed by Wolfram|Alpha. Corrected deflection angle tangent:

$$\theta_{corr} = \frac{F}{E}\cdot(0.0186547 + 0.195829) = \frac{F}{E}\cdot 0.2144837 = [rad] \tag{6.20}$$

Computation of the corrected effective deflection length, is performed by reordering the standard tangent angle formula Eq. 6.11. By substituting the constants with newly computed variables, the formula requirement of constant I is bypassed.

$$\theta_B = \frac{F\cdot L^2}{2EI} \quad \rightarrow \quad L = \sqrt{\frac{2EI}{F}\cdot\theta_B} \tag{6.21}$$

Substituting the constants:

$$l_{corr} = \sqrt{\frac{2EI_{beam}}{F}\cdot\theta_{corr}} \tag{6.22}$$

Final derived formula for corrected effective deflection length with θ_{corr} inserted. F and E cancels, making the formula independent of applied load and elasticity.

$$l_{corr} = \sqrt{\frac{2EI_{beam}}{F}\cdot\frac{F}{E}\int_0^l \frac{(l-x)}{EI(x)}dx} \tag{6.23}$$

Inserting the values, gives a numeric result of the effective beam deflection length:

$$\underline{\underline{l_{corr} = \sqrt{2I_{beam}\cdot 0.2144837} = 342.74mm}} \tag{6.24}$$

The effective beam deflection length of the rig torsion arm is 342.74 mm. Inserted in the standard beam deflection formula Eq. 6.11, results in a 6.4% lower beam deflection than the idealized beam deflection length og 350.

As this is a messy operating to compute analytically, a second numerical method was utilized to confirm the result. The result of the numerical computation is a $l_{corr} = 342.786mm$. As this was a different approach to estimate the l_{corr}, but gives equal result, implies that the analytical result should be correct.

Numerical calculation of effective beam deflection length

The following page mathematically describes what is done in the numerical computation. Briefly, it is a summing of the the incremental displacement contribution, with variable stiffness, with an increment size of 0.25mm. The total displacement u_{max} was then utilized to compute the l_{corr}, not the tangent angle as in the analytical. The computation was performed in Excel to produce the result.

End section displacement:

$$u_1 = \delta_1 = \frac{F \cdot L_1^3}{3EI_1} \tag{6.25}$$

End section length:

$$L_1 = L - R = 350 - 22.5 = 327.5mm \tag{6.26}$$

Uniform section 2. moment of area:

$$I_1 = 273852mm^4 \tag{6.27}$$

Increment size:

$$L_{inc} = 0.25mm \tag{6.28}$$

Iteration length:

$$L_{k+1} = L_k + L_{inc} \tag{6.29}$$

2. moment of area:

$$I_{k+1} = 273852 + \frac{2B}{3}\left(\sqrt{R^2 - [L - L_{k+1}]^2}\right)^3 \tag{6.30}$$

Displacement w/o rotation:

$$\delta_{k+1} = \frac{F \cdot L_{inc}^3}{3EI_{k+1}} + \frac{M \cdot L_{inc}^2}{2EI_{k+1}} \Rightarrow \frac{F \cdot L_{inc}^3}{3EI_{k+1}} + \frac{FL_k \cdot L_{inc}^2}{2EI_{k+1}} \Rightarrow \frac{F \cdot L_{inc}^2}{6EI_{k+1}}(2L_{inc} + 3L_k) \tag{6.31}$$

Deflection angle:

$$\theta_{k+1} = \frac{F \cdot L_{inc}^2}{2EI_{k+1}} + \frac{ML_{inc}}{EI_{k+1}} \Rightarrow \frac{F \cdot L_{inc}^2}{2EI_{k+1}} + \frac{FL_kL_{inc}}{EI_{k+1}} \Rightarrow \frac{F \cdot L_{inc}}{2EI_{k+1}}(L_{inc} + 2L_k) \tag{6.32}$$

Displacement included rotation:

$$u_{k+1} = \delta_{k+1} + \theta_{k+1} L_k \tag{6.33}$$

Number of iterations:

$$K = \frac{L - L_1}{L_{inc}} + 1 = \frac{350 - 327.5}{0.25} + 1 = 91 \tag{6.34}$$

Total displacement

$$u_{max} = \sum_{k=1}^{K=91} u_k = \frac{F}{E} \cdot 49.026833 = [mm] \tag{6.35}$$

This accords to:

$$u_{corrected} = u_{max} = \frac{F \cdot l_{corr}^3}{3EI} = \frac{F}{E} \cdot 49026833 \tag{6.36}$$

Final result:

$$\underline{\underline{l_{corr} = \sqrt[3]{3I \cdot 49026833} = 342.786mm}} \tag{6.37}$$

6.1.3 Rotation of the Torsion Arm

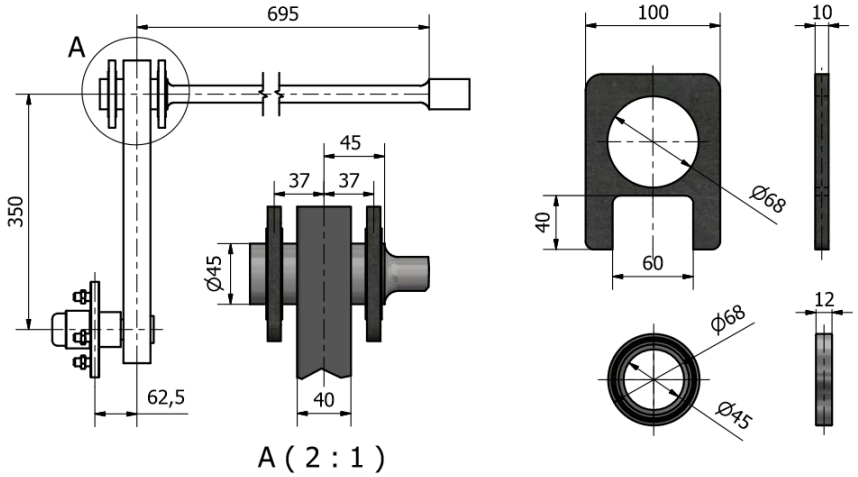

Figure 6.4: Dimensions Related to the Bearing Calculation

Assumption 5a from the exam gives that the force is directly applied at torsion arm, and not on the wheel hub. This is given to be able to neglect the rotation of the torsion arm. The consequence of a such rotation is an extra height contribution, H_β, as well as extra moment forces which may induce bending stress in the torsion bar. The nominal computation below, Eq. 6.38-6.40, reveals that the height contribution is minimal. At 3200 newtons, the contribution is only 0.135mm. On the other hand, the maximum generated moment forces are quite significant at 200Nm, Eq. 6.41, which may induce large bending stresses in the torsion bar. To evaluate the impact of assumption 5a, calculations of the bearing stiffness needs to be assessed first.
Polar moment of area:

$$I_{p,beam} = \frac{bh}{12}(h^2+b^2) - \frac{(b-t)(h-t)}{12}[(h-t)^2+(b-t)^2] = 416984mm^4 \tag{6.38}$$

Angular rotation of the torsion bar:

$$\beta_{beam} = \frac{T_{beam}\cdot l_{beam}}{I_{p,beam}\cdot G} = \frac{F\cdot 62,5mm\cdot 350mm}{416984mm^4\cdot 78000Mpa} = 6.73x10^{-7}\cdot F \tag{6.39}$$

Numeric height contribution at F = 3200N:

$$H_\beta = 62.5mm\cdot sin(\beta_{beam}) \quad \xrightarrow[F=3200N]{Numeric} = 0.135\,mm \tag{6.40}$$

Maximum generated moment forces:

$$T_{beam} = F\cdot 62.5mm \quad \xrightarrow[F=3200N]{Numeric} = 200Nm \tag{6.41}$$

The bearings supporting the torsion bar are heavy duty chrome steel bearings, with the dimensions 45x68x12mm, situated 37 mm from the torsion arm centre. Each load rated at 10.9kN static and 14.1kN dynamic [6]. The bearings are shrink fitted into the bearing houses. The dimensions are displayed in figure 6.4. To decide whether the assumption of rigid bearings [Ass: 2a] are the applicable to the rig, a worst case calculation was performed. In this calculation, the stiffness contribution from the torsion bar is ignored. Figure 6.5 displays the a free-body diagram of the forces acting on the bearings from the torsion arm. F is the 3200N vertical force from the torsion arm, whilst the M is the moment force of 200Nm generated from the wheel hub offset. F_1 and F_2 are the reaction forces from the bearings. δ is the deflection angle that would have caused bending stress in the torsion bar, and increased the total rotation of the torsion arm. By doing simple estimate of the reaction forces, it is proven that the forces are well within the bearings capacity. And a worst case calculation, Eq. 6.42-6.45, of the bearing mounts gives a nominal stress of 17 Mpa in the narrow section. Which is negligible.

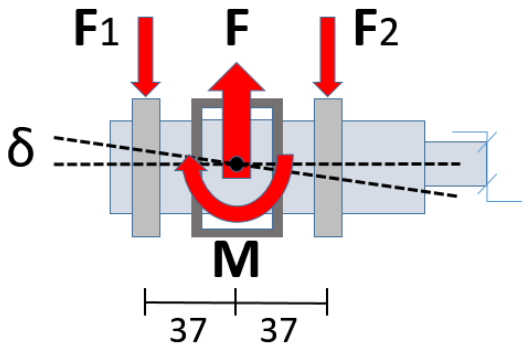

Figure 6.5: Free Body Diagram for Torsion Arm/Bearings

Reaction forces:

$$F_1 = \frac{1}{2}\left(F + \frac{M}{37mm}\right) = \frac{1}{2}\left(3200N + \frac{200Nm}{37mm}\right) = 4300N \tag{6.42}$$

$$F_2 = \frac{1}{2}\left(F + \frac{M}{37mm}\right) = \frac{1}{2}\left(3200N + \frac{200Nm}{37mm}\right) = -1100N \tag{6.43}$$

$$\Delta F = F_1 + |F_2| = 5400N \tag{6.44}$$

Worst case nominal stress in bearing mounts:

$$\sigma_{nom,Mounts} = \frac{\Delta F}{A} \Rightarrow \frac{5400N}{(100-68)\cdot 10} = 17Mpa \tag{6.45}$$

On this basis it is desirable to draw the conclusion that the bearings and mounts can be assumed rigid on the rig. There is not enough forces to generate a significant deformation. And there should not be significant deflection angle δ. To support this conclusion, the physical tests showed no compressive stress along the top of the torsion bar. The actual reading was +5.4Mpa (tension). A quick angle sensitivity test was performed to estimate of effect of a δ on the torsion bar bending stress, Eq.6.46-6.49. The test revealed that the torsion bar is stressed by 4 Mpa for every $\delta = 0.001[rad]$ $(0.057deg.)$. This implies that non rigid bearings and mounts would have inflicted significant readable compression stress in the physical tests. From this, it is concluded that the assumption of rigid bearings [Ass: 2a] is applicable for the rig.

Standard formulas for beam deflection stress and tip angle:

$$\sigma_b = \frac{My}{I}, \quad \theta_b = \frac{ML}{EI} \quad \rightarrow \sigma_b = \frac{E \cdot y \cdot \theta_b}{L} \tag{6.46}$$

Inserting values:

$$\theta_b = \delta \ \rightarrow \ \sigma_b = \frac{E \cdot y \cdot \delta}{L} = \frac{210000 \cdot \frac{25.25mm}{2}}{650mm} \cdot \delta \tag{6.47}$$

Test deflection angle of 0.001 rad:

$$\delta = 0.001\,[rad] \ \ (0.057deg.) \tag{6.48}$$

Result: 4 Mpa compression stress for every 0.001 rad:

$$\sigma_b = 4Mpa \tag{6.49}$$

6.1.4 Evaluation of assumptions

To establish an extended calculation model of the rig response, it is desirable to include all the major contributing factors. This is governed by the assumptions included in the calculation model. The calculations performed prior in this chapter enables for selecting which assumption to include. To be physical correct, Ass. 1b, "Not Infinite stiff torsion arm", is going to be included. The evaluation of the bearings and mounts argues for that the support bearings may be assumed to be rigid, Ass 2a. This is a huge advantage, as further implies that the torsion bar is only exposed to pure torsion. Considering assumption 3, idealized vs. complex geometry, it was shown that this is a major contribution factor. Both the torsion bar and torsion arm are stiffer when complex calculated. The torsion bar with a torsional stiffness of 1.8%, and the torsion arm with a 6.5% lower deflection height. This justifies for including complex geometry in the calculation, Ass. 3b. The effect of Assumption 4, small vs. large angular displacement is

not yet quantified. But Ass. 4b, large angular displacement is going to be included. This is to include the shifting force vector generating the applied torque. As the force is vertically applied, the applied torque declines in relationship with the torsion arm angle, $[T = Fl \cdot Cos(\theta)]$. This is not included in the exam model, but it essential when developing the extended model. Assumption 5, considers whether the force is applies to the wheel hub or directly to the torsion arm. The main effect from this offset is a twisting of the torsion arm generating moment forces acting on the bearings. As the bearings are assumed rigid, this is not a major factor to include. An other aspect is that the twisting causes an extra height contribution. This height is found to be 0.132 mm at 3200N, force vector not included. This equals 0.17% of the total height. From this, it appropriate to conclude that the rotation of the torsion arm is not a factor necessary to include, as there probably are other sources of errors larger than this. From this, Ass. 5a is assessed to adequate, neglecting the wheel hub offset. Assumption 6, Fixed clamping of torsion bar end section, is based on FEA form the project thesis. The chosen assumption to include in the extended model are displayed in table 6.7. This also the shows the assumptions from the exams, which is to be calculated with both Ass. 1a & 1b.

Table 6.7: Assumptions to Include in the Calculation Models

	Assumptions	Exam Model	Extended Model
1a.	Infinite stiff torsion arm	✓	
1b.	Not Infinite stiff torsion arm	✓	✓
2a.	Infinite stiff support bearings	✓	✓
2b.	Soft support bearings		
3a.	Idealized geometry	✓	
3b	Complex geometry calculation		✓
4a.	Small angular displacement	✓	
4b.	Large angular displacement		✓
5a.	Force applied to the torsion arm	✓	✓
5b.	Force applied on the wheel hub		
6.	Fixed clamping of torsion bar end section	✓	✓

6.2 Calculation Models

This section concerns using the stipulated assumptions to create an Extended calculation model. The result of this model is then compared to the calculation model from the exam, and the physical test results. The numerical values of the calculations to follow in this section are based on the built dimensions to justify a direct comparison of the exam and realistic model to the physical test results. Material constants and dimensions utilized are presented in Table 6.8. This includes the effective dimensions as stiffness factors and deflection lengths, derived prior in

this chapter. The calculations to follow includes a variety of different angles and corresponding height constants. These are visually described in figure 6.6. The two figures to the left refers to the exam model, where small angular displacement is assumed. The two figures to the right are the realistic model where the torque generating force vector follows the rotation.

Table 6.8: Dimensions and Constants

		IDEALIZED GEOMETRY	COMPLEX GEOMETRY
TORSION BAR			
Diameter	D	$25.25mm$	$25.25mm$
Torsional constant	$J_{Ø25}$	$39907mm^4$	$39907mm^4$
Stiffness factor	κ_f	$0.01629mm^{-3}$	$0.01600mm^{-3}$
TORSION ARM			
Dimensions	$h\ x\ b\ x\ t$	$60x40x3mm$	$60x40x3mm$
2. moment of area	I_x	$273852mm^4$	$273852mm^4$
Beam length	l	$350mm$	$350mm$
Deflection length	l_{corr}	$= l = 350mm$	$342.8mm$
MATERIAL COEFFICIENTS			
E-modulus	E	210 Gpa	210 Gpa
G-modulus	G	78 Gpa	78 Gpa
Yield Strength	σ_y	885 Mpa	885 Mpa

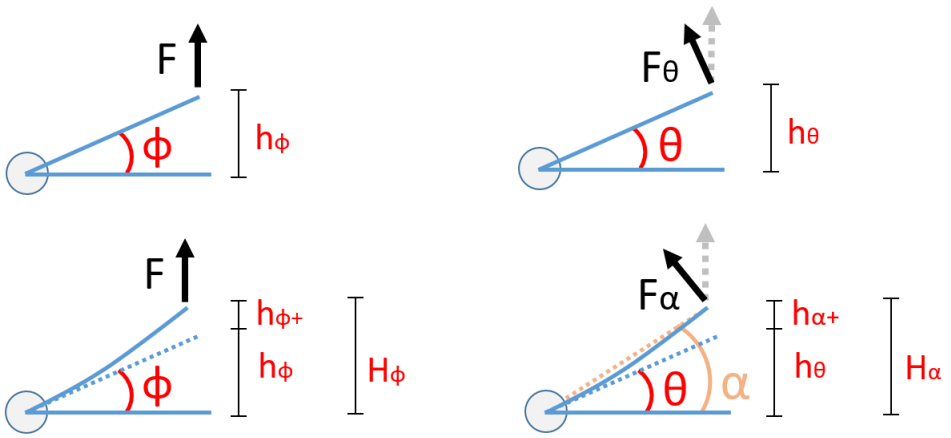

Figure 6.6: Description of Angles and Height constants

Exam calculation model

The height - load relationship in the exams is fairly simple. It includes the assumptions of; Infinite stiff support bearing, Idealized geometry, Small angular displacement, and is calculated with both infinite and non-infinite stiff torsion arm. [Ass: 1a/b, 2a, 3a, 4]. The calculation is based on basic theory which is found in the student formula tables (Irgens: Formelsamling) [4]. h_ϕ defines the vertical height of the wheel hub by a given load, with no beam deflection [Ass: 1a, 2a, 3a, 4a]. Beam deflection is defined by $h_{\phi+}$. H_ϕ is the combined total height including the beam deflection, [Ass: 1b, 2a, 3a, 4]. The Von Mises stress is based on pure torsion. The calculations below present the utilized formulas, and the numeric values. 2940N is used as force value, F, as this is the highest values from the exam assignments.

The torsion angle is defined by ϕ. The torsion bar length, L, divided on the torsional stiffness J_T is substituted with the stiffness factor, κ_f. [Ass:1a, 2a, 3a/b, 4a, 5a] Torsion Angle:

$$\phi = \frac{T \cdot L}{J_T G} \Rightarrow \frac{Fl \cdot L}{J_T G} = \frac{2940 \cdot 350 \cdot 650}{39907 \cdot 78000} = 0.215\, rad. \tag{6.50}$$

The most basic computation of the exam model is to estimate the elevation height due to the angular rotation alone. This height is defined as h_ϕ. [Ass:1a, 2a, 3a/b, 4a, 5a].

$$h_\phi = l \cdot sin\phi = 350 \cdot sin(0.214) = 74.63\, mm \tag{6.51}$$

If the assumption of non-rigid torsion arm [Ass: 1b.] is included, beam deflection is found:

$$h_{\phi+} = u_{max} = \frac{F \cdot l^3}{3EI_x} = \frac{2940 \cdot 350^3}{3 \cdot 210000 \cdot 273852} = 0.73\, mm \tag{6.52}$$

The total elevation height, H_ϕ, is the sum of the angular given height and the beam deflection. This is the final estimation of height from the exam model. [Ass:1b, 2a, 3a/b, 4a, 5a]

$$\underline{\underline{H_\phi = h_\phi + h_{\phi+} = 75.36\, mm}} \tag{6.53}$$

To compute the corresponding stresses in the torsion bar, rigid bearings are assumed [Ass: 2a]. This allows for using basic formulas for finding the principal shear stress based on pure shear. Due to this assumption, the Von Mises criterion is reduced to a simple expression:
Principal shear stress:

$$\tau_{xy} = \frac{T \cdot r}{I_{p,bar}} \Rightarrow \frac{Fl}{J_T} \cdot \frac{D}{2} = \frac{2940 \cdot 350}{39907} \cdot \frac{25.25}{2} = 325.53\,Mpa \tag{6.54}$$

Von Mises stress:

$$\underline{\underline{\sigma_{max} = \sqrt{3} \cdot \tau_{xy} = 563.83\,Mpa}} \tag{6.55}$$

Extended Model

The extended model differs from the exam model by including the angular force vector change. [Ass: 4b] The disadvantage is that this results in a transcendental equation, which is comprehensive to solve by hand. The force is applied vertically, but the force vector generating torque is the vector acting perpendicular to the torsion arm. This vector is defined as F_θ:

$$F_\theta = F \cdot cos\theta \tag{6.56}$$

The torsion angle, θ, is found by substituting F with F_θ in the basic formula. The pre-calculated $\kappa_{f,complex}$ simplifies the expression. Substituting with ϕ, gives a small expression, transcendental equation for θ :

$$\theta = \frac{F_\theta \cdot l}{G} \cdot \sum_{i=n}^{N} \frac{L_i}{J_i} \Rightarrow \frac{Fl}{G}\kappa_f \cdot cos\theta = \frac{2940 \cdot 350}{78000} 0.016 \cdot cos\theta \Rightarrow \phi \cdot cos\theta \tag{6.57}$$

Solving for θ solves the equilibrium state between the force, stiffness, and angle of the system. The equation was solved in Wolfram|Alpha:

$$\frac{\theta}{cos\theta} = \phi = 0.211\,rad \;\; , \;\; \xrightarrow[Wolfram]{Solve} \theta = 0.2065\,rad \tag{6.58}$$

The elevation height without beam deflection, h_θ , is found:

$$h_\theta = l \cdot sin\theta = 350 \cdot sin(0.2065) = 71.76mm \tag{6.59}$$

Implementing the deflection of the torsion arm is hard to get physical correct. This is due to an extra part in the non-linear equation, which is needed to include the beam deflection, in solving the equilibrium state of the system. This state is declared as α, with a corresponding

force F_α. But if the new angular contribution from the beam deflection is considered to be small, $[\alpha - \theta \approx 0]$, it is solvable. And the deflection contribution can be assumed to not affect the force vector.

$$F_\alpha \approx F_\theta = F \cdot cos\theta \ , \ \alpha \approx \theta \tag{6.60}$$

The vertical height form beam deflection is calculated from the basic deflection formula. This includes the corrected effective deflection length, l_{corr}, and F_α. The Cosine is a correcting factor to get the vertical displacement, and not the height perpendicular to the torsion arm.

$$h_{\alpha+} = \frac{F_\alpha \cdot {l_{corr}}^3}{3EI_x} \cdot cos\alpha \Rightarrow \frac{F \cdot {l_{corr}}^3}{3EI_x} cos\theta^2 \tag{6.61}$$

Nummerical vaules:

$$h_{\alpha+} = \frac{2940 \cdot 342.8^3}{3 \cdot 210000 \cdot 273852} \cdot [cos\,(0.2065)]^2 = 0.658\,mm \tag{6.62}$$

The total elevation height, H_α, is the sum of the angular given height and the beam deflection.

$$\underline{\underline{H_\alpha \approx h_\theta + h_{\alpha+} = 72.42\,mm}} \tag{6.63}$$

This corresponds to a torsion arm angle α of:

$$\underline{\underline{\alpha = sin^{-1}(\frac{H_\alpha}{l}) = 11.94\,deg}} \tag{6.64}$$

As bearings are assumed rigid, the Principal and Von Mises stresses are easily found. θ and not α is used, as θ refers to the torsion angle.
Principal stress:

$$\tau_{xy} = \frac{T \cdot R}{J_t} \Rightarrow \frac{FLcos(\theta) \cdot R}{J_t} = \frac{2940 \cdot 350 \cdot cos(0.2065)}{39907} \cdot \frac{25.25}{2} = \pm 318,61 Mpa \tag{6.65}$$

The Von Mises Stress is in the torsion bar:

$$\underline{\underline{\sigma_v = \sqrt{3}\tau_{xy} = 551.9 Mpa}} \tag{6.66}$$

6.3 Results and Evaluation

The numerical results for the exam- and the extended model are presented in Table 6.9, based on 2940N applied load. The two major values to compare are highlighted; H_ϕ - Exam model - idealized geometry, and H_α - Extended model - complex geometry. From these results, it is apparent that the H_α provides the modest results. To evaluate which model that is the most physical correct, they are compared to the physical test results. Figure 6.7 and 6.8 displays the Height/Load relation of the different models. Figure 6.7 shows the full force-range, whilst Figure 6.8 plots the top-end interval from 2200N to 3200N. From these plots, it evident that the H_α, - complex geometry, gives the most physical correlation. The deviations from the physical tests are small (1.1% @ 2940N), and it closer follows the curvature of the test results then the other models. Comparing the H_ϕ and the tests, there is a significant deviation of 5.2% at 2940N. To evaluate the Stress/Load relationship, the analytical calculated stresses from the extended model are compared with the physical tests. Figure 6.9 displays the Von Mises, principal stresses, and the stress in the radius. The comparison shows that the there is a 1.3% deviation in the compressive principal stress, 2.7% in the tensile principal stress, and 3.2% deviation in the Von Mises stress at 2940N.

The basis for the deviations between the extended model and the tests can be many; software setup, mechanical, the slightly incorrect strain gauge installation, incorrect geometry values, or analytical errors. Which of error sources that creates these deviations is hard to say, but to highlight one error source, it may be friction in the mechanical sliders and lift-plate system that is not taken into account. And that this friction influence the physical test results. Generating a higher demand of applied load to elevate the hub. Some numerical investigations has been performed, and the deviations are found to be linear to the applied force. And if a friction factor of

$$f = 1 - \frac{Force\,[N]}{200000}$$

is incorporated as $F_{real} = F \cdot f$ as a correction factor in the Physical test results, it fits the extended model. See Figure 6.10. This gives an increasing friction factor from $0 - 1.6\%$ from 0 - 3200N. It is not possible to determine if this is the real cause of the deviations, but it could be. Regardless of this, the extended computational model for the Height/Load relationship gives a satisfying result. And if the friction factor is incorporated into the rig software, it describes the static response spot on.

Table 6.9: Results Calculated at 2940 Newtons

		EXAM MODEL	
		IDEALIZED GEOMETRY	COMPLEX GEOMETRY
Torsion angle	ϕ	0.215 rad	0.211 rad
	ϕ	12.312 deg	12.090 deg
Height, no deflection	h_ϕ	74.63 mm	73.31 mm
Height inc. deflection	$h_{\phi+}$	0.73 mm	0.69 mm
Total height	H_ϕ	**75.36 mm**	**73.99 mm**
Von Mises Stress	σ_{max}	563.8 Mpa	563.8 Mpa

		EXTENDED MODEL	
		IDEALIZED GEOMETRY	COMPLEX GEOMETRY
Torsion angle	θ	0.210 rad	0.206 rad
	θ	12.04 deg	11.83 deg
Height, no deflection	h_θ	73.03 mm	71.76 mm
Height inc. deflection	$h_{\alpha+}$	0.70 mm	0.66 mm
Total height	H_α	73.73 mm	**72.42 mm**
Torsion arm angle	α	12.16 deg	11.94 deg
Von Mises Stress	σ_{max}	551.4 Mpa	551.9 Mpa

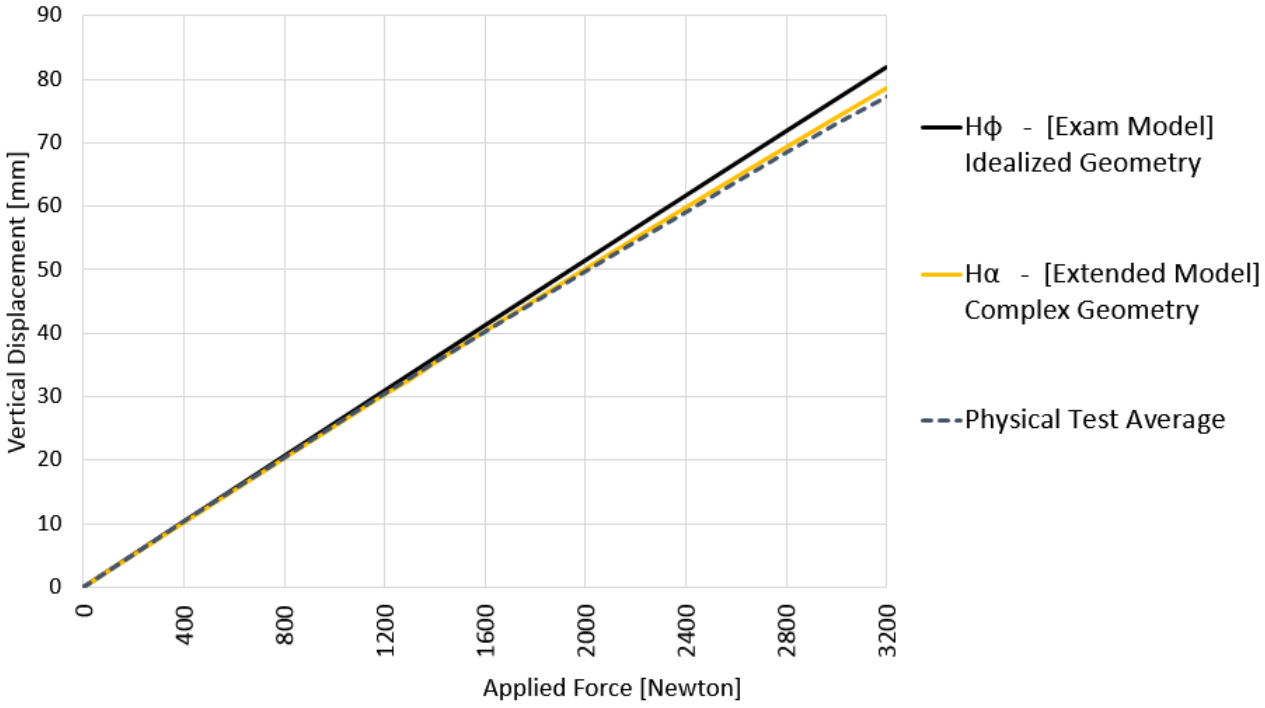

Figure 6.7: Height/Load: Analytical- vs Physical Test Results

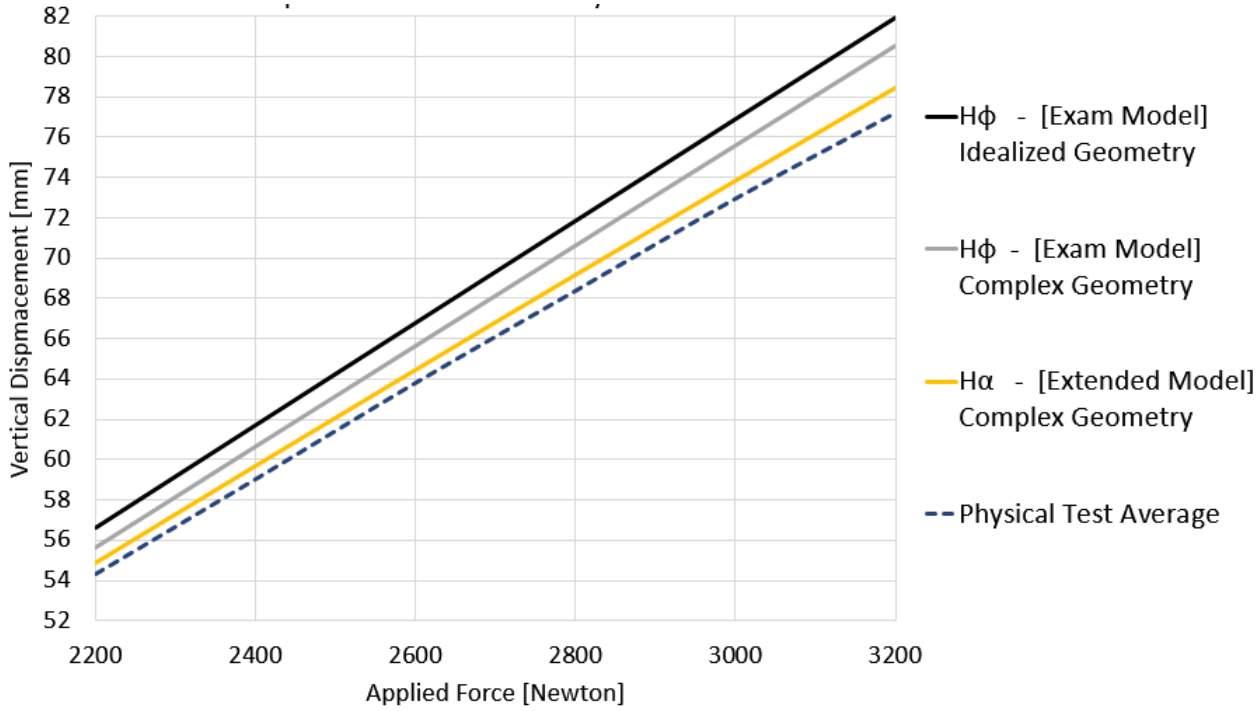

Figure 6.8: Height/Load: Analytical- vs Physical Test Results, 2200 - 3200N

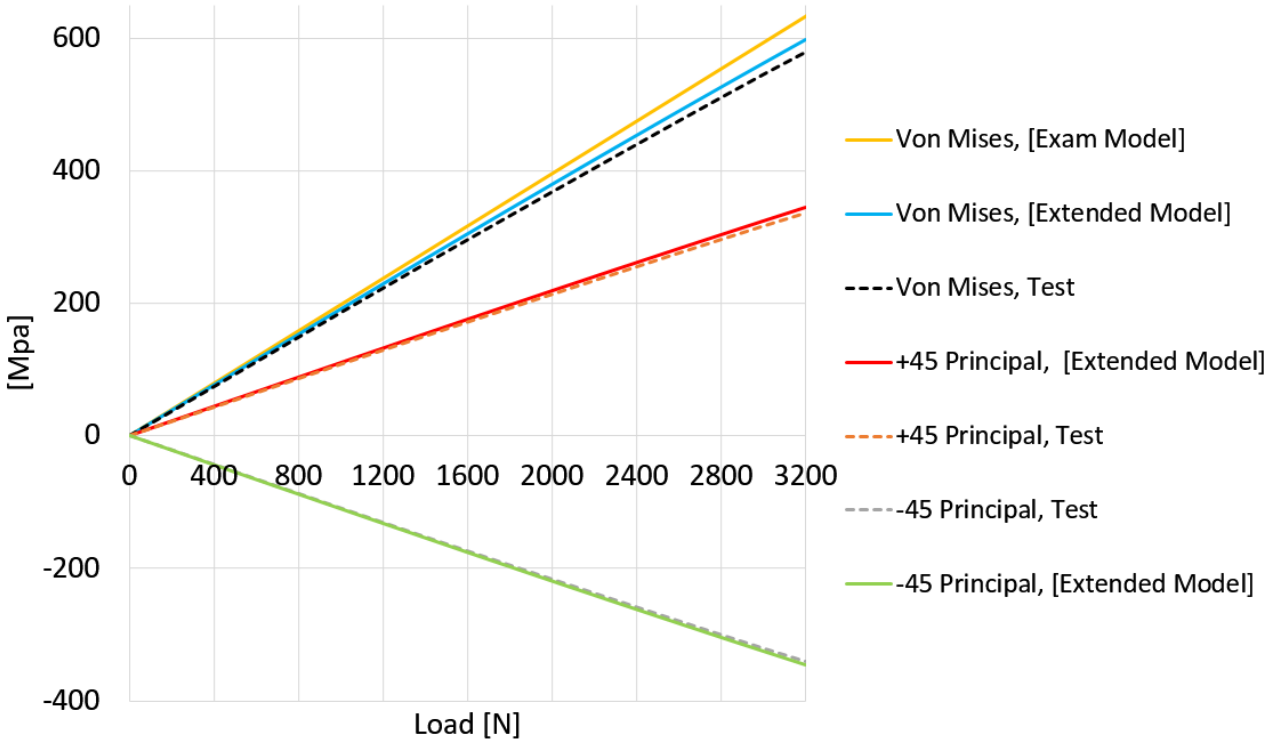

Figure 6.9: Stress/Load: Analytical- vs Physical Test Results

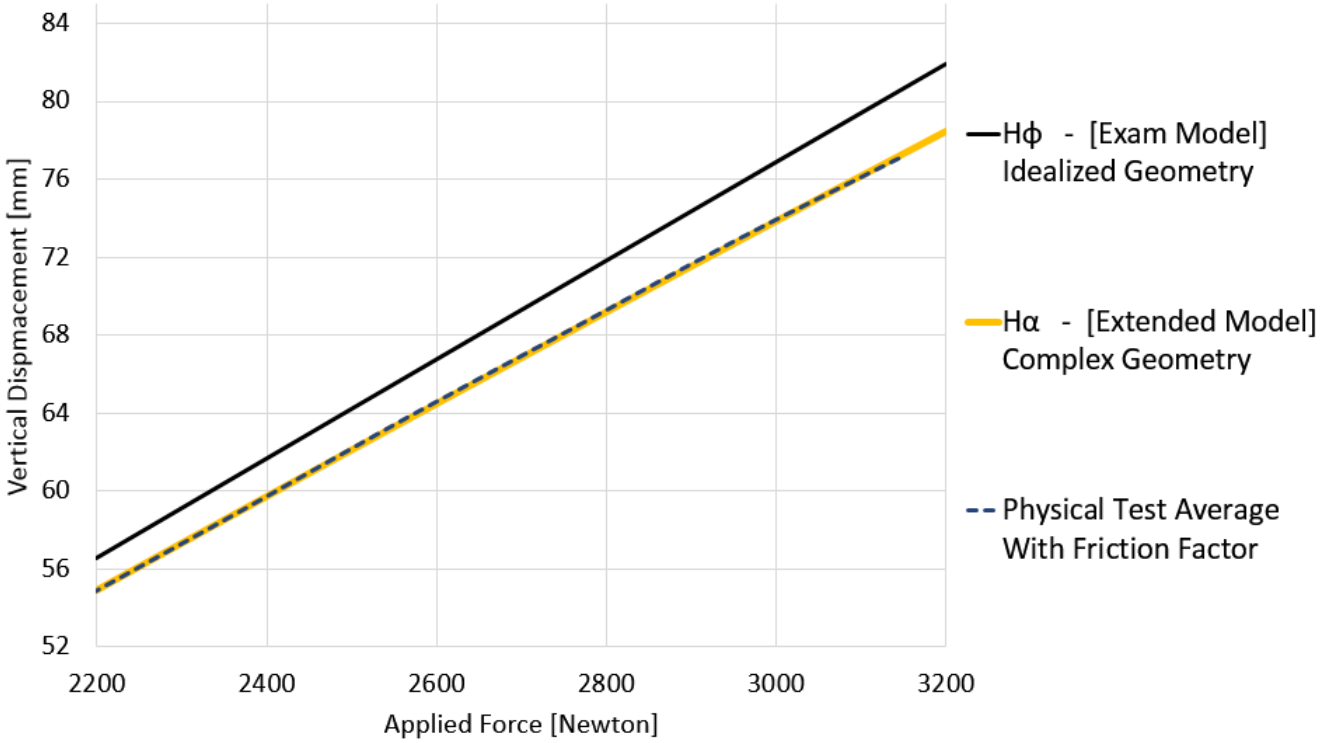

Figure 6.10: Height/Load: Analytical- vs Physical Test, included Friction Factor

Overall, the extended calculation model gives satisfying results regarding reflecting the physical rig response. It is more comprehensive to conduct than the exam model, but gives more accurate results. Concerning the height/load relation, the extended model decreases the deviation by 79% at 2940N. Whether it is worth to perform depends on the situation. The exam model gives great estimations at low angular displacement, but at relative large angles (>8 deg / 2000 N) it starts to become imprecise.

Chapter 7

Virtual simulation of Quasi-Static Response

A variety of software have been utilized during the Thesis work to design and analyze the rig. Autodesk Inventor was used as Computer-aided design (CAD) software to design the rig, but the FEA module in Inventor is not adequate to perform the desired virtual simulations. Instead, Siemens NX was used to run FEA to simulate and analyze the suspension system. Transfer of CAD models was done by Parasolid files (.X_t).

The simulations performed are quasi-static analysis of the suspension system with three different Solvers in NX. And it was conducted with both solid 3D models and 1D beam models. This Chapter only concerns the quasi-static response of the suspension system. The dynamic simulation is included in Chapter 8, Dynamic Response. The utilized solves are; SOL101 Linear Statics, SOL109 Direct Transient Response, and SOL112 Modal Transient Response. A Fatigue analysis has also been performed to evaluate the life expectancy of the rig. As the rig frame was analyzed to be considered rigid in the Project thesis [2], allows for only evaluating the torsion bar and torsion arm. This is an advantage as the simulation time is drastically reduced; Static solver SOL 101 in NX uses 1+ hour to simulate the whole rig, but only 33 seconds to run the suspension system alone. As other students likely are going to replicate these simulations in class, it is also advantageous to keep the number of simulated parts and simulation time to a minimum.

This chapter first presents the 3D simulation model and simulation setup. An introduction to the different solvers is then presented before the simulation-results of each solver. Section 7.2 concerns the 1D beam elements model, simulation setup, and the associated results. The results of all the simulations are then combined and discussed in Section 7.3, Results.

7.1 3D Solid Elements Simulation Setup

FEM- and SIM- Model

As the analytical calculations proved that the wheel hub has an insignificant impact on the results, it was excluded from the FEM model. The exception was during the dynamic frequency simulation, where the weight distribution is the foundation of the simulation. The suspension system was meshed with 8 mm Quadratic tetrahedral elements, CTETRA(10), as this mesh proves to be more accurate than quadratic hexahedral elements considering torsion [7]. In the torsion bar radii, the mesh is finer (1 mm) to capture the stress concentration in the transition area, and the decreasing stresses further out in the radii. The material properties included in the FEM model are equal to those in the analytical calculation. They are listed in Table 7.1. The material created for the torsion bar was also used in the torsion arm, as the Young's Moduli are equal, and that the torsion arm is not subjected to stresses close to its yield strength.

Table 7.1: Material Properties in the FEM-model

Material Properties				Ref.
Young's Modulus	E	210	Gpa	Matweb
Poisson's Ratio	ν	0.346	-	Matweb
Shear Modulus	G	78	Gpa	Matweb
Yield Strength	σ_{ys}	885	Mpa	Mat. Certificate
Ultimate Tensile	σ_u	1010	Mpa	Mat. Certificate

The Simulation model (SIM-model) has a basic setup of constraints and 1D Connections. They were present in all the simulations. This consists of a fully fixed constraint of the end section of the torsion bar, Pinned constrains of the bar/arm junction, and two 1D Rigid Body Elements (RBE2) to substitute the wheel hub. See Figure 7.1. The RBE2s are basically used to connect a single node to multiple nodes, and it stiffens the structure where it is located. This allows for extracting reaction forces and the displacement from a single node in the simulation post-processor. Mesh details and constrains used are summarized in Table 7.6.

Table 7.2: 3D Mesh Details and Constraints

Mesh Details	
Element Type	Quad. Tetrahedral, CTETRA(10)
Element Size	8 mm
Number of Elements	32353
Basic setup Constraints and 1D elements	
Torsion bar end-section	Fully Fixed
Bar/Arm Junction	2x Pinned
Wheel hub Substitute	2x RBE2 1D elements

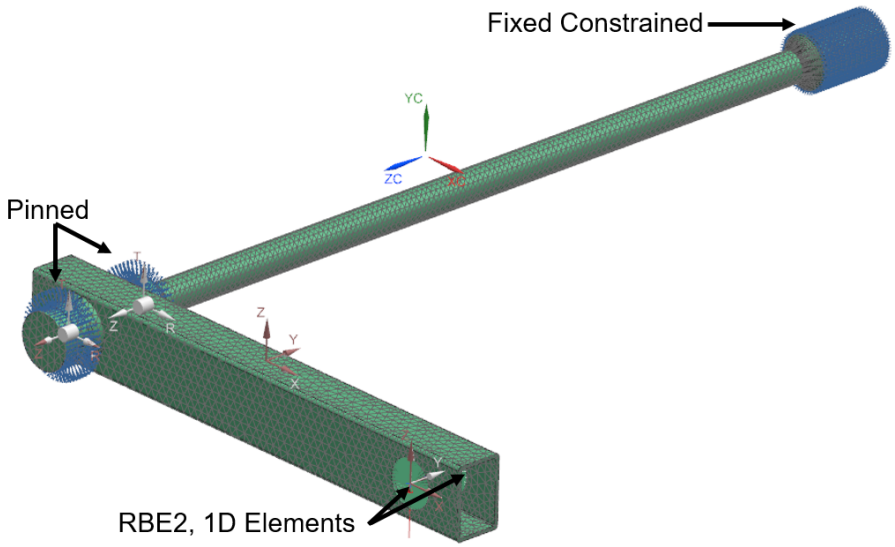

Figure 7.1: Simulation Constrains

SOL101 - Linear Statics

Solver 101 is a linear static analysis. This non-transient solver calculates the effect of static loading on a structure, where damping and inertia are ignored. Time varying load as gravity or accelerations are approximated as a static equivalent loads. The advantage of SOL 101 is that it is easy to configure, and the solution computation time is fairly low, as it only calculates one scenario. This is a good solver for a known load. The disadvantage is the lack possibility of generating a conservative load.

The simulation was performed by applying Force to the outer RBE2 element in the vertical direction. This was done three times with varying Force; 1000, 2000, and 3000 Newtons. This to confirm that the results are linear. The computation time of a simulation was 33 seconds. After the simulation, the vertical height was sampled from the RBE2 node. To make sure that the stress-sampling of the torsion bar was equal for all simulations, a Sample Group of 20 nodes was created and stored. They were random nodes situated away from the stress concentration. From this sample group, averaged elemental- and nodal- Von Mises stress was collected. See Figure 7.2. The stress concentration in the radius is sampled by the maximum elemental stress in the simulation. The results from the SOL 101 are displayed in Table 7.3. The results table shows that the result values are linear. At 3000N, the simulated height is 77.19mm. This is slightly higher than expected. The difference between the elemental stress in the torsion bar and radius gives a stress concentration factor of 1.29 in the radius.

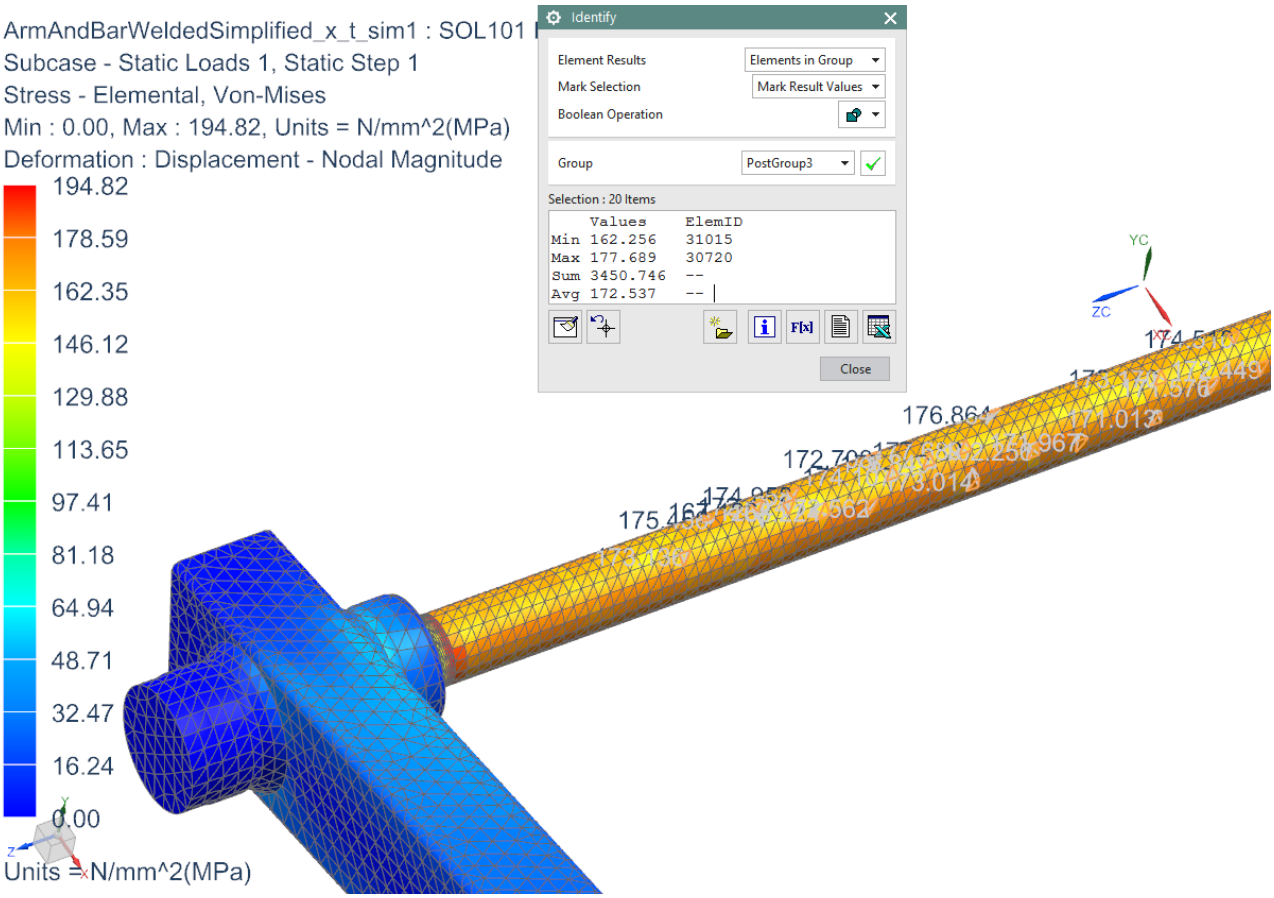

Figure 7.2: 20 Nodes to Sample Torsion Bar Stress

Table 7.3: SOL101 Results of 3D Elements Simulation

	SOL 101	**Linear Statics**	**3D Solid elements**	Run time: 33 sec
FORCE [N]	*Height [mm]*	*Elemental Stress [Mpa]*	*Nodal Stress [Mpa]*	*Radius: Elemental Stress [Mpa]*
0	0	0	0	0
1000	25,73	173	192	195
2000	51,46	345	384	390
3000	77,19	518	576	585
Norm. Results:	**25,73 mm/kN**	**173 Mpa/kN**	**192 Mpa/kN**	**195 Mpa/kN**

Transient Response

A transient analysis uses the equations of motion to compute the system response over a defined period of time, over a set of time-steps. It allows for using Enforced Motion to enforce displacement, and recover the stresses and reaction forces. By applying an enforced velocity instead of a static force, one can retrieve the system response for a series of equivalent loads (force) without running multiple static simulations, like the SOL 101.

Two different transient solvers have been used. SOL 109 Direct Transient, and SOL 112 Modal Transient. These are quite similar, but there is a significant difference: The direct solver 109 uses all the equations of motions in the computation. This gives good results, but requires a huge amount of CPU power as the equation solutions varies as the square or cube of DOFs[8]. This implies that the direct solver is great for smaller systems. On the other hand, the SOL 112 is a Modal analysis which can decouple the equations of motion. This allows for choosing which modes to compute. On a large system (many DOFs) this may save lot of computation time. Unfortunately, the suspension system is to small to induce a significant difference in computation time in this case. The time difference between the two is just 7%.

Both models have equal basic setup. A vertical enforced velocity 2mm/sec was assigned to the RBE2 element. The step increments was set to 2 seconds, with a total of 20 steps. This gives a total displacement of 80mm with 4 mm increments. This setup was a result of trail and error, due to stability problems. Lowering the velocity stabilized the system. In addition to this, Mode 1 was selected as the only mode to evaluate in SOL112. This is the mode which refers to the rotation of the torsion bar.

The results of these simulations can are displayed in Table 7.4 and 7.5. Here, Height is capitalized as it is the governing variable. The force is sampled as the vertical reaction force in the RBE2 node. The stresses are sampled with the same node-group as in SOL 101.

The results shows that the Direct SOL 109 and Modal SOL 112 generates exactly the same linear results in this case. Compared with the static SOL 101, they produce equal normalized displacement stiffness of 25.73mm/kN, but with a marginal difference considering the stresses.

Table 7.4: SOL109 Direct Transient Response of 3D Elements Simulation

	SOL 109	**Direct Transient**	**3D Solid elements**	
	Setup:	velocity: 2mm/sec	2sec inc. / 20 Steps	Run time: 153 sec
Reaction Force [N]	*HEIGHT [mm]*	*Elemental Stress [Mpa]*	*Nodal Stress [Mpa]*	*Radius: Elemental Stress [Mpa]*
0	0	0	0	0
622	16	108	119	121
1244	32	216	239	242
1865	48	324	359	363
2488	64	432	478	484
3109	80	540	597	605
Norm. Results:	**25,73 mm/kN**	**174 Mpa/kN**	**192 Mpa/kN**	**195 Mpa/kN**

Table 7.5: SOL112 Modal Transient Response of 3D Elements Simulation

	SOL 112	**Modal Transient**	**3D Solid elements**	
	Setup:	velocity: 2mm/sec	2sec inc. / 20 Steps	Run time: 143 sec
Reaction Force [N]	*HEIGHT [mm]*	*Elemental Stress [Mpa]*	*Nodal Stress [Mpa]*	*Radius Elemental Stress [Mpa]*
0	0	0	0	0
622	16	108	119	121
1244	32	216	239	242
1865	48	324	359	363
2488	64	432	478	484
3109	80	540	597	605
Norm. Results:	**25,73 mm/kN**	**174 Mpa/kN**	**192 Mpa/kN**	**195 Mpa/kN**

7.2 1D Beam Elements Simulation Setup

There are multiple benefits to run a 1D element simulation, where time and cost (in a professional setting) are the two major factors. It is simple and quick to setup and generate a model, and the reduction of degrees of freedom and elements, results in a drastic reduction of computation time. The objective with the 1D simulation is to demonstrate the simplicity of performing such a simulation, relative to the result accuracy. The solvers utilized are the same at in the 3D solid simulation. In a 1D simulation, all unnecessary features are neglected, and only the crucial elements are idealized and assessed. In this case, the model has been reduced and idealized to the absolute minimum. The model used to simulate the suspension system, is solely represented by the sketch in Figure 7.3. The torsion bar is idealized to a length of 650mm, and the torsion arm is 350mm.

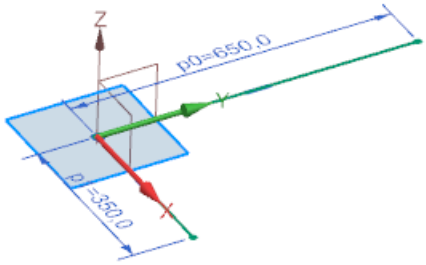

Figure 7.3: 1D Model Sketch

To give the model virtual stiffness, two cross-sections was created in the Beam Section Manager in the FEM-file. A rod-section of Ø25.25mm for the torsion bar, and a Box-section for the torsion arm. These were designated to the model in the Physical Properties Table Manager as PBEAM type, with S165M as material. The model was the meshed with 1D mesh with only 1 element in each section. This gives the model a total of 3 nodes. In the Sim-file, the model was constrained with two different constraints. The end section of the torsion bar, Node (1), was fully fixed. See Figure 7.4. The bar/arm junction node, Node (2), was fixed in all Defrees of Freedom besides the DoF 5, - the rotation around the torsion bar. The load/velocity was applied in Node (3).

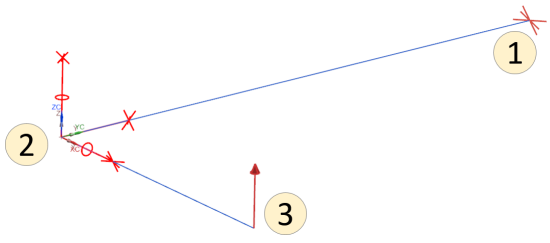

Figure 7.4: 1D Model Constraints, Node numbering

Table 7.6: 1D Mesh Details and Constraints

Mesh Details	
Element Type	PBEAM
Number of Nodes	3
Number of Elements	2

Simulation

The three solvers, SOL101 Linear static, SOL109 Direct Transient, and SOL112 Modal Transient, was also used on the 1D beam model to run the simulations. Again, SOL 101 was simulated three times with 1000, 2000, and 3000 Newtons. The transient solvers' setup was an enforced velocity of 80mm/sec on the torsion arm end node. The time-step was set to 1/30 second, with 30 steps.

The sampling of the simulation results was done in the post-processor. The displacement, force and nodal rotation was easily found in the post process navigator, but to sample the stress, it was necessary to apply the Beam Cross-section view to specific node to display the stress. Figure 7.5 displays the torsion bar stress when Beam Cross-section view is used. It shows the radial increasing stresses in the virtual cross-section.

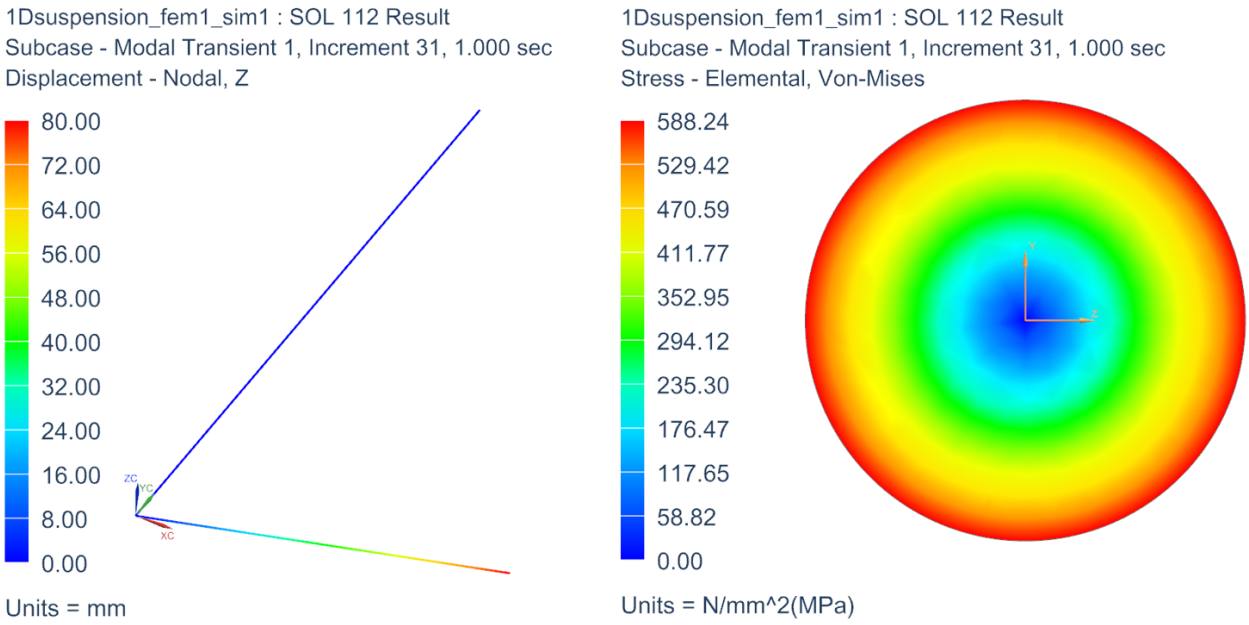

Figure 7.5: 1D SOL 112 Post-Processor; Displacement, and Nodal Stress at 80mm

The results of the simulations are displayed in Table 7.7 and Table 7.8. As SOL 109 and SOL 112 once again produced equal results, they are combined into the same Table. The first comment to the simulations is the computation time. All the simulations used less than a second to run. -Which shows the advantage of running a 1D simulation. The normalized results shows that all the solvers produce equal linear stiffness of 26,08 mm/kN. Which is 1.3% softer than the 3D simulation. A notable effect of the linear simulations is the nodal rotation; It is equally linear as the height. Physically, this makes little sense as the height is a Sine-function of the rotation . This may indicate that these solvers are is preferably reserved for simulation of small angular rotations. An other drawback of the 1D simulation is the missed possibility of measuring the stress concentration factor, as the radii in the torsion bar are not present.

Table 7.7: SOL 101 Simulation Results 1D Beam Elements

	SOL 101	**Linear Statics**	**1D Beam Elements**
Setup:	Applied Force		Run time: <1 sec.
FORCE [N]	*Height [mm]*	*Nodal Stress [Mpa]*	*Nodal Rotation,θ [Deg.]*
0	0	0	0
1000	26,08	192	4,3
2000	52,16	384	8,6
3000	78,25	575	12,9
Norm. Results:	**26,08 mm/kN**	**192 Mpa/kN**	**4.3 deg/kN**

Table 7.8: SOL 109 & 112 Simulation Results 1D Beam Elements

	SOL 109 and SOL 112	**Transient Response**	**1D Beam Elements**
Setup:	velocity: 80mm/sec	1/30sec inc. / 30 Steps	Run time: <1 sec.
Reaction Force [N]	*HEIGHT [mm]*	*Nodal Stress [Mpa]*	*Nodal Rotation,θ [Deg.]*
0	0	0	0
613	16	118	2,6
1227	32	235	5,3
1840	48	356	7,9
2453	64	471	10,6
3067	80	588	13,2
Norm. Results:	**26,08 mm/kN**	**192 Mpa/kN**	**4.3 deg/kN**

7.3 Results and Comparison with Analytical and Physical Test

Height - Load Relationship

The virtual simulations Height/Load results are best evaluated the context of the physical and analytical results. Figure 7.6 and 7.7, where the first figure shows the full force-range, and the second shows the top end interval. As all the three 3D and 1D solver generated equivalent results, they are combined into two groups in the graphs; 1D and 3D Simulations. The first thing to notice is the correlation between the 3D simulation and the idealized exam model. (only visible in Figure 7.7) They are equivalent stiff in terms of [mm]/[kN]. Initially it was expected that this correlation would be between the 1D Simulation and the idealized analytical model, not the 3D. Comparing the simulation with the physical test results also shows that the linear simulation results drifts of from the physical testing as the height increases. At 2940 Newtons the deviations are 5.7% in the 3D, and 7.2% in the 1D simulation. But when comparing with all the results at smaller rotation angles produced below 1200 Newtons ($\theta \approx 5deg$) all the approaches, except the 1D simulation, produces results within a 2% deviation of each other.

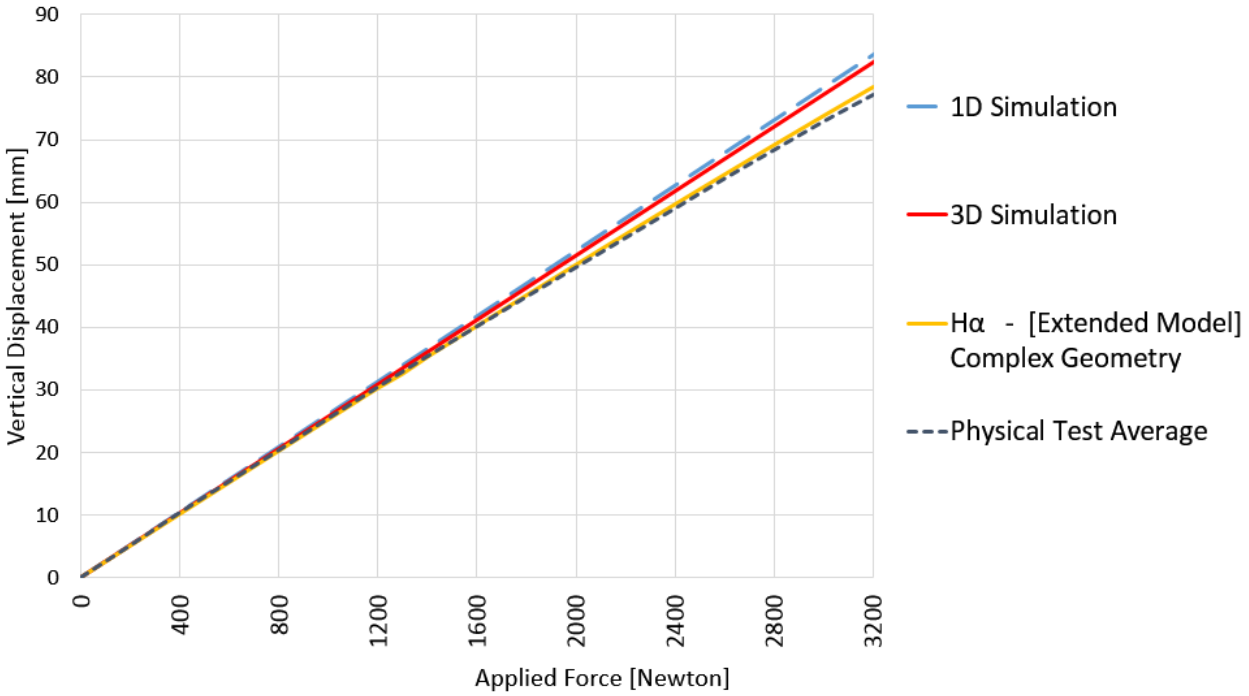

Figure 7.6: Height/Load: Simulation Results vs Analytical, and Physical Test

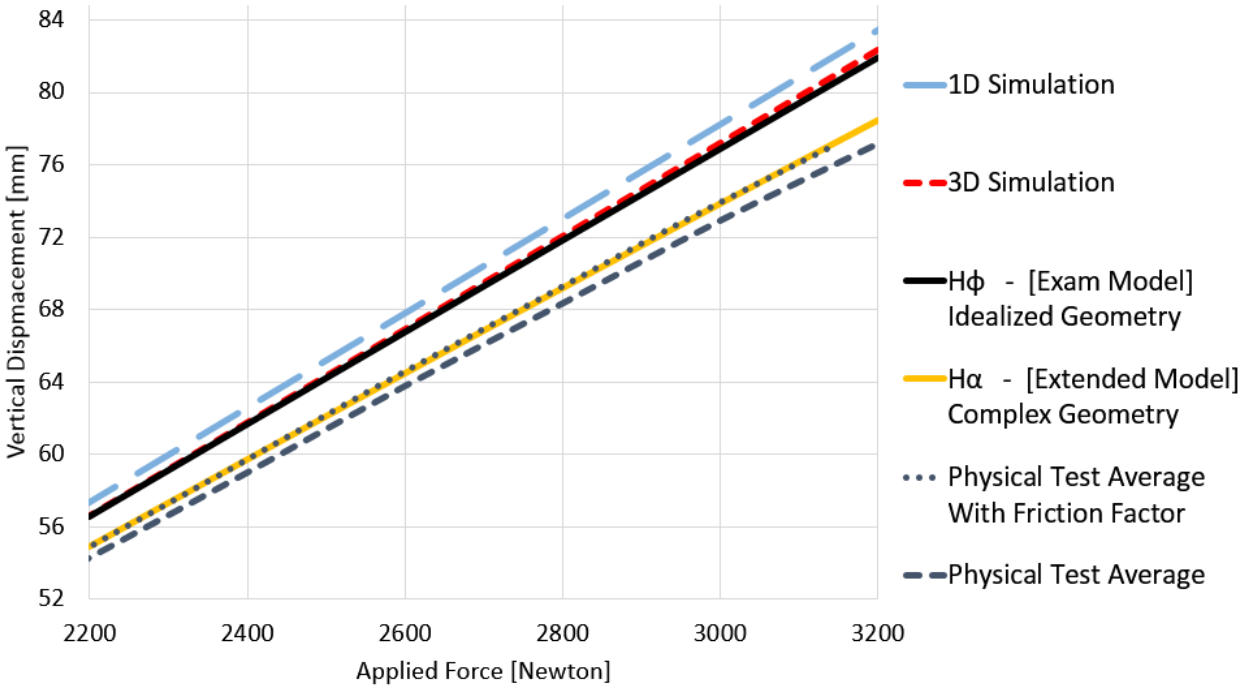

Figure 7.7: Height/Load: Simulation Results vs Analytical, and Physical Test. 2200 - 3200N

Stress

Plotting the Von Mises stress' from the uniform section of the torsion bar, Fig. 7.8, shows that the 3D- and 1D- nodal Von Mises stresses are equal. - Closely followed by the slightly lower values produced by the Extended Analytical Model. The results that stands out is the 3D Nominal Elemental stress. It is produces significant lower values (9%) than the 3D and 1D Nodal simulations. Often, it is assessed that the elemental stress is the "correct" stress in a simulation, considering that it is less affected by single-nodal extremal stains. The basis for these low elemental values, may be found in the elemental theory. Because the elemental stress is a average result of all the nodal stresses in that element. And when considering pure torsion theory, the stresses increases linearly along radius. This causes the inner nodes of the element to be subjected to less stress/stain than the outer nodes. This results in a lower average elemental stress, than the actual surface stress. So in this case, a uniform torsion bar, it is evaluated that the nodal stress gives the best and conservative results. Evaluating the physical test results versus the simulation, the physical test result gives lower values than the simulations (nodal). This is as expected as the simulations are linear. In addition, The friction factor discussed in Section 6.3, may influence the results. Which would push the physical test results closer to the simulation and analytical results. Although the simulated stresses are not spot on the physical test results, they give a close and conservative approximation, which is important considering material strength and durability.

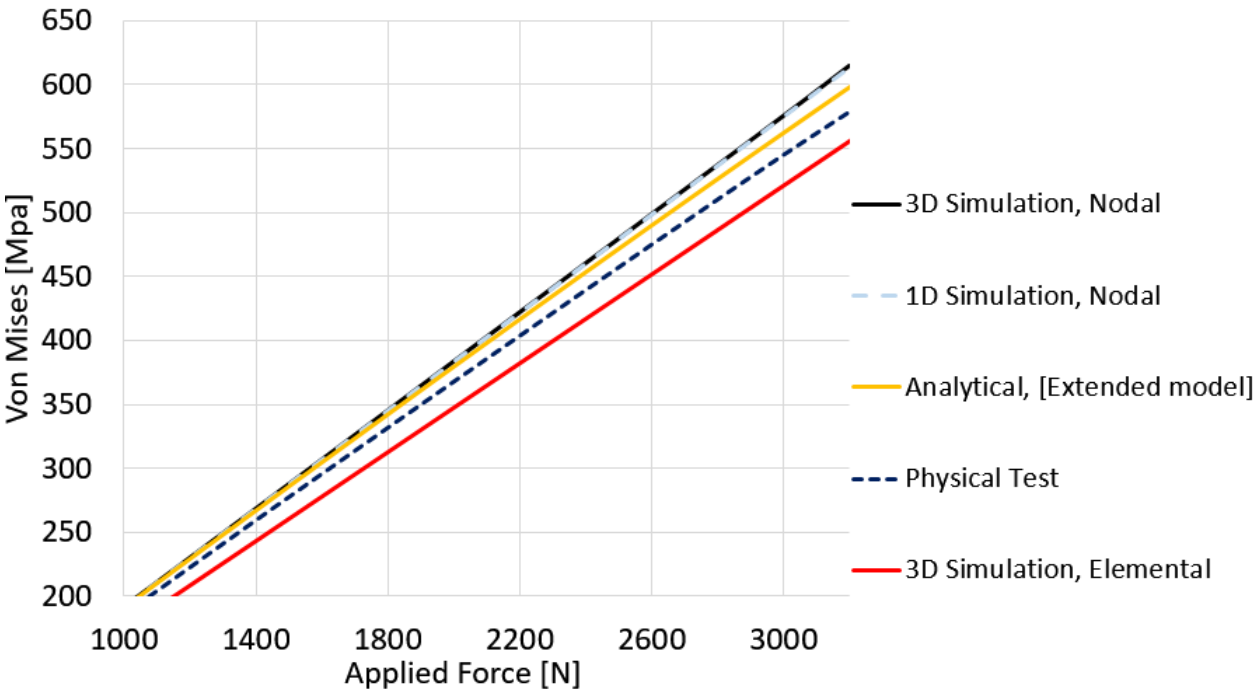

Figure 7.8: Nominal Von Mises Stress: Simulation Results vs Analytical, and Physical Test

Evaluation

The deviations between the simulations and the analytical and physical results observed above, may indicate that the solvers and/or the simulation setup used are not perfectly suited for this case where there are larger rotations. Other solvers than those described above were also tested to try to recreate the physical non-linearity of the height/load relationship. This includes the SOL106 Nonlinear Statics, and SOL129 Nonlinear Transient Response. Also in this case, the SOL106 produced equal results to the linear SOL101. Concerning the SOL129, the simulation ran for 24 hours without finishing. At this point the simulation was aborted. To conclude; the ambition to recreate the physical height/load response with virtual simulation has just partially succeeded. The simulation results for both the 1D and 3D simulations provides accurate at low angular rotation, but due to the linearity, they do not provide precise results when the angular rotation becomes large.

7.4 Fatigue

As the torsion bar is subjected to large cyclic stresses, a fatigue analysis was performed. The torsion bar is subjected to zero-to-tension (R=0), see Fig. 7.9, which is disadvantageous in terms of crack growth. The ambition with the fatigue analysis is to estimate the number of times the rig withstands the maximum loading of 3200N. The analysis was done in an embedded module in Siemens NX. The analysis module is found in the $SimulationNavigator$, by right clicking on the Sim-file $\rightarrow NewSimulationProcess \rightarrow Durability$. This creates a new fatigue simulation file in the the Simulation Navigator. This file is then linked to a previously performed simulation. In this case a 3D static SOL 101 at 3200 Newtons. When performing a fatigue analysis, it is necessary with material fatigue parameters. Unfortunately, the S165m steel used in the torsion bar is an uncommon steel. Due to this, it was unattainable to obtain the correct fatigue parameters. Instead, fatigue parameters from a steel with equivalent mechanical properties was selected. The material fatigue parameters was then included in the material physical properties in the FEM-file prior to solving the SOL 101. The parameters are displayed in Table 9.1. Before solving the fatigue analysis, different analysis parameters needs to be chosen, Fig. 7.10. This includes a Notch Factor, K_f, which is a factor that compensates for the geometric variation in the R10 radius. The K_f was found to be $K_f \approx 1.14$ [9]. To be conservative, Morrow equivalent mean stress was selected. As the Fatigue Strength Coefficient, σ'_f, is obtained for the material, Morrow is a quite good approximation [10], and is therefore chosen over Goodman and Smith-Watson-Topper (SWT). The Loading pattern was also defined, Figure 7.11. Full unit cycle was selected. By setting an offset of 0.5 sets the mean stress to be $\sigma_m = \frac{1}{2}\sigma_{max}$. This generates a R=0 loading pattern.

Table 7.9: Fatigue Parameters and Simulated Maximum Stress

Torsion Bar Fatigue Parameters			
Yield Strength	σ_{yt}	885	Mpa
Ultimate Tensile Strength	σ_{ut}	1010	Mpa
Fatigue Strength Coefficient	σ'_f	1454	Mpa
Fatigue Strength Exponent	b	-0.08	
Fatigue Ductility Coefficient	ϵ'_f	1.85	
Fatigue Ductility Exponent	c	-0.72	
Cyclic Yield Strength	σ'_s	716	Mpa
Cyclic Strength Coefficient	K'	1367	Mpa
Cyclic Strain Hardening Exponent	n'	0.10	

Static SOL 101, Maximum Stress at 3200 Newtons			
Elemental, Stress consentrarion	$\sigma_{max,El}$	623.6	Mpa
Nodal, Stress consentrarion	$\sigma_{max,No}$	728.8	Mpa

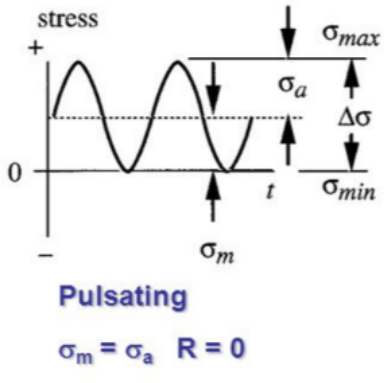

Figure 7.9: Zero-to-Tension, Cycles between 0 and σ_{max}

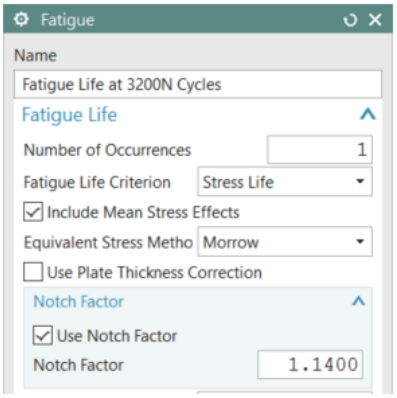

Figure 7.10: Fatigue Analysis Parameters

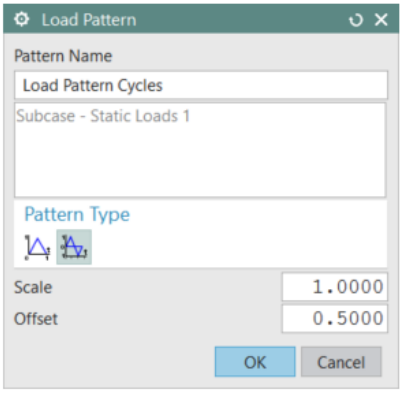

Figure 7.11: Load Pattern, Full Cycles with 50% Offset

Fatigue Simulation Results

Table 7.10: Cycles to Failure Results

Life Time Simulation Results	
Notch Factor, K_f	Cycles to Failure, N_f
1.14	$N_f = 2.50 \cdot 10^5$
1 [not inc.]	$N_f = 8.57 \cdot 10^5$

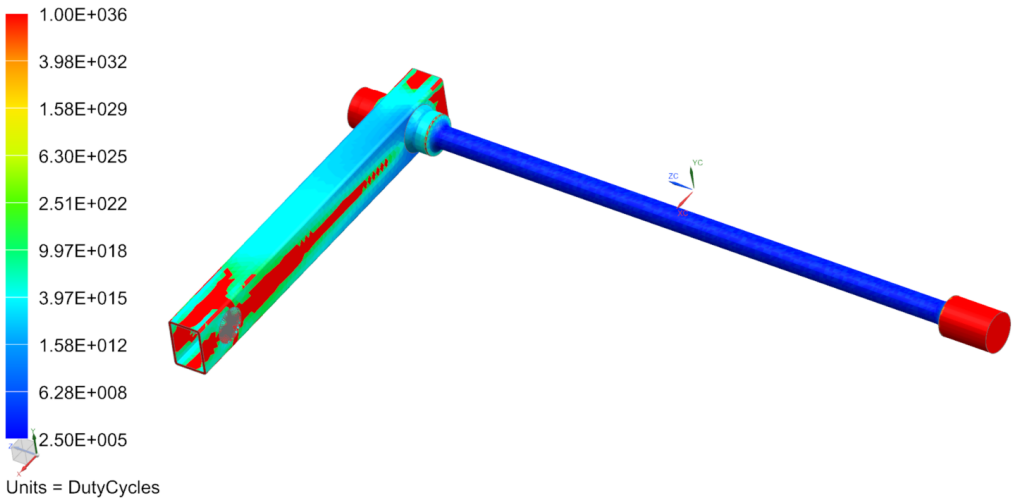

Figure 7.12: Cycles to Failure. Zero-to-Tension (F = 3200N)

The results of the fatigue simulation are displayed in Tab. 7.10 and Fig. 7.12. Included the Notch factor, the estimated number of Cycles to Failure are 250,000. Even though, the correct material fatigue parameters was not obtainable, a S-N diagram for the S165M from the steel manufacturer Industeel was found. When inserting the maximum elemental stress of 623.6 Mpa into to

the S-N diagram, Figure 7.13, it estimates a lifetime of approx. $4 \cdot 10^5$ Cycles. This value is between the simulation values of $2.5 \cdot 10^5$ cycles included notch factor, and $8.57 \cdot 10^5$ without notch. This implies that the simulation included the notch factor is a good conservative estimation of the life time of the rig. This is lower than what leads to infinite life time (10^7 cycles), but this implies that the torsion bar is not going to fail due to fatigue during its life time in service at NTNU, with a maximum of a few hundred cycles a year.

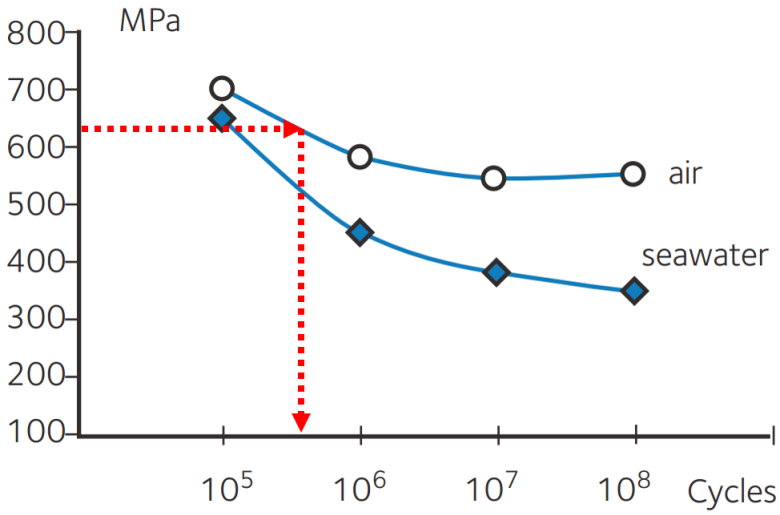

Figure 7.13: S-N diagram for S165M [Pic: Industeel [1]]

Chapter 8

Dynamic Response

The exams feature an exercises regarding the dynamic response of the suspension system. This in terms of the undamped natural frequency, and required dampening factor for a given excitation. The geometry is idealized by a 9kg mass where the wheel hub is situated 350 mm from the torsion bar. The rest of the system is assumed mass-less. This results in a undamped natural frequency, f_n = 10.48 [Hz], corrected for material properties and torsion bar diameter of the build rig, Eq. 8.1-8.2. The ambition in this chapter is to perform physical tests, simulations, and analytical calculations to evaluate the correlation between the results of the different approaches. As the dynamic response is not primary purpose of the rig, it is not equipped with a damper. So in accordance with the stipulated dynamic KIP, only the natural frequency is evaluated.

$$k = \frac{G \cdot I_p}{l^2 \cdot L} = \frac{78000 \cdot (\pi \cdot 25.25^4/32)}{350^2 \cdot 650} = 39.09\,[N/mm\ rad] \tag{8.1}$$

$$\omega_n = \sqrt{\frac{k}{m}} = \sqrt{\frac{39.74 \cdot 1000}{9}} = \underline{\underline{65.90[rad/sec] \rightarrow f_n = 10.48[Hz]}} \tag{8.2}$$

To physically emulate the idealized geometry, an extra wheel hub weight of 4.4kg has been constructed. See Fig. 8.1. When it is bolted to the wheel hub, it totals a static weight of 9 kg at the wheel hub. This weight includes half the mass of the torsion arm (0.9kg), wheel hub (3.7kg), and the extra weight (4.4kg). The wheel hub and extra weight adds to 8.1 kg. This mass is considered to be concentrated, whilst the torsion arm is considered to have dispersed mass. As the entire torsion arm is only 18% of the total dynamic mass, it was assumed that the static weight of 9kg emulates the idealized model where all the mass (9kg) is concentrated.

PARTS LIST			
ITEM	QTY	PART NUMBER	MATERIAL
1	1	Rim Hub	Steel S355
2	1	Rim Ring	Steel S355

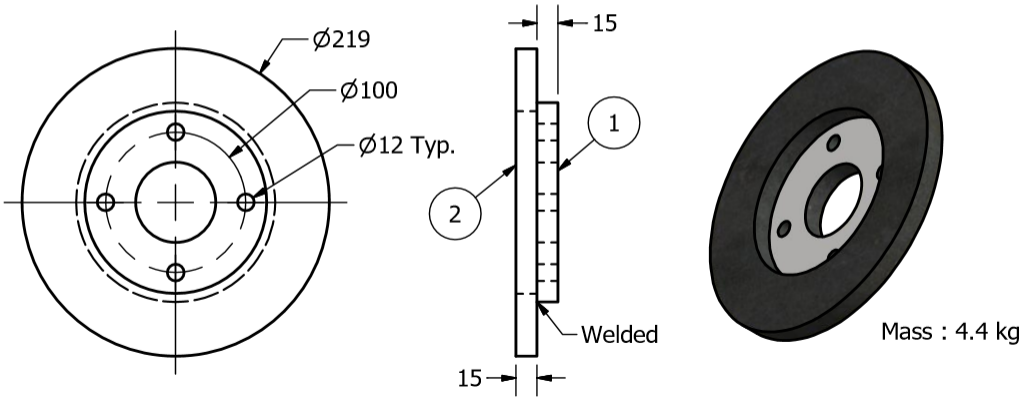

Figure 8.1: Technical Drawing of the Wheel Hub Weight

8.1 Analytical Approach

The calculation performed in this section confirms that the assumption that static weight of 9kg included the dispersed mass of the torsion arm, is a good approximation to the idealized geometry. The calculation is performed by using the Moment of Inertia of the different components. In this approach the undamped natural frequency relies on a torsional spring constant, κ_t and the Moment of inertia, I.

$$\omega_n = \sqrt{\frac{\kappa_t}{I}} \tag{8.3}$$

$$\kappa_t = \frac{G \cdot J_t}{L} \Rightarrow \frac{G}{L} \cdot \frac{\pi \cdot D^4}{32} = \frac{78000}{650} \cdot \frac{\pi \cdot 25.25^4}{32} = 4788780\,[Nmm/rad] \tag{8.4}$$

$$I = I_{arm} + I_{Hub+Weight} \tag{8.5}$$

The moment of inertia, I, Eq. 8.5, is the sum product of the torsion arm and the concentrated mass of the wheel hub and extra weight. The torsion bar is neglected, as the contribution is minimal, $\approx 0.1\%$ of the total I. The Parallel axis theorem is applied to the torsion arm and hub mass. m is the total weight-, and l_{tot} is the overall length, of the torsion arm. M is the mass of the wheel hub and the extra weight. M is considered to be a concentrated mass. Eq. 8.6 - 8.7.

$$I = \left[\frac{1}{12} m \cdot l_{tot}^2 + m\left(\frac{l}{2}\right)^2\right] + [M \cdot l^2] \tag{8.6}$$

$$I = \left[\frac{1}{12} 1.8 \cdot 450^2 + 1.8\left(\frac{350}{2}\right)^2\right] + \left[8.1 \cdot 350^2\right] = 1077750[kg \cdot mm^2] \tag{8.7}$$

$$\omega_n = \sqrt{\frac{4788780 \cdot 1000}{1077750}} = \underline{\underline{66.66[rad/sec] \rightarrow f_n = 10.61[Hz]}} \tag{8.8}$$

The result of this approach gives similar undamped natural frequency, f_n, as the idealized model at 9kg. 10.61 Hz vs. 10.48 Hz. This implies that the physical rig should behave close to the idealized model, and that idealized model is a good approximation when the dispersed mass is small (18%) of the total, as in this case. Numeric result values for the natural frequencies are displayed in Tab. 8.1. This also shows the computed frequencies without the extra weight and hub.

Table 8.1: Frequency Results with Different Mass

Frequencies Result, Moment of Inerta Approach

$f_n =$	Without Hub	With Hub	With Hub + Extra Weight
	37.67 Hz	15.0 Hz	10.61 Hz

8.2 Frequency Simulation

The dynamic response simulation was performed in NX with SOL 103 Real Eigenvalues (SOL 103RE). This solver determines the mode shapes and natural frequencies, [11]. The simulation is independent of applied forces, and relies only on the constraints to run. The frequency simulation was performed on thee different models; The model with only the torsion arm, a model with the wheel hub, and with the extra hub weight. See Fig. 8.2. The SOL 103RE allows for extracting specific modes to reduce the simulation time. In this case it is mode shape 1 which the desired one, also called the fundamental frequency. The simulation time was 1:08 min. The results are displayed in Table 8.2. The results are close to both the analytical results.

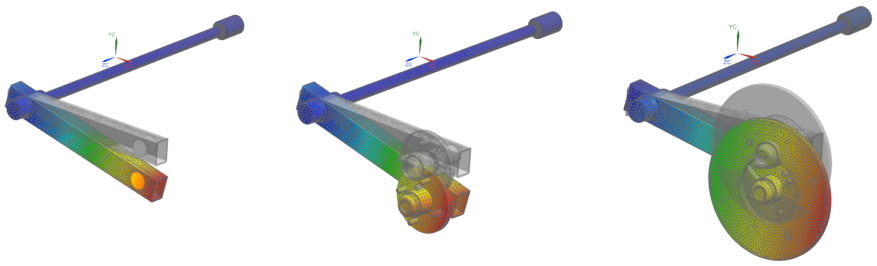

Figure 8.2: Frequency Simulation Models

Table 8.2: Frequencies with Different Simulated Mass

	Fundamental Frequency Simulation Results		
	Without Hub	With Hub	With Hub + Extra Weight
$f_n =$	37.17 Hz	14.90 Hz	10.39 Hz

8.3 Physical Testing

To obtain the natural frequency of the physical rig, the torsion arm is given a short pulse to induce the oscillation. This was sufficiently done by punching the end of the torsion arm by hand. The test was performed both with and without the extra hub weight. To collect the data, the Catman software was used to sample and process the accelerometer data. The sample rate was increased from 50 to 300 Hz to capture the oscillation. An embedded frequency analysis in Catman was then used to live monitor the frequency subjected to the accelerometer. This was adjusted to display the Root mean square (RMS) frequency amplitude, averaged every second. This makes it easy to visually identify the natural frequency. Figure 8.3 and 8.4 are screen-shots from Catman during the tests. The spike in each graph identifies the natural frequency. The

results are equal to what to expect considering the previous simulation. Numeric vales are found in Table 8.3

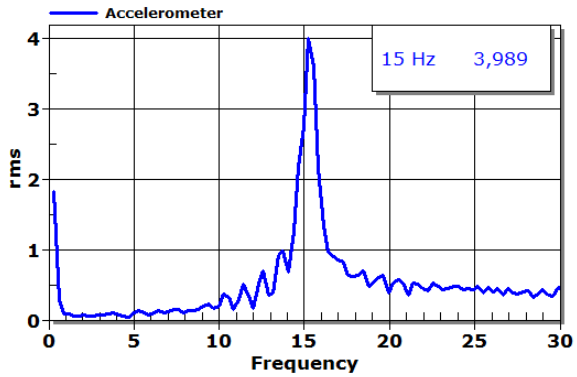

Figure 8.3: Natural Frequency: Only Wheel Hub

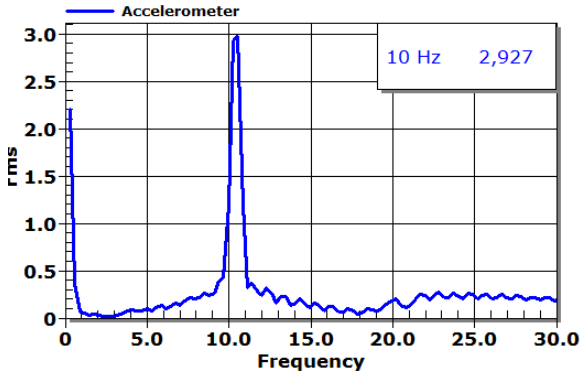

Figure 8.4: Natural Frequency: Wheel Hub And Extra Weight

Table 8.3: Frequencies Obtained from Physical Testing

	Frequencies Result, Physical Test		
	Without Hub	With Hub	With Hub + Extra Weight
$f_n =$	N/A	≈ 15.1 Hz	≈ 10.5 Hz

8.4 Evaluation of the Results

The results of the different approaches to obtain the natural frequency are combined in Table 8.4. The important fact to point out is the consistency of the results between the different approaches. This also shows that the idealized model presented in the exam is a great method for obtaining the natural frequency in this case. The comparison indicates that both an analytical approach and virtual simulation produces results that coincides with the a real physical test. Which of the methods to recommend to use i practise depends on the situation. If you have the CAD model and software, the 103RS Solver should be preferred. If not, the idealized analytical method is fast to solve, and accurate, in this case.

Table 8.4: Natural Frequency Results from all Approaches

	Natural Frequency, f_n, Results		
	Without Hub	With Hub	Hub + Extra Weight
Analytical: Idealized Geometry	N/A	14.79 Hz	10.58 Hz
Analytical: Moment of Inertia	37.67 Hz	15.0 Hz	10.61 Hz
Simulation: SOL 103RE	37.82 Hz	15.14 Hz	10.55 Hz
Physical Tests	N/A	≈ 15.1 Hz	≈ 10.5 Hz

Chapter 9

Suspension Test Rig Exercises Suggestion

In this chapter, student exercises suggestions linked to the suspension test rig has been created. The exercises are created for three different courses at IPM, TMM4112 - Machine Elements, TMM4135 - Analysis and Assessment Based on the Finite Element Method, and TMM4155 - Finite Element Applications in Mechanical Engineering. The exercises are mostly based on work performed in this thesis, with a few exceptions. The exercises are divided into three different sections, one for each respective course. The course content are presented initially in each section.
An operation manual in how to perform static and dynamic physical testing has been created. This manual is found in the appendix under Appendix C, *Physical Test Manual*. Proposed solutions for the exercises are found in Appendix D. FEM-models and Simulations for conducting relevant exercises are sent to supervisor Terje Rølvåg.

9.1 TMM4112 - Machine Elements - Exercises Suggestion

Course content *Basic functions of machines and machine elements. Mechanical integrity. Fatigue design: including Wöhler curve and Haigh diagrams, Reduction factors, Stress concentrations, Multi-axial stresses, Spectrum fatigue lifetime. Machine and rotor dynamics: Spring supported machines, critical speed/rpm, static and dynamic balancing. Mechanisms and transmissions: Mechanics of the screw, gears. Couplings and brakes. Bearings: roller bearings, bearing design, life time assessment. Springs: torsion, coil, leaf, ring and rubber springs. Press and shrink-fit connections: deformation of thick-walled tubes, tolerances and fits. Bolts: threads, load carrying capacity, pretension, tightening/torque moment, bolt diagram. Welded joints: static and fatigue analyses.* [12]

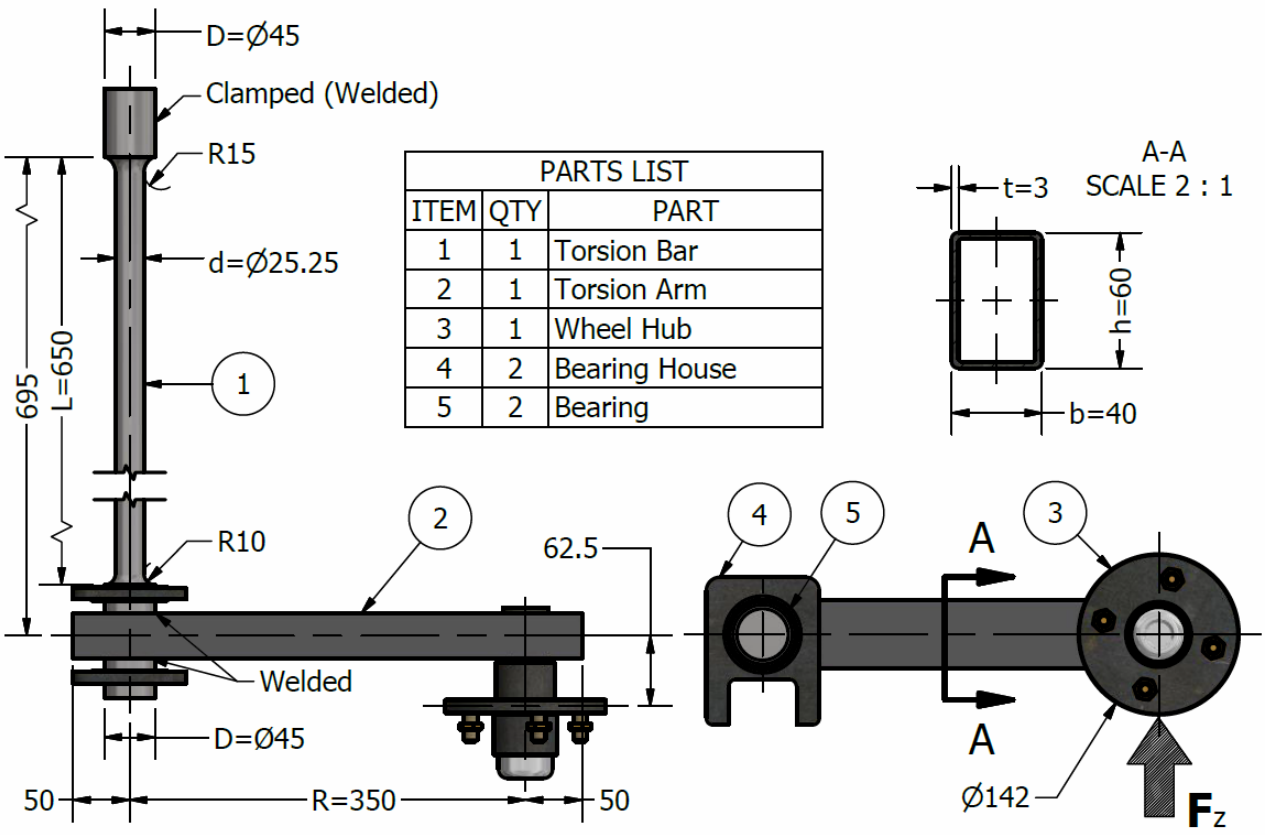

Figure 9.1: Technical Drawing of the Suspension System

Static Response

A suspension system consisting of a torsion bar, torsion arm, wheel hub, and bearings is to be evaluated. See Figure 9.1. The torsion bar material data: E-modulus: 210Gpa, G-modulus: 78Gpa, Yield-strength: 885Mpa. Poisson: 0.346. The torsion arm and bearings can be considered to be infinite stiff. The force is applied vertically on the wheel hub. The torsional length is assumed to be L=650mm with a constant cross-section of 25.25mm.

1a) Calculate the torsion angle, θ, and the vertical elevation height of the wheel hub, H, when F_z =1000N, 2000N, and 3200 Newtons are applied. Assume small angular displacement.

1b) Calculate the corresponding maximum stress (Von Mises) in the torsion bar, assumed the torsion bar is subjected to pure torsion at $F_z = 3200N$. What is the maximum allowed force considering yield?
Principal stress:

$$\tau_{xy} = \frac{T \cdot r}{I_{p,bar}} \approx \frac{FR \cdot r}{I_{p,bar}} \tag{9.1}$$

If small angular displacement is not assumed, the suspension system will not respond linear at large torsion angles, due to the decreasing distance between the torsion arm and applied force, generating less torque. $M = FRcos\theta$

2a) What is this kind non-linear suspension called?

The real torsion angle, ϕ can be found by solving a transient equation:

$$\phi = \frac{FRLcos\phi}{GI_p}$$

2b) Find ϕ and the corresponding height, H_ϕ, for F_z =1000,2000,3200 newtons. What is the height deviation in percent between the two calculation models at 1000, 2000 and 3200? Tips: solve the transient equation with Wolfram|alpha etc.

2c) Estimate the total height at 3200N if a non-infinite stiff torsion arm is included. The total height can be estimated by:

$$H_{tot} = H_\phi + H_{arm}$$

Where:

$$H_{arm} = \frac{F_\phi \cdot R^3}{3EI_x} \cdot cos\phi, \quad F_\phi = F_z \cdot cos\phi$$

2d) Perform Physical testing according to the *Physical Test Manual* and compare the results.

Natural Frequency

The physical test rig is equipped with an attachable wheel hub weight with an unknown mass. The the task is to estimate that mass by combining physical testing with numerical calculations. The torsion arm mass, m = 1.8kg. The mass of the wheel hub is $M_{wh} = 3.7kg$.

3a) Use the Moment of inertia, I, to calculate the undamped natural frequency of the suspension system without the unknown extra weight. The wheel hub, M_{wh} can be considered as a concentrated mass, whilst the torsion arm, m is dispersed mass. The torsion bar mass can be ignored.

$$\omega_n = \sqrt{\frac{\kappa_t}{I}} \tag{9.2}$$

$$\kappa_t = \frac{G \cdot J_t}{L} \tag{9.3}$$

3b) Perform physical dynamic testing according to the Physical Test Manual, to obtain the natural frequencies with and without the extra weight.

3c) Comment the relationship between the physical testing and the numerical estimate.

3d) Use the obtained frequency from the testing to estimate the mass of the extra wheel hub weight, M_{ex}.

Fatigue

The torsion bar is subjected to large cyclic stresses over its lifespan of testing. A test cycle is defined as 0 - 3200N - 0 Newtons. Material data for the torsion bar is found in Physical Test Manual.

4a) Describe and give values to the following nominal stress variables in terms of fatigue: S_{max}, S_{min}, S_a, S_m,and the stress ratio R. Hint: Exercise 1.

4b) The radii on each end of the torsion bar creates a geometric stress concentration which needs to included in a fatigue analysis. This is included in terms of a Stress concentration factor, k_t. Estimate the k_t for the R10 radius, from the graph in Figure 9.2. Geometric values are found in Figure 9.1. Hint: The graph must be extrapolated, so it is just an estimate.

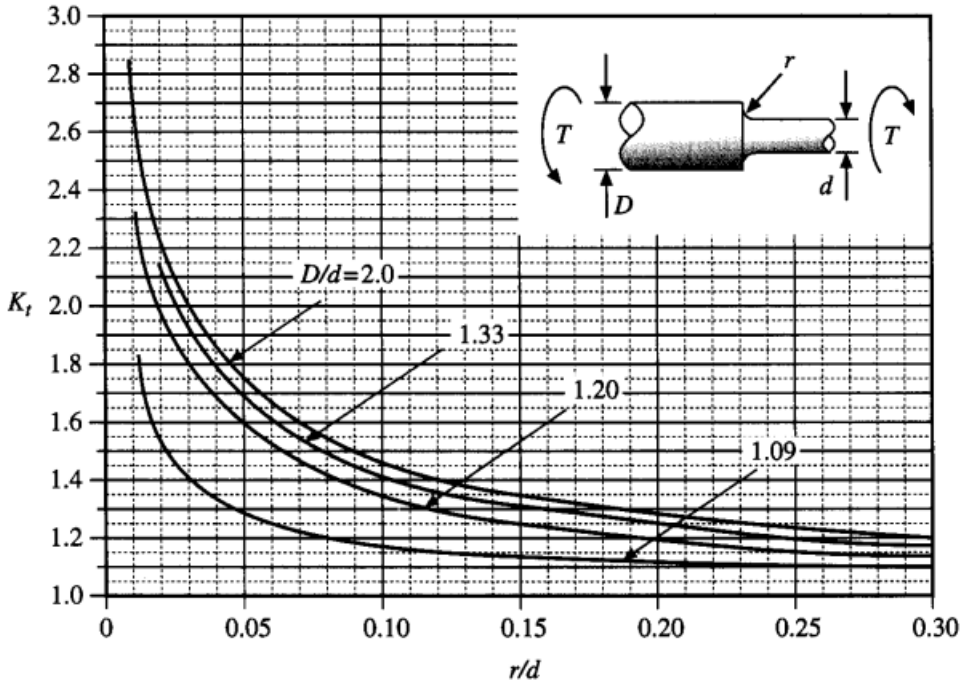

Figure 9.2: Stress Concentration Factor [Fig. 2-11, Peterson]

To be conservative, the stress, σ can be assessed to be $\sigma = k_t \cdot S$. This incorporates the effect of the stress concentration.

4c) Calculate the number of times the torsion bar can be subjected to the this force before failure, N_f. Assume High cycle fatigue, and use Morrows modified Basquin's equation, Eq.9.4. Solve with and without the stress concentration factor. The Fatigue strength coefficient, $\sigma'_f = 1454Mpa$. Fatigue Strength Exponent, $b = -0.08$.

$$\sigma_{ar} = \sigma'_f (2N_f)^b \tag{9.4}$$

$$\sigma_{ar} = \frac{\sigma_a}{1 - \frac{\sigma_m}{\sigma'_f}} \tag{9.5}$$

9.2 TMM4135 - Analysis and Assessment Based on FEM - Exercises Suggestion

Course content *Idealising of mechanical components. Boundary conditions. Elementary analysis of circular plats and cylinder shell. Element and system matrices for FE beams and plates. Compatible and non-compatible finite elements. Element requirements. Convergerce. Error estimate. Numerical integration. Isoparametric elements. Consistent load. Vibration. Heat transfer. Project assignment (weight 1/3): Modelling and analysis of mechanical products on the computer. Analysis result evaluation.* [13]

Physical Testing

Conduct Physical static testing of the suspension system according to the $PhyiscalTestManual$.
1) Sample the values for vertical displacement and rotation at 1000, 2000, 3000N.

Analytical FEM

The suspension system can be idealized as two elements: Element (1) - torsion bar, and Element (2) - torsion arm. The torsion bar has a torsion stiffness of GJ and a length L_1. The torsion arm has a bending stiffness of EI and length L_2. The force F is applied vertically at the end section of the torsion arm. Assume small angular deflection.

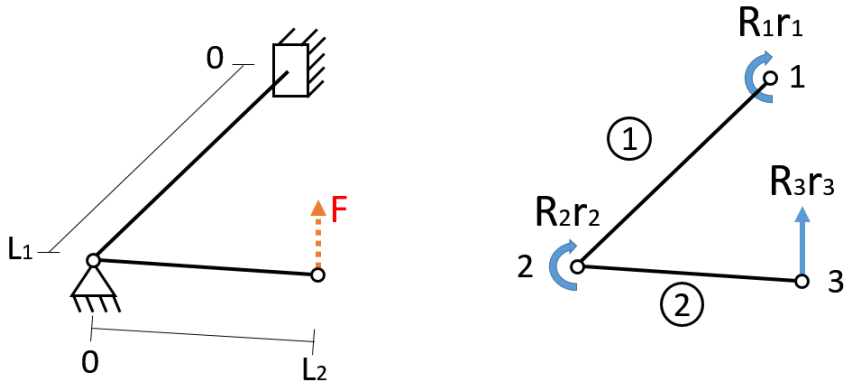

Figure 9.3: Idealized Suspension System

2a) Define the stiffness matrices k_i for each beam element where: Element 1 has angular rotation on each end. Element 2 has an angular rotation on one end, and vertical displacement on the other.

2b) Define the system stiffness matrix K. One assumes that node 1 can get rotated at this point, so that:
R = Kr
Where: **R** = $[R_1\ R_2\ R_3]^T$ and **r** = $[r_1\ r_2\ r_3]^T$

2c) Generate the equation sets, and insert the following values and solve for the displacement in node 3 and the angular rotation in node 2 for applied force of 1000N, 2000N, and 3000N

$GJ = 3.1127 \cdot 10^9 Nmm^2, \quad EI = 5.7509 \cdot 10^{10} Nmm^2$
$L_1 = 650mm\,, \quad L_2 = 350mm,$
$r_1 = 0, \quad R_1 = R_2 = 0, \quad R_3 = 1000, 2000, \&3000N$

1D Simulation

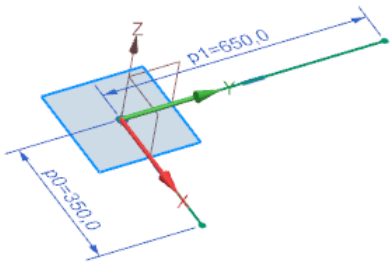

Figure 9.4: 1D Sketch of the Suspension System

In this assignment a 1D simulation of the suspension system is to be performed in NX. This is done by creating a sketch, and applying a 1D mesh and virtual cross-sections to this sketch.

3a) Create a sketch with two perpendicular lines. Torsion bar: $L_1 = 650mm$ and Torsion Arm: $L_2 = 350mm$. Figure 9.4. Save the sketch. Open $Advanced\ Simulation \rightarrow New\ FEM\ and\ Simulation$. To be able to include the sketch as a work-part: Click $Geometry\ Options$ in the appearing box. Here, $Lines$ must be ticked before clicking OK. Select SOL101 simulation.

3b) Create the virtual cross-sections. This is done under $Mesh \rightarrow 1D\ Element\ Section$. Create a ROD section for the torsion bar with Radius = 25.25mm/2, and a BOX section for the torsion arm with dimensions 40x60x3mm.

3c) Apply a 1D Mesh on each of the two lines. Choose CBEAM type, and each mesh should consist on only 1 element.

3d) Create a new material for the torsion bar called S165M with the following values: $E = 210Gpa$, $G = 78Gpa$, $\nu = 0.346$, $\rho = 7700kg/m^3$, Yield strength $885Mpa$, and Tensile strength of $1010Mpa$.

3e) Assign the Cross-sections and materials to the 1D mesh' in $Physical\ Properties$. The torsion bar should have the S165M material and ROD section, whilst the torsion arm is BOX section and steel.

3f) Open the SIM and apply suiting constraints and a Force of 1000N. Run the simulation. Evaluate the Displacement- and Rotation- results vs. the analytical and physical test results. Repeat for 2000, and 3000N

9.3 TMM4155 - FEA in ME - Exercises Suggestion

Course content *The course will include the following subjects: "geometry idealization", "advanced meshing", "identification of FE based theory and tools for problem solving", "linear and non-linear Finite Element (FE) formulations", "static and dynamic FE formulations in time and frequency domain", "simple control system design for motor and vibration control", "guidance in NX, ABAQUS and FEDEM", "guidance in static, dynamic, contact, buckling and mechanism analysis", "FE based solution of previous exams in TMM4112 Machine Element" and "FE based solutions of advanced industrial applications"* [14]

The three CAD and FEM models required for completing the tasks below are submitted to Prof. Terje Rølvåg. The models are pre-meshed, and includes the material properties of the torsion bar. This allows students to focus on running different solvers, and not preparing the FEM models.

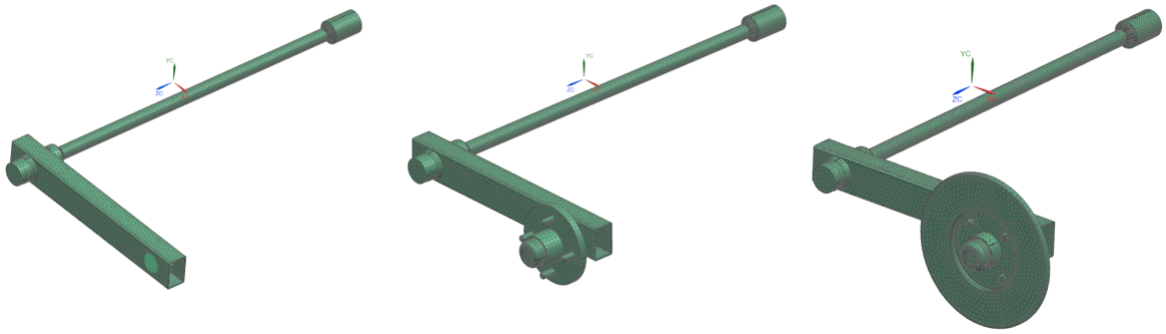

Figure 9.5: FEM Models Accompanying these Exercises

Quasi-Static Response

Use the FEM model of the suspension system without the wheel hub to evaluate the elevation height and torsion bar stress.
1a) What does a transient analysis mean?
1b) What kind of solver should preferred for a dynamic large construction if computation time is critical? - Direct Transient or Modal Transient?

In this case you are going to use a FEM model of suspension system to evaluate the quasi static response in terms of the applied force vs. torsion bar stress, and the elevation of the torsion arm. The solvers to be used are SOL 109 Direct Transient Response, and SOL 112 Modal Transient, in NX.

For the following assignments; use the FEM model of the suspension system without the wheel hub.

2a) Create a new SOL109 simulation, and apply suitable constraints to the suspension system to emulate the physical test rig; where the end-section of the torsion bar is welded to the rig-frame, and each side of the torsion bar/arm joint is fixed with rigid bearings.
2b) To enforce a rotation of the torsion arm, an enforced velocity needs to be applied. This is found under *Constraints*. Apply a vertical velocity of 2mm/sec to the RBE2 element node on the torsion arm. As the force is applied vertically, physically this simulates a progressive suspension system. (It becomes stiffer as the force increases)
2c) As the SOL 109 is a transient solver, the time step increment must be applied. This defines the number of increments and the time in-between the steps. This is done by right-clicking on the *Subcase* → *Edit* → *Time Step Intervals*. Apply the related values to displace the torsion arm by 80 mm in 20 steps. After creating the time steps interval, remember to Click *Add*-button in the List-box. Output-request must also be defined.
2d) Run the simulation and note the simulation time.
2e) Plot (Graph) the vertical displacement of the RBE2 node over the total time. Does is correlate to the applied velocity? Plot the reaction forces in the RBE2 node over the total time. What does they show in terms of the simulated system response? - Is is progressive, linear or degressive?

Natural Frequency

Task:

3) Use the 103 Real Eigenvalues solver in Siemens NX to evaluate the natural frequency of the suspension system. Two different models are to be evaluated, with and without an extra wheel hub weight. To run the simulations; three constrains needs to be added: Fix the end section of the torsion bar, and Pin side of the torsion bar/arm junction.

Compare the result with the physical testing, according to the *Physical Test Manual*.

Fatigue

As the torsion bar is subjected to large cyclic stresses, it is desirable to run a fatigue analysis. The torsion bar is subjected to zero-to-tension (R=0), see Fig. 9.6, which means that torsion bar is subjected to a constant tension cycle with variable load. The objective of the fatigue analysis is to estimate the number of times the rig withstands the maximum loading of 3200N.

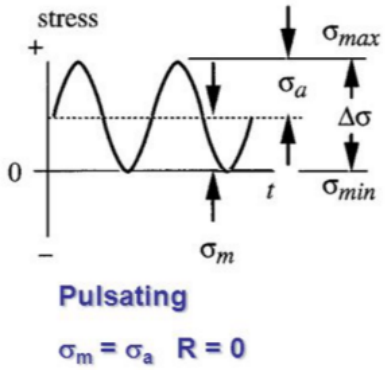

Figure 9.6: Zero-to-Tension, Cycles between 0 and σ_{max}

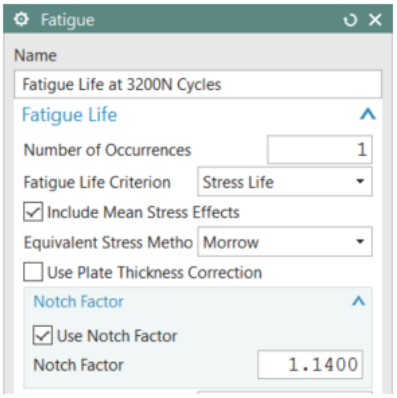

Figure 9.7: Fatigue Analysis Parameters

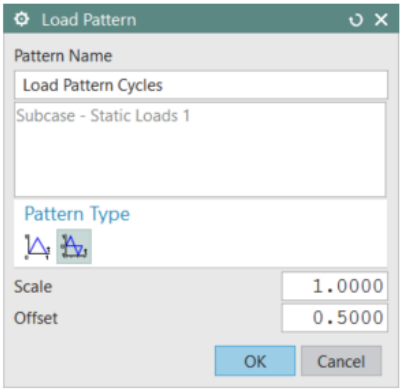

Figure 9.8: Load Pattern, Full Cycles with 50% Offset

Table 9.1: Material and Fatigue Parameters

Torsion Bar Material Data			
Elastic Modulus	E	210	Gpa
Shear Modulus	G	78	Gpa
Poisson's Number	ν	0.346	
Yield Strength	σ_{ys}	885	Mpa
Ultimate Tensile Strength	σ_{ut}	1010	Mpa
Fatigue Strength Coefficient	σ'_f	1454	Mpa
Fatigue Strength Exponent	b	-0.08	
Fatigue Ductility Coefficient	ϵ'_f	1.85	
Fatigue Ductility Exponent	c	-0.72	
Cyclic Yield Strength	σ'_s	716	Mpa
Cyclic Strength Coefficient	K'	1367	Mpa
Cyclic Strain Hardening Exponent	n'	0.10	

The analysis is to be performed in an embedded module in Siemens NX. The analysis module is found in the *Simulation Navigator*, by right clicking on the Sim-file ⇒ *New Simulation Process* ⇒ *Durability*. This creates a new fatigue simulation file in the the Simulation Navigator. This file is then linked to a previously performed simulation. In this case a static SOL 101 at 3200 Newtons. Before solving the fatigue analysis, different analysis parameters needs to be chosen, Fig. 9.7. This includes a Notch Factor, K_f, which is a factor that compensates for the geometric stress concentration in the R10 radius. The factor is found to be $K_f = 1.14$. To be conservative, Morrow equivalent mean stress is to be selected. As the Fatigue Strength Coefficient, σ'_f, is known for the material, Morrow is good approximation, and is therefore chosen over Goodman and Smith-Watson-Topper(SWT). The excitation is added by right clicking on the Static Event in the Simulation Navigator. Here a Loading pattern must be defined, Figure 9.8 Full unit cycle is the correct option. By setting an offset of 0.5 sets the mean stress to $\sigma_m = 0.5 \cdot \sigma_{max}$. This generates a 0 - 3200 - 0N loading pattern which is correct in this case.

Tasks:

4a) Use the simulation model without the wheelhub to run a linear static SOL 101 simulation, where a 3200N force is applied vertically to RBE2 element (Wheel hub substitute). Note the maximum Von Mises Stress

4b) Run the fatigue analysis according to the description above. Run the simulation twice; with and without the Notch Factor. Note the number of cycles to failure in both cases.

4c) Comment whether the rig is adequate designed considering its purpose of student testing.

4d) A S-N diagram of the torsion bar material, S165M, is displayed in Figure 9.9. How does the fatigue analysis results compare with the S-N diagram?

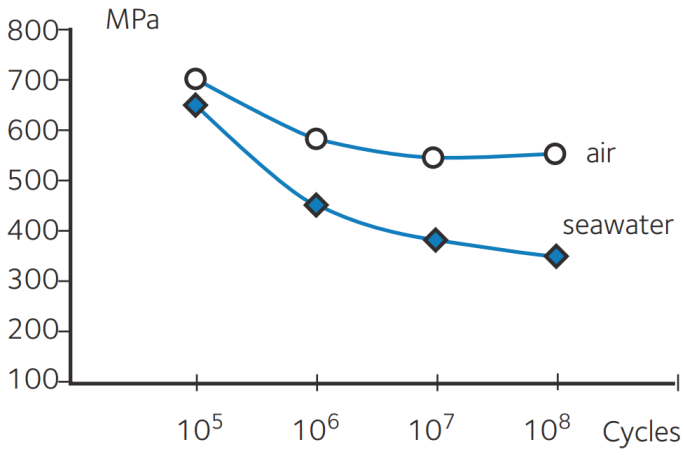

Figure 9.9: S-N diagram for S165M (Torsion Bar) [Fig: Industeel]

Chapter 10

Summary and Further Work

10.1 Summary and Conclusions

The objective of this Master's thesis was to finalize the construction of a physical torsion bar suspension test rig, and perform analytical calculations and virtual simulations related to the rig. The final physical product is a turnkey-product rig, ready to be used in lectures. For an untrained hobby mechanic, it is pleasing to say that the rig mechanically fulfills all the desired demands, and works exactly as planed. And there were few unforeseen obstacles during the construction work of the rig. Esthetically, the rig also looks good. And the visual analog indicators makes the rigs purpose more intuitive.

Instrumenting the rig, calibrating the sensors, and learning the Catman software, was a time consuming process. And a lot of troubleshooting and trail and error was needed to succeed. The result is pleasingly fully working monitoring system, ready set up for performing physical testing by students and lecturers. And the Physical Test Manual gives guidance in how to operate and perform the tests.

The static analytical calculation model that found the basis for this thesis, was analysed and revised to improved the correlation with the physical rig. This was done by examine the related assumptions, and introduce a few new. The result of the calculation model is enhanced accuracy cornering the KPIs. About 40% of the correction originates from the complex geometry calculation. The rest comes from implementing a transcendental equation which takes the angular shifting force vector into account. The disadvantage of this extended model is the transcendental equation. It makes it hard to easily compute a multi point plot of the response, as every torsion angle equation must by solved individually by e.g. Wolfram Alpha. Overall, the extended calculation model gives satisfying results regarding reflecting the physical rig response. It is

more comprehensive to conduct than the exam model, but gives more accurate results. Concerning the height/load relation, the extended model decreases the deviation from the physical test results by 79% at 2940N. Whether it is worth to perform depends on the situation. The exam model gives great estimations at low angular displacement, but at relative large angles (>8 deg / 2000 N) it starts to become imprecise.

Recreating the static response of the rig with FEA proved to be harder than expected. The results of three different solvers was presented in this thesis. All of them used on both the 3D model and the 1D representation on the rig. The simulations resulted in accurate results in terms of force, displacement and stresses at low rotations, but the results started to deviate at larger rotation. Other nonlinear solvers (SOL106, SOL129) was also tested to try to recreate the non-linearity of the height/load relationship without succeeding. But is one thing should be emphasised, it is the 1D simulations. They were the least accurate, but if one knows your way around Siemens NX, it only takes approx 2 minutes to create the whole model and run the simulation. In other terms, an extremely quick and effective way of estimating the results.

The undamped natural frequency of the suspension system tested was evaluated against analytical calculation and virtual simulation. The results was an overall great consistency between all the approaches and the physical test. An extra wheel hub weight has also been manufactured to allow students to experience the effect of added mass to a system. Without the extra mass the system has a natural frequency of ≈15Hz, whilst ≈10.5Hz with the extra mass.

To ensure that the rig is going to withstand the high-stress-testing over its service lifetime, a FEA fatigue analysis was conducted. It estimated a service life of 250000 cycles. This implies that the torsion bar is going to last the full life time of the rig, which is subjected to a few hundred cycles a year.

The student exercises was created to match the course consent of each course. They all involve comparing analytical calculation, and virtual simulating with physical testing. This allows the students to get more practical experience with transferring their knowledge between the different approaches to solve a problem. The exercise suggested solutions are found in Appendix C.

Overall, this has been a successful project. The ambition to leave behind i fully working rig, which might help students to understand difficult subjects, has been completed.

10.2 Further Work

If further work on the rig should be recommended, it would be to enhance the dynamical test capabilities. As the rig is prepared now, it is only possible to evaluate the undamped natural frequency, manually induced. A recommendation would be to install a device which induces oscillations, and an adjustable damper. This would make it possible to evaluate new aspects such as the critical damping factor, and dynamic amplification factor. To induce oscillation, it was evaluated to install an electric linear actuator from Linak instead of the hydraulic jack, in the start-up of this project. But due to cost and limited acceleration-, speed-, and force-capabilities of the actuators, this idea was discarded. To suggest an idea for further work, it would be to install a mass eccentric flywheel, driven by an electric motor. See Figure 10.1. This setup should easily generate significant oscillations with a small motor. It could be an option to use the existing wheel hub as the flywheel, but the axle friction to spin it around is quite high, which drastically increases the need of power. If such a device is installed and paired with an adjustable damper, it would open up the possibility to create many exciting student exercises.

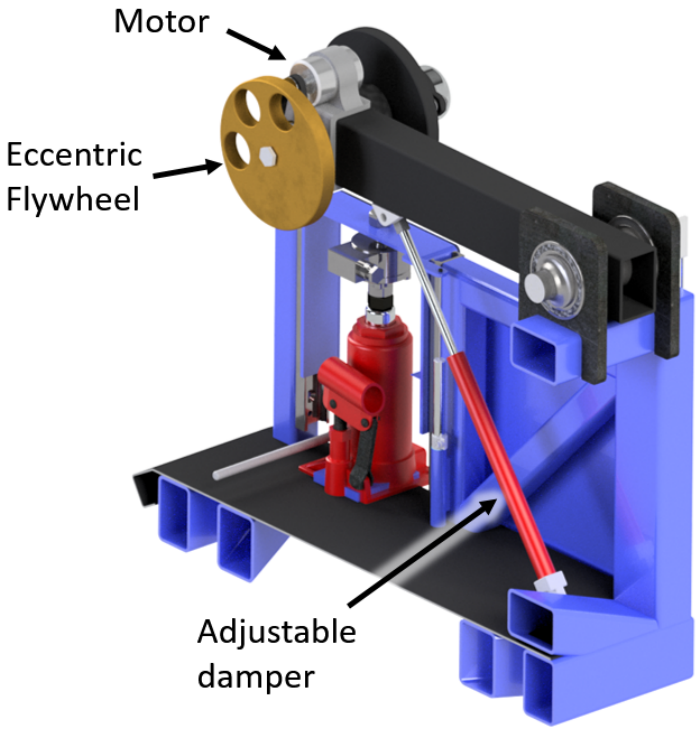

Figure 10.1: Further work suggestion, Eccentric Flywheel

Appendix A

As Built, Technical Drawings

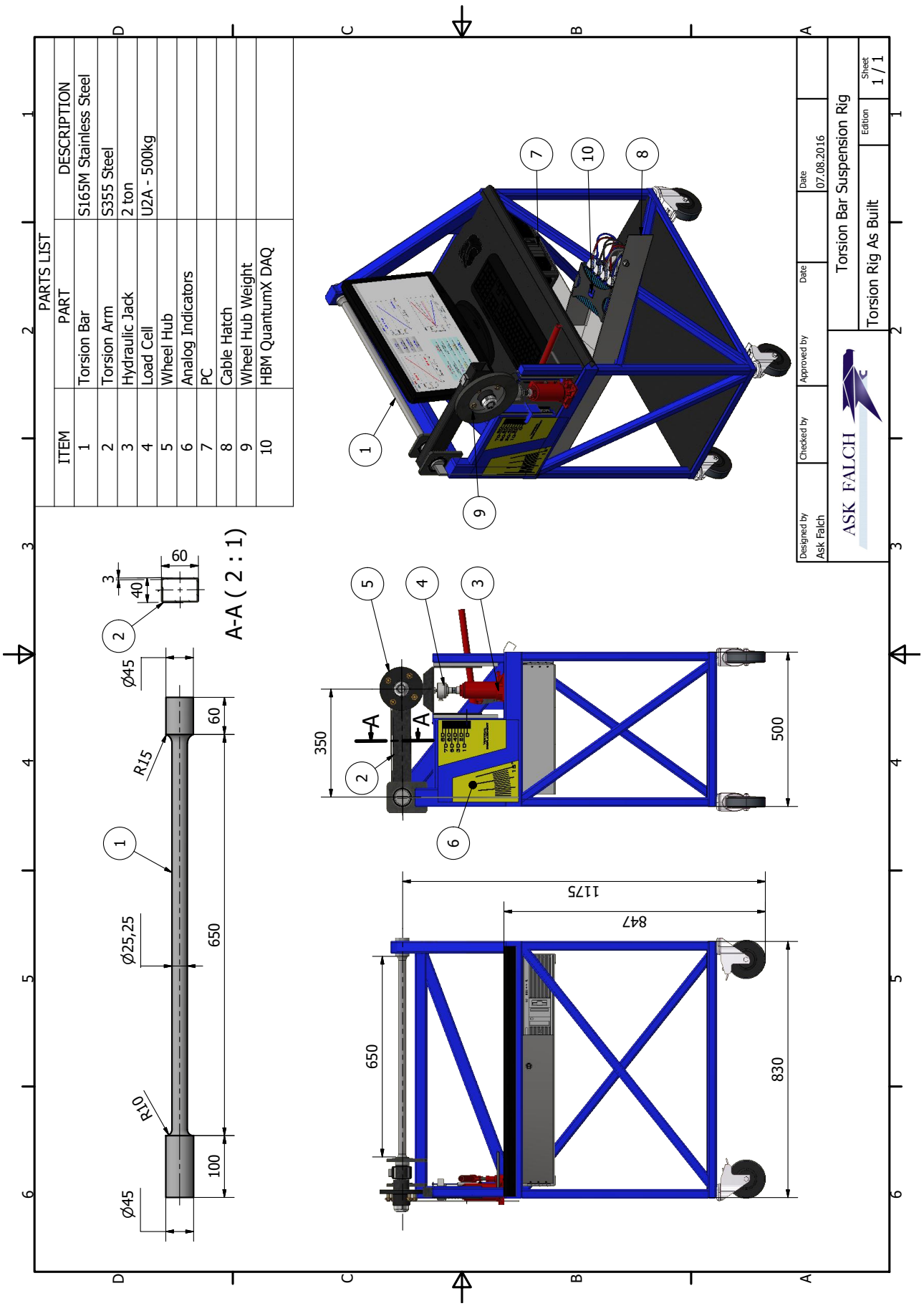
PARTS LIST
ITEM | PART | DESCRIPTION
1 | Torsion Bar | S165M Stainless Steel
2 | Torsion Arm | S355 Steel
3 | Hydraulic Jack | 2 ton
4 | Load Cell | U2A - 500kg
5 | Wheel Hub
6 | Analog Indicators
7 | PC
8 | Cable Hatch
9 | Wheel Hub Weight
10 | HBM QuantumX DAQ
A-A (2 : 1)
Ø45
R10
100
Ø25,25
650
R15
60
Ø45
3
40
60
350
500
650
847
1175
830
Designed by Ask Falch
Checked by
Approved by
Date
Date 07.08.2016
ASK FALCH
Torsion Bar Suspension Rig
Torsion Rig As Built
Edition
Sheet 1 / 1

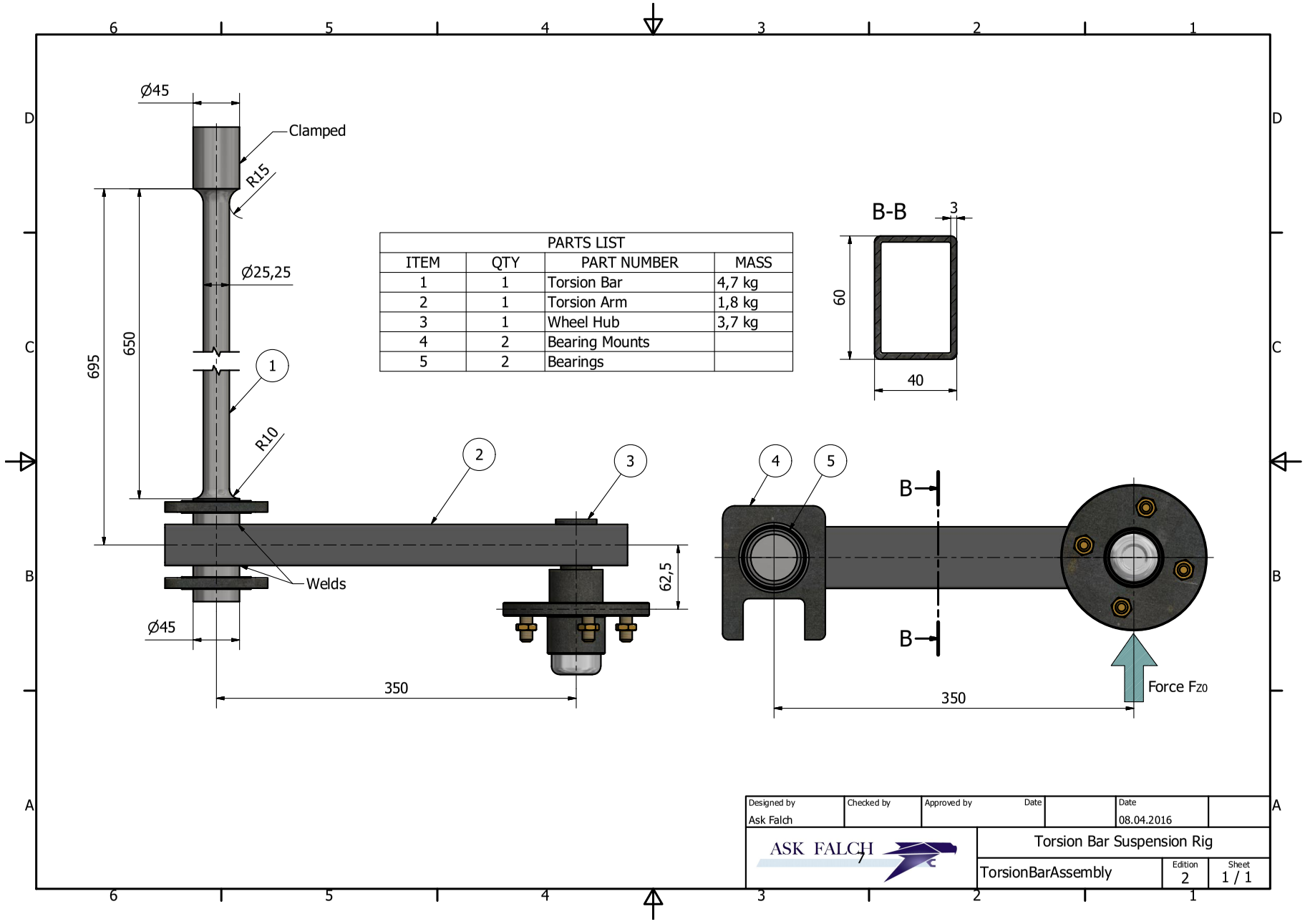

PARTS LIST			
ITEM	QTY	PART NUMBER	MASS
1	1	Torsion Bar	4,7 kg
2	1	Torsion Arm	1,8 kg
3	1	Wheel Hub	3,7 kg
4	2	Bearing Mounts	
5	2	Bearings	

Designed by	Checked by	Approved by	Date		Date
Ask Falch					08.04.2016

ASK FALCH

Torsion Bar Suspension Rig

TorsionBarAssembly | Edition 2 | Sheet 1 / 1

Appendix B

Rig Computer Background Image

Torsion Bar Suspension Rig

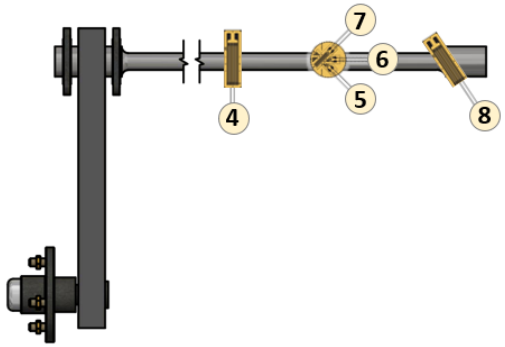

1 Load Cell
2 Displacement
3 Accelerometer
4 0° Stain Gauge
5 +45° Rosette
6 90° Rosette
7 -45° Rosette
8 +45° in Radius

DAQ Channels

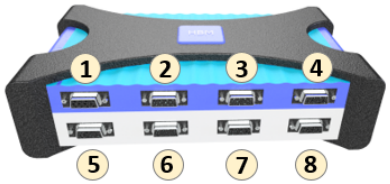

Appendix C

Physical Test Manual

Physical Test Manual

Torsion Bar Suspension Rig

Maximum Capacity

The rig is fail-proof. This means that it is OK to elevate the hydraulic jack to maximum stroke-length.

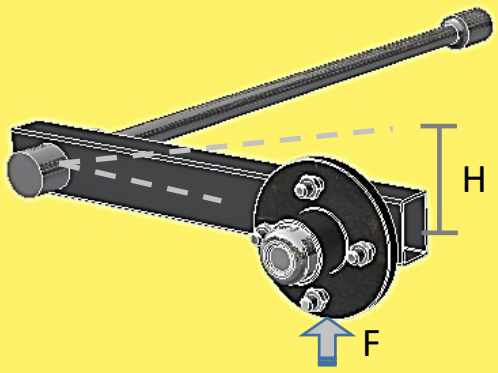

Deflection Angle	α	12,5	degrees
Elevation Height	H	81	mm
Force	F	3300	Newtons

Torsion Bar Material Data

Stainless Steel - SS2387 / S165M

E-modulus	E	210	Gpa
G-modulus	G	78	Gpa
Yield Strength	σ_{ys}	885	Mpa
Ultimate Tensile Strength	σ_{ut}	1010	Mpa
Density	δ	7700	Kg/m
Fatigue Strength Coefficient	σ'_f	1454	Mpa
Fatigue Strength Exponent	b	-0,08	
Fatigue Ductility Coefficient	ϵ'_f	1.85	
Fatigue Ductility Exponent	c	-0,72	
Cyclic Yield Strength	σ'_s	716	Mpa
Cyclic Strength Coefficient	K'	1367	Mpa
Cyclic Strain Hardening Exponent	n′	0,10	
Notch Sesitivity Factor	K_f	1,14	

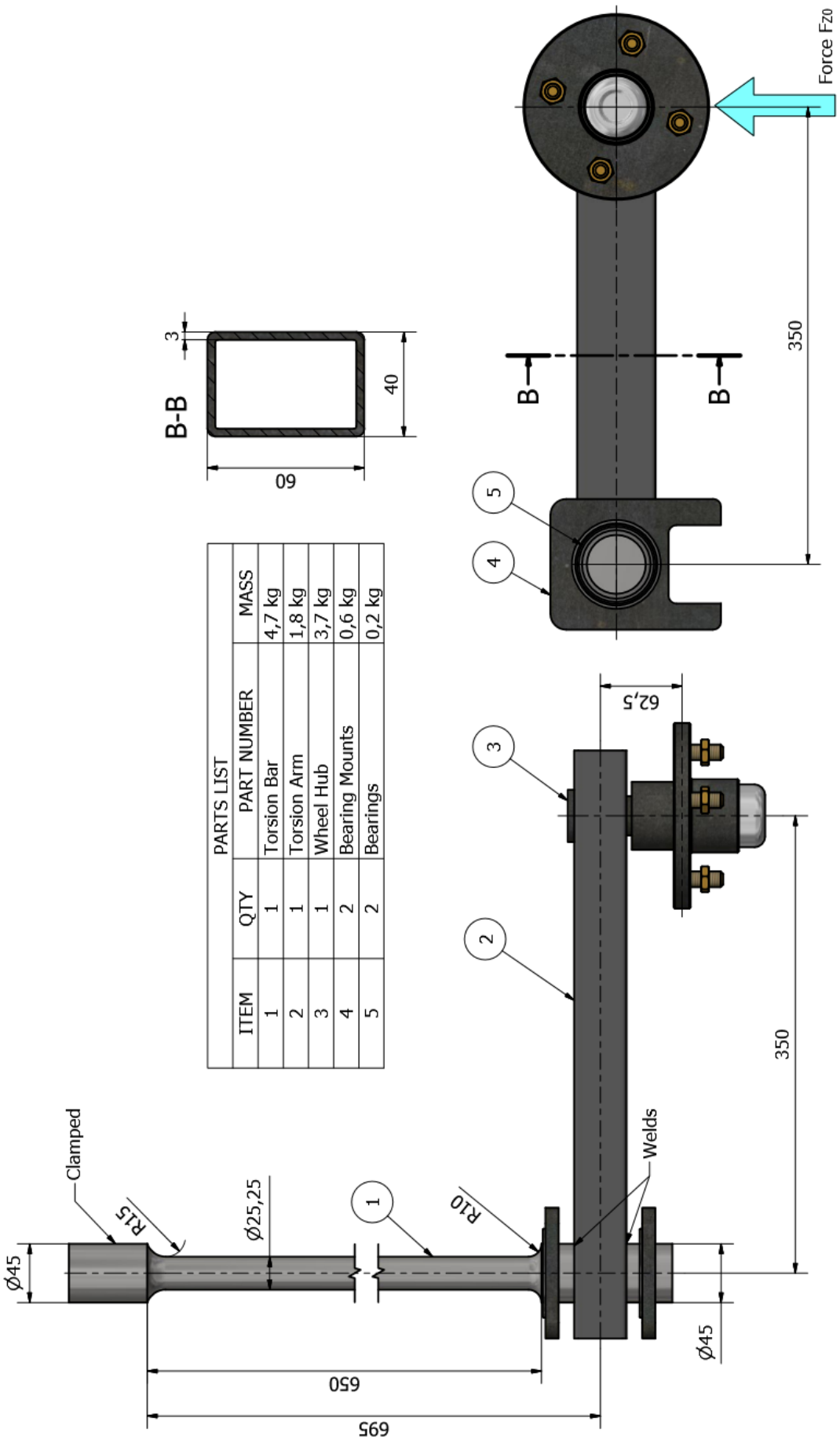

PARTS LIST			
ITEM	QTY	PART NUMBER	MASS
1	1	Torsion Bar	4,7 kg
2	1	Torsion Arm	1,8 kg
3	1	Wheel Hub	3,7 kg
4	2	Bearing Mounts	0,6 kg
5	2	Bearings	0,2 kg

Sensors & Equipment

The rig is equipped to examine quasi-static response and the Eigen frequency.

8 sensors are installed on the rig. They are connected to a Data Acquisition box (DAQ) connected to the computer to conduct live monitoring of the tests. The applied Force is monitored by a Load Cell situated directly above the hydraulic jack. A displacement probe monitors the elevation of the wheel hub. An accelerometer is used to detect the dynamic response (Eigen Frequency) of the suspension system. Five strain gauges are situated in different locations and angles on the torsion bar. These are used to compute the torsion bar stresses.

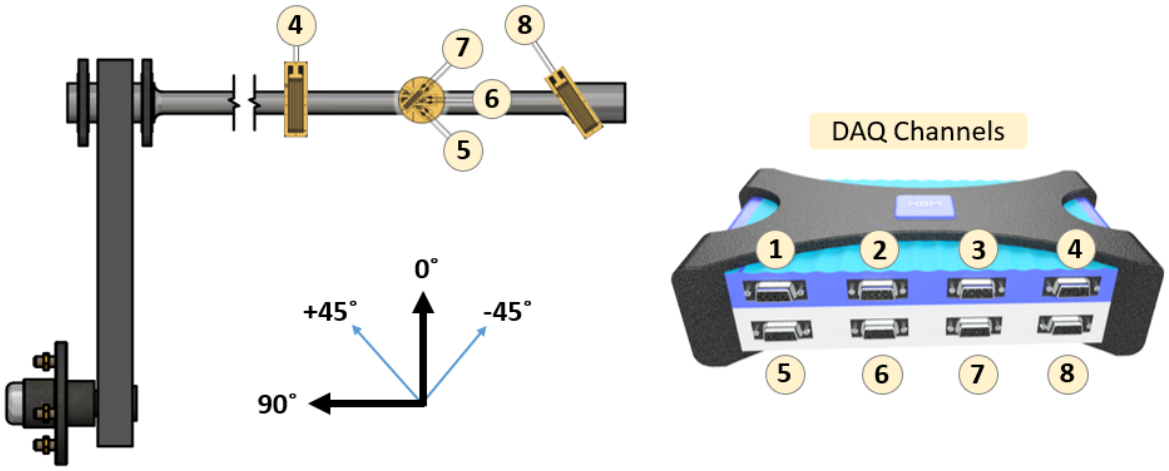

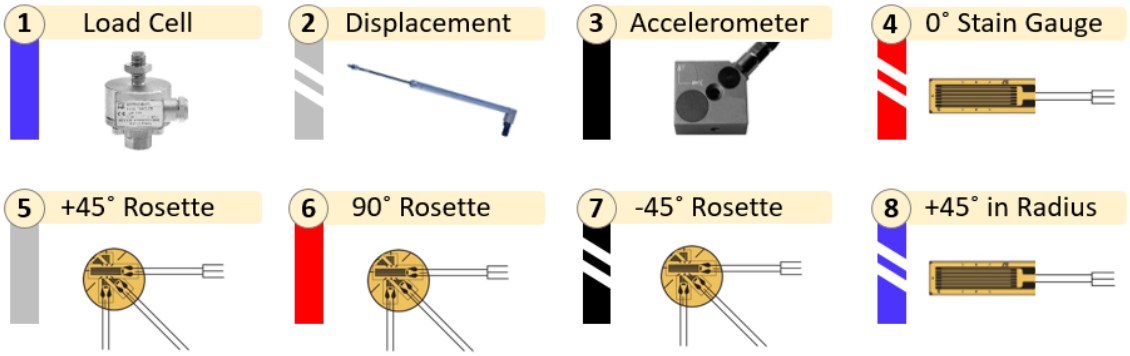

Quasi-static Test Manual

1. **Open Catman AP**
2. **Click: *Continue* (Resume my last session)**
   This opens the DAQ Channels window. Here, all the active sensors are displayed.
3. **Lower the hydraulic so the wheel hub moves freely.**
4. Before initiating a test, the sensors needs to be calibrated and zeroed. Due to the weight of the torsion arm and wheel hub (46N), this needs to be accounted for.
   Click on "A" *Live Update*. This enables live readings of the sensors. The values are visible in the Reading-column.
   Mark all the 8 sensors, "B".
   Click "C" *Execute*, to zero all the values.
   Elevate the hydraulic jack slowly, until the Load reads 46N, "D".
   Click "C" *Execute*, to zero all the values again.
5. **Click "E" *Start*** to initiate the test.

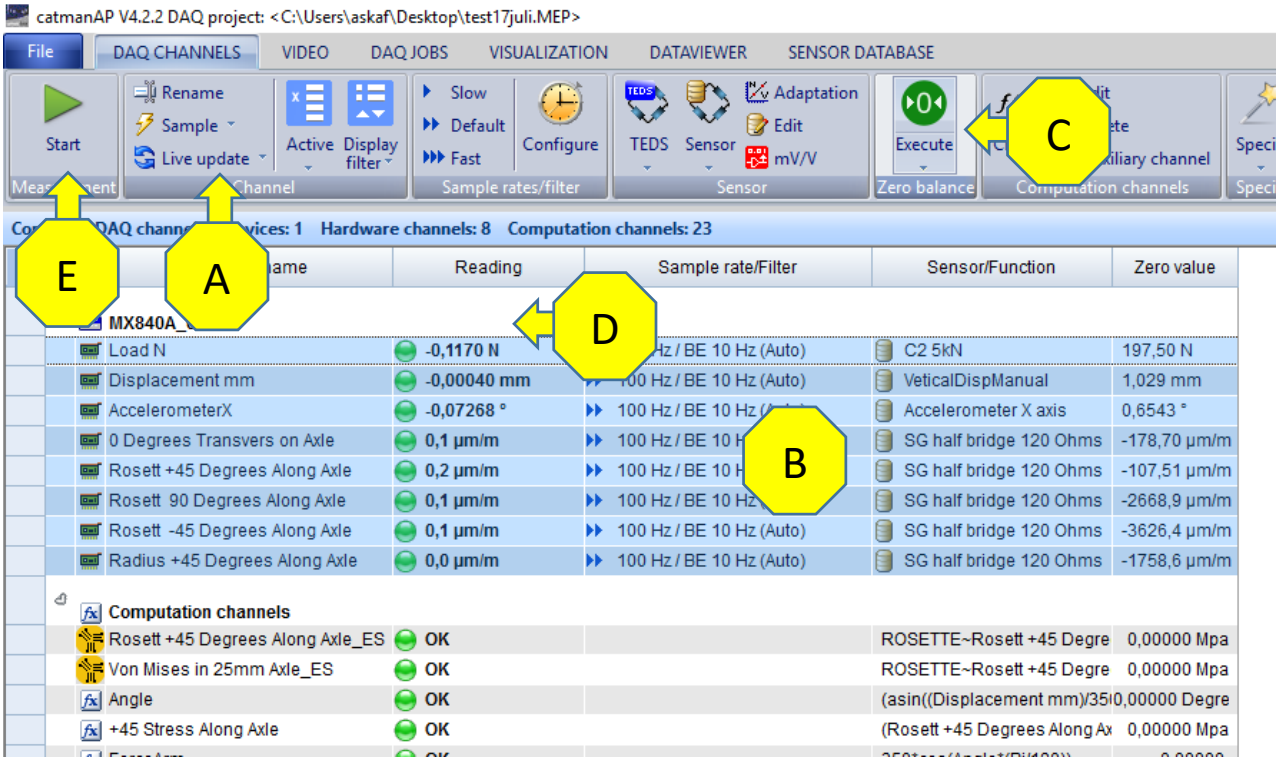

6. When a test has been started, the *VISUALIZATION panel opens.* This panel gives live monitoring of the test**. Sub-panels are prepared to visualize the quasi-static testing. Switch between these to visualize different aspects of the tests.**

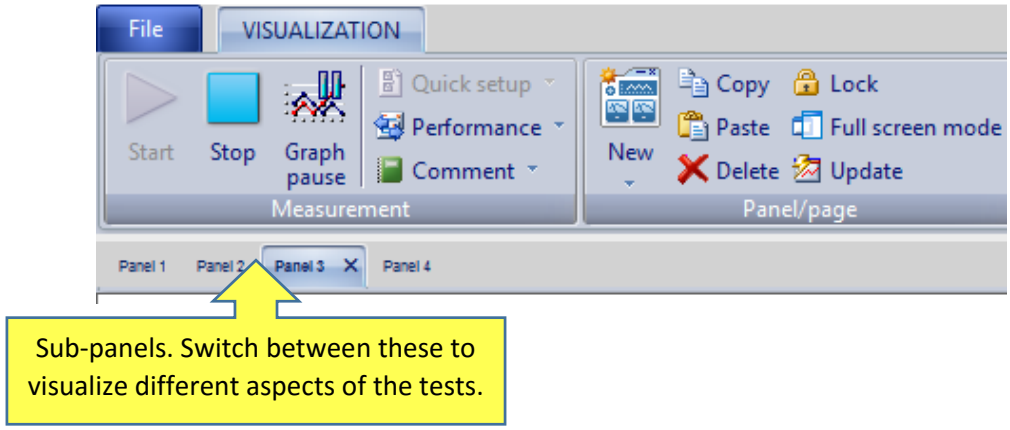

Sub-panel 1 – Stress and Overview

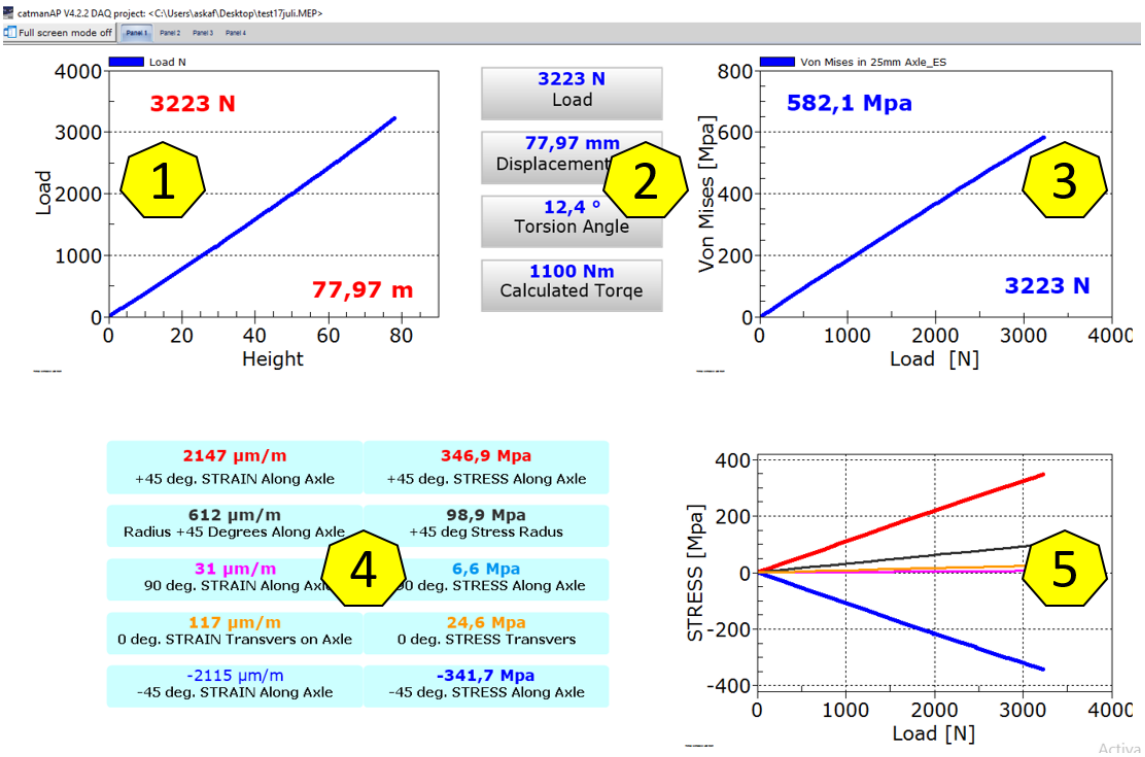

(1) Elevation height/Load.
(2) Values for Load, Elevation, Torsion angle, and Torque.
(3) Von Mises Stress in torsion bar.
(4) Strain in every strain gauge and corresponding stress.
(5) Visualization of the stresses.

Sub-panel 2 Elevation vs applied load

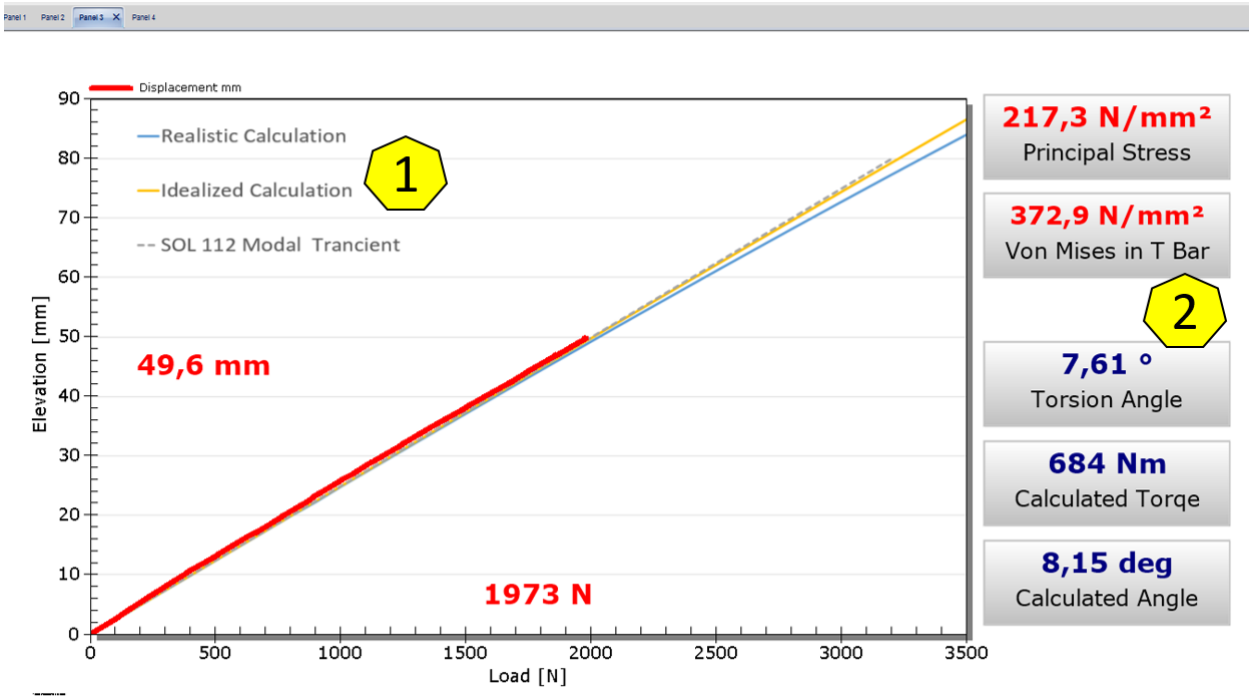

(1) Elevation height/Load. The Background picture displays analytical and virtual solutions to estimate the height/load relationship.

(2) Values: Principal and Von Mises stresses in the torsion bar. Torsion angle, Torque and calculated torsion arm angle.

7. **Use the hydraulic jack to elevate the wheel hub.** Watch the Live monitoring.

8. **When hydraulic jack reaches the maximum position, Click *Stop* to end the test.**

9. **Test data can be exported by selecting***: File → Save as → Save last DAQ job.* Choose desired format (e.g. Excel or Matlab)

Eigen Frequency Test Manual

1. **Open Catman AP**
2. **Click: *Continue* (Resume my last session)**
   This opens the DAQ Channels window. Here, all the active sensors are displayed.
3. **Lower the hydraulic so the wheel hub moves freely.**
4. Before initiating a test, the sensors needs to be calibrated and zeroed.
   Mark all the 8 sensors, "B".
   Click "C" *Execute*, to zero all the values.
5. Increase the sample rate:
   Mark all sensors and Right-click directly above the sample rate,"B". Click *Configure Sample Rate.* Set the sample rate to at least 300Hz.
6. **Click "E" *Start*** to initiate the test.
7. **Select sub-panel; Panel 4 to display the dynamic visualization.**
8. **Hit the wheel hub by hand repeatedly to initiate oscillation.** A sprike on the right graph will occour. This identifies the Eigen frequency.
9. **If desired: Attach the extra wheel hub weight to examine the difference.**
10. **End the test by clicking *Stop.***
11. **Reset the sample rate to 100Hz.**

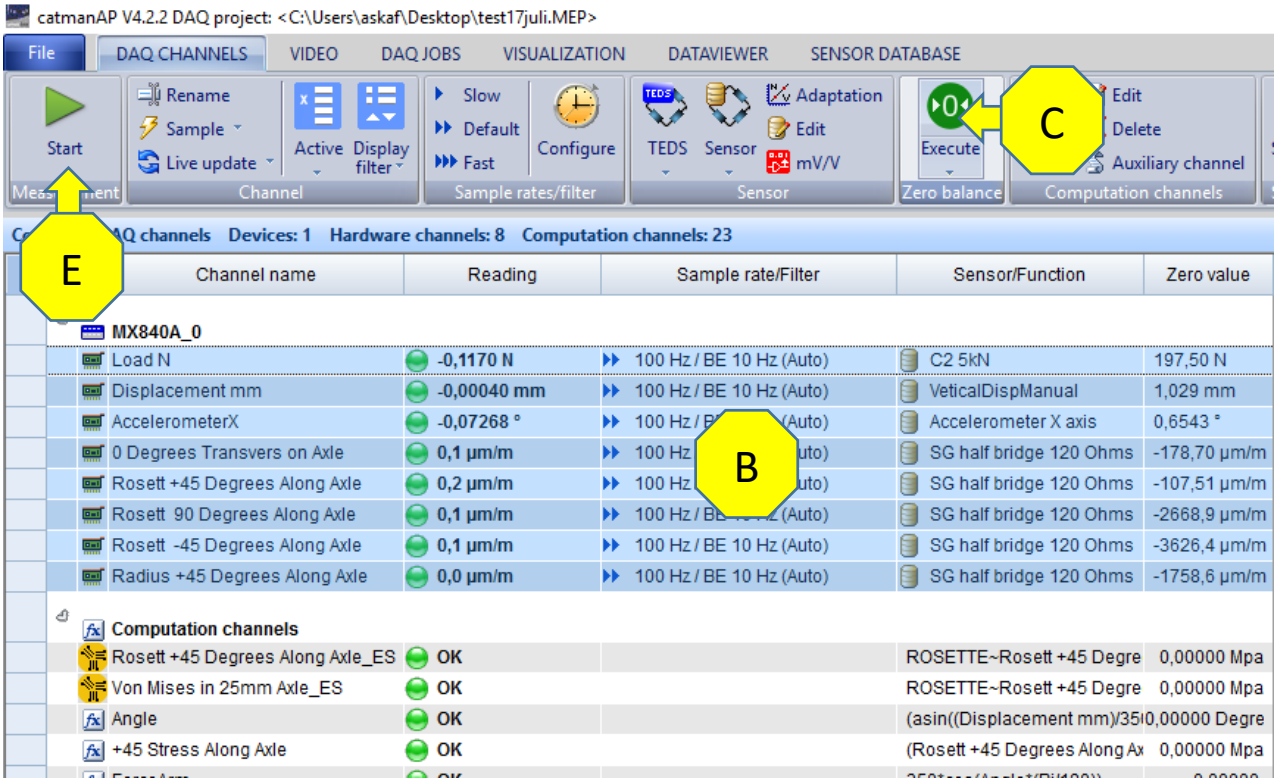

Appendix D

Suspension Test Rig Exercises Solution

D.1 TMM4112 - Machine Elements - Exercises Solution

Static Response

1a) Torsion angle:

$$\theta = \frac{TL}{G \cdot I_p} \Rightarrow \frac{F_z RL}{G \cdot I_{p,bar}} = \frac{350 \cdot 650}{78000 \cdot \frac{\pi}{32} d^4} \cdot F_z$$

vertical elevation:

$$h = R \cdot sin\theta$$

F_z = 1000N:

$$\theta_{1000N} = \frac{350 \cdot 650}{78000 \cdot \frac{\pi}{32}(25.25)^4} \cdot 1000 = 0.073rad = 4.19deg.$$

$$H_{1000N} = 350 \cdot sin(0.073) = \underline{\underline{25.53mm}}$$

F_z = 2000N:

$$\theta_{2000N} = 2 \cdot \theta_{1000N} = 0.146rad = 8.38deg.$$

$$H_{2000N} = 350 \cdot sin(0.146) = \underline{\underline{50.92mm}}$$

F_z = 3200N:

$$\theta_{3200N} = 3.2 \cdot \theta_{1000N} = 0.2336rad = 13.40deg.$$

$$H_{3200N} = 350 \cdot sin(0.2336) = \underline{\underline{81.0mm}}$$

1b) Pure torsion reduces the Von Mises Stress to:

$$\sigma_{vm} = \sqrt{3} \cdot \tau_{xy}$$

Von Mises at 3200N:

$$\sigma_{vm} = \sqrt{3} \cdot \frac{FR \cdot r}{I_p} = \sqrt{3} \cdot \frac{3200 \cdot 350 \cdot (25.25/2)}{39906} = \underline{\underline{614Mpa}}$$

Maximum force, F_{max}:

$$F_{max} = \frac{\sigma_{ys}}{\sqrt{3}} \cdot \frac{I_{p,bar}}{R \cdot r} = \frac{885}{\sqrt{3}} \cdot \frac{39906}{350 \cdot (25.25/2)} = \underline{\underline{4614Newtons}}$$

Transient System

2a) The spring becomes stiffer: Called Progressive.

2b) New torsion angle:

$$\phi = \frac{FRLcos\phi}{GI_P} \rightarrow \theta \cdot cos\phi$$

ϕ_{1000N}:

$$\frac{\phi}{cos\phi} = \theta_{1000N} \Rightarrow \frac{\phi}{cos\phi} = 0.073 \rightarrow \phi = 0.0728rad$$

$$H = 350 \cdot sin0.728 = \underline{\underline{25.45mm}}$$

ϕ_{2000N}:

$$\frac{\phi}{cos\phi} = \theta_{2000N} \Rightarrow \frac{\phi}{cos\phi} = 0.146 \rightarrow \phi = 0.1444rad$$

$$H = 350 \cdot sin0.1444 = \underline{\underline{50.36mm}}$$

ϕ_{3200N}:

$$\frac{\phi}{cos\phi} = \theta_{3200N} \Rightarrow \frac{\phi}{cos\phi} = 0.2336 \rightarrow \phi = 0.2275rad$$

$$H = 350 \cdot sin0.2275 = \underline{\underline{78.94mm}}$$

Deviations: 1000N = 0.3%, 2000N = 1.1%, 3200N = 2.6%.

2c) Total Height at 3200N.

$$H_{arm} = \frac{F \cdot R^3}{3EI_x} \cdot (cos\phi)^2 = \frac{3200 \cdot 350^3}{3 \cdot 210000 \cdot [\frac{40 \cdot 60^3}{12} - \frac{34 \cdot 54^3}{12}]} = 0.75mm$$

$$H_{tot} = 78.94 + 0.75 = \underline{\underline{79.69mm}}$$

2d) Perform testing.

Natural Frequency

3a) Natural frequency without extra weight.

$$\omega_n = \sqrt{\frac{\kappa_t}{I}}$$

$$\kappa_t = \frac{G \cdot J_t}{L} \Rightarrow \frac{G}{L} \cdot \frac{\pi \cdot d^4}{32} = \frac{78000}{650} \cdot \frac{\pi \cdot 25.25^4}{32} = 4788780\,[Nmm/rad]$$

$$I = I_{arm} + I_{Hub}$$

$$I = \left[\frac{1}{12} m \cdot R_{tot}^2 + m\left(\frac{R}{2}\right)^2\right] + [M_{wh} \cdot R^2]$$

$$I = \left[\frac{1}{12} 1.8 \cdot 450^2 + 1.8\left(\frac{350}{2}\right)^2\right] + \left[3.7 \cdot 350^2\right] = 538750[kg \cdot mm^2]$$

$$\omega_n = \sqrt{\frac{4788780 \cdot 1000}{538750}} = \underline{\underline{94.28[rad/sec] \rightarrow f_n = 15[Hz]}}$$

3b) Perform testing.

3c) Comment.

3d)

Physical test results: With hub; $\omega_n \approx 15.1Hz$, With extra weight; $\omega_n \approx 10.5Hz$.
Use $\omega_n = 10.5Hz = 66rad/s$ to find the extra mass, M_{ex}:

$$I = \frac{\kappa_t}{\omega_n^2} = \frac{4788780 \cdot 1000}{66^2} = 1099353kg \cdot mm^2$$

$$I = I_{Arm} + I_{Hub} + I_{weight} \rightarrow I_{weight} = I - (I_{Arm} + I_{Hub})$$

$$I_{weight} = 1099353 - 538750 = 560603kg \cdot mm^2$$

$$M_{ew} = \frac{I_{weight}}{R^2} = 560603kg \cdot mm^2/350mm^2 = \underline{\underline{4.57kg}}$$

Fatigue

4a) Parameters:

S_{max}: Maximum Nominal Stress

$$S_{max} = 614Mpa$$

S_{min}: Minimum Nominal Stress

$$S_{min} = 0Mpa$$

S_a: Nominal Alternating Stress Amplitude

$$S_a = \frac{\sigma_{max} - \sigma_{min}}{2} = \frac{614 - 0}{2} = 307Mpa$$

S_m: Mean Stress

$$S_m = \frac{\sigma_{max} + \sigma_{min}}{2} = \frac{614 - 0}{2} = 307Mpa$$

R: Stress Ratio

$$R = \frac{S_{min}}{S_{max}} = \frac{0Mpa}{614Mpa} = 0$$

4b) Stress Concentration

$$r/d = 0.4, D/d = 1.78 \rightarrow \underline{\underline{K_t \approx 1.15}}$$

4c) Cycles to Failure
Without stress concentration factor:

$$\sigma_a = \sigma_m = S_a = 307Mpa$$

$$\sigma_{ar} = \frac{\sigma_a}{1 - \frac{\sigma_m}{\sigma'_f}} = \frac{307}{1 - \frac{307}{1454}} = 389Mpa$$

$$\sigma_{ar} = \sigma'_f \cdot (2N_f)^b$$

$$389 = 1454 \cdot (2N_f)^{-0.08}$$

$$\underline{\underline{N_f = 7.2 \cdot 10^6 Cycles}}$$

With stress concentration factor:

$$\sigma_a = \sigma_m = \kappa_t \cdot S_a = 1.15 \cdot 307 = 353Mpa$$

$$\sigma_{ar} = \frac{\sigma_a}{1 - \frac{\sigma_m}{\sigma'_f}} = \frac{353}{1 - \frac{353}{1454}} = 466Mpa$$

$$466 = 1454 \cdot (2N_f)^{-0.08}$$

$$\underline{\underline{N_f = 7.5 \cdot 10^5 Cycles}}$$

D.2 TMM4135 - Analysis and Assessment Based on FEM - Exercises Solutions

Physical Testing

1) Static testing according to the Physical Test Manual.

Analytical FEM

2a) Stiffness matrices

ELEMENT 1, [Tilfelle 8, Elementmetoden]:

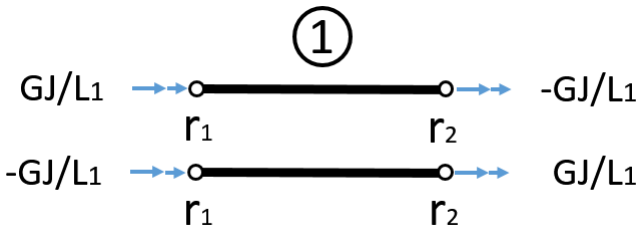

$$K_{11} = \frac{GJ}{L_1} \qquad K_{12} = \frac{-GJ}{L_1}$$

$$K_{21} = \frac{-GJ}{L_1} \qquad K_{22} = \frac{GJ}{L_1}$$

Stiffness matrix, k_1:

$$k_1 = \begin{bmatrix} \frac{GJ}{L_1} & \frac{-GJ}{L_1} \\ \frac{-GJ}{L_1} & \frac{GJ}{L_1} \end{bmatrix}$$

ELEMENT 2, [Tilfelle 7 & 6, Elementmetoden]:

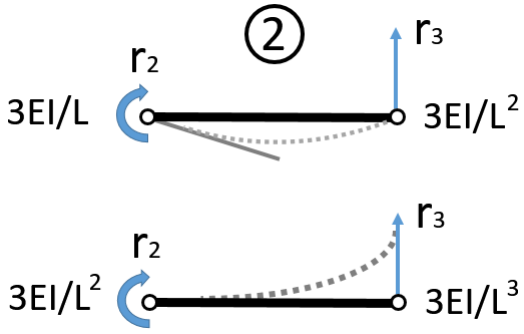

Stiffness matrix, k_2:

$$k_2 = \begin{bmatrix} \frac{3EI}{L_2} & \frac{3EI}{L_2^2} \\ \frac{3EI}{L_2^2} & \frac{3EI}{L_2^3} \end{bmatrix}$$

2b) System stiffness matrix

Stiffness matrix, K:

$$K = \begin{bmatrix} \frac{GJ}{L_1} & \frac{-GJ}{L_1} & 0 \\ \frac{-GJ}{L_1} & \frac{GJ}{L_1} + \frac{3EI}{L_2} & \frac{3EI}{L_2^2} \\ 0 & \frac{3EI}{L_2^2} & \frac{3EI}{L_2^3} \end{bmatrix}$$

R = Kr

Where: **R** = $[R_1\ R_2\ R_3]^T$ and **r** = $[r_1\ r_2\ r_3]^T$

2c) Solving for displacement and rotation

Boundary conditions:

$GJ = 3.1127 \cdot 10^9 Nmm^2, \quad EI = 5.7509 \cdot 10^{10} Nmm^2$

$L_1 = 650mm\ , \quad L_2 = 350mm,$

$r_1 = 0, \quad R_1 = R_2 = 0, \quad R_3 = 1000, 2000, \& 3000N$

Given boundary Conditions: Stiffness matrix, K:

$$K = \begin{bmatrix} 1 & 0 & 0 \\ 0 & \frac{GJ}{L_1} + \frac{3EI}{L_2} & \frac{3EI}{L_2^2} \\ 0 & \frac{3EI}{L_2^2} & \frac{3EI}{L_2^3} \end{bmatrix}$$

Equation set:

$$(1) \qquad r_1 = 0$$

$$(2) \qquad \left(\frac{GJ}{L_1}+\frac{3EI}{L_2}\right)\cdot r_2+\left(\frac{3EI}{L_2^2}\right)\cdot r_3 = 0$$

$$(3) \qquad \left(\frac{3EI}{L_2^2}\right)\cdot r_2+\left(\frac{3EI}{L_2^3}\right)\cdot r_3 = R_3$$

Solution:

$$r_2 = -0.2247\,rad = \underline{\underline{12.87\,deg.}}$$

$$r_3 = \underline{\underline{79.42mm}}$$

Analytical	**FEM Results**	
R_3	r_3	r_2
FORCE [N]	*Height [mm]*	*Nodal Rotation,θ*
0	0	0
1000	26.47	4.29
2000	52.95	8.58
3000	79.42	12.87
Norm. Results:	**26.47 mm/kN**	**4.29 deg/kN**

1D Simulation

3a - 3e) Follow the steps.

3f) Results

SOL 101	**Linear Statics**	**1D Beam Elements**
Setup:	Applied Force	Run time: <1 sec.
FORCE [N]	*Height [mm]*	*Nodal Rotation,θ [Deg.]*
0	0	0
1000	26.08	4.3
2000	52.16	8.6
3000	78.25	12.9
Norm. Results:	**26.08 mm/kN**	**4.3 deg/kN**

D.3 TMM4155 - FEA in ME - Exercises Solutions

Quasi Static Response

1a)

Transient analysis means analysing a system in unsteady state. - Where unsteady state is when variables involved in defining the state of the system varies with time. (Increasing force, velocity, acceleration, etc.)

1b)

On a large structure, modal transient should run faster. On a smaller structure (few DoFs), the difference is negligible.

2a - 3d) Follow the steps.

2d) The relationship between the height and reaction force is linear.

Natural Frequency

3) Natural frequency results of different approaches:

	Natural Frequency, f_n, Results		
	Without Hub	With Hub	Hub + Extra Weight
Simulation: SOL 103RE	37.82 Hz	15.14 Hz	10.55 Hz
Physical Tests	N/A	$\approx$ 15.1 Hz	$\approx$ 10.5 Hz

Fatigue

4a) maximum stress:

Static SOL 101, Maximum Stress at 3200 Newtons			
Elemental, Stress consentrarion	$\sigma_{max,El}$	623.6	Mpa
Nodal, Stress consentrarion	$\sigma_{max,No}$	728.8	Mpa

4b) Cycles to failure:

Life Time Simulation Results	
Notch Factor, K_f	Cycles to Failure, N_f
1.14	$N_f = 2.50 \cdot 10^5$
1 [not inc.]	$N_f = 8.57 \cdot 10^5$

4c) The rig should be just fine :)

4d) S-N Diagram

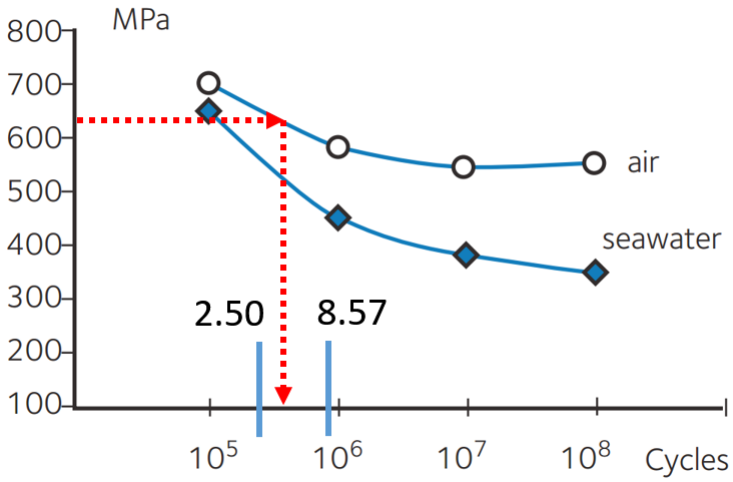

Figure D.1: S-N diagram for S165M [Pic: Industeel [1]]

Appendix E

Material Certificate & Strain Gauge Data

Material Certificate Torsion Bar

Item #	Charge #	Lot	Piece ID	Cust.art.#	Art #	Qty	Description
1	246476				6641051	0	Rustfritt rundt grovdr EN4418

TIBNOR

This document is electronically reproduced and is identical to the original.

Acciaierie Valbruna S.p.A.

36100 VICENZA (Italia) - Viale della scienza, 25 z.i.
Stab.: 39100 BOLZANO (Italia) - Via A. Volta, 4

CERTIFICATO DI COLLAUDO
ABNAHMEPRUEFZEUGNIS
INSPECTION CERTIFICATE
CERTIFICAT DE RECEPTION
EN 10204 (2005) , 3.1

Cliente / Besteller/Purchaser/Client
VALBRUNA NORDIC AB
LOVARTSGATAN 7
65224-KARLSTAD - SWEDEN-SVE

Produttore: **STABILIMENTO DI BOLZANO**
Hersteller/Item/Usine productrice

Oggetto Prove: - Hardened and Tempered Peeled
Prüfgegenstand/Item inspected/Finissage

Avviso di Spedizione: D-BZ09000462
Lieferanzeige/Packing list/B.L.

Ordine nr: R18051
Bestell/Your order/Commande

Tipo di Elaborazione: E+AOD
Erschmelzungsart/Melting process/Mode d'elaboration

Certificato nr: MEST714388/2009/
Prüfung/Test/Essai

Conferma ordine nr: EI08009108
Werks/Our Order/Ref nr.

Marchio di Fabbrica:
Zeichen des Lieferwerkes
Trade mark
Sigle de l'usine productrice

Punzone del Collaudatore:
Stempel des Werkssachverständigen
Inspector's stamp/Poinçon de l'assayeur
MR

Specifiche:
Anforderungen / Requirements / Exigences
MS-RB-4418.1 6 1.4418 QT900 EN 10088-3 2005 1.4418

Qualità: 1.4418
Werkstoff/Grade/Nuance

Marca: PKA7914
Markenbezeichnung/Brand/Nuance

Punzonatura: 1.4418
Kennzeichnung/Marking/Marquage

Pos. nr. / Item nr. / Nr. de poste	Oggetto / Gegenstand / Product description / Descrip. du produit	Dimensioni - mm / Abmessungen / Dimension / Dimension	Tolleranza / Toleranz. / Allowance / Tolerance	Lunghezza - mm / Länge / Length / Longueur	Colata / Schmelze / Heat / Coulée	Pezzi / Stückzahl / Pieces / Pieces	Peso - KG / Gewicht / Weight / Poids	Lotto nr. / Losnr. / Lot nr. / Lot nr.
1	0090 Round	51,200	h12	3635 / 5735	246476		865,0	817703920

Sono state soddisfatte tutte le condizioni richieste
Die gestellten Anforderungen sind it. Anlage erfüllt
The material has been furnished in accordance with the requirements
Le materiel à été trouvé conforme aux exigences

Controllo antimescolanza: OK
Verwechslungsprüfung: spectralanalytisch durchgeführt
Antimixing testing performed: OK
Contrôle anàmelange fait: r.a.s.

Controllo visivo e dimensionale: soddisfa le esigenze:
Besichtigung und Ausmessung: ohne Beanstandung
Visual inspection and dimensional checks:satisfactory
Contrôle visuel et dimensions: satisfaisant

TEST	Provetta/Probestab / Specimen/Eprouvette / Larg.diam.Spess. / Breite Diam. Dicke / Width Diam. Thickness / Larg. diam. epais. mm	°C	Posiz. Saggio / Probelage / Location / Emplacement 1)	Snervamento / Streckgrenze / Yield Stress / Limite elastique Rp 0,2% N/mm2	Snervamento / Streckgrenze / Yield Stress / Limite elastique Rp 1% N/mm2	Resistenza / Zugfestigkeit / Tensile strength / Resistance a traction Rm N/mm2	Allungamento / Bruchdehnung / Elongation / Allongement A5 %		Strizione / Einschnürung / Reduction of area / Striction Z %		Resilienza / Kerbschlagarbeit / Impact Value / Resilience			Durezza / Härte / Hardness / Dureté HB		
Valori richiesti 1 / Anforderungen/Required values / Valeurs demandées		min / max		750	800	900 / 1050	16	-	40	-	-			280 / 340		
A	10.00	20	L	885	902	1010	20		58					320		

TEST	Provetta/Probestab / Specimen/Eprouvette / Larg.diam.Spess. / Breite Diam. Dicke / Width Diam. Thickness / Larg. diam. epais. mm	°C	Posiz. Saggio / Probelage / Location / Emplacement 1)	Resilienza / Kerbschlagarbeit / Impact Value / Resilience KV J			Espansione laterale / Lateral Expansion			Shear / Shear		
Valori richiesti 1 / Anforderungen/Required values / Valeurs demandées		min / max		32	32	32	-	-	-	-	-	-
B	10X10	-40	L	109	111	110						

1)L=longitudinale/längs, T=trasversale/quer, Q=Tangenziale/tangential

Analisi chimica

Chemische Zusammensetzung/Chemical Analysis/Analyse chimique

Colata / Heat / Schmelze/Coulée	C %	Si %	Mn %	Cr %	Mo %	Cu %	Ni %	Ti %	P %	S %	N %	Cb-Nb
min 0,020 / max 0,050	0,30 / 0,70	0,60 / 1,00	15,00 / 17,00	0,80 / 1,25	- / 0,60	4,50 / 5,50	- / 0,025	- / 0,040	0,005 / 0,015	0,020 / 0,050	- / 0,050	- / -	- / -	- / -
246476	0,025	0,44	0,78	15,42	0,94	0,26	5,12	0,001	0,029	0,013	0,043	0,015

Hardened 1040 C x 1.50h/air. Tempered 560 C x 4h.
UT-TESTING ACCORDING TO MS-RB-4418.1: OK

Melted and manufactured in Italy No welding or weld repair Material free from Mercury or radio-activity contamination
The Quality Management System is Certified acc. Pressure Equipment Directive [97/23/EC] Annex 1,s.,4.3 by TUEV and LLOYD'S

Bolzano,04/02/09 BBL006 (Mod. MCER)	*Il collaudatore di stabilimento / der Werkssachverständige / Works Inspector / L'agent d'usine* M.Rizzotto	Pagina - 1 di 1

Material Data Torsion Bar

Industeel VIRGO 39 16% Cr, 5% Ni, Martensitic Stainless Steel

Categories: Metal; Ferrous Metal; Martensitic; Stainless Steel

Material Notes: **Description:** Virgo 39 is a 16% Cr, 5% Ni, 1% Mo low carbon martensitic stainless steel. The grade is specially designed to combine high mechanical properties including toughness and improved corrosion resistance properties when compared to other martensitic stainless steels, like 13 Cr and 13 Cr 4 Ni grades. The alloy has been primarily designed to resist to erosion-corrosion or cavitation encountered in hydraulic applications. The alloy is also used for hydrofoils legs, as anti-seismic compounds or offshore structures, boats, landing grids for helicopters… where the combined mechanical and corrosion resistance properties are needed. Mining, cement plants, and hydraulic applications take also advantage of its combined abrasion-corrosion resistance properties.

Information provided by manufacturer.

Key Words: EN 10088/10028 1.4418 - X4 Cr Ni Mo 16-5-1, AFNOR Z6 CND 16.05.01, DIN W.Nr 1.4418

Vendors: No vendors are listed for this material. Please click here if you are a supplier and would like information on how to add your listing to this material.

Physical Properties	Metric	English	Comments
Density	7.70 g/cc	0.278 lb/in³	

Mechanical Properties	Metric	English	Comments
Hardness, Brinell	230 - 320	230 - 320	Typical
Tensile Strength, Ultimate	850 MPa	123000 psi	Quenched Tempered
Tensile Strength, Yield	615 MPa @Strain 0.200 %	89200 psi @Strain 0.200 %	Quenched Tempered
Elongation at Break	>= 15 %	>= 15 %	
Modulus of Elasticity	210 GPa	30500 ksi	
Poissons Ratio	0.346	0.346	Calculated
Shear Modulus	78.0 GPa @Temperature 20.0 °C	11300 ksi @Temperature 68.0 °F	
Charpy Impact	35.0 J	25.8 ft-lb	Guaranteed in T Direction
	60.0 J	44.3 ft-lb	Guaranteed in L Direction
	100 J	73.8 ft-lb	Typical

Electrical Properties	Metric	English	Comments
Electrical Resistivity	0.0000750 ohm-cm @Temperature 20.0 °C	0.0000750 ohm-cm @Temperature 68.0 °F	

Thermal Properties	Metric	English	Comments
CTE, linear	10.0 µm/m-°C @Temperature 20.0 - 100 °C	5.56 µin/in-°F @Temperature 68.0 - 212 °F	
	11.0 µm/m-°C @Temperature 20.0 - 200 °C	6.11 µin/in-°F @Temperature 68.0 - 392 °F	
Specific Heat Capacity	0.460 J/g-°C @Temperature 20.0 °C	0.110 BTU/lb-°F @Temperature 68.0 °F	
Thermal Conductivity	20.0 W/m-K @Temperature 20.0 °C	139 BTU-in/hr-ft²-°F @Temperature 68.0 °F	

Component Elements Properties	Metric	English	Comments
Carbon, C	0.045 %	0.045 %	
Chromium, Cr	16 %	16 %	
Iron, Fe	77.934 %	77.934 %	As remainder
Molybdenum, Mo	1.0 %	1.0 %	
Nickel, Ni	5.0 %	5.0 %	
Phosphorous, P	0.020 %	0.020 %	
Sulfur, S	0.0010 %	0.0010 %	

Material Fatigue Data

42CrMo4 1.7225		
Data under fatigue +20 °C		
+N	328	Cyclic yield strength, σ_y'
+QT	716	N/mm² low cycle number
+N	0.12	Cyclic strength exponent, n'
+QT	0.10	low cycle number
+N	673	Cyclic strength coefficient, K '
+QT	1367	N/mm² low cycle number
+N	1000	Fatigue strength coefficient, σ_f '
+QT	1454	N/mm² low cycle number
+N	-0.11	Fatigue strength exponent, b
+QT	-0.08	low cycle number
+N	-1.00	Fatigue ductility exponent, c
+QT	-0.72	low cycle number
+N = normalization +QT = quenching and tempering		

EUROPE EN	ITALY UNI	CHINA GB	GERMANY DIN	FRANCE AFNOR	U.K. B.S.	RUSSIA GOST	USA AISI/SAE
42CrMo4	42CrMo4	ML42CrMo	42CrMo4	42CD4	708M40	42HM	4140

T.T.T. curve

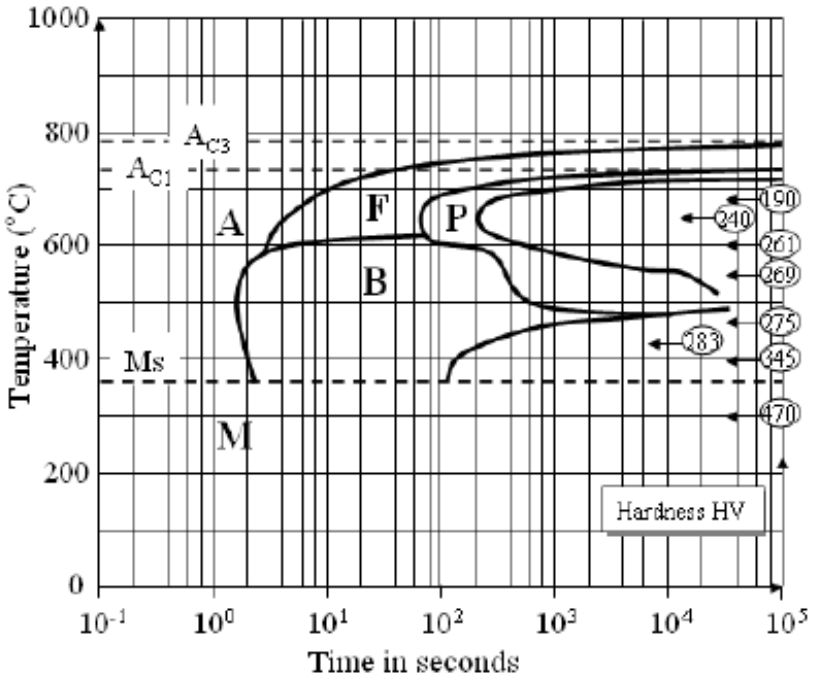

THE DATA CONTAINED HEREIN ARE INTENDED AS REFERENCE ONLY AND ARE SUBJECT TO CONSTANT CHANGE. LUCEFIN S.P.A. DISCLAIMS ANY AND ALL LIABILITY FOR ANY CONSEQUENCES THAT MAY RESULT FROM THEIR USE.

Material Data Torsion Arm

ThyssenKrupp Materials International

Mechanical properties at room temperature

Steel grade	Yield strength R_{eH} N/mm² Nominal wall thickness in mm						Tensile strength R_m N/mm² Nominal wall thickness in mm			Elongation A [1)2)] min. in % Nominal thickness in mm				Impact energy KV[3)] J min. at a temperature °C of		
(Material No.)	≤ 16	> 16 ≤ 40	> 40 ≤ 63	> 63 ≤ 80	> 80 ≤100	>100 ≤120	< 3	≥ 3 ≤100	> 100 ≤ 120	≤ 40	> 40 ≤ 63	> 63 ≤ 100	> 100 ≤ 120	-20	0	+20
S235JRH (1.0039)	235	225	215	215	215	195	360 - 510	360 - 510	350 - 500	26	25	24	22	-	-	27
S275J0H (1.0149)	275	265	255	245	235	225	430 - 580	410 - 560	400 - 540	23	22	21	19	-	27	-
S355J0H (1.0547)	355	345	335	325	315	295	510 - 680	470 - 630	450 - 600	22	21	20	18	-	27	-
S355J2H (1.0576)														27	-	-

[1)] Longitudinal values. Transverse values are 2 % below.

[2)] For thicknesses < 3 mm see DIN EN 10210-1:2006, 9.2.2

[3)] For sections with a nominal thickness > 100 mm the values are to be agreed. If test pieces with a width lower than 10 mm are applied, the mentioned minimum values have to be decreased proportional corresponding to the cross-section of the test piece. With nominal thicknesses < 6 mm no impact test are required.

Reference data for some physical properties

Density at 20°C	Modulus elasticity kN/mm² at				Thermal conductivity at 20 °C	spec. thermal capacity at 20 °C	spec. electrical resistivity at 20 °C
Kg/dm³	20 °C	100 °C	200 °C	300 °C	W/m K	J/kg K	Ω mm²/m
7,85	210	205	197	190	54	461	0,15

Linear coefficient 10^{-6} K^{-1} of thermal expansion between 20 °C and

100 °C	200 °C	300 °C
11,1	12,1	12,9

Hot forming / Heat treatment (for guidance only)

Hot Forming		Heat Treatment		
Temperature °C	Cooling Type	Normalizing [1)]	Stress relieving anneal [2)]	Cooling Type
700 - 750	Air	850 - 950 °C	580 - 630 °C	Air

[1)] Normalizing: Holding time 1 minute per mm plate thickness, minimum 30 minutes

[2)] Stress relieving anneal: Holding time 1-2 minutes per mm plate thickness, minimum 30 minutes

Stain Gauge Data

TML STRAIN GAUGE TEST DATA

GAUGE TYPE	: FRA-6-11	TESTED ON	: SS 400
LOT NO.	: A513731	COEFFICIENT OF THERMAL EXPANSION	: 11.8 $\times 10^{-6}$/℃
GAUGE FACTOR	: 1=2.11 2=2.11 3=2.11 ±1%	TEMPERATURE COEFFICIENT OF G.F.	: +0.1±0.05 %/10℃
ADHESIVE	: P-2	DATA NO.	: A0492

THERMAL OUTPUT (ε app : APPARENT STRAIN)

$\varepsilon app = -2.33\times10^{1}+1.57\times T^{1}-1.21\times10^{-2}\times T^{2}-4.97\times10^{-4}\times T^{3}+4.55\times10^{-6}\times T^{4}$ (μm/m)

TOLERANCE : ±0.85 [(μm/m)/℃] , T : TEMPERATURE

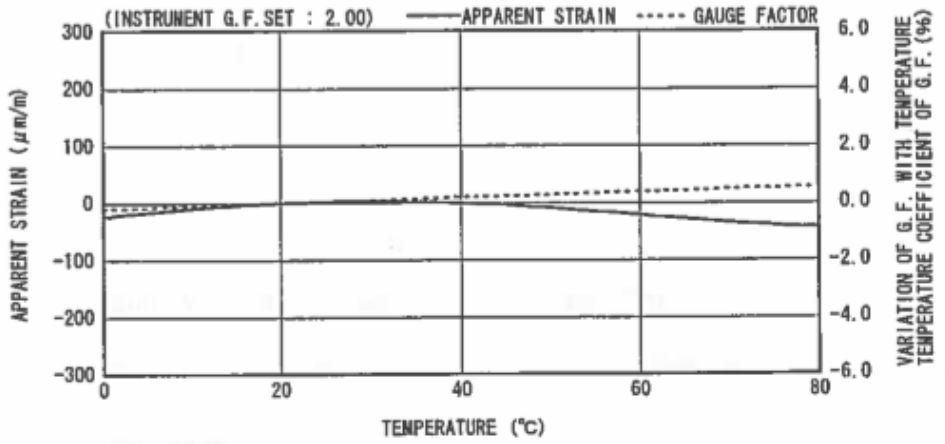

ひずみゲージ取扱いの注意事項

- ●上記の特性データは、リード線の取付けによる影響を含んでおりません。裏面記載のリード線の測定値への影響に従って補正してください。
- ●ゲージの使用温度は、接着剤の耐熱温度などにより変わります。
- ●絶縁抵抗などの点検は、印加電圧を５０Ｖ以下にしてください。
- ●ゲージリード線に無理な力を加えないでください。
- ●ゲージ裏面に接着剤を塗布して接着してください。
- ●ひずみゲージの裏面は脱脂洗浄してありますので、汚さないように取扱いしてください。
- ●ゲージの包装を開封後は、乾燥した場所で保管してください。
- ●ご使用に際してご不明な点などがございましたら、当社までお問い合わせください。

CAUTIONS ON HANDLING STRAIN GAUGES

- ● The above characteristic data do not include influence due to lead wires. Correct the data in accordance with the influence of lead wires on measured values described overleaf.
- ● The service temperature of strain gauge depends on the operating temperature of adhesive, etc.
- ● Check of insulation resistance, etc. should be made at a voltage of less than 50V.
- ● Do not apply an excessive force to the gauge leads.
- ● Apply an adhesive to the back of a strain gauge and stick the gauge to a specimen.
- ● As the back of strain gauge has been degreased and washed, do not contaminate it.
- ● After unpacking, store strain gauges in a dry place.
- ● If you have any questions on strain gauges or installation, contact TML or your local agent.

Made in Japan

Stain Gauge Data

TML STRAIN GAUGE TEST DATA

GAUGE TYPE	: FCA-3-11	TESTED ON	: SS 400
LOT NO.	: A601522	COEFFICIENT OF THERMAL EXPANSION	: 11.8 $\times 10^{-6}$/℃
GAUGE FACTOR	: 1=2.12 2=2.12 ±1%	TEMPERATURE COEFFICIENT OF G.F.	: +0.1±0.05 %/10℃
ADHESIVE	: P-2	DATA NO.	: A0263

THERMAL OUTPUT (εapp : APPARENT STRAIN)

$\varepsilon app = -1.55\times10^{1}+1.96\times T^{1}-7.01\times10^{-2}\times T^{2}+5.69\times10^{-4}\times T^{3}-2.08\times10^{-6}\times T^{4}$ (μm/m)

TOLERANCE : ±0.85 [(μm/m)/℃] , T : TEMPERATURE

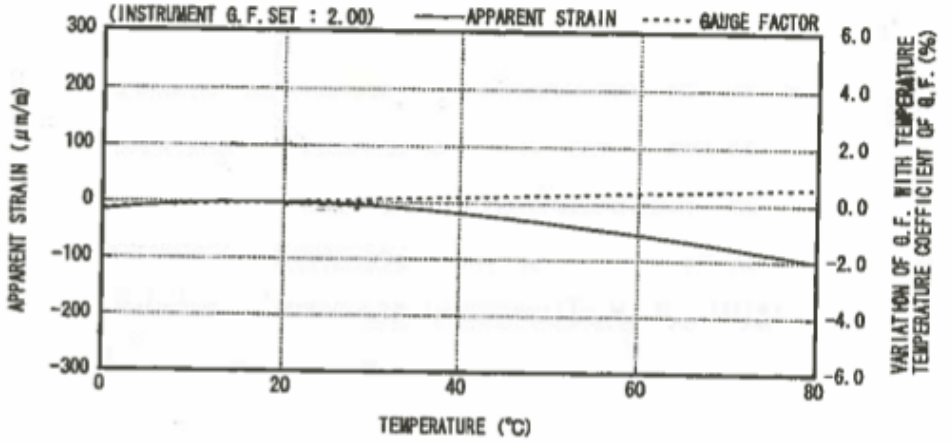

ひずみゲージ取扱いの注意事項

- 上記の特性データは、リード線の取付けによる影響を含んでおりません。裏面記載のリード線の測定値への影響に従って補正してください。
- ゲージの使用温度は、接着剤の耐熱温度などにより変わります。
- 絶縁抵抗などの点検は、印加電圧を50V以下にしてください。
- ゲージリード線に無理な力を加えないでください。
- ゲージ裏面に接着剤を塗布して接着してください。
- ひずみゲージの裏面は脱脂洗浄してありますので、汚さないように取扱いしてください。
- ゲージの包装を開封後は、乾燥した場所で保管してください。
- ご使用に際してご不明な点などがございましたら、当社までお問い合わせください。

CAUTIONS ON HANDLING STRAIN GAUGES

- The above characteristic data do not include influence due to lead wires. Correct the data in accordance with the influence of lead wires on measured values described overleaf.
- The service temperature of strain gauge depends on the operating temperature of adhesive, etc.
- Check of insulation resistance, etc. should be made at a voltage of less than 50V.
- Do not apply an excessive force to the gauge leads.
- Apply an adhesive to the back of a strain gauge and stick the gauge to a specimen.
- As the back of strain gauge has been degreased and washed, do not contaminate it.
- After unpacking, store strain gauges in a dry place.
- If you have any questions on strain gauges or installation, contact TML or your local agent.

Appendix F

Risk Assessment

NTNU HMS	Kartlegging av risikofylt aktivitet	Utarbeidet av	Nummer	Dato
		HMS-avd.	HMSRV2601	22.03.2011
		Godkjent av		Erstatter
		Rektor		01.12.2006

Enhet: **IPM** **Dato: 30.05.2016**

Linjeleder: Terje Rølvåg

Deltakere ved kartleggingen (m/ funksjon)**: Ask Falch, student**

(Ansv. veileder, student, evt. medveiledere, evt. andre m. kompetanse)

Kort beskrivelse av hovedaktivitet/hovedprosess: Masteroppgave Ask Falch. Hjulopphengsrigg for tilhenger

Er oppgaven rent teoretisk? (JA/NEI)**:** **Nei** *«JA» betyr at veileder innestår for at oppgaven ikke inneholder noen aktiviteter som krever risikovurdering. Dersom «JA»: Beskriv kort aktiviteteten i kartleggingsskjemaet under. Risikovurdering trenger ikke å fylles ut.*

Signaturer: *Ansvarlig veileder:* Terje Rølvåg *Student:* Ask Falch

ID nr.	Aktivitet/prosess	Ansvarlig	Eksisterende dokumentasjon	Eksisterende sikringstiltak	Lov, forskrift o.l.	Kommentar
1	Bæring av materiale	Ask	Interne prosedyrer for labarbeid på NTNU	Verneutstyr, Godkjent utstyr		
2	Kapping av materiale	Ask	Interne prosedyrer for labarbeid på NTNU	Verneutstyr, Godkjent utstyr		
3	Sveising	Ask	Interne prosedyrer for labarbeid på NTNU	Verneutstyr, Godkjent utstyr		
4	Klemfare under testing	Ask	Interne prosedyrer for labarbeid på NTNU	Verneutstyr, Godkjent utstyr		
5	Lakkering	Ask	Interne prosedyrer for labarbeid på NTNU	Verneutstyr, Godkjent utstyr		
6	Maskinering av komponenter	Ask	Interne prosedyrer for labarbeid på NTNU	Verneutstyr, Godkjent utstyr		

NTNU HMS	Risikovurdering	Utarbeidet av	Nummer	Dato
		HMS-avd.	HMSRV2601	22.03.2011
		Godkjent av		Erstatter
		Rektor		01.12.2006

Enhet: IPM **Dato: 30.05.2016**

Linjeleder: Terje Rølvåg

Deltakere ved kartleggingen (m/ funksjon): Ask Falch

(Ansv. Veileder, student, evt. medveiledere, evt. andre m. kompetanse)

Risikovurderingen gjelder hovedaktivitet: Masteroppgave Ask Falch. Hjulopphengsrigg for tilhenger.

Signaturer: *Ansvarlig veileder:* Terje Rølvåg *Student:* Ask Falch

ID nr	Aktivitet fra kartleggings-skjemaet	Mulig uønsket hendelse/ belastning	Vurdering av sannsynlighet	Vurdering av konsekvens:				Risiko-Verdi	Kommentarer/status Forslag til tiltak
			(1-5)	Menneske (A-E)	Ytre miljø (A-E)	Øk/ materiell (A-E)	Om-dømme (A-E)		
1a	Bæring av materiale	Skade på finger/hender, klemsituasjon	4	A		A		A4	Være oppmerksom under arbeid
2a	Kapping av materiale	Kuttskader, metallspon i øyne	3	B			B	B3	Utføre arbeid etter instruks, bruke vernebriller
2b	Sveising	Øyeskader, brannskader	3	B			B	B3	Bruke korrekt verneutstyr
3a	Klemfare under testing	Skade på finger/hender, klemsituasjon	3	B			A	B3	Utføre arbeid etter instruks
4a	Lakkering	Uønsket avgass	2	A	A	A		A2	Sikre tilstrekkelig avtrekk
4b	Maskinering av komponenter	Øyeskader, fysisk skade på armer.	2	D		B	B	D2	Bruke vernebriller, Utføre arbeid etter instruks

NTNU HMS	Risikovurdering	Utarbeidet av	Nummer	Dato
		HMS-avd.	HMSRV2601	22.03.2011
		Godkjent av		Erstatter
		Rektor		01.12.2006

Sannsynlighet vurderes etter følgende kriterier:

Svært liten 1	Liten 2	Middels 3	Stor 4	Svært stor 5
1 gang pr 50 år eller sjeldnere	1 gang pr 10 år eller sjeldnere	1 gang pr år eller sjeldnere	1 gang pr måned eller sjeldnere	Skjer ukentlig

Konsekvens vurderes etter følgende kriterier:

Gradering	Menneske	Ytre miljø Vann, jord og luft	Øk/materiell	Omdømme
E Svært Alvorlig	Død	Svært langvarig og ikke reversibel skade	Drifts- eller aktivitetsstans >1 år.	Troverdighet og respekt betydelig og varig svekket
D Alvorlig	Alvorlig personskade. Mulig uførhet.	Langvarig skade. Lang restitusjonstid	Driftsstans > ½ år Aktivitetsstans i opp til 1 år	Troverdighet og respekt betydelig svekket
C Moderat	Alvorlig personskade.	Mindre skade og lang restitusjonstid	Drifts- eller aktivitetsstans < 1 mnd	Troverdighet og respekt svekket
B Liten	Skade som krever medisinsk behandling	Mindre skade og kort restitusjonstid	Drifts- eller aktivitetsstans < 1uke	Negativ påvirkning på troverdighet og respekt
A Svært liten	Skade som krever førstehjelp	Ubetydelig skade og kort restitusjonstid	Drifts- eller aktivitetsstans < 1dag	Liten påvirkning på troverdighet og respekt

Risikoverdi = Sannsynlighet x Konsekvens
Beregn risikoverdi for Menneske. Enheten vurderer selv om de i tillegg vil beregne risikoverdi for Ytre miljø, Økonomi/materiell og Omdømme. I så fall beregnes disse hver for seg.

Til kolonnen "Kommentarer/status, forslag til forebyggende og korrigerende tiltak":
Tiltak kan påvirke både sannsynlighet og konsekvens. Prioriter tiltak som kan forhindre at hendelsen inntreffer, dvs. sannsynlighetsreduserende tiltak foran skjerpet beredskap, dvs. konsekvensreduserende tiltak.

NTNU	Risikomatrise	utarbeidet av	Nummer	Dato	
		HMS-avd.	HMSRV2604	08.03.2010	
HMS/KS		godkjent av		Erstatter	
		Rektor		09.02.2010	

MATRISE FOR RISIKOVURDERINGER ved NTNU

KONSEKVENS						
	Svært alvorlig	E1	E2	E3	E4	E5
	Alvorlig	D1	D2	D3	D4	D5
	Moderat	C1	C2	C3	C4	C5
	Liten	B1	B2	B3	B4	B5
	Svært liten	A1	A2	A3	A4	A5
		Svært liten	Liten	Middels	Stor	Svært stor
		SANNSYNLIGHET				

Prinsipp over akseptkriterium. Forklaring av fargene som er brukt i risikomatrisen.

Farge	Beskrivelse
Rød	Uakseptabel risiko. Tiltak skal gjennomføres for å redusere risikoen.
Gul	Vurderingsområde. Tiltak skal vurderes.
Grønn	Akseptabel risiko. Tiltak kan vurderes ut fra andre hensyn.

Appendix G

Project Thesis

Trailer suspension rig for viritual and physical testing

Ask Arildsønn Falch

April 2016

PROJECT THESIS

Department of Engineering Design and Materials

Norwegian University of Science and Technology

Supervisor: Terje Rølvåg

THE NORWEGIAN UNIVERSITY
OF SCIENCE AND TECHNOLOGY
DEPARTMENT OF ENGINEERING DESIGN
AND MATERIALS

PROJECT WORK SPRING 2016
FOR
STUD.TECHN. ASK FALCH

TRAILER SUSPENSION RIG FOR VIRTUAL AND PHYSICAL TESTING

Tilhenger hjuloppheng rig for virtuell og fysisk dynamisk testing

IPM professors are teaching various courses in static and dynamic analysis of mechanical systems. Different methods and cases are used and it's hard for the students to know when and where the different methods and tools are applicable. Analytical calculations are sometimes applicable while simulation tools are required for more complex analysis.

The intention with the physical test rig is to establish a common benchmark model and link between the different methods and tools used in various courses. Then the students can compare calculations with physical test results and evaluate the difference in accuracy and speed.

This project work will prepare the test rig for use in several IPM courses. The learning objective is to give the students a better understanding of structural dynamics and motivate them for further studies in this challenging area.

Tasks to be completed:

1. Study the trailer suspension model and tasks described in the Machine Elements 2009 exams.
2. Identify structural and mechanism key performance indicators (KPIs) to be tested and benchmarked
3. Build and instrument the virtual and physical test rig with sensors to capture the KPIs
4. Perform physical tests and document the performance (KPIs)
5. Perform analytical calculations, virtual tests and compare with physical test KPIs

If time permits:

6. Suggest suspension test rig exercises for TMM4112 (Maskindeler), TMM4135 (Elementmetoden grunnkurs) and TMM4155 (FEAinME).

Formal requirements:

Students are required to submit an A3 page describing the planned work three weeks after the project start as a pdf-file. A template can be found on IPM's web-page (https://www.ntnu.no/ipm/prosjekt-og-fordypningsemner).

Performing a risk assessment is mandatory for any experimental work. Known main activities must be risk assessed before they start, and the form must be handed in within 3 weeks after you receive the problem text. The form must be signed by your supervisor. Risk assessment is an ongoing activity, and must be carried out before starting any activity that might cause injuries or damage materials/equipment or the external environment. Copies of the signed risk assessments have to be put in the appendix of the project report.

No later than 1 week before the deadline of the final project report, you are required to submit an updated A3 page summarizing and illustrating the results obtained in the project work.

Official deadline for the delivery of the report is 25 May 2016 at 2 p.m. The report is to be delivered in two paper copies and one electronic version.

When evaluating the project, we take into consideration how clearly the problem is presented, the thoroughness of the report, and to which extent the student gives an independent presentation of the topic using his/her own assessments.

The report must include the signed problem text, and be written as a scientific report with summary of important findings, conclusion, literature references, table of contents, etc. Specific problems to be addressed in the project are to be stated in the beginning of the report and briefly discussed. The report should not exceed thirty pages including illustrations and sketches.

Additional tables, drawings, detailed sketches, photographs, etc. can be included in an appendix at the end of the thirty page report. References to the appendix must be specified. The report should be presented so that it can be fully understood without referencing the Appendix. Figures and tables must be presented with explanations. Literature references should be indicated by means of a number in brackets in the text, and each reference should be further specified at the end of the report in a reference list. References should be specified with name of author(s) and book, title and year of publication, and page number.

Contact persons:
The contact persons at IPM are Bjørn Haugen and Torgeir Welo.

Torgeir Welo
Head of Division

Terje Rølvåg
Professor/Supervisor

NTNU
Norges teknisk-naturvitenskapelige universitet
Institutt for produktutvikling og materialer

Abstract

The objective of this thesis is to design and build a physical torsion bar suspension test rig. This report describes the work that has been done to achieve this goal. The basis for this work are two exams from TMM4112 Machine Elements of 2009. The aim is to build a user friendly physical rig that behaves as a suspension system presented in these exams. The physical rig is later on going to be instrumented with numerous sensors. This is to compare the physical performance with the analytical values from the exams, and computer simulations. FEA simulations has been utilized during the design process to ensure that the design criteria was met. The design and constitution of the rig was preformed by the author of this paper. The ambition to build a finished rig was completed during this Thesis. Initial physical testing indicates that the finished rig behaves as desired.

Sammendrag

Målet for denne prosjektoppgaven var å designe og bygge en fysisk testrigg for et torsjons-stag-hjuloppheng. Denne oppgaven beskriver arbeidet som har blitt gjort for å oppnå dette målet. Bakgrunnen for dette arbeidet er to eksamener i faget TMM4112 maskindeler i fra 2009. Ambisjonen var å bygge en brukervennlig fysisk testrigg som oppfører seg som hjulopphenget som er presentert i disse eksamenene. Den fysiske riggen vil på et senere tidspunkt bli utrustet med en rekke måleinstrumenter. Dette vil gi et grunnlag for å sammenlikne riggens fysiske ytelser mot analytiske verdier i fra eksamenene, samt mot datasimuleringer. FEA simuleringer ble benyttet igjennom utarbeidelsen av designet av riggen. Dette ble gjort for å forsikre seg om at gitte designkriterier ble møtt. Desigingen og byggingen av riggen ble utført av undertegnede. Ambisjonen om å ferdigstille riggen i løpet av denne oppgaven, ble gjennomført. Initiell fysisk testing tyder på at riggen oppfører seg som ønsket.

Preface

This project thesis considers the work of designing and constructing a physical torsion bar suspension test rig. The rig is going to be utilized in lecturing several courses at the Department of Engineering Design and Materials, NTNU. The work was carried out during the spring semester of 2016. The idea for this projects is provided by supervisor Professor Terje Rølvåg. The basis for this project are two exams in Machine Elements of 2009, created by Professor Torgeir Welo. The ambition is to provide students with an opportunity to perform physical testing of theory, in a convenient way.

Trondheim, 2016-04-22

Ask A. Falch

Acknowledgment

I would like to thank the following people for their great help during my project thesis.
Supervisor, Professor Terje Rølvåg has been a great help and support, throughout this project. By providing an exciting project I find interesting, and expecting great results, he has pushed me to preform my best. A big thanks goes to Halvard Støwer for being a great asset concerning the sensors and software, which is going to be utilized on the finished rig. Gabriela Dahle has been a great help, by dealing with orders and vendors during this project.

A.F.

Contents

Abstract . . . iii

Preface . . . iv

Acknowledgment . . . v

1 Introduction **2**

1.1 Background . . . 2

1.2 Objectives . . . 4

1.3 Approach . . . 4

1.4 Structure of the Report . . . 4

2 Analyzing Exams **5**

2.1 Key Performance Indicators . . . 6

2.2 Evaluation of Assumptions . . . 7

3 Rig Design **8**

3.1 Initial Design Process . . . 8

3.1.1 Materials . . . 9

3.1.2 Size and layout . . . 9

3.1.3 Torsion bar . . . 10

3.1.4 Torsion arm . . . 11

3.2 CAD . . . 12

3.2.1 Software . . . 12

3.2.2 Revision 1 - Concept . . . 13

3.2.3 Revision 2 . . . 14

3.2.4 Revision 3 . . . 15
3.2.5 Revision 4 . . . 16
3.3 Simulation / Results . . . 17
3.3.1 Displacement . . . 18
3.3.2 Stresses . . . 18

4 Building process **20**
4.1 Production Planing . . . 20
4.1.1 Procurement of parts . . . 20
4.1.2 Time and cost . . . 21
4.1.3 Technical drawings . . . 22
4.1.4 Assembly procedure . . . 23
4.2 Fabrication . . . 25
4.2.1 Torsion bar . . . 25
4.2.2 Welding . . . 25
4.2.3 Modified components . . . 27
4.2.4 Paint . . . 27
4.3 Final product . . . 27

5 Summary **29**
5.1 Summary and Conclusions . . . 29
5.2 Further Work . . . 30

A As Built, Technical Drawings **31**

B Acronyms **34**

C Material Certificate **35**

D Risk Assessment **37**

Chapter 1

Introduction

Throughout five years of a Mechanical Engineering education, students primary learn the necessary theory to construct mechanical components. This leaves some students to have limited hands on experience with transferring their theoretical knowledge into manufactured components. And to experience deviations and unforeseen obstacles that may occur. This thesis' objective is to provide students with an opportunity to preform physical testing of theory, in a convenient setting. This by construing a physical version of a theoretical exercise most IPM students have tried to solve. Hopefully, this thesis will inspire other students to conduct similar projects themselves.

1.1 Background

IPM professors are teaching various courses in static and dynamic analysis of mechanical systems. Different methods and cases are used and it is hard for students to know when and where the different methods and tools are applicable. Analytical calculations are sometimes applicable while simulation tools are required for more complex analysis. The intention with the physical test rig is to establish a common benchmark model and link between the different methods and tools used in various courses. Then, students can compare calculations with physical test results and evaluate the difference in accuracy and speed. This project thesis will prepare the test rig for use in several IPM courses. The learning objective is to give the students a better understanding of structural dynamics and motivate them for further studies in this challenging area.

Problem Formulation

The objective of this thesis is to construct a physical test rig, on the basis of two exams in Machine Elements of 2009. The test rig is to be utilized by professors and students at IPM, to compare physical testing with analytical calculations and FEA

Tasks to be completed:

1. Study the trailer suspension model and tasks described in the Machine Elements 2009 exams.
2. Identify structural and mechanism key performance indicators (KPIs) to be tested and benchmarked.
3. Build and instrument the virtual and physical test rig with sensors to capture the KPIs.
4. Perform physical tests and document the performance (KPIs).
5. Perform analytical calculations, virtual tests and compare with physical test KPIs.
6. (If time permits:) Suggest suspension test rig exercises for TMM4112 (Maskindeler), TMM4135 (Elementmetoden grunnkurs) and TMM4155 (FEAinME).

Restriction of Problem Formulation

The problem formulation of this thesis is dimensioned to be a Master Thesis (20 weeks). Due to this, it is chosen to restrict the problem formulation to adapt it to a Project Thesis (10 weeks). To not compromise the quality of the work, due to time-consume, the problem formulation for this thesis is restricted to pullet-in number. 1, 2, and building the rig (partially nr. 3). Instrumenting and testing the rig is not included in this thesis.

1.2 Objectives

After restricting the problem formulation, the following objectives are set to be completed.

1. Study the trailer suspension model and tasks described in the Machine Elements 2009 exams.
2. Identify structural and mechanism key performance indicators (KPIs) to be tested and benchmarked.
3. Design a physical test rig based on the theoretical trailer suspension model.
4. Perform building of physical test rig.

1.3 Approach

The exams with solutions were analyzed to retrieve important KPIs. These became the basis for a set of engineering criteria, essential to designing the physical version of the suspension system. Product Demand Specifications, (PDS), were created on the basis of the intended use of the rig. Different component/material solutions where analyzed and chosen in regards to cost/benefit. To ensure that the design was adequate, FEA simulation was performed of the design throughout the design process. The construction of the rig was performed at the Institute's realization workshop.

1.4 Structure of the Report

The rest of the report is structured to separate the different stages of developing and building the rig. Some of these stages were performed simultaneously during the work described, but are sectioned for practical reasons. The report is sectioned as following:

Chapter 2 Presents the essence of the analyze of the Machine Elements exams of 2009.

Chapter 3 Describes the work of designing the physical rig, including FEA.

Chapter 4 Describes the building process and finished product.

Chapter 5 Includes a summary and further work.

Chapter 2

Analyzing Machine Elements Exams of 2009

The Machine Elements Exams include a variety of different exercises related to a technical drawing of a torsion bar suspension system. See Figure 2.1. The primary focus in these exercises is to analyze static and dynamic response and limitations of the system. Calculation are made on the basis of given material properties and dimensions. Assumptions are also given to ease the hand calculations. In this Thesis, the focus is the static behavior and limitations.

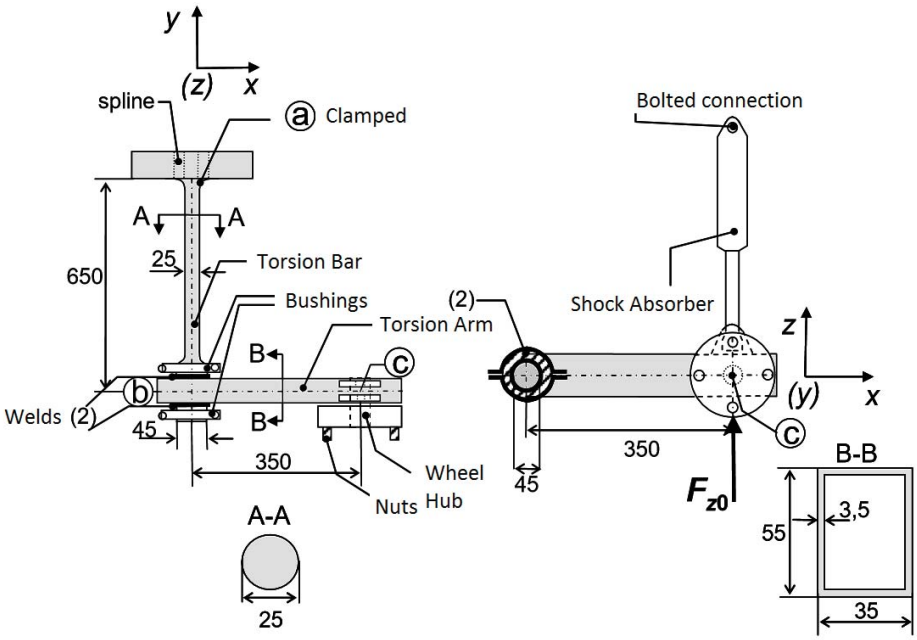

Figure 2.1: Technical drawing from 2009 Exam

2.1 Key Performance Indicators

The key performance indicators, (KPIs), relevant to this thesis, are the relationship between; applied force, elevation of the wheel hub, and stress in the torsion bar. The assumptions given in the exams, sums up to that the entire system can be considered to behave linearly. The main assumptions are: Force is applied in Point C, not on the wheel hub, at a constant horizontal distance from the torsion bar. See Figure 2.1. The torsion arm is infinite stiff, and assume small deformations. Yield stress σ is 640 Mpa. The material coefficient γ is 1.1, which gives maximum allowed stress = 582 Mpa in the torsion bar. Tabel 2.1, displays the important KPI values from the exams. The relationship between these are linear from 0. See Figure 2.2.

Table 2.1: Linear relationship between KPIs

Applied Force	Elevation of Hub	Von Mises, Torsion Bar	Principal stress, Torsion Bar
1000N	25,8mm	198 Mpa	114 Mpa
2940N	76mm	582 Mpa (maximum allowed)	336 Mpa

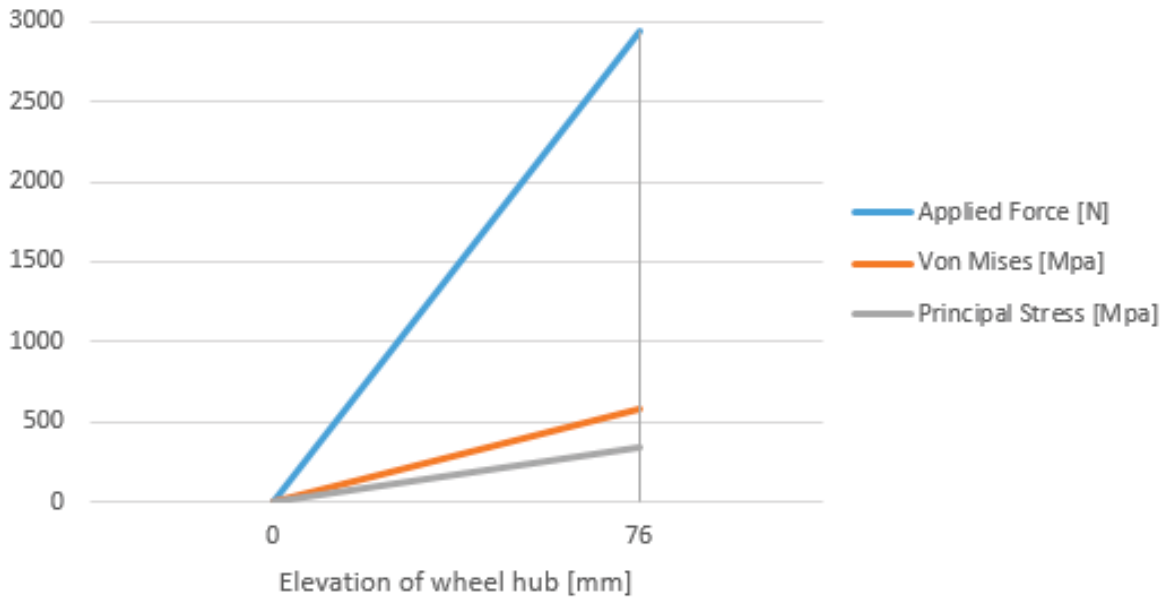

Figure 2.2: Linear response of the torsion bar system

2.2 Evaluation of Assumptions

When analyzing the exams in order to build a physical version, it was necessary to evaluate the structural and computational assumptions. Structural assumptions and data was evaluated of whether they needed to taken into account. As seen in Table 2.2, there were several issues that needed to be resolved. These were addressed during the design process later on.

Table 2.2: Assumptions and structural data from the Exams

Item	Given assumptions	Needs addressing
TORSION BAR		
Cross-section	Ø25mm, and Ø45mm at each end	No
Section Lengths	Effective torsion length reaches centerline of arm	Yes: Not realistic
Material	Yield Strength = 640 Mpa, E-modulus = 210 Gpa	Yes: High tension steel
Fixing	Clamped end section	Yes: Need a rigid frame
Welds	Welds joining torsion bar and arm	Dependant on weldability
TORSION ARM		
Cross-section	55x35x3.5mm	Yes. Stock dimension?
Section Length	350mm effective length	No
Material	Yield Strength = 640 Mpa, E-modulus = 210 Gpa	Yes: Unnecessary quality
Other	Assumed infinite stiff	Yes: Not realistic
FORCE		
Force offset	Force assumed applied at torsion arm centerline	Yes: Want an offset
Moment force	Force leverage arm assumed to be constant	Yes: Not physical correct

Chapter 3

Designing a Physical Rig

The purpose of constructing this physical test rig, is to be able to demonstrate practical examples of theory in the classroom. The ambition is to construct a rig that is physically behaves close to the exams of 2009, based on the KPIs. The rig will be used in lecturing of different courses, of various professors. This means that the rig must be mobile, and preferably be intuitive to use.

3.1 Initial Design Process

A decision on whether the rig should be quasi static or dynamically loaded, took some time to make. This choice would influence the overall design of the rig, considering that fluctuations in the frame may influence the results. Due to cost, versus the benefit of having a dynamic loaded rig, dynamic loading was discarded. The focus shifted to creating a quasi static loaded design, and finding suitable materials and components, that wound make the rig behave similar to the theoretical model.

3.1.1 Materials

Table 3.1: Steel from the exam vs. chosen steel

	Steel Exams	SS2387 Torsion Bar	S355 Torsion Arm
Yield Strength, σ_0	640 Mpa	750 Mpa	355 Mpa
Tensile Strength, R_m	800 Mpa	900 Mpa	420 Mpa
Young's Modulus, E	210 Gpa	205-210 Gpa	210 Gpa
Poisson's Number, ν	0.3	0.3	0.3

In the exams, the material is given as a generic steel with the following values; see Table 3.1. Finding a steel that matches these values was a challenge . High tensile steel is needed to the torsion bar, as it is the only component that exposed to stresses > 300 Mpa. Preferably a steel with similar mechanical properties as the generic steel from the exams, or stronger. After a lot of research, a good matching steel, and a Norwegian supplier was found. The chosen steel is named SS2387. A high tensile strength stainless steel, with good weldability without preheating. The only issue is that the Young's modulus is somewhere between 205 and 210 Gpa. Which can result in a softer stiffness than desired. When considering a material for the torsion arm, the stresses it is exposed to are < 200 Mpa. These stresses are found in the area joining the torsion bar and arm. For the torsion arm, regular construction steel, S335, is sufficient. It has the correct modulus of elasticity, and a yield strength of 355 Mpa.

3.1.2 Size and layout

As the rig is to be hauled between classrooms, the overall size of the rig must be narrow enough to fit between regular doors. The torsion bar suspension should be mounted high enough to make it possible for all students in the classroom to spot. The rig-operator should be able to operate the rig while standing or sitting. A surface to place a computer connected to the instruments, is also preferable. On this basis, and the stipulated measurements of the torsion bar and arm, guiding measurements were set: The width = 55 ± 10cm. The length = 90 ± 15cm. And the suspension system needs to be situated higher than 110 cm.

3.1.3 Torsion bar

To create a physical test rig that behaves equally to the theoretical model, some modifications have to be made. The main issue is the length of the torsion bar. In the theoretical model, calculations are based on a total torsion length, L = 650 mm. Where the cross-section is Ø25 mm throughout the length of the bar. All the way from where the torsion bar is is clamped, to the centre line of the torsion arm. This is not applicable to the physical rig. This is due to the width of the torsion arm, welds, and the need of an inner support bearing. The theoretical model in the exams assume that the torsion bar behaves similar to Model A in Figure 3.1. Which is not correct compared to a real suspension. Because of this, it was decided to alter the lengths of the different sections of the torsion bar. Figure 3.1 displays four different options that were evaluated. To make the physical rig behave as the theoretical model, the relationship between applied torque and angular deflection, ϕ, is important. This is determined by: $\phi = \frac{Torque \cdot BarLength}{G \cdot I_p}$, were the Polar moment of inertia, $I_p = \frac{\pi d^4}{32}$. In Table 3.2, the different solutions from Figure 3.1 are compared with respect to the angular deflection. Model A is true to the theoretical model. Model B is similar to the technical drawing from the exams. This model is 7,5% stiffer than A. Both Model C and D are almost identical to the theoretical model. Considering that 650mm is utilized as the calculating length in the exams, it is desirable to keep this number in the new model. The selected concept was therefore Model C. This model provides 99,3% of the torsional stiffness of the theoretical model, given equal material constants, but is realistic to build.

Remark: Altering the length of the bar does not affect the torsional stresses in the torsion bar, as stresses are a function of the Radius, Torque, and Material Constants. Which remain unchanged.

Table 3.2: Relative angular-stiffness of different torsion bar lengths

Model	A	B	C	D
Dimentions [mm]	650xØ25	600xØ25 + 50xØ45	650xØ25 + 50xØ45	645xØ25 + 50xØ45
$I_{p,Ø25}$ [mm^4]	38330	38330	38330	38330
$I_{p,Ø45}$ [mm^4]	402374	402374	402374	402374
Length$_{,Ø25}$ / $I_{p,Ø25}$	0,01696	0,01565	0,01696	0,01683
Length$_{,Ø45}$ / $I_{p,Ø45}$	0,00000	0,00012	0,00012	0,00012
Sum of Lengths / I_p	0,01696	0,01578	0,01708	0,01695
Ratio relative to A	1,00000	1,07480	0,99273	1,00036

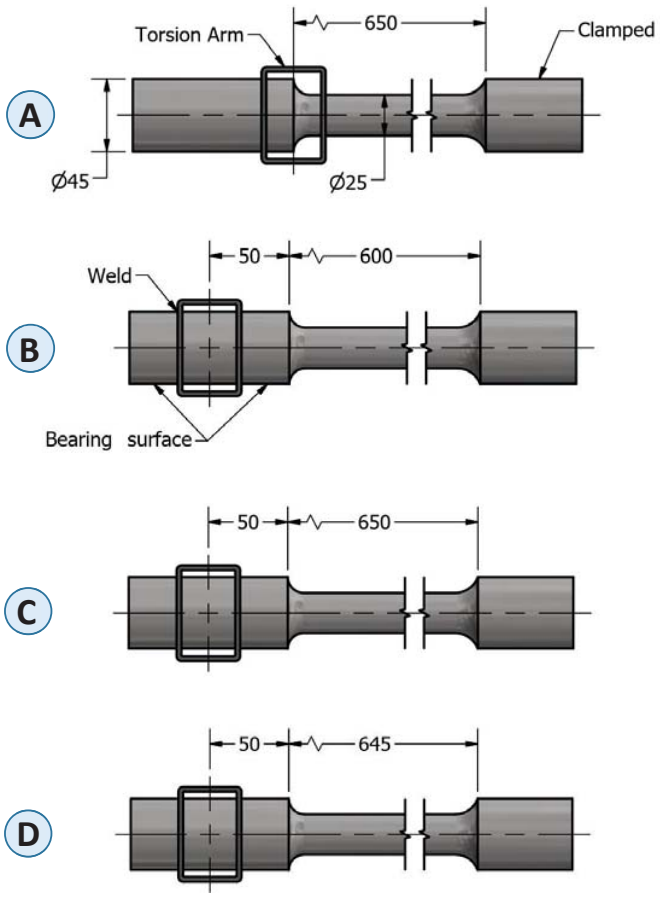

Figure 3.1: Different torsion bar length options. Model A -D

3.1.4 Torsion arm

The torsion arm cross-section in the exams is a rectangular hollow section with dimensions; 55x35x3,5 mm. Due to that this dimension is not a stock item at local dealerships, another dimension is chosen. The selected dimension for the physical rig is 60x40x3mm. This cross-section has an identical surface area, but 20% higher Second Moment of Inertia, I_{xx}. See Figure 3.2. The increased stiffness makes the rig behave closer to the theoretical model, where the torsion arm is assumed rigid. But it will still make a small deflection contribution, which is wished for.

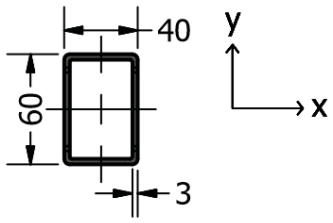

Figure 3.2: Cross section of torsion arm

3.2 CAD

3.2.1 Software

The chosen CAD program for this project is Autodesk Inventor 2016. This choice is based on the author of this paper's five years' experience with this program, through school and work. A familiar program reduces time spent on CAD, and frees up time to other work. Inventor 2016 is a program that has a great CAD console, but a poor FEA console. Due to this, all FEA in this project has been done in Siemens NX 10.0.

3.2.2 Revision 1 - Concept

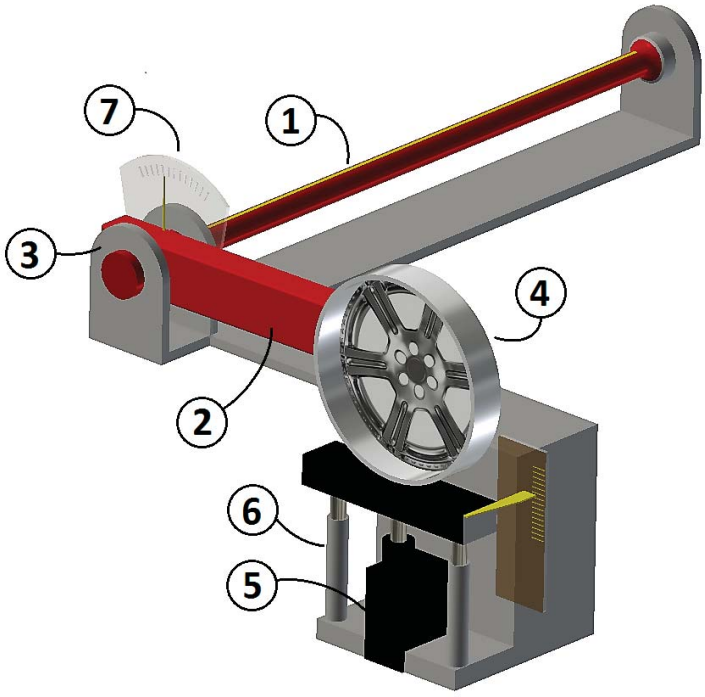

Figure 3.3: Revision 1 - Concept

Designing of the rig started with a concept, Figure 3.3. This was to get a feeling about sizes, and to stipulate mechanical features and functions needed for the rig. Technical data and dimensions from the exams are roughly incorporated at this stage. Features that are necessary:

(1) Torsion Bar

(2) Torsion Arm

(3) Bearings / bushings to stabilize the torsion bar

(4) Wheel Hub

(5) Force loading unit

(6) Sliding mechanism to stabilize the Force loading unit

(7) Analog and digital Instruments; Load cell, Strain gauges, Distance and Angle sensors

3.2.3 Revision 2

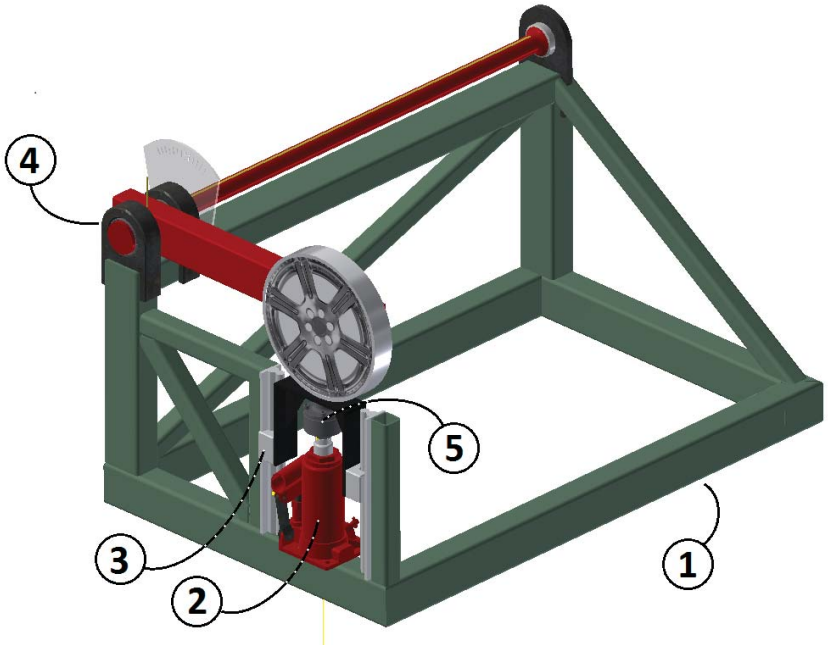

Figure 3.4: Revision 2

See Figure 3.4

(1) At this point in the development, it was chosen to utilize the same cross-section as the torsion arm in the rig frame. This is a 60x40x3 mm hollow section. It would have been easier to create a super rigid frame by scaling up the steel beams, but this minimizes the need of FEA and fine tuning. In other words; no engineering challenge. By utilizing the same cross-section, discarding of 5.5 meters of material is also avoided. (Materials are delivered in 6m lengths)

(2) As a force loading unit, a 2 ton hydraulic jack from Clas Ohlson was chosen. It is compact, and have a stroke length of 110 mm. The CAD model of the jack was downloaded and re-sized to correct measurement.

(3) As the wheel hub´s horizontal position varies with elevation, it is necessary to stabilize the travel-plate between the hub and jack. Linear sliders was implemented as stabilizers.

(4) Copper bushings was chosen to stabilize the torsion bar.

(5) A 500kg Load Cell was selected. CAD model downloaded from manufacturer.

3.2.4 Revision 3

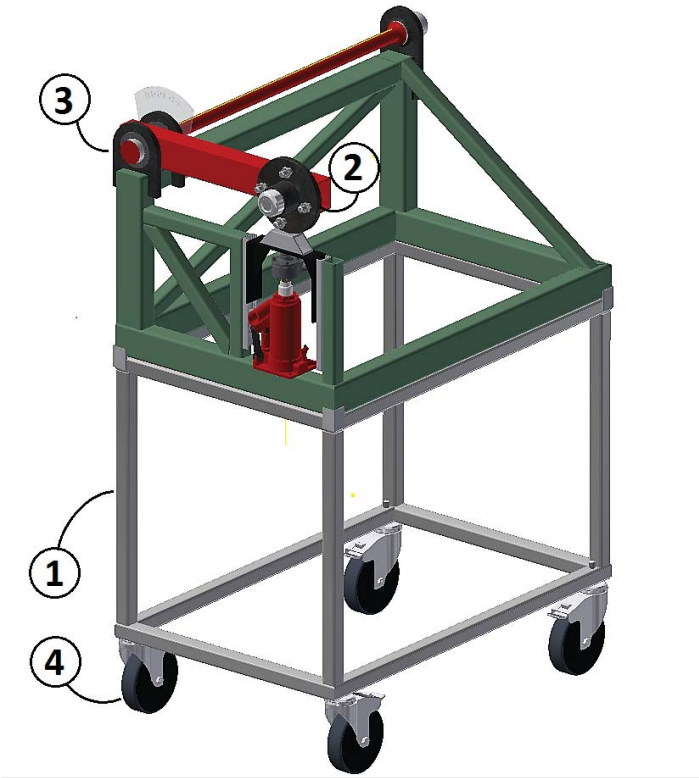

Figure 3.5: Revision 3

See Figure 3.5

(1) 30x30x3mm hollow sections are utilized as frame-legs/subframe.

(2) A prefabricated wheel hub and axle from Biltema.

(3) Copper bushings are changed in favor of ball bearings. The ball bearings are 12mm wide, versus the 35mm bushings. This makes the length between the torsion arm and the slender section of the the torsion bar shorter.

(4) Transport wheels from Biltema. 100mm diameter wheels makes it easy to roll over door sills.

3.2.5 Revision 4

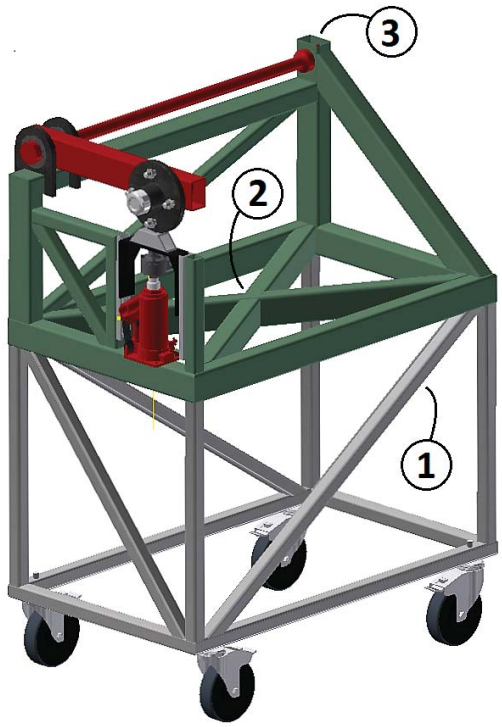

Figure 3.6: Revision 4

Revision 4 is the last revision before production. This involved more detailed Finite Element Analyzes in NX to ensure the design lives up to the expectations. In this revision stiffeners where set in place. If FEA had reveled any weaknesses, the cross-sections would have been increased.

See Figure 3.6

(1) Stiffeners are added to the sub frame. These reduces the twisting of the frame.

(2) Crossing stiffeners are added to the main frame. These also acts as a supporting structure for a table top to be placed on. A computer monitoring the sensors may be placed on this table top.

(3) The the torsion bar is to be welded directly into the frame, instead of machining a fixing bracket.

3.3 Simulation / Results

Final Element Analysis was done in NX 10.0 with the Linear Static SOL 101 Solver. Since there are no non-linearities in the material, this is an sufficient solver for this operation. The physical properties utilized are generic steel from NX, with an Young's-modulus = 210 Gpa. The rig has been meshed with two different types of mesh. The frame and torsion arm are meshed with tetrahedral, CTETRA(10), due to complex shapes. This has an element size of 10 mm. The torsion bar and bearings have been meshed with both tetrahedral and hexahedral CHEXA(20) in different simulations to compare. All components are connected by using Surface-to-Surface Gluing or Contact. See Figure 3.7. The force is 2940 Newton, applied to the wheel hub. The rig is only fixed in the spot where the hydraulic jack base is situated. By doing this, it is not necessary to apply a downwards force at this point. And if there is any deflection or twisting in the frame, the displacement of the hub is calculated from this fixed spot. And not a point that has been relatively displaced.

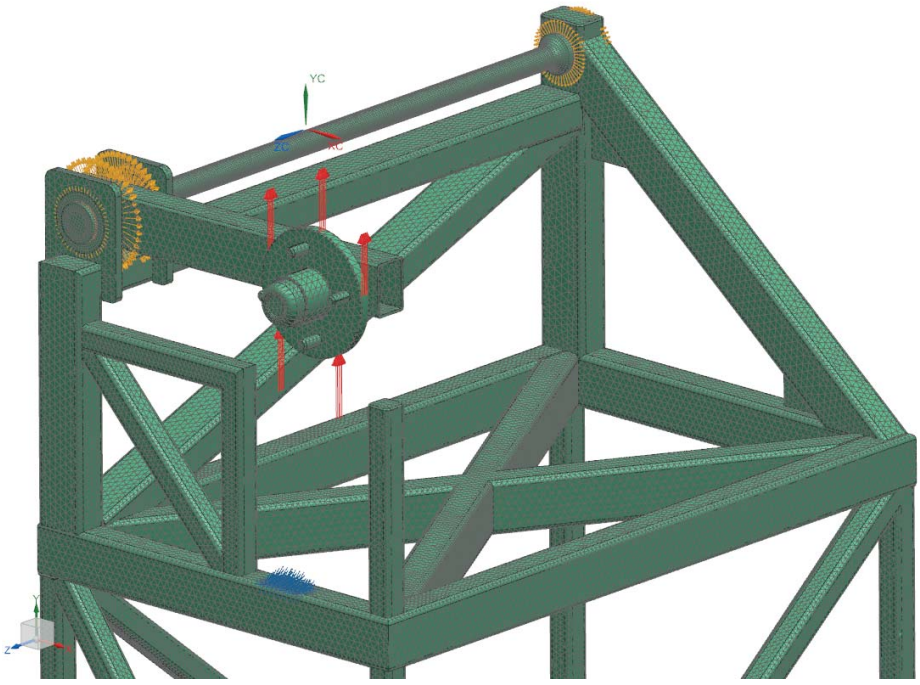

Figure 3.7: Meshed rig with applied simulation objects.

3.3.1 Displacement

The torsional forces from the torsion bar could have caused the frame to twist. The analysis reveals that the frame is totally rigid. The frame will twist <0.1 mm, which is negligible. See Figure 3.8. This approves the frame for production. The centre of the hub is elevated 74.38 mm at 2940 N. The analytical value from the exams predicts 76 mm. It is expected that these two values differs, as the force leverage arm is shortened by an increasing angle of the torsion arm. At this point (12.3 degrees), the force leverage arm is 97.7% of the initial length of 350 mm. If this is incorporated in the theoretical linear model, the prediction becomes 74.25 mm.

3.3.2 Stresses

The critical areas considering stresses are the torsion bar and torsion arm. During the project, the torsion bar has been simulated a number of times with different types of mesh. And the mesh influence the results. Meshed with tetrahedral CTETRA(10), 7mm elements, the uniform elemental stress in the torsion bar is found to be 580.5 Mpa, (Von Mises). This is almost identical to the theoretical 582 Mpa. The stress consecration in the radius is 727 Mpa, (K_t = 1.25). It is suspected that this is unlikely high. A finer mesh in the radius would presumably produce a lower stress consecration. The torsion bar was also meshed with hexahedral CHEXA(20), 3mm element size. The uniform elemental stress was then 527.5 Mpa. Which is significant lower than 582 Mpa. But the stress consecration is only 2.5%, (K_t = 1.025). This deviation between the types of mesh, might be be explained by the way stress is sampled in the hexa mesh. The stresses are sampled in the integration points, and not at the surface, where the stress is highest. Unaveraged Nodal, gives uniform stress of 564.7 Mpa. Which is closer to what to expect. See Figure 3.9 Evaluating this, it is believed that the tetrahedral produces the most correct value for uniform stress in this case. The highest elemental stress in the torsion arm is found to be 190 Mpa. This is located in the area joining the torsion bar and arm. As the stress is way below the material yield stress of 355 Mpa, it is nothing to worry about. Considering the rest of the frame, the stresses are <30 Mpa, which is negligible. The only section where the stress is higher than 30 Mpa, is the joint between the torsion bar and frame. Here, the stresses are similar to in the torsion arm. Based on the simulation results, the rig should hopefully behave as desired.

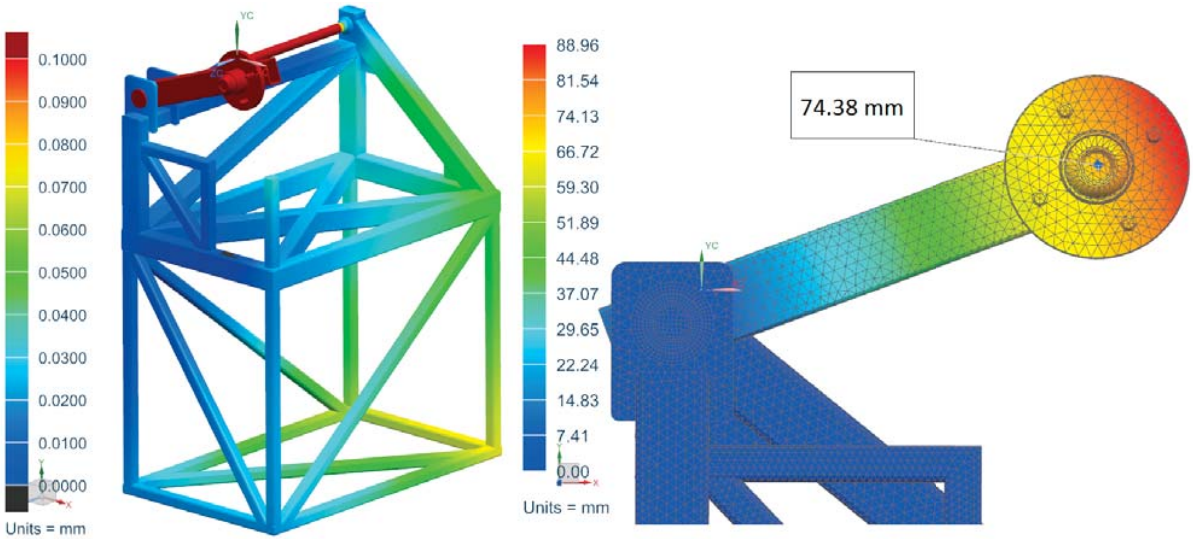

Figure 3.8: Displacement magnitude at 2940N

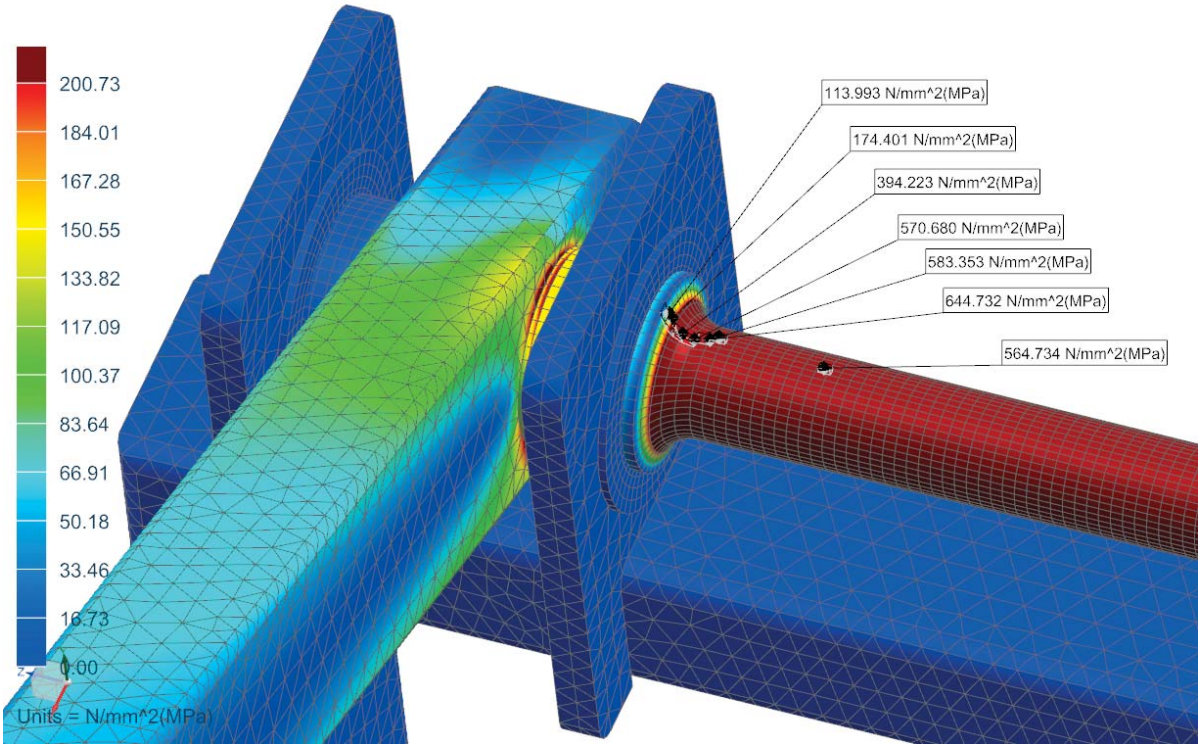

Figure 3.9: Unaveraged Nodal, Von Mises Stress in torsion bar and arm, at 2940N. (overflow from 200Mpa)

Chapter 4

Buiding process

4.1 Production Planing

Preparing for production is an important task. This consists of order parts and materials, creating an assembly manual, and keeping track of the economy. In addition, one must ensure that the tools needed for production actually are available in the workshop. Proper preparation reduces the risk of downtime and last minute changes before/during fabrication. The Department of Engineering Design and Materials has its own fully equipped realization lab available for students. This is where the production of the rig happened. All construction work was done by the author of this paper. The exception was the machining of the torsion bar and bearing mounts, as this require trained personnel operating CNC machines.

4.1.1 Procurement of parts

The procurement of parts and components was done in two batches. Round one was to be able to finish the design, as the size and design was unknown for three components. Thus, the hydraulic jack and wheel hub were purchased. The third component, the Load Cell, was borrowed from the Institute. Round two, occurred after finishing the design of the rig. This consisted of ordering all the construction material from a local dealer, Tibnor, and purchasing the rest of the components needed. See Table 4.1 for all purchased parts and materials.

4.1.2 Time and cost

It has been a focus to keeping cost and expenses to a minimum. By design-choices like utilizing the same material for the rig frame, as for the Torsion Arm. The rest of the components are the most cost effective components found. Keeping the need for advanced machining to a minimum, also reduces cost. The total material and component cost of the build is 6336 NOK Excl. VAT. , see Table 4.1 . 75% of the expenses are related to construction materials. Although the material expenses has been kept low, the project has probably hit a budget overrun. This is due to the machining of the torsion bar. This turned out to be more complicated than expected. The Realization lab lacks adequate equipment, which led to that the torsion bar had to be finished at SINTEF. Estimated fabrication-time was to be around 3 weeks / 15 effective workdays. The estimate was quite spot on, but due to easter and a HSE shutdown of the workshop, the 15 effective workdays were scattered across five weeks.

Table 4.1: Components and Material cost

Item	Dim.	Order quantum	Need (m) or (pcs)	NOK Excl. VAT	NOK Incl. VAT	Supplier
Hollow section	60x40x3mm	2x6 m	9 m	1005	-	Tibnor
Hollow section	30x30x3 mm	2x6 m	10 m	944	-	Tibnor
Circular bar	Ø51 mm	1 m	0,8 m	2222	-	Tibnor
Hydraulic jack	2 ton	1 pcs	1 pcs	-	129	Clas Ohlson
Bearings	45x68x12	2 pcs	2 pcs	-	400	Kulelager24
Wheels	100mm	4 pcs	4 pcs	-	280	Biltema
Wheel hub	40mm axle	1 pcs	1 pcs	-	399	Biltema
Paint	Blue, Black	2 pcs	1 pcs	-	550	E. Tønderdal
Slider mechanism		2 pcs	2 pcs	-	198	Clas Ohlson
Delivery		1 pcs	1 pcs	600	-	Tibnor
			Sum	4771	1956	

Total Sum	Excl. VAT	6336,-
Total Sum	Incl. VAT	7920,-

4.1.3 Technical drawings

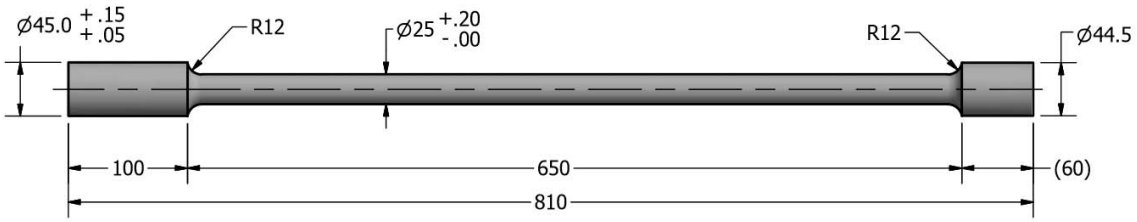

Figure 4.1: Torsion Bar drawing

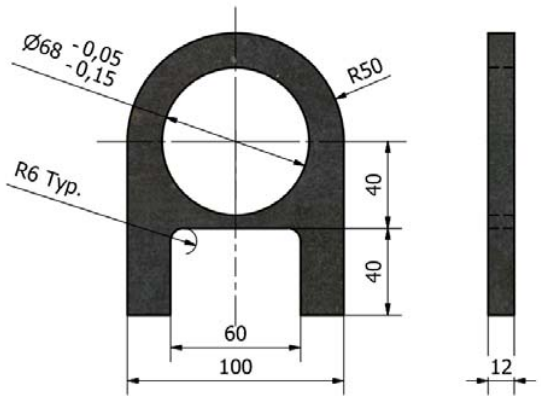

Figure 4.2: Bearing Mounts drawing

Technical production drawings was made for the torsion bar and bearing mounts. Section views from these drawings can be seen of the Figures 4.1, and 4.2. As it was the author of this paper that was manufacturing the rig, it was chosen not to fabricate technical drawings of all the components. Instead, a cutting-list for all the steel members, was made. This displays the cross-section, lengths and angles of the steel members. This cutting-list corresponds with an illustration (Figure 4.3) to where the members are situated. This illustration may seem messy, but there is a color- and number-coding-system of personal preference.

#	X-section	Presise Length	Cut to length	Angle
1	30x30	480		
2	30x30	480		
3	30x30	480		
4	30x30	480		
5	30x30	500		45 - 45
6	30x30	830		45 - 45
7	30x30	500		45 - 45
8	30x30	830		45 - 45
9	30x30		700	Messure
10	30x30		930	Messure
11	30x30		700	Messure
12	30x30		930	Messure
		Rig top		
21	60x40	500		45 - 45
22	60x40	830		45 - 45
23	60x40	500		45 - 45
24	60x40	830		45 - 45
25	60x40	290		0 - 45
26	60x40	380		
27	30x30		830	Messure
28	60x40		600	Messure
29	60x40	790		0 - 45
30	60x40		900	Messure
31	60x40		450	Messure
32	60x40		450	Messure
33	30x30	230		
34	30x30	230		0 - 45
35	30x30	300		Messure
36	30x30	225		0 - 45
37	60x40	450		

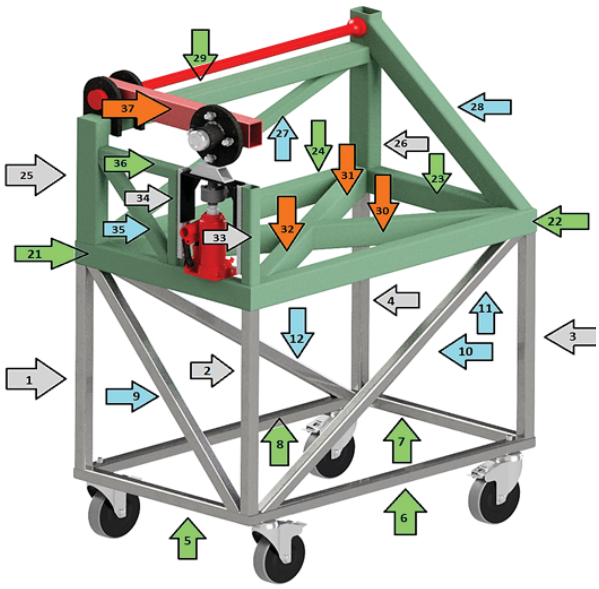

Figure 4.3: Cutting-list and steel member placement. To personal use

4.1.4 Assembly procedure

Planing how the rig is assembled together is crucial. If some steel members are welded on before it should, the assembly will not fit together. Twisting caused by the weld process must also be taken into account. A 12 step production/assembly was planed before production start, see Figure 4.4. The most crucial element was to make sure the torsion bar was not being bend. Hence, the frame-part combining the bearing mounts to the main frame is welded on after the torsion bar. This is to ensure a good fit without bending the torsion bar, see step 11 and 12 on Figure 4.4.

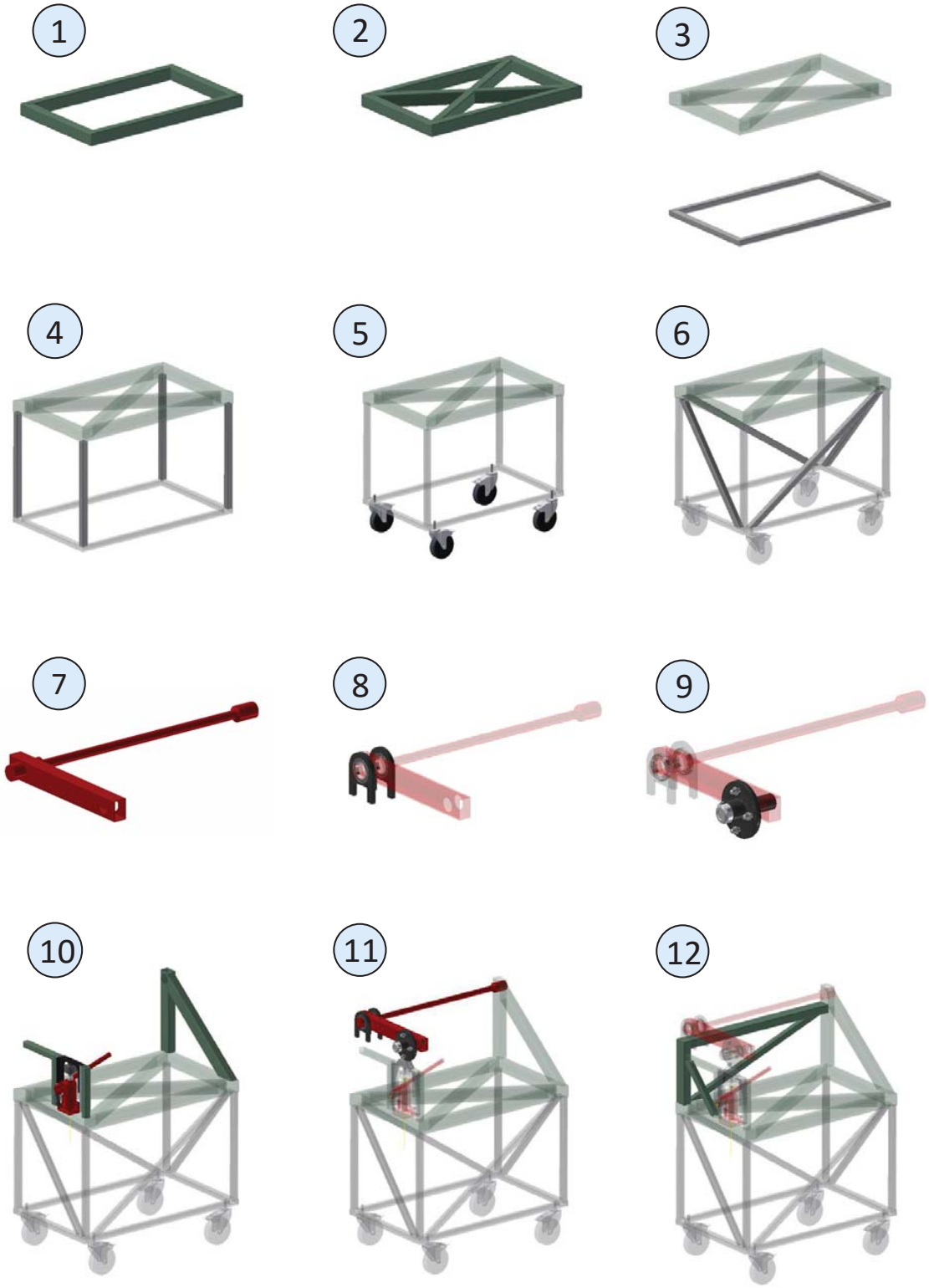

Figure 4.4: Assembly procedure

4.2 Fabrication

4.2.1 Torsion bar

The job with machining the torsion bar was given to the personnel employed in the realization lab. The reason for this is that the slender geometry, in combination with high tensile stainless steel, is complex to machine. As this results in flexing of the bar during turning. Considering the stress concentration factor, the torsion bar is designed with a R12 radius on both sides. The realization lab lacked the adequate radial tool for this job. The bar was therefore sent to SINTEF to make these radii, and the correct surface finish, with a CNC machine. Even due to professional machining, the finished torsion bar is slightly convex. The center diameter is 0.25mm lager than designed. This convex shape may create an extra deviation factor on the physical model versus the analytical. Some misconception happened concerning the radii as-well. Resulting in that the torsion bar has a radius of R10 at one end, and R15 at the other. The overall result of the torsion bar is satisfying.

4.2.2 Welding

Welding is a major element of producing the rig, as the construction contains more than hundred weld seams. The welding method used on this project is Metal Inert Gas (MIG) welding. Prior to this build, research was done on basic welding-theory and practical tips, to make sure that it gets correctly preformed. About 90% of the welds are on the hollow section main frame. Which is 3mm carbon steel. As some of the weld-joints is exposed to local high stresses, it is important to have a full penetration weld. To achieve this, it is necessary to prepare the weld-joint by grooving the edges to be welded. Figure 4.5 displays four steps of the welding of the rig frame. As welding generates a lot of heat, one has to take material distortion into account. By spot welding all corners prior to seam-welding, one reduces the risk of distortion. Many of corners of the main frame are grinded down to a smooth finish. This is to be able to attach other beams perpendicular to these joints. Welding the torsion bar to both the torsion arm and rig frame was more of a concern. Welding two different materials may induce weld cracking. As the torsion bar is stainless steel, and the frame is mild carbon steel, this could become a problem. Ordinary

austenitic stainless steel (316L) has a thermal expansion that is 50% higher than carbon steel. This may induce cold cracking as the weld cools down. The stainless chosen for the torsion bar is ferritic martensitic. This steel has a thermal expansion coefficient of $11,0x10^{-6}K^{-1}$, almost identical with the carbon steel frame's coefficient of $11,1x10^{-6}K^{-1}$. This reduces the risk of cold cracking. As the welds between the torsion bar and frame are critical due to high stresses, adjustments to the welding machine was done. The polarity of the MIG welder was changed from Direct Current Electrode Negative, (DCEN), to Direct Current Electrode Positive, (DCEP). This changes the direction of the current-flow of the welder. This generates a lot of heat in the construction, but results in a deeper weld in the torsion bar. These welds was designed to have an A-measurement of 4 mm. The finished welds have about 5 mm, which is good.

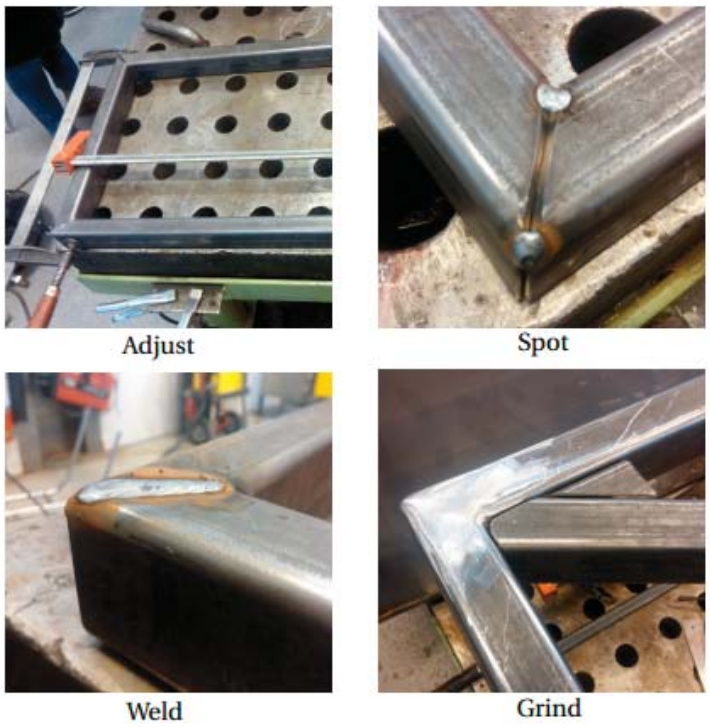

Figure 4.5: Steps of welding

4.2.3 Modified components

Some of the purchased components had to be customized before assembly. This includes the hydraulic jack, the slider mechanism, and wheel hub. The hydraulic jack needed a custom fitting between it and the force cell. A M16 Male - M12 Male fitting was made for this purpose. To make it easier to operate the the hydraulic jack, the release valve got an extended handle. The sliders that stabilizes the jack was shortened. This was done to situate the internal ball-bearing-cage at the perfect spot, to maximize the stiffness of the sliders. The wheel hub axle was shortened.

4.2.4 Paint

Prior to paint, the rig got sanded down by hand, and cleaned. A two-tone paint-job was chosen. A black finish on the torsion arm and bearings mounts reinforces the impression of a suspension system. Whilst a blue frame is just great contrast. The torsion bar is not painted as large strains may cause cracks in the paint. And as it is stainless, it do not require paint to prevent corrosion indoors.

4.3 Final product

The finalized product is almost exactly as intended. There where no unforeseen obstacles that led to any major alterations of the design. There is a few changes, but mostly cosmetic. The analog angular indicator was changed. From being situated on the top of the rig, it was moved to the front side. See Figure 4.6. The initial tests indicates that the rig works as planed. The rig is designed to withstand at least 76 mm vertical displacement of the torsion arm. Due to the material, it is safe to elevate the arm to about 95 mm. It is tested to 85 mm, and works perfect. When elevating the torsion arm, the wheel hub and jack becomes vertically aligned. This is to prevent large moment forces in the jack as the vertical force increases. The rig also is constructed to be fail-secure. The hydraulic jack is mounted in a way that makes it impossible to provoke yield in the torsion bar. This prevents anyone form ruining the rig unintentionally. Top and bottom table tops are also installed. See Figure 4.7. Appendix A includes As-Built technical drawings of the finished rig.

Figure 4.6: Front view, directed towards audience

Figure 4.7: Side view. Table top to locate a computer.

Chapter 5

Summary and Further Work

5.1 Summary and Conclusions

The objective of this thesis was to design an build a Torsion Bar Suspension Test Rig. The basis for this work are two exams from TMM4112 Machine Elements from 2009. The aim was to build a user friendly, physical test rig that behaves as a suspension system presented in these exams. The physical rig is later on going to be instrumented with numerous sensors. This is to compare the physical performance with the analytical values from the exams, and computer simulation. FEA simulations was utilized during the design process to ensure that the design criteria were met, based on KPIs. The ambition to design and build the rig was completed during this Thesis. Only a few unforeseen obstacles were met during the development and production of the rig. The finished torsion bar has a slightly larger diameter than planned. How much this affects the rigs behavior, is going to be interesting to investigate. On the positive side, all chosen components seem to work as intended. And initial testing indicates that the rig behaves as desired. However, thorough testing will be required before concluding whether the rig is a success or not.

5.2 Further Work

The author of this paper will continue to work with this project, as a Master Thesis. The following work consists of instrument and test the rig, and compare the physical results with FEA and hand calculations. Both static and dynamical behavior will be analyzed. The rig it going to be instrumented with strain-gauges, load cell, vertical displacement sensor, angular twist sensor, and an accelerometer. Interpreting these signals will be done by utilizing Catman AP software. The comparison between simulation, hand calculation, and the physical test results, may uncover discrepancies. These will be analyzed and described. Student work-tasks, linked to this project, is also going to be developed. Figure 5.1 displays how the rig is going to look like after instrumentation.

Figure 5.1: Rendering of finished rig with instrumentation

Appendix H

Exams of 2009 in Machine Elements

Norges teknisk-naturvitenskapelige universitet
Institutt for produktutvikling og materialer

EKSAMENSOPPGAVE I TMM4112 - Maskindeler

Faglig kontakt under eksamen: Professor Torgeir Welo; Vit. Ass. Jan Magnus G. Farstad

Tlf.: 41440061; 98074461

Eksamensdato : 30.05.2009

Eksamentid : 09:00 – 13:00

Studiepoeng : 7,5

Tillatte hjelpemidler: C; F. Igrens, Formelsamling i mekanikk
Bestemt, enkel kalkulator tillatt.

Samtlige oppgaver skal besvares. Hvert svar forsynes med det tilsvarende oppgavenummer og spørsmålindeks. Svarene skal være ordentlig og pent innført. Det legges vekt på at teksten er klar og konsis og at skissene er ordentlig og tydelig tegnet og inneholder alle nødvendige påskrifter. Skisser utføres i en slik målestokk at man tydelig kan se det som skal beskrives. Hvis du føler at oppgaveteksten mangler essensielle opplysninger, eller ikke har funnet svaret på en oppgave som skal brukes i en etterfølgende oppgave, kan du gjøre dine egne antagelser og bruke disse videre.

Språkform : Norsk

Antall sider bokmål : 8 (inklusiv vedlegg)

Antall sider vedlegg : 1

Sensurdato : 3 uker fra eksamensdato

Merk! Studentene må primært gjøre seg kjent med sensur ved å oppsøke sensuroppslagene. Evt. telefoner om sensur må rettes til instituttet eller sensurtelefonene. Eksamenskontoret vil ikke kunne svare på slike telefoner.

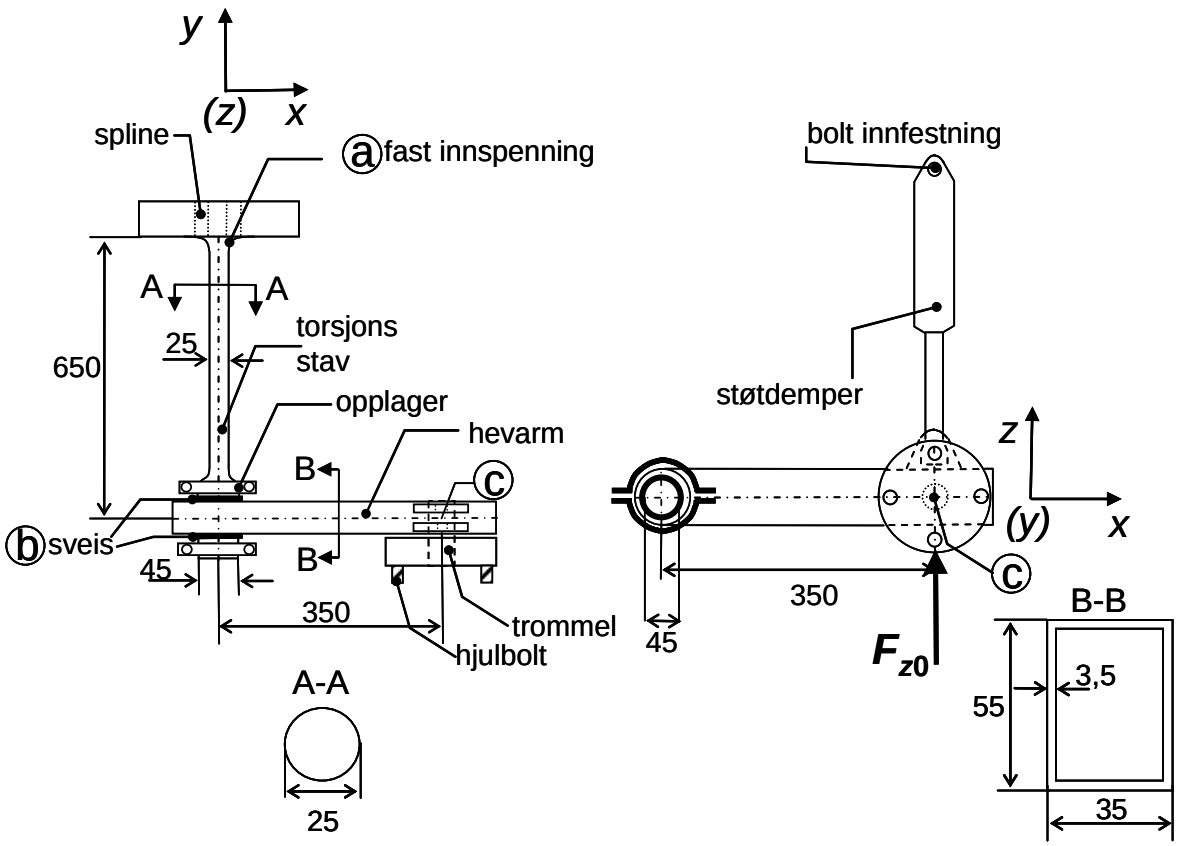

Figur 1: Hjulopphengssystem for en liten personbiltilhenger.

Oppgave 1.

Figur 1 viser et hjulopphengssystem for en enkel to-hjuls personbiltilhenger som bruker en torsjonsstav som fjærelement. Torsjonsstaven er lagret i tilhengerens understell i pkt ⓑ (fastholdt i *x* og *z* retning, men kan rotere fritt om *y*-aksen) hvor den er forbundet med hevarmen, for å unngå bøyespenninger langs førstnevnte, og er fast innspent til tilhengerens understell i motsatt ende ⓐ. Torsjonsstaven er ført gjennom et maskinert hull i hevarmen i ⓑ og en kilsveis på hver side av hevarmen overfører krefter mellom de to komponentene. I denne oppgaven skal vi anta at hevarmen er uendelig stiv/sterk og at sveisene er overdimensjonerte m.h.t. statiske belastninger.
Materialdata: Flytespenning, σ_0 = 640 MPa; Elastisitetsmodul, E = 210.000 MPa; Tverrkontraksjon (Poissons tall) $\nu = 0{,}3$ Materialkoeffisient γ_m = 1,1; von Mises dimensjoneringskriterium:

$$\sigma_e^2 = (\sigma_1 - \sigma_2)^2 + (\sigma_2 - \sigma_3)^2 + (\sigma_1 - \sigma_3)^2 \le \frac{2\sigma_0^2}{\gamma_m^2}$$ (der σ_i er hovedspenninger)

a) Lag en forenklet statisk beregningsmodell der en (statisk) vertikal kraft F_{z0} overført fra hjulet virker på systemet. Du kan anta at hjulets eksentrisitet er så liten at lasten angriper i senter av tverrsnittet til hevarmen. Tegn bøyemoment-, torsjonsmoment- og skjærkraftdiagram for hele systemet.
b) Vis spenningstilstanden (største spenningsnivå) i snitt ⓐ i Mohrs spenningsdiagram for en last F_{z0} = 1.000 N, og indiker største og minste hovedspenning, samt hovedspenningsretning.

c) Finn den maksimale statiske lasten $F_{z0}^{\max}$ som systemet kan ta opp basert på feil (overskridelse av dimensjonerende spenning) i snitt ⓐ.

d) Se bort fra deformasjon av hevarmen—dvs. anta at denne er uendelig stiv—og beregn største deformasjon/bevegelse ($w^{\max}$) i pkt ⓒ for den maksimale lasten $F_{z0}^{\max}$. Anta *små deformasjoner* i beregningsmodellen (dvs. lasten virker normalt på et fast punkt på hevarmen, uavhengig av deformasjon, slik at det er en lineær sammenheng mellom kraft i ⓒ og moment i ⓑ; d.v.s. $\tan\theta \approx \sin\theta \approx \theta; \cos\theta = 1$, der θ er rotasjon av hevarmen).

e) Beregn fjæringssystemets stivhet k for en vertikal last påført i punkt ⓒ på hevarmen. Her kan du som over anta *små deformasjoner* slik at dette punktet beveger seg kun vertikalt *w*(*z*) (dvs. $u(x) = 0$). Hvordan vil du betegne modellens fjær-karakteristikk ut fra disse antagelser?

Oppgave 2.

Vi skal gjøre noen betraktninger rundt dynamisk oppførsel til det samme hjulopphenget som er vist i figur 1. Vi skal anta at halve massen (*M*) til to-hjuls tilhengeren er mye større enn den ekvivalent massen (*m* = 9 kg) til hvert hjul/trommel i pkt ⓒ. Vi kan videre anta at stivheten til dekket (*K*) er mye større enn fjærstivhet til hjulopphenget, *k* (fra oppgave 1e). Anta at systemets masse *m* er konsentrert i pkt. ⓒ (resten av systemet er 'vektløst') og at fleksibiliteten er konsentrert til torsjonsstaven ⓐ-ⓑ (d.v.s. hevarmen er uendelig stiv). En støtdemper med dempningskonstant *c* er montert i enden av hevarmen ⓒ. Vi forutsetter igjen små deformasjoner (utslag) slik at det er en lineær sammenheng mellom kraften $F_z(\omega)$ overført fra veibanen og bevegelsen *w* i pkt ⓒ. Øvrige data som i oppgave 1.

a) Skisser en forenklet modell for å analysere dynamisk oppførsel av fjæringssystemet, og sett opp den dynamiske bevegelsesligningen for systemet (Newtons 2. lov) der du inkluderer den ytre, harmoniske kraften $F_z(\omega)$.

b) Hva mener vi med følgende betegnelser: *systemets egenfrekvens (p)*; *naturlig frekvens for fri svingning av dempet system* (ω_{nd})*;* *dynamisk forstørrelsesfaktor* ($D(\omega)$)*;* *resonansfrekvens* (ω_r)?

c) Beregn systemets egenfrekvens (naturlige), *p*, for den spesifikke svingemoden vi får med forutsetningene angitt i teksten over.

d) Løsningen for fri svingning av et dempet system er gitt på formen,
$w = \left(A\cos p\sqrt{1-\xi^2}t + B\sin p\sqrt{1-\xi^2}t\right)e^{-\xi pt}$,
der $\xi = c/(2\sqrt{km})$ og *c* er dempning. Vis prinsippene for å komme fram til denne løsningen, og skisser svingeforløpet for en valgt løsning. Skisser hvordan økt/redusert dempning påvirker svingeforløpet.

e) Bestem nødvendig dempning (*c*) for støtdemperen under forutsetningen av at minimum 96 % av utslaget skal dempes ned gjennom en svingesyklus fra ett utslag til det neste.

f) Produsenten av tilhengeren ønsker å finne den maksimale dynamiske forstørrelsesfaktoren for systemet under tvungen svingning ($F_z(\omega)$). Sjefsingeniøren argumenterer for å sette på en påtrykt frekvens ω lik egenfrekvensen for et udempet system *p* og så registrere maksimalt utslag for en gitt påtrykt kraft eller forskyvning. Hva ville du gjøre hvis du var en del av testgruppen til sjefsingeniøren?

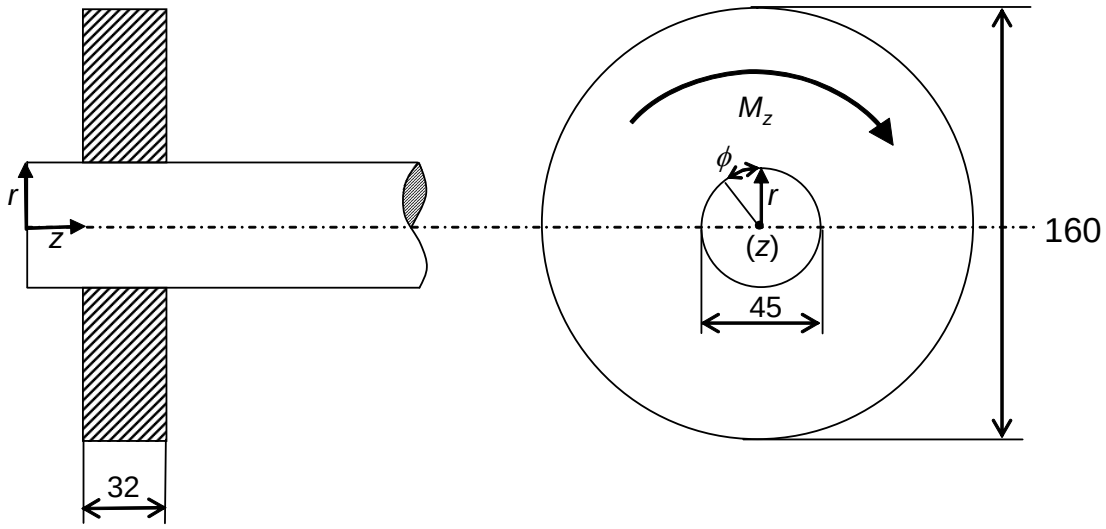

Figur 2: Dimensjoner for krympeforbindelse blir utsatt for ren torsjonsbelastning (M_z).

Oppgave 3.

Vi skal undersøke torsjonskapasitet og spenninger i presspasningen 45H8/u7 som er vist i figur 2. Aksel og nav er av samme materiale (smidd stål). Elastisitetsmodul og tverrkontraksjon (Poisson-tall) er henholdsvis E = 210.000 MPa og $\nu = 0{,}3$. Materialets flytespenning (σ_0) er 640 MPa og materialkoeffisient (γ_m) er 1.15. Øvrige data tas fra figur 3.

a) Forklar hva tallene og bokstavene står for i betegnelsen 45H8/u7, og bruk tabellene i figur 3 til å bestemme øvre og nedre avvik for henholdsvis boring (*ES*, *EI*) og aksel (*es*, *ei*). Vis toleranseområdene og indiker midlere pressmonn i en enkel skisse.
b) Beregn midlere pressmonn (δ_m) og det mest sannsynlige avviket ($\Delta\delta$) fra denne middelverdien. Her kan du anta at boringens og akslingens diameter er uavhengige og normalfordelte, hver med diameterstandardavvik på halve toleranseområdet (fra a)).
c) Forklar hvorfor vi i praksis opererer med effektivt pressmonn (δ_{eff}) som er avhengig av overflateruhet til både boring ($R_{a,b}$) og aksel ($R_{a,a}$).
d) Anta at overflateruhet kan settes til 10 % av diametertoleransen for hver av de to delene (aksel og nav/boring), og at det effektive pressmonnet kan beregnes av $\delta_{eff} = \delta - 4(R_{a,a} + R_{a,b})$, der δ er pressmonn. Beregn forventet maksimum ($\delta_{\max,\ eff}$), midlere ($\delta_{m,\ eff}$) og minimum ($\delta_{\min,\ eff}$) effektivt pressmonn.
e) Forklar hvorfor vi må sjekke forbindelsen for både maksimalt pressmonn og minimalt (effektivt) pressmonn.
f) Beregn torsjonskapasitet til forbindelsen for minste effektivt pressmonn $M_z(\delta_{\min,\text{eff}})$. Her kan du anta at friksjonskoeffisienten mellom nav og aksel, $\mu = 0{,}35$. Følgende formler er oppgitt (notasjon som i læreboka, der α er fleksibilitetskoeffisienter, indeksene *a* og *n* refererer til henholdsvis aksel og nav, indeksene *i* og *y* refererer til henholdsvis indre og ytre, *E* er elastisitetsmodul og ν er tverrkontraksjon:

$$(\alpha_{ni} + \alpha_{ay})p = \delta / 2;$$

$$\alpha_{ni} = \frac{1}{E_n}\frac{r_{ni}^2}{r_{ny}^2 - r_{ni}^2} r_{ni}\left[1-\nu+(1+\nu)\frac{r_{ny}^2}{r_{ni}^2}\right];$$

$$\alpha_{ay} = \frac{1}{E_a}\frac{r_{ay}^2}{r_{ay}^2 - r_{ai}^2} r_{ay}\left[1-\nu+(1+\nu)\frac{r_{ai}^2}{r_{ay}^2}\right]$$

g) Sjekk spenningstilstanden og finn sikkerhetsfaktoren hvis en spesifikk forbindelse med maksimalt effektivt pressmonn ($\delta_{\max,eff}$) belastes med torsjonsmomentet fra f), dvs. $M_z(\delta_{\min,\text{eff}})$. (Tips: kontakttrykk kan skaleres direkte fra f) siden det varierer lineært med pressmonnet.) Skisser spenningskomponentene for et element som ligger i overflaten til navet.

$$\sigma_{r,ay} = \sigma_{r,ni} = -p$$

$$\sigma_{\varphi,ay} = -p\frac{r_{ay}^2 + r_{ai}^2}{r_{ay}^2 - r_{ai}^2}; \qquad \sigma_{\varphi,ni} = p\frac{r_{ny}^2 + r_{ni}^2}{r_{ny}^2 - r_{ni}^2}$$

$$\sigma_e = \sqrt{\sigma_r^2 + \sigma_\varphi^2 - \sigma_r\sigma_\varphi + 3\tau_{r\varphi}^2 + 3\tau_{rz}^2} \le \frac{\sigma_0}{\gamma_m}$$

Basismål Basic size mm		t[1]				u				
Over Above	T.o.m. Up to and including	5	6	7	8	5	6	7	8	9
–	3					+ 22 + 18	+ 24 + 18	+ 28 + 18	+ 32 + 18	+ 43 + 18
3	6					+ 28 + 23	+ 31 + 23	+ 35 + 23	+ 41 + 23	+ 53 + 23
6	10					+ 34 + 28	+ 37 + 28	+ 43 + 28	+ 50 + 28	+ 64 + 28
10	18					+ 41 + 33	+ 44 + 33	+ 51 + 33	+ 60 + 33	+ 76 + 33
18	24					+ 50 + 41	+ 54 + 41	+ 62 + 41	+ 74 + 41	+ 93 + 41
24	30	+ 50 + 41	+ 54 + 41	+ 62 + 41	+ 74 + 41	+ 57 + 48	+ 61 + 48	+ 69 + 48	+ 81 + 48	+ 100 + 48
30	40	+ 59 + 48	+ 64 + 48	+ 73 + 48	+ 87 + 48	+ 71 + 60	+ 76 + 60	+ 85 + 60	+ 99 + 60	+ 122 + 60
40	50	+ 65 + 54	+ 70 + 54	+ 79 + 54	+ 93 + 54	+ 81 + 70	+ 86 + 70	+ 95 + 70	+ 109 + 70	+ 132 + 70
50	65	+ 79 + 66	+ 85 + 66	+ 96 + 66	+ 112 + 66	+ 100 + 87	+ 106 + 87	+ 117 + 87	+ 133 + 87	+ 161 + 87
65	80	+ 88 + 75	+ 94 + 75	+ 105 + 75	+ 121 + 75	+ 115 + 102	+ 121 + 102	+ 132 + 102	+ 148 + 102	+ 176 + 102
80	100	+ 106 + 91	+ 113 + 91	+ 126 + 91	+ 145 + 91	+ 139 + 124	+ 146 + 124	+ 159 + 124	+ 178 + 124	+ 211 + 124
100	120	+ 119 + 104	+ 126 + 104	+ 139 + 104	+ 158 + 104	+ 159 + 144	+ 166 + 144	+ 179 + 144	+ 198 + 144	+ 231 + 144
120	140	+ 140 + 122	+ 147 + 122	+ 162 + 122	+ 185 + 122	+ 188 + 170	+ 195 + 170	+ 210 + 170	+ 233 + 170	+ 270 + 170
140	160	+ 152 + 134	+ 159 + 134	+ 174 + 134	+ 197 + 134	+ 208 + 190	+ 215 + 190	+ 230 + 190	+ 253 + 190	+ 290 + 190
160	180	+ 164 + 146	+ 171 + 146	+ 186 + 146	+ 209 + 146	+ 228 + 210	+ 235 + 210	+ 250 + 210	+ 273 + 210	+ 310 + 210
180	200	+ 186 + 166	+ 195 + 166	+ 212 + 166	+ 238 + 166	+ 256 + 236	+ 265 + 236	+ 282 + 236	+ 308 + 236	+ 351 + 236
200	225	+ 200 + 180	+ 209 + 180	+ 226 + 180	+ 252 + 180	+ 278 + 258	+ 287 + 258	+ 304 + 258	+ 330 + 258	+ 373 + 258
225	250	+ 216 + 196	+ 225 + 196	+ 242 + 196	+ 268 + 196	+ 304 + 284	+ 313 + 284	+ 330 + 284	+ 356 + 284	+ 399 + 284
250	280	+ 241 + 218	+ 250 + 218	+ 270 + 218	+ 299 + 218	+ 338 + 315	+ 347 + 315	+ 367 + 315	+ 396 + 315	+ 445 + 315
280	315	+ 263 + 240	+ 272 + 240	+ 292 + 240	+ 321 + 240	+ 373 + 350	+ 382 + 350	+ 402 + 350	+ 431 + 350	+ 480 + 350
315	355	+ 293 + 268	+ 304 + 268	+ 325 + 268	+ 357 + 268	+ 415 + 390	+ 426 + 390	+ 447 + 390	+ 479 + 390	+ 530 + 390
355	400	+ 319 + 294	+ 330 + 294	+ 351 + 294	+ 383 + 294	+ 460 + 435	+ 471 + 435	+ 492 + 435	+ 524 + 435	+ 575 + 435
400	450	+ 357 + 330	+ 370 + 330	+ 393 + 330	+ 427 + 330	+ 517 + 490	+ 530 + 490	+ 553 + 490	+ 587 + 490	+ 645 + 490
450	500	+ 387 + 360	+ 400 + 360	+ 423 + 360	+ 457 + 360	+ 567 + 540	+ 580 + 540	+ 603 + 540	+ 637 + 540	+ 695 + 540

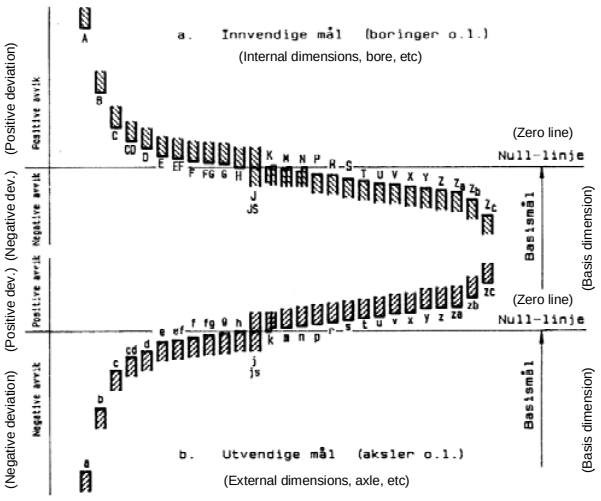

Figur 1.1. ISO-toleransenes beliggenhet
(Location of ISO tolerances)

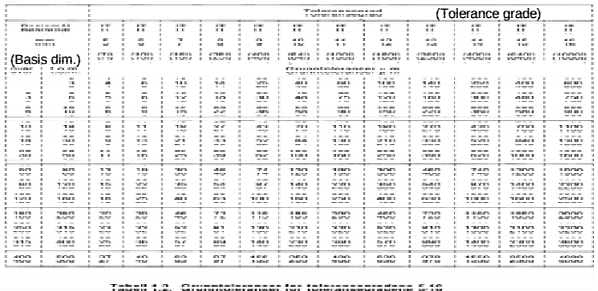

Tabell 1.2. Grunntoleranser for toleransegradene 5-16
(basis tolerances for tolerance grades 5-16)

Figur 3: Toleranseklasser og toleransegrader.

Oppgave 4.

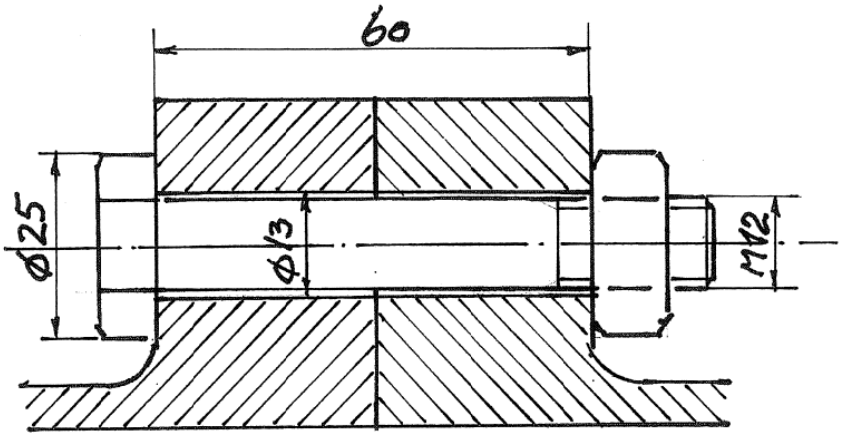

Figur 4. Geometri for flensforbindelse.

Den viste flensforbindelsen skal undersøkes med hensyn på virkningen av temperatur-endringer. Aksialkraften i røret er uten betydning i denne sammenheng, og settes ut av betraktning.
Skruen er av stål, dimensjon M12, maks tillatt strekkraft er F_{Smax}=72.000N.
Flensene er i aluminium.
Materialdata:

Elastisitetsmodul: Stål: $E_{St} = 2 \cdot 10^5$ MPa
Al: $E_{Al} = 7 \cdot 10^4$ MPa

Varmeutvidelsestall: Stål: $\alpha_{St} = 1{,}2 \cdot 10^{-5}$ mm/mm˚C
Al: $\alpha_{Al} = 2{,}4 \cdot 10^{-5}$ mm/mm˚C

Forbindelsen monteres ved vanlig romtemperatur. Driftsbetinget temperaturvariasjon er $\Delta t = 100$˚C.
Temperaturutvidelse regnes slik: $\Delta l = \alpha \cdot l \cdot \Delta t$

a) Velg forspenningskraft og tegn skruediagram.
b) Vis i skruediagrammet hva som skjer når
   i. Flensene oppvarmes men ikke skruen
   ii. Alle delene oppvarmes like mye
c) Hva blir kraftvariasjonen i skruen?

Oppgave 5.

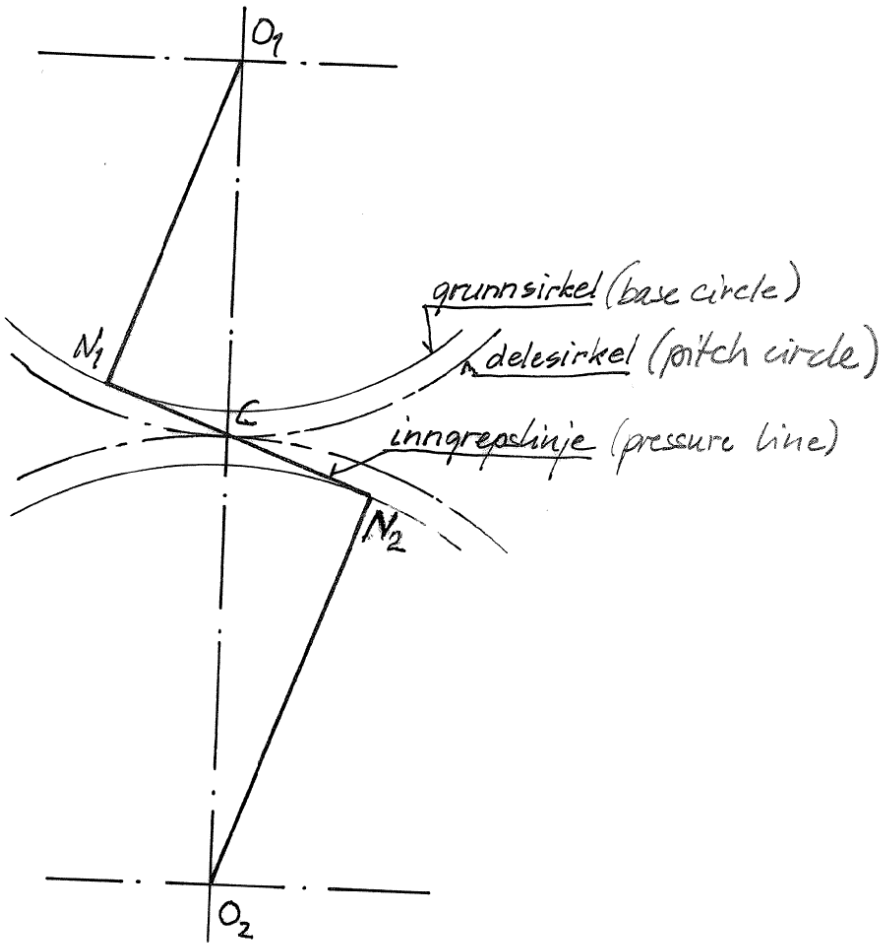

Figur 5. Skisse av system for to tannhjul i inngrep.

Skissen viser skjema til to tannhjul i inngrep.
Tannhjulene er normhjul med modul 5 og tilvirkningsinngrepsvinkel $\alpha_0 = 20^\circ$.
Hjul 1 med tanntall $z_1 = 20$, hjul 2 med tanntall $z_2 = 24$. En grafisk løsning er tilfredsstillende hvis den er nøyaktig og i målestokk.

a) Tegn inn tanntoppsirkelen til de to hjulene.

b) Bestem den del av inngrepslinjen N1N2 der det er tenner i inngrep.

c) Det viste skjema er tegnet for normal akseavstand O1O2 = $a = r1 + r2$. Vis hvordan skjemaet forandres hvis akseavstanden økes med 5mm.

d) Bestem inngrepsvinkelen i denne situasjonen.

NB: Tegn løsningen på løsningsarket som er lagt inn bakerst i oppgaveheftet.
Husk å skrive på studnr og sidenr.
Riv arket ut og legg det ved besvarelsen.

Fagnr.: TMM4112 Maskindeler Dato: 30. mai 2009 Sidenr.: ……

Studentnr.: ……..

Vedlegg 1: Ark for å tegne løsning på oppgave 5.

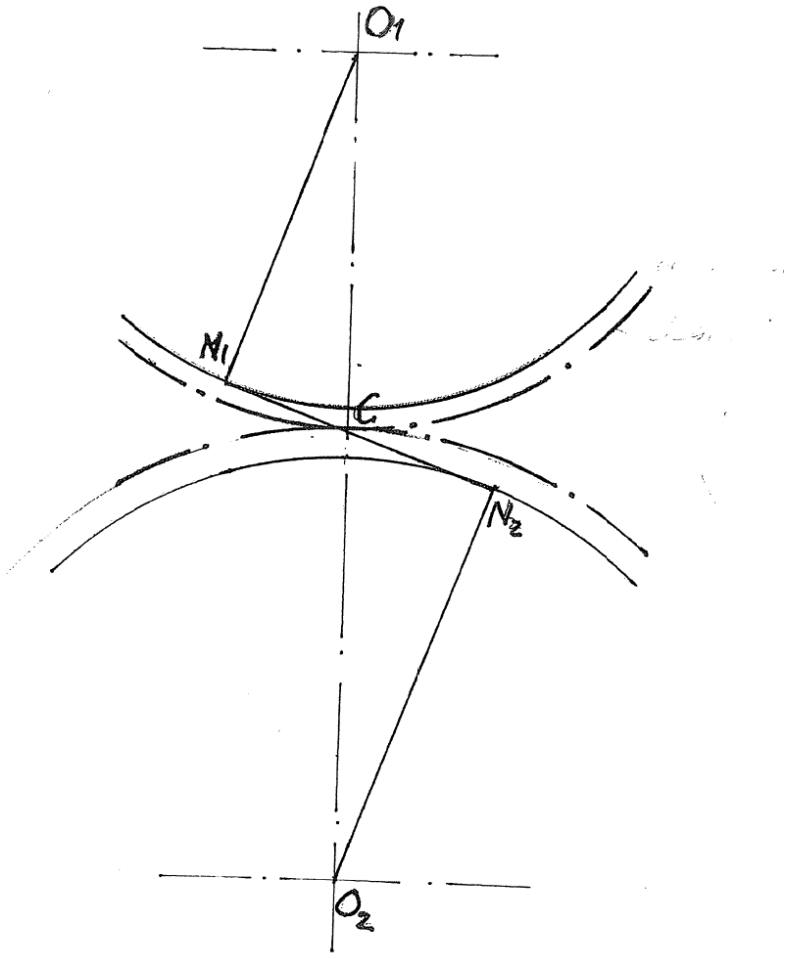

Husk løsning på dette arket. Riv det ut og legg det ved besvarelsen. Skriv på studentnummer og sidenummer.

Norges teknisk-naturvitenskapelige universitet
Institutt for produktutvikling og materialer

KONTINUASJONSEKSAMEN TMM4112 - Maskindeler

Faglig kontakt under eksamen: Professor Torgeir Welo; Knud-Helmer Knudsen

Tlf.: 41440061; 99579815

Eksamensdato : 15.08.2009

Eksamentid : 09:00 – 13:00

Studiepoeng : 7,5

Tillatte hjelpemidler: C; F. Igrens, Formelsamling i mekanikk
Bestemt, enkel kalkulator tillatt.

Samtlige oppgaver skal besvares. Hvert svar forsynes med det tilsvarende oppgavenummer og spørsmålindeks. Svarene skal være ordentlig og pent innført. Det legges vekt på at teksten er klar og konsis og at skissene er ordentlig og tydelig tegnet og inneholder alle nødvendige påskrifter. Skisser utføres i en slik målestokk at man tydelig kan se det som skal beskrives. Hvis du føler at oppgaveteksten mangler essensielle opplysninger, eller ikke har funnet svaret på en oppgave som skal brukes i en etterfølgende oppgave, kan du gjøre dine egne antagelser og bruke disse videre.

Språkform : Norsk

Antall sider bokmål : 7 (inklusiv vedlegg)

Antall sider vedlegg : 0

Sensurdato : 3 uker fra eksamensdato

Merk! Studentene må primært gjøre seg kjent med sensur ved å oppsøke sensuroppslagene. Evt. telefoner om sensur må rettes til instituttet eller sensurtelefonene. Eksamenskontoret vil ikke kunne svare på slike telefoner.

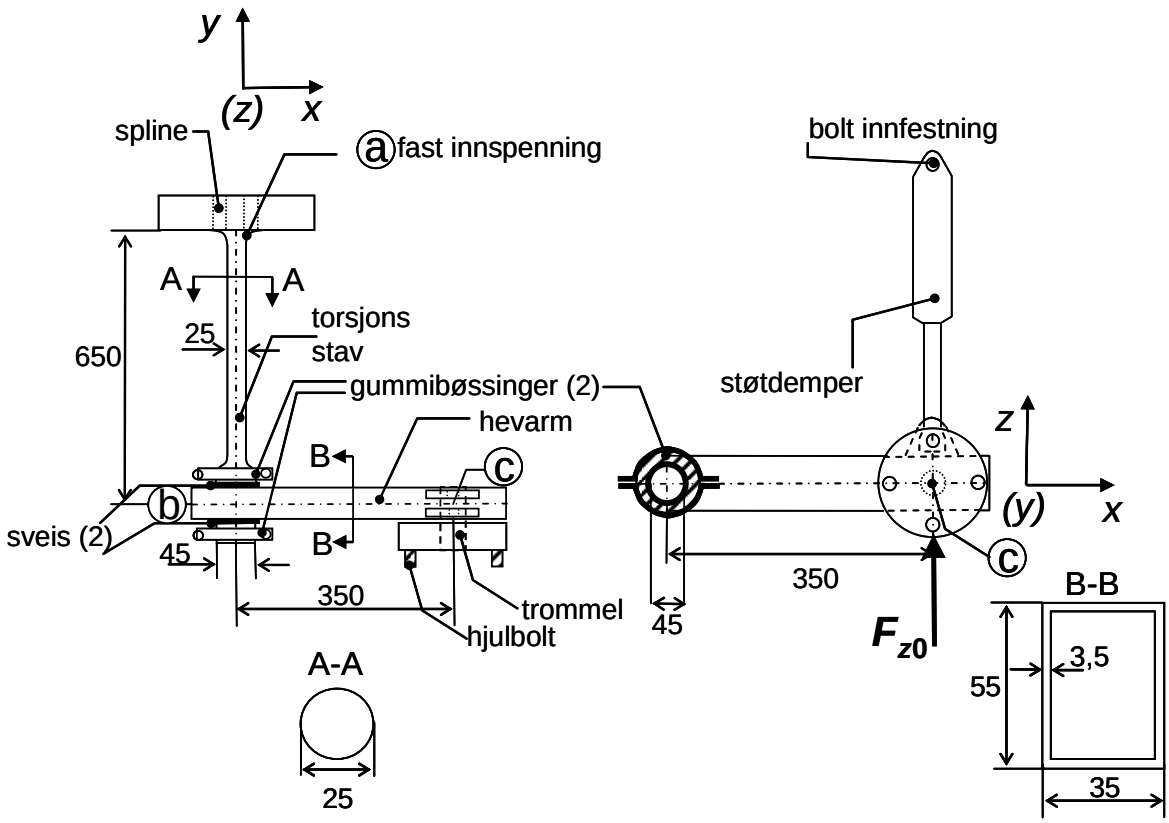

Figur 1: Hjulopphengssystem for en liten personbiltilhenger.

Oppgave 1.

Hjulopphenget for en to-hjuls personbiltilhenger vist i Figur 1 bruker en torsjonsstav som fjærelement. Torsjonsstaven er lagret i tilhengerens understell via to like elastiske **gummibøssinger** for bl.a. å redusere bøyespenningene langs torsjonsstaven. Modelleringsteknisk kan disse to bøssingene representeres med en sentrisk bøssing med samlet (radiell) stivhet k_g. Torsjonsstaven kan rotere fritt om y-aksen pkt ⓑ, og er fast innspent til tilhengerens understell i motsatt ende ⓐ. Torsjonsstaven er ført gjennom et maskinert hull i hevarmen i ⓑ, og en kilsveis på hver side av hevarmen overfører krefter mellom de to komponentene. I denne oppgaven skal vi anta at hevarmen er uendelig stiv/sterk og at sveisene er overdimensjonerte m.h.t. statiske belastninger.
De tre utviklingsingeniørene Fritz, Günter og Hansi, som jobber hos av en av Biltemas underleverandører i Syd-Tyrol, har ulik oppfatning (modeller) over hvordan kreftene tas opp i systemet. Din oppgave er å se på forskjeller som modellene gir m.h.t. belastingen på systemet med en statisk (vertikal) last F_{z0} påført fra hjulet i ⓒ.

Materialdata: Flytespenning, σ_0 = 640 MPa; Elastisitetsmodul, E = 210.000 MPa; Tverrkontraksjon (Poissons tall) $\nu = 0{,}3$ Materialkoeffisient γ_m = 1,1; von Mises dimensjoneringskriterium:

$$2\sigma_e^2 = (\sigma_1 - \sigma_2)^2 + (\sigma_2 - \sigma_3)^2 + (\sigma_1 - \sigma_3)^2 \le \frac{2\sigma_0^2}{\gamma_m^2}$$ (der σ_i er hovedspenninger)

a) Fritz mener at gummibøssingen(e) er så myk ($k_g \approx 0$) at man kan se bort fra reaksjonskraften (R_z) som den eventuelt tar opp. Lag en forenklet statisk beregningsmodell der en vertikal kraft F_{z0} overført fra hjulet virker på systemet. Du kan anta at hjulets eksentrisitet er så liten at lasten angriper i senter av tverrsnittet til hevarmen. Beregn snittkreftene (skjær, bøyning og torsjonsmoment ved F_{z0} =1.000 N) i snitt ⓐ.

b) Günter derimot påstår hardnakket at torsjonsstaven er myk i forhold til de relativt kompakte gummibøssingene slik at systemet kan antas å være fastholdt i *z*- og *x*-retning i punkt ⓑ ($1/k_g \approx 0$). Beregn snittkreftene i ⓐ tilsvarende oppgave a).

c) Hansi, som for øvrig har ett semester som utvekslingsstudent ved NTNU, mener at man må ta hensyn til stivheten til gummibøssingen(e) hvis man skal beregne realistiske krefter i snitt ⓐ. Han foreslår en modell for reaksjonskraften i bøssingen: $R_z = F_{z0}/(1+\alpha)$, der et enkelt måleoppsett i verkstedet gav α = 0,2. Beregn snittkreftene i ⓐ tilsvarende oppgave a) og b).

d) Anta α = 0,2 og vis spenningstilstanden (største spenningsnivå) i snitt ⓐ i Mohrs spenningsdiagram for lasten F_{z0} = 1.000 N. Finn største og minste hovedspenning.

e) Finn sikkerhetsfaktoren med hensyn på materialflyt i det mest påkjent punktet i snitt ⓐ for α = 0,2 og F_{z0} = 1.000 N.

f) Det forventet at fleksibiliteten til gummibøssingen øker over tid etter hvert som den morkner og sprekker opp. Forklar kort hvordan dette vil påvirke spenningstilstanden og dermed sikkerhetsfaktoren beregnet i f) (ingen beregninger er nødvendig).

Oppgave 2.

Vi skal vurdere utmattingslevetiden til torsjonsstaven i figur 1 som er laget av seigherdet smidd stål med flytespenning σ_0 = 640 MPa og bruddspenning R_m = 820 MPa. Anta at overflatefaktor $r_{\text{overflate}}$ = 0,65 og dimensjonsfaktor r_{dim} = 0,95. Videre skal vi anta at vi har kjervfaktor K_t = 1,2 i overgangen mellom torsjonsstaven og 'spline'.

Data: Elastisitetsmodul, E = 210.000 MPa; Skjærmodul $G = E/2{,}6$; treghetsmoment for torsjonsstav, $I = \pi D^4/64$; polart treghetsmoment for torsjonsstav $I_T = \pi D^4/32$.

a) Utmattingsgrensen settes til $N_D = 10^7$ og vi skal benytte Basquins ligning til å beregne Wøhler spenningen, $\sigma_{AN} = 2R_m(2N)^{-b} \approx \sigma_W$, der konstanten b = 0,10. Tegn in Goodman linjen i et Haig-diagram basert på opplysningene som er gitt over.

b) Korriger Haigh-diagrammet for overflate- og dimensjonseffekter, og tegn inn den dimensjonerende Goodman linjen.

c) Vis i det samme diagrammet hvordan man kan korrigere 'begrensningskurven' slik at den tar hensyn til kjerveffekten (K_t = 1,2) i overgang mellom torsjonsstav og 'spline'.

d) Ved hjelp av stivhetsberegninger (og testing) finner de tyske ingeniørene at sammenhengen mellom vertikal deformasjon og kraft påført ved ⓒ er gitt av $w = \dfrac{F_z h^2 L}{GI_T}\left[1+\left(\dfrac{L}{h}\right)^2 \dfrac{\alpha}{1+\alpha}\dfrac{GI_T}{EI}\right]$,

der L og h er henholdsvis lengde av torsjonsstav og svingarm, og 'bøssningparameteren' α = 0,2 (fra oppgave 1). Vis at Hansis modell reduserer stivheten til systemet med 30 % i forhold Günter's modell (som antok at bøssingen er uendelig stiv), mens forskjell i ekvivalent spenning beregnet med de to modellene kun er 6 % (hvis du mangler svar fra oppgave 1. kan du anta at ekvivalent spenning $\sigma_e = 210$ Mpa for $F_z = 1.000$ N med Hansis modell).

e) Systemets skal dimensjoneres for en statisk middeldeformasjon (w_m i z-retning ved ⓒ) fra vekt av henger og en karakteristisk syklisk deformasjon (w_a i z-retning ved ⓒ) fra ujevnheter i vegbanen, $w = w_m \pm w_a$ =15 mm $\pm$ 20 mm. Finn de tilhørende spenningskomponentene som inngår i utmattingsanalysen av snitt ⓐ. **Tips:** Finn kraft F_z fra formel gitt i 2.d) med α = 0,2 og bestem spenninger relativt til de du fant for F_{z0}=1.000N.

f) Anta at ekvivalent spenningsamplitude kan beregnes av $\sigma_a = \sqrt{\sigma_{1a}^2 + \sigma_{2a}^2 - \sigma_{1a}\sigma_{2a}}$, og ekvivalent midtspenning, $\sigma_m = \min\left\{\sqrt{\sigma_{1m}^2 + \sigma_{2m}^2 - \sigma_{1m}\sigma_{2m}} \;\; ; \sigma_{1m} + \sigma_{2m}\right\}$ der '1' og '2' referer til henholdsvis største og minste hovedspenning. Beregn disse størrelsene for den beskrevne lastsituasjonen.

g) Plott inn spenningstilstanden i Haigh-diagrammet og bestem sikkerhetsfaktoren. Er denne innenfor det som anses akseptabelt i forbindelse med utmattingsdimensjonering?

Oppgave 3.

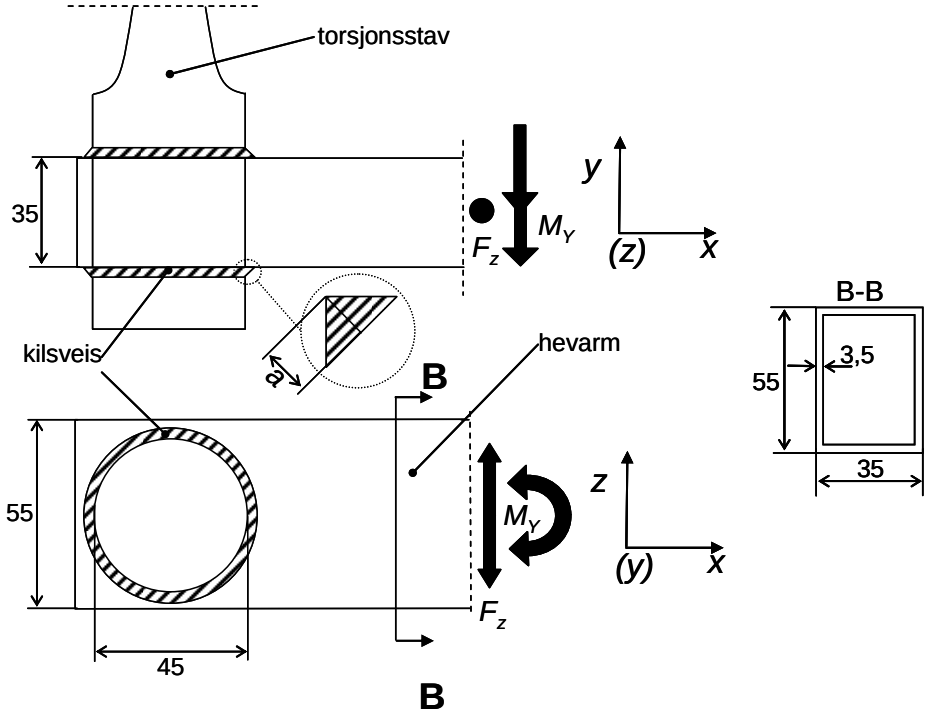

Figur 2: Detaljer av sveist forbindelse mellom hevarm og torsjonsstav.

Vi skal dimensjonere sveisene som overfører krefter mellom hevarm og torsjonsstav i hjulopphenget til biltilhengeren. Hovedsystemet er angitt i Figur 1, mens detaljer av sveiseforbindelsen er angitt i Figur 2. Vi skal anta at *krefter fordeles jamt* mellom de to sveisene slik at begge er like effektive. Vi skal bruke dimensjoneringskriteriet for kilsveis:

$$\sqrt{\sigma_\perp^2 + 3\tau_\perp^2 + 3\tau_\parallel^2} \; < 355 \text{ MPa}/\gamma_m$$

Her kan vi anta at $\gamma_m = 1{,}1$.

a) Anta at når hjulet ruller langs veibane genererer dette en vertikal kraft som overføres til hevarmen. Definer/vis hvilke indre krefter som denne kraften generer langs hevarmen. Beregn sammenhengen mellom største bøyemoment ($M_{\max}$) langs hevarm og største torsjonsmoment ($T_{\max}$) langs torsjonsstaven.

b) Sett opp sammenhengene mellom spenningskomponenten(e) som opptrer i et snitt langs kilsveisen(e) og en last F_z påført i punkt ⓒ.

c) Den maksimale statiske lasten som kan overføres til det globale systemet uten at man overskrider maksimal tillatt spenning for torsjonsarmen i ⓐ er beregnet til $F_z^{\max} = 2{,}75$ kN. Pga utmattingsegenskapene for sveiser vil man at sveiseforbindelsen skal ha en statisk lastkapasitet som er 3 ganger den til torsjonsstaven, dvs. $F_z^{\max-s} = 3F_z^{\max} = 8{,}25$ kN. Finn minste teoretiske *a*-mål for sveisene (neglisjer skjærkraften), og velg et praktisk *a*-mål ut fra dette.

d) Forklar hvorfor middelspenning ikke inngår som en dimensjoneringsvariabel ved dimensjonering av sveiser mot utmatting.

e) Sveisen utføres i Detaljkategori 100 (figur 3). Finn den tillatte spenningsvidden ($\Delta\sigma$), dvs. minste spenningsvidde (som gir opphav til utmattingsskade) som kan tillates når det antas at en eller flere av belastningssyklusene kan ligge over utmattingsgrensen.

f) Anta at den sykliske deformasjonen $w_a \pm 20$ mm (i *z*-retning ved ⓒ, figur 1) tilsvarer en syklisk last $F_{za} \pm 600$ N. Sjekk om tilhørende spenningsvidde for valgt *a*-mål er under *avskjæringsgrensen* når sveisen er utført i Detaljkategori 100 (figur 3).

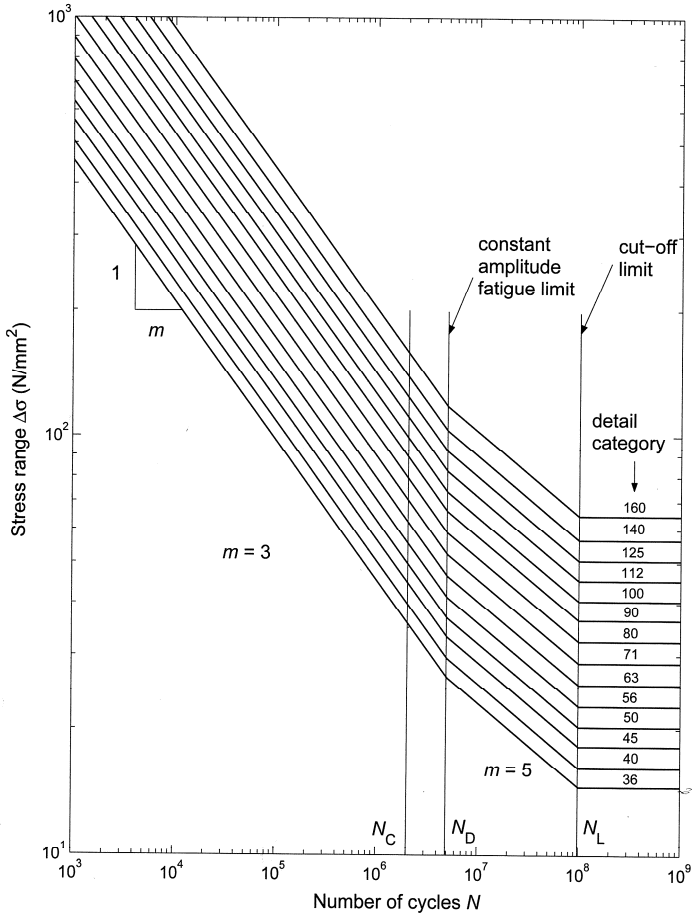

Figur 3: Tillatte antall spenningssykler *N* som funksjon av normalspenningsvidden med detaljkategorien (36 – 160) som parameter (Eurocode 3 1993).

Oppgave 4.

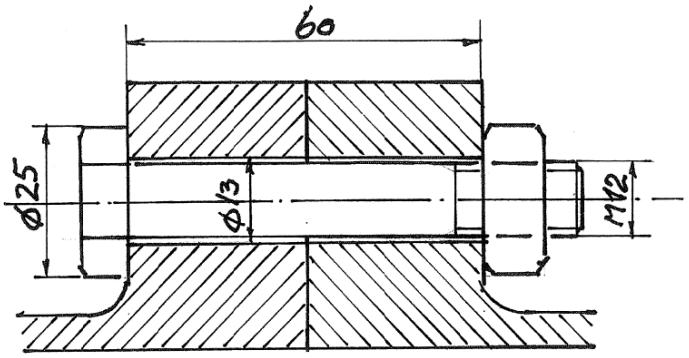

Figur 4: Geometri for flensforbindelse.

Flensforbindelsen som er vist i figur 4 skal forspennes til F_o = 40.000 N. Skruen er av stål dimensjon M12, stigning p = 1,75 mm, flankediameter d = 10,8 mm.
Flensene er av aluminium.

	Stål	**Aluminium**
Elastisitetsmodul:	E_{St} = 200 GPa;	E_{Al} = 70 GPa
Temperaturutvidelseskoeffisient:	$\alpha_{St} = 12 \cdot 10^{-6}\ {}^{mm}/_{mm^\circ C}$	$\alpha_{Al} = 24 \cdot 10^{-6}\ {}^{mm}/_{mm^\circ C}$

a) Tegn skruediagram for den oppgitte forspenningskraften.

b) Forspenningen skjer ved at mutteren skrues til med fingrene til anslag, deretter dreies den til en viss vinkel til den ønskede forspenningskraft er oppnådd. Hvor stor er denne vinkelen?

c) Har delenes temperatur ved montasjen noe å si for forspenningen?

d) Hva skjer når temperaturen endrer seg etter at forbindelsen er montert?

Oppgave 5.

Kraftoverføringen i en moped/scooter er arrangert som vist skjematisk i skissen i figur 5.

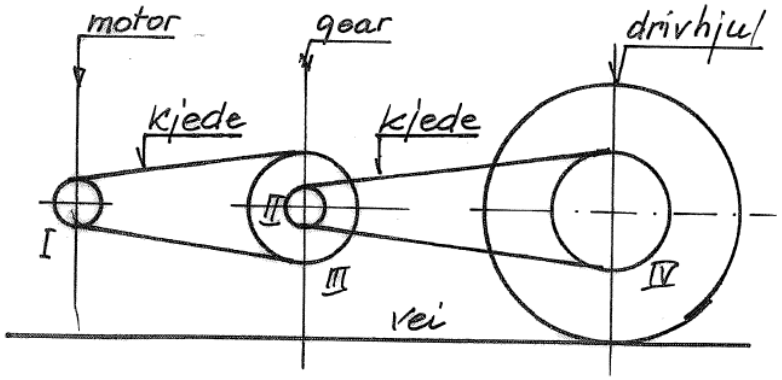

Figur 5: Kraftoverføring i en moped/scooter.

Fra motoren overføres effekt med kjede til gearvekselen og videre med kjede til drivhjulet.
Kjedehjul I på motorakselen har $z_I = 18$ tenner
Kjedehjul II på gearvekselen (inngående aksel) har $z_{II} = 45$ tenner
Kjedehjul III på gearvekselen (utgående aksel) har $z_{III} = 18$ tenner
Kjedehjul IV på drivhjulet (utgående aksel) har $z_{IV} = 50$ tenner
Drivhjulets diameter er 440 mm.
Motorens maksimale effekt $P = 3{,}3$ kW, tilsvarende omløpshastighet er $n = 5.000$ omløp/minutt (RPM)

a) Bestem total oversetning mellom hjul og drivhjul.
b) Bestem drivhjulets rotasjonshastighet når motoren går med maksimal hastighet.
c) Bestem tangentialkraften på drivhjulet når motoren går med maksimal effekt.
d) Hva er tilsvarende tangentialhastighet på hjulet
e) Bestem strekkraften i kjedet mellom gearvekselen og drivhjulet.

Bibliography

[1] Virgo 39. Datasheet for virgo 39 (s165m), Industeel, 2010.

[2] Ask Falch. Trailer suspension rig for virtual and physical testing. Project Thesis, April 2016.

[3] Gunnar Härkegård. *Dimensjonering av maskindeler*. Tapir akademisk forlag, 2012.

[4] Fridtjof Irgens. *Formel samling mekanikk*. Tapir akademisk forlag, 2010.

[5] Omega. *Strain Gauge Installation How to Position Strain Gauges to Monitor Bending, Axial, Shear and Torsional Loads*.

[6] Ball bearings. http://www.vxb.com/6909-2RS-Bearing-45x68x12-Sealed-p/kit1028.htm.

[7] Rainer Rauch Erke Wang, Thomas Nelson. Back to elements - tetrahedra vs. hexahedra. 2004.

[8] John R. Brauer. *What Every Engineer Should Know About Finite Element Analysis*. Marcel Dekker, 2. edition, 1993.

[9] University of Tennessee at Martin. Stress concentration factors and notch sensitivity notch sensitivity. Lecture 4 - Engineering 473 Machine Design,.

[10] Norman E. Dowling. Mean stress effects in stress-life and strain-life fatigue. 2004.

[11] Siemens. *Basic Dynamic Analysis User's Guide*. Siemens, 2014.

[12] Course description tmm4112. http://www.ntnu.edu/studies/courses/TMM4112tab=omEmnet.

[13] Course description tmm4135. http://www.ntnu.edu/studies/courses/TMM4135tab=omEmnet.

[14] Course description tmm4155. http://www.ntnu.edu/studies/courses/TMM4155tab=omEmnet.